Recombinant Expression and Functional Characterization of Cannabinoid Producing Enzymes in *Komagataella phaffii*

Zur Erlangung des akademischen Grades eines

Dr.rer.nat

von der Fakultät Bio- und Chemieingenieurwesen
der Technischen Universität Dortmund
genehmigte Dissertation

vorgelegt von

M. Sc. Bastian Zirpel

aus

Hannover

Tag der mündlichen Prüfung: 02.05.2018

1. Gutachter/-in: Prof. Dr. Oliver Kayser

2. Gutachter/-in: Prof. Dr. Ida van der Klei

Dortmund 2018

ACKNOWLEDGEMENTS

I would like to express my gratitude towards the people who supported and encouraged me over the last years. First of all, I want to thank my supervisor **Prof. Dr. Oliver Kayser** (Technical Biochemistry, TU Dortmund) for offering me the possibility to research in my field of preference. He promoted my scientific ideas and gave me the opportunity to freely develop my skills and expertise in the desired research areas. I would like to thank **Dr. Felix Stehle** for guidance and support in the first two years of my PhD thesis.

I also want to express my gratitutude towards all people who contributed with their work to the successful publications: **Dirk Münker**, **David Dannheisig** and **Madeleine Dorsch** for their student work regarding chapter 3; **Julia Grühn**, **Martin Obholzer**, **Christian Staubach** and **Martin Kares** for their student work regarding chapter 6; **Angela Sester** (Technical Biology, TU Dortmund) for her help with NMR analysis (chapter 5); **Wolfgang Brandt** (IPB Halle) for sharing ideas about possible enzyme variants (chapter 5); **Michael Kubicki** (CCB, TU Dortmund) for performing the HPLC-MS^3 measurements (chapter 5); **Jan Schonert** for performing NMR measurements (chapter 6). **Peter Kötter** (Goethe University Frankfurt) for supplying us with the strain CEN.PK2-1C (chapter 6). **Prof. Dr. Jörn Kalinowski** and **Daniel Wibberg** (CeBiTec, University Bielefeld) for strain sequencing and analysis (chapter 4).

I would like to thank the Ministry of Innovation, Science and Research of the German Federal State of North Rhine-Westphalia (NRW) and TU Dortmund for awarding me with a scholarship from the **CLIB-Graduate Cluster Industrial Biotechnology** (CLIB2021). Furthermore, I want to thank co-workers of the chair of technical biochemistry, particularly **Kristine Hemmer** and **Jörg Fischer** who facilitated the day-to-day work. A special thanks goes to **Chantale Zammarelli** for always assisting my research whether in good or not-so-nice times as well as sharing the passion for funny cat videos.

I also want to thank fellow PhD students **Friederike Degenhardt**, **Laura Kohnen**, **Nouman Almofti**, **Friederike Ullrich**, **Eva Gruchattka**, **Angela Sester**, **Julia Schachtsiek**, **Tajammul Hussain**, **Parijat Kusari**, **Kathleen Pamplanyil**, **Torsten Arndt**, **Niklas Wolters** (APT, TU Dortmund) and **Jan Schwarzhans** (University Bielefeld) as well as **Pawel Rodziewicz** for their support in the laboratory, fruitful discussions and pleasant times outside of the laboratory. Furthermore, I want to thank our students **Tobias Graef**, **Daniel Stalinski**, **Nico Biermann**, **Florian Worm** and **Christian Staubach** for the fun times we shared.

Finally, a special thanks goes to my **family** and **friends** for their support and encouragement as well as offering welcome distractions where necessary.

TABLE OF CONTENTS

I. ABSTRACT

Cannabinoids are secondary natural products predominantly found in the oil compartments of trichomes of the plant *Cannabis sativa* L. Up to now more than 100 cannabinoids have been isolated, the most prominent being the psychoactive Δ^9-tetrahydrocannabinol (THC) and cannabidiol (CBD). As THC-derived products are already available for medical use and CBD is currently investigated for its application in several disease treatments, the demand of cannabinoid-based products is expected to further rise in the future.

A biotechnological production presents a promising alternative to meet the demand, while also offering environmentally friendly, highly controllable and reproducible, GMP compliant processes as well as the reduction of agricultural area.

In this regard, the cannabinoid producing enzymes from *C. sativa*, Δ^9-tetrahydrocannabinolic acid synthase (THCAS) and cannabidiolic acid synthase (CBDAS), were recombinantly produced in the yeast *Komagataella phaffii*. The expression of *thcas* was enhanced in *K. phaffii* by optimization of cultivation conditions as well as identification and co-expression of helper protein genes.

Insights were gained into structure-function relationships of the THCAS and CBDAS. The influence on the enzyme activities of glycosylation sites, of amino acid residues in the berberine-bridge-domain as well as in the active site were investigated. Important amino acid residues for enzyme activity were identified yielding enzyme variants with improved catalytic and stability properties.

Additionally, a first approach to establish the late cannabinoid biosynthesis pathway in yeasts is presented. Production of the soluble prenyltransferase NphB from *Streptomyces* sp. strain CL190, which enables the replacement of the native transmembrane prenyltransferase cannabigerolic acid synthase from *C. sativa*, was simultaneously produced with THCAS, thereby enabling a production of Δ^9-tetrahydrocannabinolic acid from precursors olivetolic acid and geranyl diphosphate.

The studies presented here contribute to increased fundamental and industrially relevant knowledge and will help promoting a biotechnological cannabinoid production in yeasts.

II. ZUSAMMENFASSUNG

Cannabinoide sind sekundäre Naturstoffe, die vorrangig in den Öl-Kompartimenten von Trichomen der Pflanze *Cannabis sativa* L. vorkommen. Bis heute wurden mehr als 100 Cannabinoide isoliert, wobei die bekanntesten von ihnen die psychoaktiven Stoffe Δ9-Tetrahydrocannabinol (THC) und Cannabidiol (CBD) sind. THC-haltige Produkte finden bereits medizinische Anwendung und CBD wird momentan für mögliche Anwendungen in der Behandlung von diversen Krankheiten untersucht, weswegen in der Zukunft mit einem Anstieg der Nachfrage von cannabinoidhaltigen Produkten gerechnet wird.

Eine biotechnologische Produktion stellt eine vielversprechende Alternative dar, um diesen Bedarf zu decken. Zusätzlich bietet sie eine Aussicht auf ökologische, kontrollierbare und reproduzierbare, GMP-konforme Prozesse, ohne den Bedarf an landwirtschaftlicher Nutzfläche zu steigern.

Die Cannabinoid-produzierenden Enzyme aus *C. sativa*, Δ9-Tetrahydrocannabinolsäure Synthase (THCAS) and Cannabidiolsäure Synthase (CBDAS), wurden recombinant in der Hefe *Komagataella phaffii* produziert. Die *thcas* Expression wurde in *K. phaffii* erhöht, indem Kultivierungsbedingungen optimiert und Helferproteine identifiziert und co-produziert wurden.

Neue Erkenntnisse bezüglich der Struktur-Funktion-Beziehungen der THCAS und CBDAS wurden gewonnen. Die Einflüsse der Glykosylierungsstellen, von Aminosäurereste in der Berberine-Bridge-Enzyme Domäne, sowie von Aminosäureresten in der aktiven Tasche auf die Enzymaktivitäten wurden untersucht. Dabei wurden wichtige Aminosäurereste für die Enzymaktivität identifiert und Enzymvarianten mit verbesserten katalytischen und Stabilitätseigenschaften erstellt.

Weiterhin wurde ein erster Versuch unternommen, die letzten beiden Schritte der Cannabinoid Biosynthese in Hefen zu integrieren. Die simultane Produktion der löslichen Prenyltransferase NphB aus *Streptomyces* sp. Stamm CL190, welche die native transmembrane Prenyltransferase Cannabigerolsäure Synthase aus *C. sativa* ersetzt, mit der THCAS wurde etabliert. Dadurch wurde die Produktion von THC aus den Vorstufen Olivetolsäure und Geranyldiphosphat ermöglicht.

Die hier präsentierten Studien tragen zu einem grundlegenden und speziell industriell relevanten Verständnis bei, um eine Entwicklung zur biotechnologischen Produktion von Cannabinoiden in Hefen voranzutreiben.

CHAPTER 1

SCOPE OF THE THESIS

1.1. AIMS AND OBJECTIVES

The aim of this project was to establish a biotechnological approach for the production of cannabinoids from *Cannabis sativa* L. In this regard, this study investigates the production and its optimization of cannabinoid producing enzymes from *C. sativa*, namely Δ^9-tetrahydrocannabinolic acid synthase and cannabidiolic acid synthase, in different heterologous hosts, as well as an elucidation of structure-function relationships of these enzymes. Furthermore, this project should provide a basis for the cannabinoid production in a heterologous host and accordingly a first approach to establish the late cannabinoid pathway in yeasts is presented. The goals of this cumulative thesis are addressed as individual chapters describing the following points:

A. **Chapter 2** provides an introduction to the thesis and its relevant literature. It highlights on the one hand the pharmaceutical interest in different cannabinoids from *C. sativa*, their synthesis and state of the art production. On the other hand, possible hosts for the recombinant production of cannabinoid producing enzymes are compared and available strains, regulatory elements and genetic tools of *Komagataella phaffii* are described in detail.

B. **Chapter 3** gives insights into the possibilities of a recombinant host for the production of cannabinoids. In this regard, the Δ^9-tetrahydrocannabinolic acid synthase is recombinantly produced in the hosts *Escherichia coli*, *Saccharomyces cerevisiae* and *K. phaffii*. The cultivation conditions for recombinant production in *K. phaffii* are investigated, optimized and a whole cell bioconversion of cannabigerolic acid to Δ^9-tetrahydrocannabinolic acid is performed.

C. **Chapter 4** provides insights into possible bottlenecks during the folding and production of Δ^9-tetrahydrocannabinolic acid synthase in *K. phaffii*. Effects of the co-production of several helper proteins from *K. phaffii* on the production of Δ^9-tetrahydrocannabinolic acid synthase are investigated by employing a low-throughput screening system. Helper proteins with a positive effect on the production of Δ^9-tetrahydrocannabinolic acid synthase are identified and an optimized strain developed.

D. **Chapter 5** elucidates structure-function relationships of the cannabinoid producing enzymes Δ^9-tetrahydrocannabinolic acid synthase and cannabidiolic acid synthase by employing site-directed mutagenesis and a low-throughput screening system. Optimized enzyme variants of the Δ^9-tetrahydrocannabinolic acid synthase and the cannabidiolic acid synthase are identified. A whole cell bioconversion of cannabigerolic acid to cannabidiolic acid is performed.

E. **Chapter 6** provides a first approach to establish the final steps of the cannabinoid biosynthesis in a recombinant host by co-production of the Δ^9-tetrahydrocannabinolic acid synthase from *C. sativa* and NphB from *Streptomyces* sp. strain CL190. Co-production of both enzymes yielded Δ^9-tetrahydrocannabinolic acid formation from geranyl diphosphate and olivetolic acid.

F. **Chapter 7** discusses the presented results in a combined manner and evaluates the potential and future possibilities regarding the biotechnological approach for the production of cannabinoids.

CHAPTER 2

INTRODUCTION

2.1. *CANNABIS SATIVA* L.

Cannabis sativa L. is a predominantly dioeciously flowering (i.e. male and female flowers are found on separate plants), annual herb. Humans have deliberately grown the plant for at least 6000 years (Fleming and Clarke, 1998) and utilized it for its fiber, oil production and recreational purposes. It contains a number of medicinally interesting compounds, such as cannabinoids (chapter 2.2.1 and 2.2.2), terpenoids (Ross and ElSohly, 1996), flavonoids (Vanhoenacker et al., 2002) or alkaloids (Turner et al., 1976).

The genus *Cannabis* belongs to the family of *Cannabaceae*. There has been controversy in the number of species in the genus *Cannabis* and therefore in nomenclature as well. Several propositions can be found in literature for the number of *Cannabis* species, mainly reflecting geographical, phenotypic or chemical composition differences of the plants. For example, there are polyspecific descriptions of *Cannabis* distinguishing *C. sativa*, *C. indica*, *C. ruderalis* and/or *C. afghanica*. However, due to its long history of domestication and breeding, discrimination is often problematic and most authors regard the genus as a highly polymorphic (highly variable), monotypic species of *Cannabis sativa* L. (Chandra et al., 2017). To prevent misinterpretations, in this thesis the polymorphic, monotypic description is used and in the subsequent text *Cannabis*, *Cannabis sativa* and *Cannabis sativa* L. are used synonymously.

In the last decades, *Cannabis* has gained increasing popularity not only for being an illicit drug (Bridgeman and Abazia, 2017), but also for its medicinal potential - mainly owed to its primary pharmacologically active compounds Δ^9-tetrahydrocannabinol (THC or Δ^9-THC) and cannabidiol (CBD) (Pertwee, 2006; Pisanti et al., 2017) (see chapter 2.2.2 for further information). Generally, *Cannabis* is classified into drug-type and fiber-type (hemp) depending on the THC content in the dried flowering portion of the plant. In Europe, *Cannabis* plants are considered as drug-type if their THC content exceeds 0.2 % (Mead, 2017). Drug-type *Cannabis* is the most commonly used, illicit drug worldwide with approximately 147 million consumer individuals per year (~ 2.5 % of global population) (Bridgeman and Abazia, 2017).

2.2. CANNABINOIDS

Historically, 'cannabinoids' are defined as the terpenophenolic constituents of *C. sativa* L. (Gertsch et al., 2010). However, since the discovery of the first plant-isolated cannabinoids from *C. sativa* – cannabidiol (CBD) (Mechoulam and Shvo, 1963), THC (Gaoni and Mechoulam, 1964a), cannabigerol (CBG) (Gaoni and Mechoulam, 1964b), cannabidivarin (CBDV) (Vollner et al., 1969) and Δ^9-tetrahydrocannabidivarin (THCV) (MERKUS, 1971) - the terminology expanded over the years. On the one hand, the discovery of the endocannabinoid receptor CB_1 (Devane et al., 1988) started the exploration of the endocannabinoid system (ECS). These ligands are called endocannabinoids and were first described with anandamide (Devane et al., 1992) and 2-arachidonylglycerol (Mechoulam et al., 1995). On the other hand, many synthetic cannabinoids have been produced in the recent years – some of them were developed seeking interaction with other signalling systems, but found to interact with the ECS (Shevyrin et al., 2016; Soderstrom et al., 2017). Additionally, several non-cannabinoid natural plant compounds have been reported to act as cannabinoid receptor ligands. Hence, three definitions for cannabinoid-type compounds are necessary.

Phytocannabinoids are ‘any plant-derived natural product capable of either directly interacting with cannabinoid receptors or sharing chemical similarity with cannabinoids or both’ (Gertsch et al., 2010).

A total of 565 chemical compounds have been isolated from *C. sativa* so far, out of which 120 are phytocannabinoids (ElSohly et al., 2016; Turner et al., 2017). These lipophilic products generally have a typical bicyclic or tricyclic structure and the majority of them are derived from the most abundant acidic phytocannabinoids - namely Δ^9-tetrahydrocannabinolic acid-A (THCA), cannabigerolic acid (CBGA), cannabinolic acid (CBNA), cannabichromenic acid (CBCA) and cannabidiolic acid (CBDA) - by non-enzymatic transformations and degradation reactions upon heat and light exposure as well as auto-oxidation (Crombie et al., 1968; Degenhardt et al., 2017). The main phytocannabinoids are C5-phytocannabinoids due to their n-pentyl side chain. C4-phytocannabinoids and C3-phytocannabinoids with shorter side chains have also been isolated from plant material (Chandra et al., 2017). It should be noted that there are also phytocannabinoids described, such as beta-caryophyllene, which have no structural similarity to THC but are cannabinoid receptor effectors. Table 2-1 shows the most important phytocannabinoids as well as some examples of the other classes. A full display of the 120 phytocannabinoids has been reported elsewhere (Chandra et al., 2017).

Endocannabinoids are ‘naturally occurring chemical compounds produced by living organisms that are associated with the cannabinoid receptors (CB_1 and CB_2) or more generally considered part of the endocannabinoid system’ (Shevyrin et al., 2016).

The ECS is a ubiquitous lipid signaling system in vertebrates with homeostatic and physiological functions that include pain modulation and inflammation. It comprises both the classical endocannabinoid receptors CB_1 and CB_2, potentially also the G-protein-coupled receptor GPR55, the endogenous ligands as well as the enzymes involved in synthesis, uptake and degradation of the endocannabinoids. The most important enzymes involved are the fatty acid amide hydrolase (FAAH) and the monoacylglycerol lipase (MAGL) which are responsible for the degradation of the endocannabinoids (Gertsch et al., 2010).

Synthetic cannabinoids are ‘non-naturally occurring chemical compounds that either affect the endocannabinoid system or that are structural analogues of an endocannabinoid, phytocannabinoid, or other synthetic cannabinoids’ (Shevyrin et al., 2016).

There are different classes of synthetic cannabinoids, *inter alia* the classical synthetic cannabinoids which are derivatives of the dibenzopyran THC (see nabilone or HU-210 in Table 2-1), but also structurally unrelated compounds such as WIN55,212-2. A deeper insight into classification and potential use of synthetic cannabinoids is given by Shevyrin et al. (2016) and Pertwee (2010).

Table 2-1: Overview of different cannabinoids, the common abbreviation and their chemical structure. Adapted from Chandra et al. (2017).

Name	**Common abbreviation**	**Structure and residues**
Phytocannabinoids		
Δ^9-THC type		
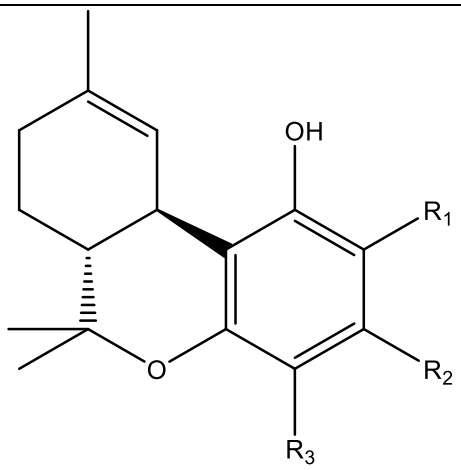		
(-)-Δ^9-*trans*-tetrahydrocannabinolic acid A	THCA or THCA-A	R_1=COOH R_2=C_5H_{11} R_3=H
(-)-Δ^9-*trans*-tetrahydrocannabinolic acid B	THCA-B	R_1=H R_2=C_5H_{11} R_3=COOH
(-)-Δ^9-*trans*-tetrahydrocannabinol	THC or Δ^9-THC	R_1=H R_2=C_5H_{11} R_3=H
(-)-Δ^9-*trans*-tetrahydrocannabivarinic acid	THCVA	R_1=COOH R_2=C_3H_7 R_3=H
(-)-Δ^9-*trans*-tetrahydrocannabivarin	THCV	R_1=H R_2=C_3H_7 R_3=H

Table 2-1: Overview of different cannabinoids, the common abbreviation and their chemical structure - continued.

Δ^8-THC type		
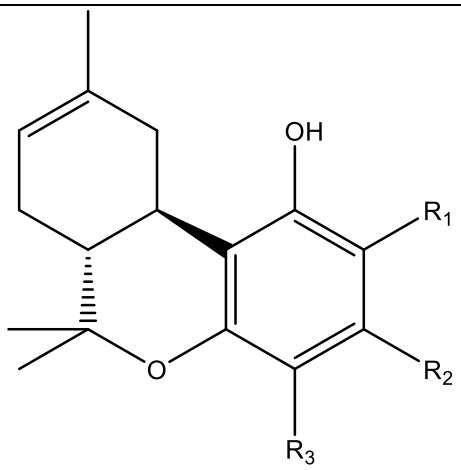		
(-)-Δ^8-*trans*-tetrahydrocannabinolic acid	Δ^8-THCA	R_1=COOH R_2=C_5H_{11} R_3=H
(-)-Δ^8-*trans*-tetrahydrocannabinolic acid	Δ^8-THC	R_1=H R_2=C_5H_{11} R_3=H
CBG type		
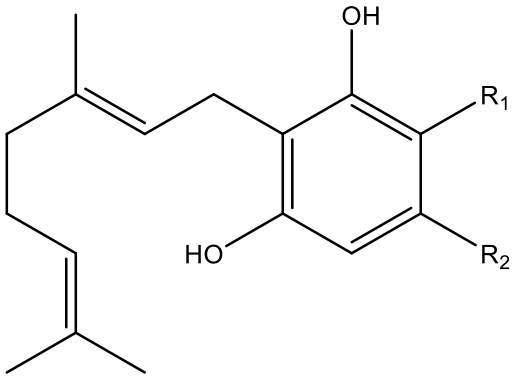		
Cannabigerolic acid	CBGA or (*E*)-CBGA	R_1=COOH R_2=C_5H_{11}
Cannabigerol	CBG or (*E*)-CBG	R_1=H R_2=C_5H_{11}
Cannabigerovarinic acid A	CBGVA or (*E*)-CBGVA	R_1=COOH R_2=C_3H_7
Cannabigerovarin	CBGV or (*E*)-CBGV	R_1=H R_2=C_3H_7

Table 2-1: Overview of different cannabinoids, the common abbreviation and their chemical structure - continued.

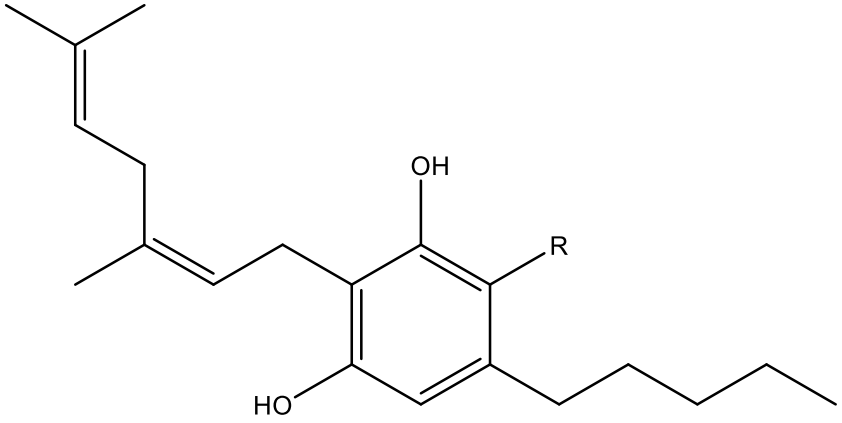		
Cannabinerolic acid A	(*Z*)-CBGA	R=COOH
Cannabinerol	(*Z*)-CBG	R=H
CBC type		
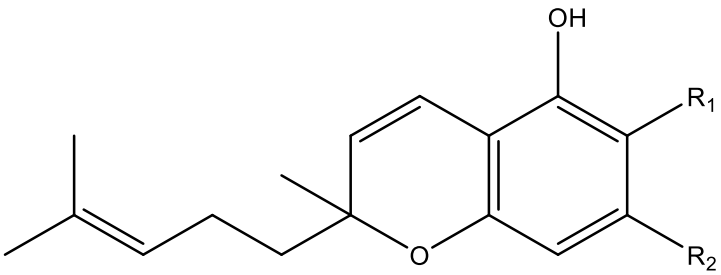		
(±)-Cannabichromenic acid	CBCA	R_1=COOH R_2=C_5H_{11}
(±)-Cannabichromene	CBC	R_1=H R_2=C_5H_{11}
(±)-Cannabivarichromenic acid	CBCVA	R_1=COOH R_2=C_3H_7
(±)-Cannabivarichromene	CBCV	R_1=H R_2=C_3H_7
CBD type		
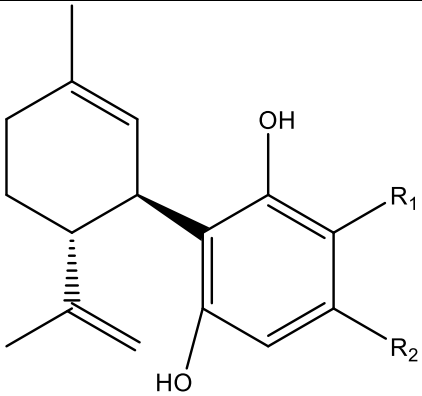		

Table 2-1: Overview of different cannabinoids, the common abbreviation and their chemical structure - continued.

Cannabidiolic acid	CBDA	R_1=COOH R_2=C_5H_{11}
Cannabidiol	CBD	R_1=H R_2=C_5H_{11}
Cannabidivarinic acid	CBDVA	R_1=COOH R_2=C_3H_7
Cannabidivarin	CBDV	R_1=H R_2=C_3H_7
Endocannabinoids		
Anandamide/ N-arachidonoylethanolamine	AEA	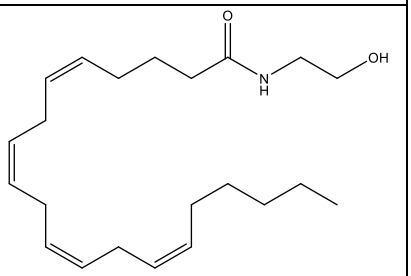
2-arachidonylglycerol	2-AG	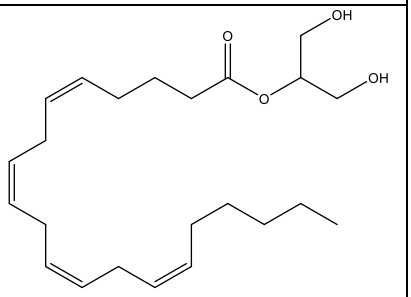
Synthetic cannabinoids		
Racemic mixture of (*R*,*R*)-(−)-nabilone and (*S*,*S*)-(+)-nabilone	Nabilone	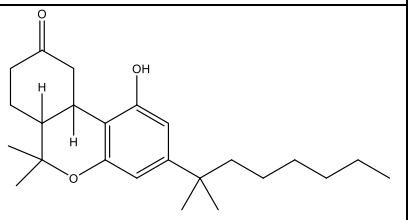
WIN55,212-2	WIN55,212-2	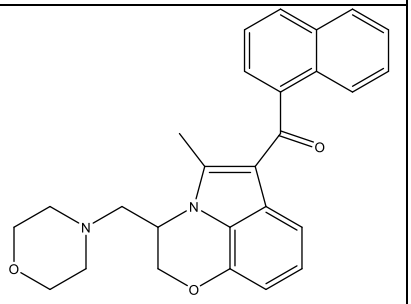
HU-210	HU-210	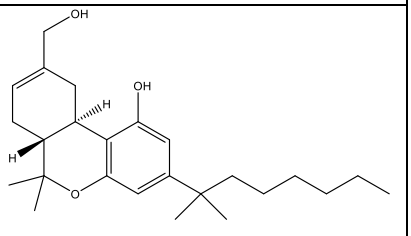

2.2.1. Cannabinoid biosynthesis in *Cannabis sativa* L.

In the recent years, the biosynthetic pathway for the production of cannabinoids in *C. sativa* has been elucidated. In this regard, phytocannabinoids include an alkylresorcinol (typically olivetolic acid (OA) or olivetol) and a monoterpene moiety (typically geranyl diphosphate (GPP) which is synthesized from its precursor isopentyl diphosphate (IPP)) (Fig. 2-1) and are hence produced from fatty acids and isoprenoid precursors as part of the secondary metabolism of *Cannabis* (Fig. S VI-1 and Fig. S VI-2).

In planta, the isoprenoid precursors are either provided through the mevalonate (MVA) pathway which proceeds in the cytosol or the 2-C-methyl-D-erythritol 4-phosphate or 1-deoxy-D-xylulose 5-phosphate pathway (MEP/DOXP pathway) which occurs in the plastids. Thus, the MVA pathway is mainly involved in the plant primary metabolism and the MEP pathway contributes to a greater extend to the plant secondary metabolism (Fig. S VI-1) (Eisenreich et al., 2004).

The biosynthesis of olivetolic acid in *C. sativa* has been recently elucidated as well (Fig. S VI-2). Starting from the activation of hexanoic acid by an acyl activating enzyme (Stout et al., 2012), three malonyl-CoA moieties and hexanoyl-CoA are converted by the olivetol synthase (OLS) to olivetol, which is subsequently cyclized to olivetolic acid by the olivetolic acid cyclase (OAC) (Gagne et al., 2012).

The central metabolite in the cannabinoid biosynthesis, CBGA, is produced from GPP and OA by the cannabigerolic acid synthase (CBGAS) (also called geranyl diphosphate:olivetolate geranyltransferase (GOT)) (Degenhardt et al., 2017). The CBGAS is supposedly an integral membrane protein, however up to date only inconclusive scientific knowledge about the CBGAS is available. While there is evidence of the CBGAS being an integral membrane protein (Ohara et al., 2009; Yamamoto et al., 1997), Fellermeier and Zenk detected CBGAS activity only in the soluble fraction of the plant crude extract, but not in the isolated, particulate fractions (Fellermeier and Zenk, 1998). Furthermore, a patent is available stating CBGAS as an integral membrane protein (Page and Boubakir, 2014). The CBGAS accepts other substrates as well. For example, prenylation of OA with neryl diphosphate instead of GPP yields (*Z*)-CBGA. While prenylation of OA leads to the synthesis of C5-phytocannabinoids, e.g. prenylation of divarinic acid yields cannabidivarinic acid (CBDVA) and subsequently the C3-phytocannabinoids THCVA, CBDVA or CBCVA.

Presumably, one of three different enzymes performs the final catalytic step of the cannabinoid synthesis. The tetrahydrocannabinolic acid synthase (THCAS), cannabidiolic acid synthase (CBDAS) or cannabichromenic acid synthase (CBCAS) perform different oxidative cyclizations of the prenyl moiety of CBGA yielding THCA, CBDA or CBCA. These main cannabinoids are synthesized in an acidic form and only exert their major pharmacological features after decarboxylation to the neutral forms (THC, CBD and CBC) (see chapter 2.2.2). Most of the other phytocannabinoids, which can be isolated from the plant, are degradation or isomerization products of these main cannabinoids (Crombie et al., 1968; Degenhardt et al., 2017).

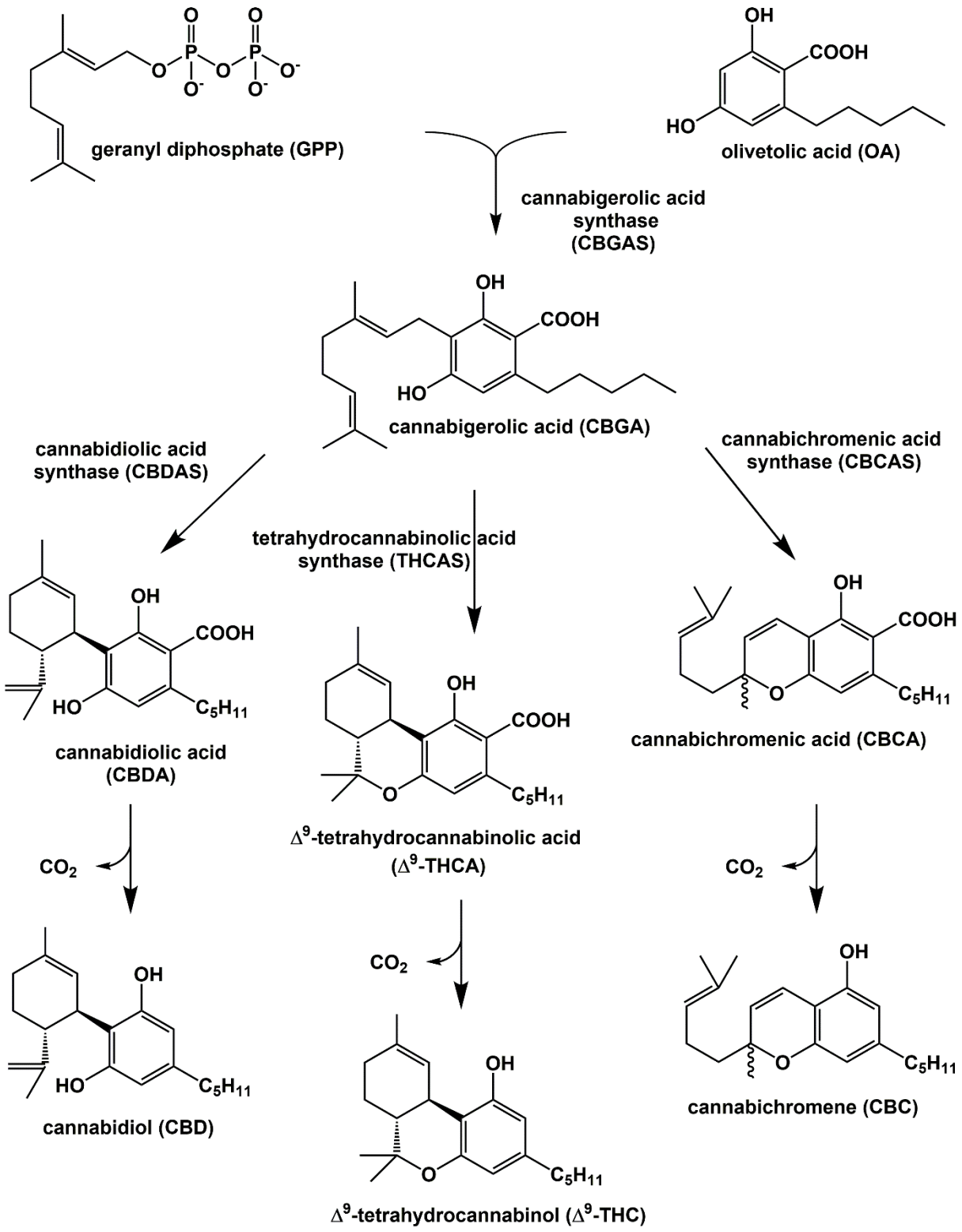

Fig. 2-1: Final biosynthetic steps of cannabinoid production in *Cannabis sativa* L. Adapted from Degenhardt et al. (2017). The central precursor in cannabinoid production, cannabigerolic acid (CBGA), is converted by three enzymes – the cannabidiolic acid synthase (CBDAS), tetrahydrocannabinolic acid synthase (THCAS) or the cannabichromenic acid synthase (CBCAS) – to one of the major acidic cannabinoids cannabidiolic acid (CBDA), Δ^9-tetrahydrocannabinolic acid (THCA) or cannabichromenic acid (CBCA). The neutral cannabinoids are obtained upon heat-induced decarboxylation.

The THCAS and CBDAS are soluble oxidoreductases that belong to the berberine-bridge-enzyme (BBE)-like enzyme family (Pfam 08031). These enzymes form a subgroup of the superfamily of flavine adenine dinucleotide (FAD)-linked oxidases (SCOPe d58.32). The name assignment of the BBE-like enzyme family stems from the

(*S*)-reticuline oxidase or berberine bridge enzyme from *Eschscholzia californica* which catalyzes the oxidative ring closure from (*S*)-reticuline to (*S*)-scoulerine (Daniel et al., 2017). The THCAS contains several glycosylation sites, one disulfide bridge and a bi-covalently bound FAD cofactor. The enzyme has been purified to homogeneity from *Spodoptera frugiperda* Sf9 insect cells enabling the generation of a structural protein model (PDB:3vte) (Shoyama et al., 2012, 2005; Sirikantaramas et al., 2004). Coding sequences of the THCAS and CBDAS have been published (Sirikantaramas et al., 2004; Taura et al., 2007b). The CBCAS protein has been identified, partially purified and characterized some time ago (Morimoto et al., 1998), however until now - besides a filed patent containing a coding sequence - no further scientific research regarding the CBCAS has been published (Page and Stout, 2015). Catalytic parameters of the THCAS have been determined (k_{cat} = 0.888 s^{-1}, K_M = 1.31 * 10^{-4} M^{-1}, k_{cat}/K_M = 0.7 *10^4) (Taura et al., 2007a). Correlating these parameters with a database analysis from 2011, the catalytic efficiency of this enzyme is low even for a member of the secondary metabolism (k_{cat} = 2.5 s^{-1}, k_{cat}/K_M = 7.1 * 10^4) (Bar-Even et al., 2011). The THCAS and CBDAS share a high sequence similarity of 83 % and THCAS and the CBCAS sequence of the filed patent even share a similarity of 92 %. These differences determine the catalytic parameters of the enzymes as well as their product specificity. Detailed information on the THCAS and CBDAS are further presented in chapters 3-6 and chapter 6, respectively.

2.2.2. Interest in *Cannabis* and (phyto-) cannabinoids

Cannabis is mostly known for its psychoactive effect caused by THC. However, it is also used in the treatment of several medical conditions, such as immune deficiency syndrome-related appetite loss, chemotherapy-associated nausea and vomiting or relief of multiple sclerosis-associated symptomatic pain. Other potential applications are under investigation (Carlini, 2004; Chandra et al., 2017; Pertwee, 2006). Currently, several pharmaceutical formulations which are orally administered are on the market globally: Dronabinol (synthetic Δ^9-THC), nabilone (racemic mixture of Δ^9-THC-derivate) and nabiximols (plant extract of *C. sativa* containing Δ^9-THC). Besides these THC formulations, dried flower tips of *Cannabis* (Bedrocan®) are also authorized as *Cannabis*-based medicine for inhalation in several European countries. Other cannabinoids have not yet found their way onto the market, but are investigated for several therapeutical effects and features. THCA is currently examined for its immunomodulatory, anti-inflammatory, neuroprotective and anti-neoplastic effects (Moreno-Sanz, 2016). CBC is investigated for its anti-inflammatory, anti-fungal, antibiotic and analgesic effects (Elsohly et al., 1982; Maione et al., 2011; Romano et al., 2013). CBD is investigated for its application in treatment of Alzheimer's disease, Parkinson's disease and epilepsy, as well as for its anti-tumor properties and neuroprotective efficacy (Pisanti et al., 2017). Furthermore, CBD and other cannabinoids and terpenoids act in synergy with THC leading to pharmacological potentiation or decrease of adverse effects (Johnson et al., 2010; Russo, 2011; Whittle et al., 2001).

Besides the growing medicinal interest in the last years, the public interest in *Cannabis* both as medicine and as a recreational drug has increased as well. The public opinion regarding botanical *Cannabis* use, i.e. the dried *Cannabis* flowers, has changed significantly in the United States over the last decades. Support for legal *Cannabis* use increased in the late 1960s and early 1970s but plateaued at about 25 % of the population. In the last years however, an increase to nowadays 58 % support of *Cannabis* legalization has been noted (Mead, 2017). This is reflected in an increased *Cannabis* consumption as well, especially by younger people (Burns et al., 2013). The public opinion has also been driving policy changes up to date. In 1996, the first state law was enacted in the

United States allowing the medical use of *Cannabis*. Today, more than 50 % of the states in the United States have issued such laws (Mead, 2017; The National Academies of Science Engineering Medicine, 2017). Similar observations can be made for the European Union where several *Cannabis*-related laws have changed in the recent years, e.g. in Germany *Cannabis* can be prescribed for medicinal use since March 2017 (Müller-Vahl and Grotenhermen, 2017). Next to Germany and the United States, the Netherlands, Israel, Spain, Portugal, Czech Republic, Finland and Greece, Denmark and Italy have already legalized botanical *Cannabis* for medical purposes. (Abuhasira et al., 2018; Hughes, 2017). It should be noted that up to now no European state parliament has expressed support of legislation for the recreational use, although an increasing number of citizen petitions ask national governments to legalize *Cannabis* production or the use for recreational purposes (Hughes, 2017).

Contrary to these policy changes, botanical *Cannabis* is not approved by the United States Food and Drug Administration (FDA) or the European Medicines Agency (EMA) for safety and efficacy. *Cannabis* and THC as well as CBD are defined as Schedule I substances in the United States according to the federal Controlled Substances Act, thus medical use in the United States is currently not accepted, they have high risk of abuse and lack accepted safety for use of the drug under medical supervision (Mead, 2017). In Europe, *Cannabis* and THC are classified according to the United Nations Single Convention on Narcotic Drugs and the Convention on Psychotropic Substances in a similar way. Additionally, many CBD-based products are available over the internet despite its potential therapeutic effects and hence lack consistent quality and quality control.

Considering the importance for the public health, it should be highly desirable to gain FDA or EMA approval. A medical, botanical *Cannabis* product needs to be 'consistent, standardized and display a quality equal to any New Chemical Entity that has passed muster as a pharmaceutical' (Russo, 2016). *Inter alia*, analyses of pharmacokinetic and pharmacodynamic properties, as well as toxicity studies are necessary. All these investigations, however, can only be conducted with controlled plant material of continuous quality.

Street market *Cannabis* and home-grown *Cannabis* cannot meet these desired criteria and thus not gain regulatory approval. Besides the biochemical variability, pesticide residues, molds, bacteria and heavy metals endanger public health (Russo, 2016). But even if the agricultural production is highly regulated and standardized, e.g. by a certified company such as Bedrocan International B.V., it faces several challenges such as a future increasing demand of agricultural area that could be used otherwise, the plant susceptibility to climate and diseases as well as a difficult standardization of cultivation conditions and supply chain management (Carvalho et al., 2017; Russo, 2016). Furthermore, the common delivery system of smoking itself inherits risks like chronic cough, phlegm production, bronchitis and inhalation of pyrolytic by-products (Tashkin, 2013). Additionally, irrelevant of whether vaporizers are used or *Cannabis* is administered via smoking, a pulmonary administration seems not desirable as the risk of rapid intoxication is opposing the aims of most therapeutic applications, especially in treatments of chronic conditions (Russo, 2016).

Other approaches for the production of cannabinoids are chemical synthesis or a biotechnological concept. Chemical synthesis currently fails to be a cost-effective, environmentally-friendly alternative, mainly due to a complex, multi-step synthesis leading to low yields and high production costs (Carvalho et al., 2017). Compared to a cannabinoid production in plants, the production using a heterologous host system harbors several potential advantages, such as a good process scalability enabling higher space-time yields, highly controllable and standardized processes including Good Manufacturing Practices and supply management as well as a decreased

risk of an illicit use or production. Furthermore, the enzymes THCAS, CBDAS and CBCAS use the same substrate for conversion. The establishment of a chassis strain able to produce CBGA would therefore allow for a tailored production of different cannabinoids or cannabinoid compositions depending on which genes of these cannabinoid producing enzymes are expressed in the chassis strain.

2.3. HETEROLOGOUS HOSTS FOR CANNABINOID BIOSYNTHESIS

When deciding on a heterologous host, it is necessary to define the intended purpose. Some yeasts and prokaryotic hosts are popular for the recombinant production of enzymes especially when the proteins are needed in high amounts for subsequent purifications and characterizations. When proteins are produced as an active pharmaceutical ingredient, often mammalian cells are used as a recombinant host. However, implementation of complete foreign, biosynthetic pathways and tailoring the host for high titer production of cannabinoids by metabolic engineering requires the consideration of additional aspects for host selection.

In general, availability of host genetic information, of tools for the expression of heterologous genes (targeting sequences, promoters, terminators, vectors, strains, selection markers etc.), the protein production capacity and ability to perform post-translational modifications as well as the availability of classical and modern molecular biological tools for targeted genetic engineering has to be evaluated. Additionally, successful application of systems metabolic engineering requires the existence of -omics data and computational systems biology tools for the respective host (Keasling, 2010). So far, systems metabolic engineering has only been established in the prokaryotic organisms *Escherichia coli* and *Bacillus subtilis* as well as the eukaryotic model-yeast *Saccharomyces cerevisiae* (Kelwick et al., 2014). Promising features can be found in several organisms, although often requirements are only partly fulfilled.

Higher eukaryotic cells, like mammalian or insect cells, might prove suitable for production of a single protein used as a pharmaceutical ingredient, but are unsuitable for a metabolic engineering project due to their complexity, expensive media and slow growth rates, as well as a reduced means of genetic tools available compared to yeast and prokaryotic cells. On the contrary, *E. coli* as a representative prokaryotic organism, offer easy genetic modifications, the fastest growth known, availability of defined cultivation media, high protein production rates and extensive scientific knowledge for metabolic engineering projects (Carvalho et al., 2017; Schwarzhans et al., 2017a; Vogl et al., 2013).

As described before, IPP is a precursor for the production of GPP and subsequently cannabinoids. In yeasts the MVA pathway is the only IPP synthesis pathway and exhibits high efficiencies. This results in IPP making up to 5 % of the cell's dry weight (Lamacka and Sajbidor, 1997) rendering yeasts a promising heterologous host for production of IPP-based compounds. Furthermore, yeast cells offer the capability of post-translational modifications. The most prominent yeast candidates are *S. cerevisiae* and *Komagataella phaffii* (formerly known as *Pichia pastoris* and recently reclassified to *Komagataella phaffii* (Kurtzman, 2009), thus *Pichia pastoris* and *Komagataella phaffii* will be used synonymously in this thesis). While there are also other promising yeast, such as the oleaginous yeast *Yarrowia lipolytica, Hansenula polymorpha, Candida boidinii or Kluyveromyces marxianus*, they mostly lack regarding their genetic toolbox and availability of strains and promoters (Carvalho et al., 2017).

In Table 2-2 a brief overview is given on the heterologous production hosts *S. cerevisiae*, *E. coli* and *K. phaffii*, regarding their potential to produce cannabinoids by evaluating their ability to produce foreign proteins, the availability of molecular techniques and ease of genetic modifications, as well as the available research and successful projects of metabolic engineering.

Table 2-2: Potential of heterologous hosts for cannabinoid production. Table adapted from literature (Carvalho et al., 2017; Vogl et al., 2013).

	Saccharomyces cerevisiae	*Komagataella phaffii*	*Escherichia coli*
Ease of genetic modifications	Simple	Simple	Simple
Cultivation	Fast and robust growth, high cell densities	Fast and robust growth, very high cell densities	Fastest growth
Genetic toolbox	Very good	Good (only recently improved)	Very good
Strains, promoters, vectors	Very good	Good (only recently improved)	Very good
(Plant) protein yields and secretory pathway capacity	Good	Very good	Possible
Post-translational modifications	Possible, hyperglycosylation	Possible, hyperglycosylation less pronounced than in *S. cerevisiae*	Not possible
Compartmentalization of biosynthetic pathways	Possible	Possible	Not possible
Available literature (omics data, metabolic engineering)	Very good	Available	Very good

All three depicted organisms have promising features, however, for the metabolic engineering project yeast cells offer the capability to functionally express more complex enzymes including post-translational modifications, the possibility to compartmentalize intracellular biosynthetic pathways and stable genomic integrations (Schwarzhans et al., 2017a). Comparing both yeast strains with each other, *S. cerevisiae* is considered a model organism for yeasts and therefore - with its large scientific community - profits from an extensive genetic toolbox as well as available scientific -omics data and metabolic engineering data. However, besides the recent advancements regarding genetic tools for *K. phaffii* (discussed in chapter 2.4.1 and 2.4.2), the suitability of this organism for the expression of various proteins from humans, animals, plants, algae, fungi and bacteria is beyond doubt. Membrane protein expression is potentially more successful than in *S. cerevisiae* (Bill, 2014; Öberg et al., 2011). The hyperglycosylation in yeasts is less pronounced in *K. phaffii* as well, making the expression of glycoproteins in *K.*

phaffii more likely to succeed (Hamilton and Gerngross, 2007). Additionally, *K. phaffii* is compared to *S. cerevisiae* Crabtree-negative allowing for better substrate utilization in batch cultivations.

As this work mostly focuses on *K. phaffii*, a deeper insight into the organism, available strains and promoters as well as the genetic toolbox is given in the next chapters.

2.4. KOMAGATAELLA PHAFFII

Komagataella phaffii is a methylotrophic, non-conventional budding yeast and can grow on methanol as sole carbon source. It is predominantly known for its extraordinary protein production and secretion capacities that made it an interesting platform not only for academia but also for industry. *K. phaffii* was first used for production of technical enzymes. However, the granting of the GRAS (generally regarded as safe) status by the United States Food and Drug Administration (Ciofalo et al., 2006) paved the way for the use of *K. phaffii* in biopharmaceutical productions as well, such as the aglycosylated protease Jetrea® or the kallikrein inhibitor Kalbitor® (Corchero et al., 2013; Meehl and Stadheim, 2014). Furthermore, the organism has shown its suitability for the functional expression of proteins that proved difficult to express in other hosts, e.g. integral membrane proteins and glycoproteins (Byrne, 2015; Laukens et al., 2015; Vogl et al., 2014). The assembled genomes of the commonly used *K. phaffii* strains GS115 and CBS7435 were first published between 2009 and 2011 and later refined (De Schutter et al., 2009; Küberl et al., 2011; Mattanovich et al., 2009; Sturmberger et al., 2016). Convenient access to genome sequences and current annotations is provided by an online database (www.pichiagenome.org). So far, over five thousand different proteins have been produced in *K. phaffii* (www.pichia.com). The increasing popularity of this organism comes from its ease of genetic manipulation, the utilization of tightly regulated, strong promoters leading to production of high amounts of protein in robust high-cell density cultivations, as well as good post-translational modification and secretion capabilities (Ahmad et al., 2014; Macauley-Patrick et al., 2005).

2.4.1. *K. phaffii* - strains and regulatory elements

The availability of genome sequences and annotations constitutes a milestone not only towards rational strain engineering, but also for identification of e.g. autonomously replicating sequences (ARS), new promoters and terminators. Nowadays, an extensive repertoire of strains and vectors are available promoting the use of *K. phaffii* as a production platform.

Strains

Available *K. phaffii* strains can be generally classified into wild-type strains, auxotrophic strains, protease-deficient strains as well as glyco-engineered strains. An overview of the most important strains is given in Table 2-3, a more detailed overview of available strains is described elsewhere (Ahmad et al., 2014; Schwarzhans et al., 2017a).

Table 2-3: Overview of the most important *Komagataella phaffii* strains. Table adapted from Ahmad et al. (2014).

Strain	**Phenotype**	**References**
Wild-type strains		
X-33	WT	ThermoFisher Scientific
CBS704	WT	Centraalbureau voor Schimmelcultures, the Netherlands
CBS7435	WT	Centraalbureau voor Schimmelcultures, the Netherlands
Auxotrophic strains		
GS115	His^-	ThermoFisher Scientific
PichiaPink™ strain 1	Ade^-	ThermoFisher Scientific
KM71	His^-, Mut^S (slow methanol utilizer)	ThermoFisher Scientific
KM71H	Mut^S (slow methanol utilizer)	ThermoFisher Scientific
CBS7435 *his4*	His^-	(Näätsaari et al., 2012), Pichia Pool
CBS7435 Mut^S *his4*	His^-, Mut^S (slow methanol utilizer)	(Näätsaari et al., 2012), Pichia Pool
Protease-deficient strains		
SMD1168	His^-, Protease PEP4 knockout	ThermoFisher Scientific
SMD1168H	Protease PEP4 knockout	ThermoFisher Scientific
PichiaPink™ strain 2-4	Ade^-, various protease knockouts	ThermoFisher Scientific
CBS7435 *his4 pep4 prb1*	His^-, Protease PRB1 and PEP4 knockouts	(Ahmad et al., 2014), Pichia Pool
Other strains		
CBS7435 *ku70*	WT, reduced NHEJ mechanism	(Näätsaari et al., 2012), Pichia Pool
CBS7435 *ku70 ade1*	Ade^-, $Zeocin^R$, reduced NHEJ mechanism	(Näätsaari et al., 2012), Pichia Pool
Glycoengineered strains		
$SuperMan_5$	His^-, α1,2-mannosidase production	BioGrammatics

A lot of these strains are commercially available, most of them are distributed by ThermoFischer Scientific. Among them are the wild-type strain X-33, the auxotrophic strains GS115 or KM71/KM71H, as well as protease-deficient strains like SMD1168H and PichiaPink™ strains 2-4. While these strains are commonly used in research, their commercial use is restricted by patent protection.

Several auxotrophies and combinations of these have been established in *K. phaffii*, e.g. adenine-, histidine-, lysine-, arginine-, uracil-, methionine-, proline- or tyrosine-auxotrophies. When no genetic deficiency of the strain is used for transformation selection, common antibiotics, such as Zeocin, Hygromycin, Geneticin, Blasticidin or Nourseothricin in combination with the respective resistance genes may be used for selection (Ahmad et al., 2014).

K. phaffii as a methylotrophic yeast is able to grow on methanol as sole carbon source. This ability is owed to enzymes involved in the methanol utilization pathway (MUT pathway), although mainly to two alcohol oxidases (AOX1 and AOX2) that convert methanol to formaldehyde in an initial step. During growth on methanol, both *aox1* and *aox2* are strongly upregulated, however, due to its stronger promoter P_{AOX1}, AOX1 constitutes to the majority of alcohol oxidases within the cell (Cregg et al., 1989). Additionally, the alcohol oxidase I promoter P_{AOX1} is one of the most used promoters for the recombinant protein production in this organism (see below for further information), thus methanol is often used as a carbon source and expression inducer simultaneously. In order to reduce methanol consumption and prolong induction, knockouts of *aox1* or *aox1* and *aox2* have been generated. These strains have either a reduced capacity to utilize methanol (slow methanol utilizer Mut^S - *aox1* knockout) or lost its capacity (no methanol utilizer Mut^- - *aox1, aox2* knockouts) (Hartner and Glieder, 2006). It was shown that Mut^S phenotypes can have a positive effect on protein production, especially when mixed carbon source feeds are used, e.g. methanol and sorbitol (Jungo et al., 2007; Ramón et al., 2007) .

The popularity of *K. phaffii* cultivations stems - among other things - from its ability to grow to high cell densities and efficiently secrete proteins into the culture supernatant. However, especially at high cell densities nutrient or oxygen shortage might occur, leading to cell lysis, release of proteases into the supernatant and ultimately proteolysis of target proteins. Additionally, proteolysis may occur during vesicular transport of the target protein by secretory pathway-resident proteases (Ni et al., 2008; Werten and de Wolf, 2005). The use of protease-deficient strains has therefore been an effective strategy to prevent recombinant protein degradation, especially for protease-sensitive proteins. Most commonly *pep4, prb1* or *prc1* knockouts or a combination of these are generated to sufficiently prevent proteolysis. PEP4 encodes the major vacuolar aspartyl protease proteinase A which in turn is able to activate itself as well as other proteases such as the carboxypeptidase Y (PRC1) and proteinase B (PRB1) (Gleeson et al., 1998).

Contrary to the commercially distributed strains, strains derived from *K. phaffii* CBS7435 are not covered by patent protection and thus present an alternative for production purposes especially in industry. A lot of auxotrophic strains, Mut^S and protease-deficient strains have been established recently and are available in the Pichia Pool at the TU Graz, a strain collection without patent restrictions aiming for industrial uses (Ahmad et al., 2014). The same working group also established KU70 deficient strains for improved targeting efficiencies of foreign DNA and less off-target integrations (see chapter 2.4.2. for detailed information on clonal variability) (Näätsaari et al., 2012).

Regulatory elements

While the recombinant production of proteins foremost requires a promoter with a high transcriptional rate as well as being tightly regulated for the possibility to decouple production and cell growth phases, the demands of an efficient production of pharmaceuticals in a heterologous host are considerably higher. To prevent pathway bottlenecks, misdirection of metabolites as well as overburden of the host cell, strategies are required allowing fine-tuning and switching on and off of expression of the different genes (Roquet and Lu, 2014). Therefore, a broad range of inducible and constitutive promoters with different transcriptional strengths, as well as terminator sequences are imperative for successful metabolic engineering projects in eukaryotes.

In *K. phaffii* soluble recombinant protein titers of more than 15 g L^{-1} have been obtained intracellularly or secreted to the culture supernatant (Hasslacher et al., 1997; Werten et al., 1999). Besides the ability to grow to high cell densities, these protein yields is additionally owed to the used alcohol oxidase I promoter P_{AOX1}.The methanol inducible P_{AOX1} has been the most used promoter for the heterologous protein production in *K. phaffii* due to its extraordinary transcriptional strength and tight regulation that also allows for decoupling of growth phase and production phase. When *K. phaffii* cells are grown on common carbon sources, such as glucose or glycerol, no AOX1 production can be observed due to transcriptional repression (Couderc and Baratti, 1980). While strong induction is achieved via methanol, several derepressing carbon sources are known as well, e.g. sorbitol or mannitol (Inan and Meagher, 2001). Under derepressed, induced conditions, the amount of alcohol oxidase 1 can reach levels up to 30 % of total protein in the cell (Vogl and Glieder, 2013). However, the use of a methanol induced P_{AOX1} system is also accompanied by concerns of toxicity and flammability of methanol as well as an increased oxygen consumption and heat generation, especially in industrial processes (Looser et al., 2015). Among the constitutive promoters, the glyceraldehyde-3-phosphate dehydrogenase promoter P_{GAP} is the most used for foreign gene expression with a comparable strength to the P_{AOX1} (Waterham et al., 1997). As decoupling of growth and production phase is not possible and constitutive promoters are less suitable for host toxic products. In this regard, new promoter variants of P_{AOX1} and P_{GAP} with varying transcriptional activity have been developed in the last years that increase the applicability for fine-tuned expression. Variants of the P_{GAP} showed 0.6 % to ~ 2000 % of wild-type P_{GAP} transcriptional activity (Qin et al., 2011) and variants of P_{AOX1} spanned a range of 6 to 160 % of wild-type P_{AOX1} transcriptional activity (Hartner et al., 2008). Furthermore, a pool of promoters with diverse expression and regulatory properties has been discovered and applied over the years, among them natural promoters as well as synthetic core promoters (de Almeida et al., 2005; Portela et al., 2017; Shen et al., 1998; Stadlmayr et al., 2010; Vogl et al., 2016, 2014). Recently, bidirectional promoters were added to the *K. phaffii* portfolio as well (Vogl et al., 2015b; Weninger et al., 2016) Table 2-4 gives an overview about the most prominent promoters used in *K. phaffii* and their recent advancements.

Table 2-4: Overview of promoters available for use in *K. phaffii*. Estimated expression levels were taken from literature (Ahmad et al., 2014; Schwarzhans et al., 2017a; Vogl and Glieder, 2013).

Promoter	**Native gene product**	**Regulation**	**Expression level**	**References**
		<u>Inducible promoters</u>		
P_{AOX1}	Alcohol oxidase 1	Induced by methanol	Strong (up to 5 % of mRNA/ 30 % of total protein)	(Ellis et al., 1985)
P_{AOX2}	Alcohol oxidase 2	Induced by methanol	~5 – 10 % of P_{AOX1}	(Koutz et al., 1989)
P_{DAS}	Dihydroxyacetone synthase	Induced by methanol	Strong (similar to P_{AOX1})	(Ellis et al., 1985)
P_{ADH3}	Alcohol dehydrogenase	Induced by ethanol	Strong (similar to P_{AOX1})	(Karaoglan et al., 2016)

Table 2-4: Overview of promoters available for use in *K. phaffii* – continued.

P_{FLD1}	Formaldehyde dehydrogenase	Induced by methanol and methylamine	Strong (similar to P_{AOX1})	(Shen et al., 1998)
P_{PEX8}	Peroxisomal matrix protein	Induced by methanol or oleate	Weak	(Snyder et al., 1999)
P_{CAT1}	Function related to H_2O_2 detoxification	Glucose derepression, methanol and oleate induction	100 – 180 % of P_{AOX1}	(Vogl et al., 2016)
P_{PHO89}	Sodium-coupled phosphate symporter	Induced by phosphate limitation	Strong (similar to P_{GAP})	(Ahn et al., 2009)
P_{AOD}	Alternative oxidase	Expression on glucose but not on methanol	~40 % of P_{GAP}	(Kern et al., 2007)
P_{LRA3}		Rhamnose induction	~ 80 % of P_{GAP}	(Liu et al., 2016)
Synthetic β-estradiol promoter		β-estradiol induction	Stronger than P_{AOX1}	(Perez-Pinera et al., 2016)
P_{AOX1} variant library	Alcohol oxidase	Induced by methanol	~6 % - > 160 % of P_{AOX1}	(Hartner et al., 2008)
$P_{AOX1\text{-}mi3}$ (mutated)	Alcohol oxidase	Dihydroxyacetate induction	~50 – 60 % of P_{AOX1}	(Shen et al., 2016)
$P_{AOX1\text{-}syn(d6)}$ (synthetic; based on P_{AOX1})	Alcohol oxidase	Glucose/glycerol derepression	~ 400 % of P_{AOX1}	(Hartner et al., 2008; Looser et al., 2017)
P_{AOX1} variant library	Alcohol oxidase	Induced by methanol	25 % - 350 % of P_{AOX1}	(Yang et al., 2018)
Constitutive promoters				
P_{GAP}	Glyceraldehyde-3-phosphate dehydrogenase	Constitutive	Strong (similar to $P_{AOX1)}$	(Waterham et al., 1997)
P_{GAP} variant library	Glyceraldehyde-3-phosphate dehydrogenase	Constitutive	0.6 % - 19.6 – fold of wild-type P_{GAP}	(Qin et al., 2011)
P_{TEF1}	Translation elongation factor 1 alpha	Constitutive, strong growth association	Strong (similar to P_{GAP})	(Stadlmayr et al., 2010)
P_{ENO1}	Enolase	Constitutive	~20 – 70 % of P_{GAP}	(Stadlmayr et al., 2010)

Table 2-4: Overview of promoters available for use in *K. phaffii* – continued.

P_{KAR2}	Endoplasmatic reticulum resident chaperone	Constitutive	~10 – 70 % of P_{GAP}	(Stadlmayr et al., 2010)
P_{PET9}	ADP/ATP carrier of the inner mitochrondrial membrane	Constitutive	~10 – 1700 % of P_{GAP}	(Stadlmayr et al., 2010)
P_{TPI1}	Triose phosphate isomerase	Constitutive	~10 – 80 % of P_{GAP}	(Stadlmayr et al., 2010)
P_{PGK1}	Phosphoglycerate kinase	Constitutive	~10 % of P_{GAP}	(de Almeida et al., 2005; Stadlmayr et al., 2010)
P_{THI11}	Thiamine synthesis	Constitutive, thiamine derepression	Strong (similar to P_{GAP})	(Landes et al., 2016)
$P_{AOX1\text{-}mi1}$ (mutated)	Alcohol oxidase	Glucose derepression, no glycerol repression, no methanol induction	77 % of P_{AOX1}	(Wang et al., 2017)
Bidirectional promoters				
P_{HTX1}		Constitutive		(Vogl et al., 2015b; Weninger et al., 2016)
P_{GAP}/P_{TEF}		Constitutive		(Vogl et al., 2015b)
P_{DAS1}/P_{DAS2}		Induction by methanol		(Vogl et al., 2015b)

In the recent years, the diversity of *K. phaffii* strains and regulatory elements has increased in size and versatility to facilitate metabolic engineering projects. In order to increase use of *K. phaffii* for more than just recombinant protein secretion, different strain and plasmid pools are made publicly available. As mentioned before, several strains and vectors are available at the Pichia Pool of the TU Graz (Ahmad et al., 2014; Näätsaari et al., 2012). The same group also constructed a total of 40 plasmids for use with type IIS restriction enzymes (Vogl et al., 2015a). Additionally, a modular toolkit for generating *K. phaffii* secretion libraries was recently established and added to the Addgene repository (Obst et al., 2017). Based on the popular yeast toolkit for *S. cerevisiae* (Lee et al., 2015), this kit has been expanded with *K. phaffii* specific parts, such as the P_{AOX1} and P_{GAP}. The kit comprises a total of 26 genetic parts that can be combined into 264 different vectors or more than 4000 vectors when including the compatible *S. cerevisiae* parts. While the *K. phaffii* toolkit focuses on protein secretion, utilization of other cellular targeting sequences is possible.

2.4.2. *K. phaffii* - genetic toolbox and clonal variability

The typical approach in *K. phaffii* is the chromosomal integration of the linearized expression vector harboring the gene of interest and an auxotrophic or antibiotic selection marker. This procedure ensures a high genetic stability (Cereghino and Cregg, 2000). While the preferred genomic integration mechanism in *S. cerevisiae* is via homologous recombination (HR) of usually terminal sequences of the linearized DNA fragment with homologous DNA sequences on the chromosomes, the dominant mechanism in *K. phaffii* is non-homologous end joining (NHEJ) (Daley et al., 2005). Non-homologous end joining is the host repair mechanism for double-strand breaks that integrates DNA without requiring homologous sequences. Thereby, NHEJ events can happen at random loci on the chromosome, potentially leading to disruption of genes or regulatory intergenic regions within the host. Furthermore, the locus of chromosomal integration might influence the expression strength of the gene of interest in eukaryotic systems e.g. due to epigenetic factors (Day, 2000). Another phenomenon in *K. phaffii* is the relatively high occurrence of transformants with gene copy numbers (GCN) greater than one due to multi-copy integrations of the linearized expression vector. *In vivo* multimerisation and subsequent integration of several expression cassettes at once are suspected to be the underlying cause occurring in 5 - 10 % of the transformed cells (Aw and Polizzi, 2013; Schwarzhans et al., 2016a). These phenomena are not necessarily disadvantageous for recombinant protein production. Studies of intracellular recombinant protein flux models supported that a higher GCN often correlates proportionally to protein synthesis rates as long as the secretory pathway capacity does not become saturated and limiting (Love et al., 2012; Pfeffer et al., 2011). For example, an up to 30 fold difference in product formation was observed in strains producing the tetanus toxin fragment C (Clare et al., 1991). While there are multiple approaches to increase the GCN (Aw and Polizzi, 2013), it could also be shown for *K. phaffii* that copy numbers of the integrated vector can be increased post-transformationally (Aw and Polizzi, 2016). When the integrated vector DNA contains an antibiotic selection marker cassette and the transformed cells are exposed to increasing concentrations of the antibiotic, cells were adapting to increased concentrations by increasing the GCN. However, especially for proteins targeted through the endoplasmic reticulum (ER) and (parts of) the secretory pathway, an increased GCN does not necessarily correlate with the product titer, but might even have negative effects due to the unfolded protein response (Marx et al., 2009).

Bottom line, these combined phenomena in *K. phaffii* lead to an increased clonal variability that might be beneficial for sole protein production, but poses a challenge for metabolic and genetic strain engineering where defined features and a clear cause-effect relationship is important (Schwarzhans et al., 2017a). To isolate the clone with the optimal features for a desired application from a heterogeneous population, which is displaying changes in physiology and differences in productivity characteristics, a time-consuming screening process has to be performed (Looser et al., 2015; Schwarzhans et al., 2016a, 2016b). The clonal variability is therefore considered as the major factor holding back further metabolic engineering of *K. phaffii* with the aim of value-added chemical production (Kelwick et al., 2014).

Several approaches of controlling clonal variability have been discussed by Schwarzhans et al. (Schwarzhans et al., 2017a), however the most promising to date might be the knockout of the *ku70* gene which is part of the NHEJ pathway in *K. phaffii*. Knockout of the *ku70* gene greatly reduced the probability of NHEJ events and thereby increased the targeting efficiency during the transformation. Nevertheless, strains with a *ku70* knockout also exerted an increased susceptibility to DNA damage and about 20 % lower growth rates (Näätsaari et al., 2012).

An alternative to genomic integration and a valuable tool for metabolic engineering present episomal vectors. For use in *K. phaffii*, vectors have been available that use the native autonomously replicating sequences (ARS) *PARS1* and *PARS2* (Cregg et al., 1985; Lee et al., 2005). However, these were scarcely used due to poor stability and low expression levels of the gene of interest compared to genomic integrations. A genome wide search for ARS in *K. phaffii* led to the discovery of potential ARS sequences, their features and applicability for an episomal vector (Liachko et al., 2014, 2013). In search for an ARS that functions in a broad range of yeasts, the *panARS* from *Kluyveromyces lactis* was discovered and subsequently investigated for heterologous protein production in *K. phaffii* and other yeasts (Camattari et al., 2016; Liachko and Dunham, 2014). Protein production levels in *K. phaffii* using an episomal vector with the *panARS* were similar to levels using genomic integration and, more importantly, the clonal variability was greatly reduced. While the genome-wide search of Liachko et al. only considered chromosomal DNA, recently a mitochrondrial ARS was discovered that displayed comparable features to *panARS* and also allowed replication in *S. cerevisiae* (Schwarzhans et al., 2017b). Due to their decreased clonal variability, high stability under selective conditions and similar expression levels compared to genomic integrations, both episomal vector systems have expanded the genetic toolbox of *K. phaffii*.

Another important step in metabolic engineering is the possibility to re-use the selection markers. For sequential gene deletions, an enhanced Cre-*lox* system has been established in *K. phaffii* making use of mutated *lox* sites (Pan et al., 2011). Upon cell selection after transformation, expression of Cre-recombinase can be induced by methanol addition, which in turn leads to excision of the integrated DNA via the *lox* sites. However, with this method of genetic engineering the problem of clonal variability is not addressed and reduced. Recently, a new recombinase based system has been developed employing the recombinases *BxbI, R4* and *Tp901-1* (Perez-Pinera et al., 2016). A 'landing pad' of heterologous DNA was integrated into the *K. phaffii* genome beforehand to allow for a standardized integration protocol of linearized vector DNA into the 'landing pad'. This system displayed increased targeting efficiencies and reduced off-target integrations.

After discovery of the CRISPR/Cas9 (clustered regularly interspaced short palindromic repeats/CRISPR associated protein 9) technology, it quickly became one of the most valuable tools in biotechnology and has thus been established for various organisms (Komor et al., 2017). The technology is based on a bacterial defense mechanism against host invading, foreign DNA. The Cas9 nuclease is targeted to a specific genomic locus via a ca. 20 bp long guide RNA to induce a double strand break. The double strand break is subsequently repaired by the host repair mechanisms, i.e. either by NHEJ or, if a homologous template is provided, by HR. Based on this mechanism, CRISPR/Cas9 technology offers markerless, targeted genome modifications with major advantages over classical techniques. Only recently, this method has also been developed for use in *K. phaffii* (Weninger et al., 2016). The major obstacle impeding the development in *K. phaffii* was the lack and/or inefficiency of RNA polymerase III promoters for guide RNA transcription. Weninger et al. solved this problem by flanking the guide RNA with ribozymes and putting transcription under control of an efficient RNA polymerase II promoter. After transcription, guide RNA is cleaved and released by the flanking ribozymes to allow binding to the target locus and recruiting Cas9 nuclease. While this technique offered near 100 % efficiency for insertions and deletions via the NHEJ mechanism, the efficiency for integrating donor cassettes via the HR mechanism was still low due to *K. phaffii*'s predominant NHEJ mechanism. An optimized system with efficiencies approaching 100 % for integrating donor cassettes was later established using the *KU70* deletion strain. By placing an ARS on the donor cassette, the

efficiency in the *K. phaffii* wild type strain as well as the *KU70* deletion strain could also be significantly increased(Weninger et al., 2017).

For metabolic cell engineering purposes, the simultaneous expression of several genes under control of different promoters might be necessary. Golden Gate cloning is one of the techniques offering these possibilities. It is based on restriction enzyme type II reactions, i.e. employing *Bsa*I and *Bpi*I enzymes that cut out of their recognition site, allowing for scar-less, standardized and universal DNA assembly in one-pot reactions (Engler et al., 2008). Recently, the popular Golden Gate technique has been transferred to the *K. phaffii* system, called Golden*Pi*CS (Prielhofer et al., 2017). This cloning system deploys 20 promoters of different strength, 10 transcription terminators, 4 genome integration loci and 4 resistance marker cassettes for the assembly of modular genetic parts that can be combined in a versatile order. The method enables the flexible and efficient generation of DNA constructs not only for protein production but also for all applications where multiple DNA product integrations are required simultaneously, such as pathway expressions or cofactor co-expressions. Golden*Pi*CS vectors have been added to the Addgene repertoire as well.

2.5. REFERENCES

Abuhasira, R., Shbiro, L., Landschaft, Y., 2018. Medical use of *Cannabis* and cannabinoids containing products – Regulations in Europe and North America. Eur. J. Intern. Med. 0–1. doi:10.1016/j.ejim.2018.01.001

Ahmad, M., Hirz, M., Pichler, H., Schwab, H., 2014. Protein expression in Pichia pastoris: recent achievements and perspectives for heterologous protein production. Appl. Microbiol. Biotechnol. 98, 5301–5317. doi:10.1007/s00253-014-5732-5

Ahn, J., Hong, J., Park, M., Lee, H., Lee, E., Kim, C., Lee, J., Choi, E. -s., Jung, J. -k., Lee, H., 2009. Phosphate-Responsive Promoter of a Pichia pastoris Sodium Phosphate Symporter. Appl. Environ. Microbiol. 75, 3528–3534. doi:10.1128/AEM.02913-08

Aw, R., Polizzi, K.M., 2016. Liquid PTVA: a faster and cheaper alternative for generating multi-copy clones in Pichia pastoris. Microb. Cell Fact. 15, 29. doi:10.1186/s12934-016-0432-8

Aw, R., Polizzi, K.M., 2013. Can too many copies spoil the broth? Microb. Cell Fact. 12, 128. doi:10.1186/1475-2859-12-128

Bar-Even, A., Noor, E., Savir, Y., Liebermeister, W., Davidi, D., Tawfik, D.S., Milo, R., 2011. The Moderately Efficient Enzyme: Evolutionary and Physicochemical Trends Shaping Enzyme Parameters. Biochemistry 50, 4402–4410. doi:10.1021/bi2002289

Bill, R.M., 2014. Playing catch-up with Escherichia coli: using yeast to increase success rates in recombinant protein production experiments. Front. Microbiol. 5, 1–5. doi:10.3389/fmicb.2014.00085

Bridgeman, M.B., Abazia, D.T., 2017. Medicinal *Cannabis*: History, Pharmacology, And Implications for the Acute Care Setting. P T 42, 180–188.

Burns, R.M., Caulkins, J.P., Everingham, S.S., Kilmer, B., 2013. Statistics on *Cannabis* Users Skew Perceptions of *Cannabis* Use. Front. Psychiatry 4, 1–10. doi:10.3389/fpsyt.2013.00138

Byrne, B., 2015. Pichia pastoris as an expression host for membrane protein structural biology. Curr. Opin. Struct. Biol. 32, 9–17. doi:10.1016/j.sbi.2015.01.005

Camattari, A., Goh, A., Yip, L.Y., Tan, A.H.M., Ng, S.W., Tran, A., Liu, G., Liachko, I., Dunham, M.J., Rancati, G., 2016. Characterization of a panARS-based episomal vector in the methylotrophic yeast Pichia pastoris for recombinant protein production and synthetic biology applications. Microb. Cell Fact. 15, 139. doi:10.1186/s12934-016-0540-5

Carlini, E.., 2004. The good and the bad effects of (−) trans-delta-9-tetrahydrocannabinol (Δ9-THC) on humans. Toxicon 44, 461–467. doi:10.1016/j.toxicon.2004.05.009

Carvalho, Â., Hansen, E.H., Kayser, O., Carlsen, S., Stehle, F., 2017. Designing microorganisms for heterologous biosynthesis of cannabinoids. FEMS Yeast Res. 17. doi:10.1093/femsyr/fox037

Cereghino, J.L., Cregg, J.M., 2000. Heterologous protein expression in the methylotrophic yeast Pichia pastoris.

FEMS Microbiol. Rev. 24, 45–66.

Chandra, S., Lata, H., ElSohly, M.A., 2017. *Cannabis* sativa L. - Botany and Biotechnology. Springer International Publishing, Cham. doi:10.1007/978-3-319-54564-6

Ciofalo, V., Barton, N., Kreps, J., Coats, I., Shanahan, D., 2006. Safety evaluation of a lipase enzyme preparation, expressed in Pichia pastoris, intended for use in the degumming of edible vegetable oil. Regul. Toxicol. Pharmacol. 45, 1–8. doi:10.1016/j.yrtph.2006.02.001

Clare, J.J., Rayment, F.B., Ballantine, S.P., Sreekrishna, K., Romanos, M.A., 1991. High-Level Expression of Tetanus Toxin Fragment C in Pichia Pastoris Strains Containing Multiple Tandem Integrations of the Gene. Nat. Biotechnol. 9, 455–460. doi:10.1038/nbt0591-455

Corchero, J.L., Gasser, B., Resina, D., Smith, W., Parrilli, E., Vázquez, F., Abasolo, I., Giuliani, M., Jäntti, J., Ferrer, P., Saloheimo, M., Mattanovich, D., Schwartz, S., Tutino, M.L., Villaverde, A., 2013. Unconventional microbial systems for the cost-efficient production of high-quality protein therapeutics. Biotechnol. Adv. 31, 140–153. doi:10.1016/j.biotechadv.2012.09.001

Couderc, R., Baratti, J., 1980. Oxidation of Methanol by the Yeast, Pichia pastoris . Purification and Properties of the Alcohol Oxidase. Agric. Biol. Chem. 44, 2279–2289. doi:10.1080/00021369.1980.10864320

Cregg, J.M., Barringer, K.J., Hessler, A.Y., Madden, K.R., 1985. Pichia pastoris as a host system for transformations. Mol. Cell. Biol. 5, 3376–85.

Cregg, J.M., Madden, K.R., Barringer, K.J., Thill, G.P., Stillman, C.A., 1989. Functional characterization of the two alcohol oxidase genes from the yeast Pichia pastoris. Mol. Cell. Biol. 9, 1316–1323. doi:10.1128/MCB.9.3.1316

Daley, J.M., Palmbos, P.L., Wu, D., Wilson, T.E., 2005. Nonhomologous End Joining in Yeast. Annu. Rev. Genet. 39, 431–451. doi:10.1146/annurev.genet.39.073003.113340

Daniel, B., Konrad, B., Toplak, M., Lahham, M., Messenlehner, J., Winkler, A., Macheroux, P., 2017. The family of berberine bridge enzyme-like enzymes: A treasure-trove of oxidative reactions. Arch. Biochem. Biophys. 632, 88–103. doi:10.1016/j.abb.2017.06.023

Day, C.D., 2000. Transgene integration into the same chromosome location can produce alleles that express at a predictable level, or alleles that are differentially silenced. Genes Dev. 14, 2869–2880. doi:10.1101/gad.849600

de Almeida, J.R.M., de Moraes, L.M.P., Torres, F.A.G., 2005. Molecular characterization of the 3-phosphoglycerate kinase gene (PGK1) from the methylotrophic yeastPichia pastoris. Yeast 22, 725–737. doi:10.1002/yea.1243

De Schutter, K., Lin, Y.-C., Tiels, P., Van Hecke, A., Glinka, S., Weber-Lehmann, J., Rouzé, P., Van de Peer, Y., Callewaert, N., 2009. Genome sequence of the recombinant protein production host Pichia pastoris. Nat. Biotechnol. 27, 561–566. doi:10.1038/nbt.1544

Degenhardt, F., Stehle, F., Kayser, O., 2017. The Biosynthesis of Cannabinoids, in: Preedy, V. (Ed.), Handbook of *Cannabis* and Related Pathologies. Elsevier, pp. 13–23. doi:10.1016/B978-0-12-800756-3.00002-8

Devane, W.A., Dysarz, F.A., Johnson, M.R., Melvin, L.S., Howlett, A.C., 1988. Determination and characterization of a cannabinoid receptor in rat brain. Mol. Pharmacol. 34, 605–13. doi:88/050605-09$02.OO/O

Devane, W.A., Hanus, L., Breuer, A., Pertwee, R.G., Stevenson, L.A., Griffin, G., Gibson, D., Mandelbaum, A., Etinger, A., Mechoulam, R., 1992. Isolation and structure of a brain constituent that binds to the cannabinoid receptor. Science 258, 1946–9.

Eisenreich, W., Bacher, A., Arigoni, D., Rohdich, F., 2004. Biosynthesis of isoprenoids via the non-mevalonate pathway. Cell. Mol. Life Sci. 61, 1401–1426. doi:10.1007/s00018-004-3381-z

Ellis, S.B., Brust, P.F., Koutz, P.J., Waters, A.F., Harpold, M.M., Gingeras, T.R., 1985. Isolation of alcohol oxidase and two other methanol regulatable genes from the yeast Pichia pastoris. Mol. Cell. Biol. 5, 1111–1121. doi:10.1128/MCB.5.5.1111

Elsohly, H.N., Turner, C.E., Clark, A.M., Elsohly, M.A., 1982. Synthesis and Antimicrobial Activities of Certain Cannabichromene and Cannabigerol Related Compounds. J. Pharm. Sci. 71, 1319–1323. doi:10.1002/jps.2600711204

ElSohly, M.A., Mehmedic, Z., Foster, S., Gon, C., Chandra, S., Church, J.C., 2016. Changes in *Cannabis* potency over the last 2 decades (1995-2014): Analysis of current data in the United States. Biol. Psychiatry 79, 613–619. doi:10.1016/j.biopsych.2016.01.004

Engler, C., Kandzia, R., Marillonnet, S., 2008. A One Pot, One Step, Precision Cloning Method with High Throughput Capability. PLoS One 3, e3647. doi:10.1371/journal.pone.0003647

Fellermeier, M., Zenk, M.H., 1998. Prenylation of olivetolate by a hemp transferase yields cannabigerolic acid, the precursor of tetrahydrocannabinol. FEBS Lett. 427, 283–5.

Fleming, M.P., Clarke, R.C., 1998. Physical evidence for the antiquity of *Cannabis* sativa L . J. Int. Hemp Assoc. 5, 80–92.

Gagne, S.J., Stout, J.M., Liu, E., Boubakir, Z., Clark, S.M., Page, J.E., 2012. Identification of olivetolic acid cyclase from *Cannabis* sativa reveals a unique catalytic route to plant polyketides. Proc. Natl. Acad. Sci. 109, 12811–12816. doi:10.1073/pnas.1200330109

Gaoni, Y., Mechoulam, R., 1964a. Isolation, Structure, and Partial Synthesis of an Active Constituent of Hashish. J. Am. Chem. Soc. 86, 1646–1647. doi:10.1021/ja01062a046

Gaoni, Y., Mechoulam, R., 1964b. The structure and function of cannabigerol, a new hashish constituent. Proc Chem Soc 82.

Gertsch, J., Pertwee, R.G., Di Marzo, V., 2010. Phytocannabinoids beyond the *Cannabis* plant - do they exist? Br. J. Pharmacol. 160, 523–529. doi:10.1111/j.1476-5381.2010.00745.x

Gleeson, M.A.G., White, C.E., Meininger, D.P., Komives, E. a, 1998. Generation of Protease-Deficient Strains and Their Use in Heterologous Protein Expression, in: Pichia Protocols. Humana Press, New Jersey, pp. 81–94. doi:10.1385/0-89603-421-6:81

Hamilton, S.R., Gerngross, T.U., 2007. Glycosylation engineering in yeast: the advent of fully humanized yeast. Curr. Opin. Biotechnol. 18, 387–392. doi:10.1016/j.copbio.2007.09.001

Hartner, F.S., Glieder, A., 2006. Regulation of methanol utilisation pathway genes in yeasts. Microb. Cell Fact. 5, 39. doi:10.1186/1475-2859-5-39

Hartner, F.S., Ruth, C., Langenegger, D., Johnson, S.N., Hyka, P., Lin-Cereghino, G.P., Lin-Cereghino, J., Kovar, K., Cregg, J.M., Glieder, A., 2008. Promoter library designed for fine-tuned gene expression in Pichia pastoris. Nucleic Acids Res. 36, e76–e76. doi:10.1093/nar/gkn369

Hasslacher, M., Schall, M., Hayn, M., Bona, R., Rumbold, K., Lückl, J., Griengl, H., Kohlwein, S.D., Schwab, H., 1997. High-level intracellular expression of hydroxynitrile lyase from the tropical rubber tree Hevea brasiliensis in microbial hosts. Protein Expr. Purif. 11, 61–71. doi:10.1006/prep.1997.0765

Hughes, B., 2017. *Cannabis* legislation in Europe. doi:10.2810/4682

Inan, M., Meagher, M.M., 2001. Non-Repressing Carbon Sources for Alcohol Oxidase (AOXI) Promoter of Pichia pastoris Non-Repressing Carbon Sources for Alcohol Oxidase (AOXI) Promoter of Pichia pastoris. Pap. Biochem. Eng. 92, 585–589.

Johnson, J.R., Burnell-Nugent, M., Lossignol, D., Ganae-Motan, E.D., Potts, R., Fallon, M.T., 2010. Multicenter, Double-Blind, Randomized, Placebo-Controlled, Parallel-Group Study of the Efficacy, Safety, and Tolerability of THC:CBD Extract and THC Extract in Patients with Intractable Cancer-Related Pain. J. Pain Symptom Manage. 39, 167–179. doi:10.1016/j.jpainsymman.2009.06.008

Jungo, C., Schenk, J., Pasquier, M., Marison, I.W., von Stockar, U., 2007. A quantitative analysis of the benefits of mixed feeds of sorbitol and methanol for the production of recombinant avidin with Pichia pastoris. J. Biotechnol. 131, 57–66. doi:10.1016/j.jbiotec.2007.05.019

Karaoglan, M., Karaoglan, F.E., Inan, M., 2016. Comparison of ADH3 promoter with commonly used promoters for recombinant protein production in Pichia pastoris. Protein Expr. Purif. 121, 112–117. doi:10.1016/j.pep.2016.01.017

Keasling, J.D., 2010. Manufacturing Molecules Through Metabolic Engineering. Science (80-.). 330, 1355–1358. doi:10.1126/science.1193990

Kelwick, R., MacDonald, J.T., Webb, A.J., Freemont, P., 2014. Developments in the Tools and Methodologies of Synthetic Biology. Front. Bioeng. Biotechnol. 2, 1–23. doi:10.3389/fbioe.2014.00060

Kern, A., Hartner, F.S., Freigassner, M., Spielhofer, J., Rumpf, C., Leitner, L., Frohlich, K.-U., Glieder, A., 2007. Pichia pastoris “just in time” alternative respiration. Microbiology 153, 1250–1260. doi:10.1099/mic.0.2006/001404-0

Komor, A.C., Badran, A.H., Liu, D.R., 2017. CRISPR-Based Technologies for the Manipulation of Eukaryotic Genomes. Cell 169, 559. doi:10.1016/j.cell.2017.04.005

Koutz, P., Davis, G.R., Stillman, C., Barringer, K., Cregg, J., Thill, G., 1989. Structural comparison of thePichia pastoris alcohol oxidase genes. Yeast 5, 167–177. doi:10.1002/yea.320050306

Küberl, A., Schneider, J., Thallinger, G.G., Anderl, I., Wibberg, D., Hajek, T., Jaenicke, S., Brinkrolf, K., Goesmann, A., Szczepanowski, R., Pühler, A., Schwab, H., Glieder, A., Pichler, H., 2011. High-quality genome sequence of Pichia pastoris CBS7435. J. Biotechnol. 154, 312–320. doi:10.1016/j.jbiotec.2011.04.014

Kurtzman, C.P., 2009. Biotechnological strains of Komagataella (Pichia) pastoris are Komagataella phaffii as determined from multigene sequence analysis. J. Ind. Microbiol. Biotechnol. 36, 1435–1438. doi:10.1007/s10295-009-0638-4

Lamacka, M., Sajbidor, J., 1997. Ergosterol determination in Saccaromyces cerevisiae. Comparison of different methods. Biotechnol. Tech. 11, 723–725. doi:10.1023/A:1018484015806

Landes, N., Gasser, B., Vorauer-Uhl, K., Lhota, G., Mattanovich, D., Maurer, M., 2016. The vitamin-sensitive promoter P THI11 enables pre-defined autonomous induction of recombinant protein production in Pichia pastoris. Biotechnol. Bioeng. 113, 2633–2643. doi:10.1002/bit.26041

Laukens, B., De Visscher, C., Callewaert, N., 2015. Engineering yeast for producing human glycoproteins: where are we now? Future Microbiol. 10, 21–34. doi:10.2217/fmb.14.104

Lee, C.C., Williams, T.G., Wong, D.W.S., Robertson, G.H., 2005. An episomal expression vector for screening mutant gene libraries in Pichia pastoris. Plasmid 54, 80–85. doi:10.1016/j.plasmid.2004.12.001

Lee, M.E., DeLoache, W.C., Cervantes, B., Dueber, J.E., 2015. A Highly Characterized Yeast Toolkit for Modular, Multipart Assembly. ACS Synth. Biol. 4, 975–986. doi:10.1021/sb500366v

Liachko, I., Dunham, M.J., 2014. An autonomously replicating sequence for use in a wide range of budding yeasts. FEMS Yeast Res. 14, 364–367. doi:10.1111/1567-1364.12123

Liachko, I., Youngblood, R.A., Keich, U., Dunham, M.J., 2013. High-resolution mapping, characterization, and optimization of autonomously replicating sequences in yeast 698–704. doi:10.1101/gr.144659.112.Freely

Liachko, I., Youngblood, R.A., Tsui, K., Bubb, K.L., Queitsch, C., Raghuraman, M.K., Nislow, C., Brewer, B.J., Dunham, M.J., 2014. GC-Rich DNA Elements Enable Replication Origin Activity in the Methylotrophic Yeast Pichia pastoris. PLoS Genet. 10, e1004169. doi:10.1371/journal.pgen.1004169

Liu, B., Zhang, Y., Zhang, X., Yan, C., Zhang, Y., Xu, X., Zhang, W., 2016. Discovery of a rhamnose utilization pathway and rhamnose-inducible promoters in Pichia pastoris. Sci. Rep. 6, 27352. doi:10.1038/srep27352

Looser, V., Brühlmann, B., Bumbak, F., Stenger, C., Costa, M., Camattari, a, Fotiadis, D., Kovar, K., 2015. Cultivation strategies to enhance productivity of Pichia pastoris: A review. Biotechnol. Adv. 33, 1177–1193. doi:10.1016/j.biotechadv.2015.05.008

Looser, V., Lüthy, D., Straumann, M., Hecht, K., Melzoch, K., Kovar, K., 2017. Effects of glycerol supply and specific growth rate on methanol-free production of CALB by P. pastoris: functional characterisation of a novel promoter. Appl. Microbiol. Biotechnol. 101, 3163–3176. doi:10.1007/s00253-017-8123-x

Love, K.R., Politano, T.J., Panagiotou, V., Jiang, B., Stadheim, T.A., Love, J.C., 2012. Systematic single-cell analysis of pichia pastoris reveals secretory capacity limits productivity. PLoS One 7, 1–11. doi:10.1371/journal.pone.0037915

Macauley-Patrick, S., Fazenda, M.L., McNeil, B., Harvey, L.M., 2005. Heterologous protein production using thePichia pastoris expression system. Yeast 22, 249–270. doi:10.1002/yea.1208

Maione, S., Piscitelli, F., Gatta, L., Vita, D., De Petrocellis, L., Palazzo, E., de Novellis, V., Di Marzo, V., 2011. Non-psychoactive cannabinoids modulate the descending pathway of antinociception in anaesthetized rats through several mechanisms of action. Br. J. Pharmacol. 162, 584–596. doi:10.1111/j.1476-5381.2010.01063.x

Marx, H., Mecklenbräuker, A., Gasser, B., Sauer, M., Mattanovich, D., 2009. Directed gene copy number amplification in Pichia pastoris by vector integration into the ribosomal DNA locus. FEMS Yeast Res. 9, 1260–70. doi:10.1111/j.1567-1364.2009.00561.x

Mattanovich, D., Graf, A., Stadlmann, J., Dragosits, M., Redl, A., Maurer, M., Kleinheinz, M., Sauer, M., Altmann, F., Gasser, B., 2009. Genome, secretome and glucose transport highlight unique features of the protein production host Pichia pastoris. Microb. Cell Fact. 8, 29. doi:10.1186/1475-2859-8-29

Mead, A., 2017. The legal status of *Cannabis* (marijuana) and cannabidiol (CBD) under U.S. law. Epilepsy Behav. 70, 288–291. doi:10.1016/j.yebeh.2016.11.021

Mechoulam, R., Ben-Shabat, S., Hanus, L., Ligumsky, M., Kaminski, N.E., Schatz, A.R., Gopher, A., Almog, S., Martin, B.R., Compton, D.R., Pertwee, R.G., Griffin, G., Bayewitch, M., Barg, J., Vogel, Z., 1995. Identification of an endogenous 2-monoglyceride, present in canine gut, that binds to cannabinoid receptors. Biochem. Pharmacol. 50, 83–90. doi:10.1016/0006-2952(95)00109-D

Mechoulam, R., Shvo, Y., 1963. Hashish—I. The structure of cannabidiol. Tetrahedron 19, 2073–2078. doi:10.1016/0040-4020(63)85022-X

Meehl, M.A., Stadheim, T.A., 2014. Biopharmaceutical discovery and production in yeast. Curr. Opin. Biotechnol. 30, 120–127. doi:10.1016/j.copbio.2014.06.007

MERKUS, F.W.H.M., 1971. Cannabivarin and Tetrahydrocannabivarin, Two New Constituents of Hashish. Nature 232, 579–580. doi:10.1038/232579a0

Moreno-Sanz, G., 2016. Can You Pass the Acid Test? Critical Review and Novel Therapeutic Perspectives of Δ 9 -Tetrahydrocannabinolic Acid A. *Cannabis* Cannabinoid Res. 1, 124–130. doi:10.1089/can.2016.0008

Morimoto, S., Komatsu, K., Taura, F., Shoyama, Y., 1998. Purification and characterization of cannabichromenic acid synthase from *Cannabis* sativa. Phytochemistry 49, 1525–9.

Müller-Vahl, K., Grotenhermen, F., 2017. Medizinisches *Cannabis*: Die wichtigsten Änderungen. Dtsch Arztebl 114, A-352 / B-306 / C-300.

Näätsaari, L., Mistlberger, B., Ruth, C., Hajek, T., Hartner, F.S., Glieder, A., 2012. Deletion of the Pichia pastoris KU70 Homologue Facilitates Platform Strain Generation for Gene Expression and Synthetic Biology. PLoS One 7, e39720. doi:10.1371/journal.pone.0039720

Ni, Z., Zhou, X., Sun, X., Wang, Y., Zhang, Y., 2008. Decrease of hirudin degradation by deleting theKEX1 gene in recombinantPichia pastoris. Yeast 25, 1–8. doi:10.1002/yea.1542

Öberg, F., Sjöhamn, J., Conner, M.T., Bill, R.M., Hedfalk, K., 2011. Improving recombinant eukaryotic membrane protein yields in Pichia pastoris : The importance of codon optimization and clone selection. Mol. Membr. Biol. 28, 398–411. doi:10.3109/09687688.2011.602219

Obst, U., Lu, T.K., Sieber, V., 2017. A Modular Toolkit for Generating Pichia pastoris Secretion Libraries. ACS Synth. Biol. 6, 1016–1025. doi:10.1021/acssynbio.6b00337

Ohara, K., Muroya, A., Fukushima, N., Yazaki, K., 2009. Functional characterization of LePGT1, a membrane-bound prenyltransferase involved in the geranylation of p -hydroxybenzoic acid. Biochem. J. 421, 231–241. doi:10.1042/BJ20081968

Page, J., Stout, J., 2015. CANNABICHROMENIC ACID SYNTHASE FROM *CANNABIS* SATIVA. WO2015196275.

Page, J.E., Boubakir, Z., 2014. Aromatic prenyltransferase from *Cannabis*. US 20120144523 A1.

Pan, R., Zhang, J., Shen, W.-L., Tao, Z.-Q., Li, S.-P., Yan, X., 2011. Sequential deletion of Pichia pastoris genes by a self-excisable cassette. FEMS Yeast Res. 11, 292–8. doi:10.1111/j.1567-1364.2011.00716.x

Perez-Pinera, P., Han, N., Cleto, S., Cao, J., Purcell, O., Shah, K.A., Lee, K., Ram, R., Lu, T.K., 2016. Synthetic biology and microbioreactor platforms for programmable production of biologics at the point-of-care. Nat. Commun. 7, 12211. doi:10.1038/ncomms12211

Pertwee, R., 2010. Receptors and Channels Targeted by Synthetic Cannabinoid Receptor Agonists and Antagonists. Curr. Med. Chem. 17, 1360–1381. doi:10.2174/092986710790980050

Pertwee, R.G., 2006. Cannabinoid pharmacology: the first 66 years. Br. J. Pharmacol. 147 Suppl, S163-71. doi:10.1038/sj.bjp.0706406

Pfeffer, M., Maurer, M., Köllensperger, G., Hann, S., Graf, A.B., Mattanovich, D., 2011. Modeling and measuring intracellular fluxes of secreted recombinant protein in Pichia pastoris with a novel 34S labeling procedure. Microb. Cell Fact. 10, 47. doi:10.1186/1475-2859-10-47

Pisanti, S., Malfitano, A.M., Ciaglia, E., Lamberti, A., Ranieri, R., Cuomo, G., Abate, M., Faggiana, G., Proto, M.C., Fiore, D., Laezza, C., Bifulco, M., 2017. Cannabidiol: State of the art and new challenges for therapeutic applications. Pharmacol. Ther. 175, 133–150. doi:10.1016/j.pharmthera.2017.02.041

Portela, R.M.C.C., Vogl, T., Kniely, C., Fischer, J.E., Oliveira, R., Glieder, A., 2017. Synthetic Core Promoters as Universal Parts for Fine-Tuning Expression in Different Yeast Species. ACS Synth. Biol. 6, 471–484. doi:10.1021/acssynbio.6b00178

Prielhofer, R., Barrero, J.J., Steuer, S., Gassler, T., Zahrl, R., Baumann, K., Sauer, M., Mattanovich, D., Gasser, B., Marx, H., 2017. GoldenPiCS: a Golden Gate-derived modular cloning system for applied synthetic biology in the yeast Pichia pastoris. BMC Syst. Biol. 11, 123. doi:10.1186/s12918-017-0492-3

Qin, X., Qian, J., Yao, G., Zhuang, Y., Zhang, S., Chu, J., 2011. GAP Promoter Library for Fine-Tuning of Gene Expression in Pichia pastoris. Appl. Environ. Microbiol. 77, 3600–3608. doi:10.1128/AEM.02843-10

Ramón, R., Ferrer, P., Valero, F., 2007. Sorbitol co-feeding reduces metabolic burden caused by the overexpression of a Rhizopus oryzae lipase in Pichia pastoris. J. Biotechnol. 130, 39–46. doi:10.1016/j.jbiotec.2007.02.025

Romano, B., Borrelli, F., Fasolino, I., Capasso, R., Piscitelli, F., Cascio, M., Pertwee, R., Coppola, D., Vassallo, L., Orlando, P., Di Marzo, V., Izzo, A., 2013. The cannabinoid TRPA1 agonist cannabichromene inhibits nitric oxide production in macrophages and ameliorates murine colitis. Br. J. Pharmacol. 169, 213–229. doi:10.1111/bph.12120

Roquet, N., Lu, T.K., 2014. Digital and analog gene circuits for biotechnology. Biotechnol. J. 9, 597–608. doi:10.1002/biot.201300258

Ross, S.A., ElSohly, M.A., 1996. The Volatile Oil Composition of Fresh and Air-Dried Buds of *Cannabis* sativa. J. Nat. Prod. 59, 49–51. doi:10.1021/np960004a

Russo, E.B., 2016. Current Therapeutic *Cannabis* Controversies and Clinical Trial Design Issues. Front. Pharmacol. 7, 1–19. doi:10.3389/fphar.2016.00309

Russo, E.B., 2011. Taming THC: Potential *Cannabis* synergy and phytocannabinoid-terpenoid entourage effects. Br. J. Pharmacol. 163, 1344–1364. doi:10.1111/bph.2011.163

Schwarzhans, J.-P., Luttermann, T., Geier, M., Kalinowski, J., Friehs, K., 2017a. Towards systems metabolic engineering in Pichia pastoris. Biotechnol. Adv. 35, 681–710. doi:10.1016/j.biotechadv.2017.07.009

Schwarzhans, J.-P., Luttermann, T., Wibberg, D., Winkler, A., Hübner, W., Huser, T., Kalinowski, J., Friehs, K., 2017b. A Mitochondrial Autonomously Replicating Sequence from Pichia pastoris for Uniform High Level Recombinant Protein Production. Front. Microbiol. 8, 1–15. doi:10.3389/fmicb.2017.00780

Schwarzhans, J.-P., Wibberg, D., Winkler, A., Luttermann, T., Kalinowski, J., Friehs, K., 2016a. Integration event induced changes in recombinant protein productivity in Pichia pastoris discovered by whole genome sequencing and derived vector optimization. Microb. Cell Fact. 15, 84. doi:10.1186/s12934-016-0486-7

Schwarzhans, J.-P., Wibberg, D., Winkler, A., Luttermann, T., Kalinowski, J., Friehs, K., 2016b. Non-canonical integration events in Pichia pastoris encountered during standard transformation analysed with genome sequencing. Sci. Rep. 6, 38952. doi:10.1038/srep38952

Shen, S., Sulter, G., Jeffries, T.W., Cregg, J.M., 1998. A strong nitrogen source-regulated promoter for controlled expression of foreign genes in the yeast Pichia pastoris. Gene 216, 93–102. doi:10.1016/S0378-1119(98)00315-1

Shen, W., Xue, Y., Liu, Y., Kong, C., Wang, X., Huang, M., Cai, M., Zhou, X., Zhang, Y., Zhou, M., 2016. A novel methanol-free Pichia pastoris system for recombinant protein expression. Microb. Cell Fact. doi:10.1186/s12934-016-0578-4

Shevyrin, V., Melkozerov, V., Endres, G.W., Shafran, Y., Morzherin, Y., 2016. On a New Cannabinoid Classification System: A Sight on the Illegal Market of Novel Psychoactive Substances. *Cannabis* Cannabinoid Res. 1, 186–194. doi:10.1089/can.2016.0004

Shoyama, Y., Takeuchi, A., Taura, F., Tamada, T., Adachi, M., Kuroki, R., Shoyama, Y., Morimoto, S., 2005. Crystallization of Δ 1 -tetrahydrocannabinolic acid (THCA) synthase from *Cannabis* sativa. Acta Crystallogr. Sect. F Struct. Biol. Cryst. Commun. 61, 799–801. doi:10.1107/S1744309105023365

Shoyama, Y., Tamada, T., Kurihara, K., Takeuchi, A., Taura, F., Arai, S., Blaber, M., Shoyama, Y., Morimoto, S., Kuroki, R., 2012. Structure and Function of Δ1-Tetrahydrocannabinolic Acid (THCA) Synthase, the Enzyme Controlling the Psychoactivity of *Cannabis* sativa. J. Mol. Biol. 423, 96–105. doi:10.1016/j.jmb.2012.06.030

Sirikantaramas, S., Morimoto, S., Shoyama, Y., Ishikawa, Y., Wada, Y., Shoyama, Y., Taura, F., 2004. The Gene Controlling Marijuana Psychoactivity. J. Biol. Chem. 279, 39767–39774. doi:10.1074/jbc.M403693200

Snyder, W.B., Koller, A., Choy, a J., Johnson, M. a, Cregg, J.M., Rangell, L., Keller, G. a, Subramani, S., 1999. Pex17p is required for import of both peroxisome membrane and lumenal proteins and interacts with Pex19p and the peroxisome targeting signal-receptor docking complex in Pichia pastoris. Mol. Biol. Cell 10, 4005–19.

Soderstrom, K., Soliman, E., Van Dross, R., 2017. Cannabinoids Modulate Neuronal Activity and Cancer by CB1 and CB2 Receptor-Independent Mechanisms. Front. Pharmacol. 8, 1–28. doi:10.3389/fphar.2017.00720

Stadlmayr, G., Mecklenbräuker, A., Rothmüller, M., Maurer, M., Sauer, M., Mattanovich, D., Gasser, B., 2010. Identification and characterisation of novel Pichia pastoris promoters for heterologous protein production. J. Biotechnol. 150, 519–529. doi:10.1016/j.jbiotec.2010.09.957

Stout, J.M., Boubakir, Z., Ambrose, S.J., Purves, R.W., Page, J.E., 2012. The hexanoyl-CoA precursor for cannabinoid biosynthesis is formed by an acyl-activating enzyme in *Cannabis* sativa trichomes. Plant J. 71, 353–365. doi:10.1111/j.1365-313X.2012.04949.x

Sturmberger, L., Chappell, T., Geier, M., Krainer, F., Day, K.J., Vide, U., Trstenjak, S., Schiefer, A., Richardson, T., Soriaga, L., Darnhofer, B., Birner-Gruenberger, R., Glick, B.S., Tolstorukov, I., Cregg, J., Madden, K., Glieder, A., 2016. Refined Pichia pastoris reference genome sequence. J. Biotechnol. 235, 121–131. doi:10.1016/j.jbiotec.2016.04.023

Tashkin, D.P., 2013. Effects of Marijuana Smoking on the Lung. Ann. Am. Thorac. Soc. 10, 239–247.

doi:10.1513/AnnalsATS.201212-127FR

Taura, F., Dono, E., Sirikantaramas, S., Yoshimura, K., Shoyama, Y., Morimoto, S., 2007a. Production of Δ1-tetrahydrocannabinolic acid by the biosynthetic enzyme secreted from transgenic Pichia pastoris. Biochem. Biophys. Res. Commun. 361, 675–680. doi:10.1016/j.bbrc.2007.07.079

Taura, F., Sirikantaramas, S., Shoyama, Y., Yoshikai, K., Shoyama, Y., Morimoto, S., 2007b. Cannabidiolic-acid synthase, the chemotype-determining enzyme in the fiber-type *Cannabis* sativa. FEBS Lett. 581, 2929–2934. doi:10.1016/j.febslet.2007.05.043

The National Academies of Science Engineering Medicine, 2017. The Health Effects of *Cannabis* and Cannabinoids, The Health Effects of *Cannabis* and Cannabinoids: The Current State of Evidence and Recommendations for Research. National Academies Press, Washington, D.C. doi:10.17226/24625

Turner, C.E., Hsu, M.H., Knapp, J.E., Schiff, P.L., Slatkin, D.J., 1976. Isolation of *Cannabis*ativine, an Alkaloid, from *Cannabis* sativa L. Root. J. Pharm. Sci. 65, 1084–1085. doi:10.1002/jps.2600650736

Turner, S.E., Williams, C.M., Iversen, L., Whalley, B.J., 2017. Molecular Pharmacology of Phytocannabinoids, in: Progress in the Chemistry of Organic Natural Products. pp. 61–101. doi:10.1007/978-3-319-45541-9_3

Vanhoenacker, G., Van Rompaey, P., de Keukeleire, D., Sandra, P., 2002. Chemotaxonomic Features Associated with Flavonoids of Cannabinoid-Free *Cannabis* (*Cannabis* sativa subsp. sativa L.) in Relation to hops (Humulus Lupulus L.). Nat. Prod. Lett. 16, 57–63. doi:10.1080/1057563029001/4863

Vogl, T., Ahmad, M., Krainer, F.W., Schwab, H., Glieder, A., 2015a. Restriction site free cloning (RSFC) plasmid family for seamless, sequence independent cloning in Pichia pastoris. Microb. Cell Fact. 14, 1–15. doi:10.1186/s12934-015-0293-6

Vogl, T., Glieder, A., 2013. Regulation of Pichia pastoris promoters and its consequences for protein production. N. Biotechnol. 30, 385–404. doi:10.1016/j.nbt.2012.11.010

Vogl, T., Hartner, F.S., Glieder, A., 2013. New opportunities by synthetic biology for biopharmaceutical production in Pichia pastoris. Curr. Opin. Biotechnol. 24, 1094–1101. doi:10.1016/j.copbio.2013.02.024

Vogl, T., Kickenweiz, T., Sturmberger, L., Glieder, A., 2015b. Bidirectional promoter.

Vogl, T., Ruth, C., Pitzer, J., Kickenweiz, T., Glieder, A., 2014. Synthetic core promoters for Pichia pastoris. ACS Synth. Biol. 3, 188–191. doi:10.1021/sb400091p

Vogl, T., Sturmberger, L., Kickenweiz, T., Wasmayer, R., Schmid, C., Hatzl, A.-M., Gerstmann, M.A., Pitzer, J., Wagner, M., Thallinger, G.G., Geier, M., Glieder, A., 2016. A Toolbox of Diverse Promoters Related to Methanol Utilization: Functionally Verified Parts for Heterologous Pathway Expression in Pichia pastoris. ACS Synth. Biol. 5, 172–186. doi:10.1021/acssynbio.5b00199

Vollner, L., Bieniek, D., Korte, F., 1969. [Hashish. XX. Cannabidivarin, a new hashish constituent]. Tetrahedron Lett. 145–7.

Wang, J., Wang, X., Shi, L., Qi, F., Zhang, P., Zhang, Y., Zhou, X., Song, Z., Cai, M., 2017. Methanol-Independent Protein Expression by AOX1 Promoter with trans-Acting Elements Engineering and Glucose-Glycerol-Shift Induction in Pichia pastoris. Sci. Rep. 7, 41850. doi:10.1038/srep41850

Waterham, H.R., Digan, M.E., Koutz, P.J., Lair, S. V., Cregg, J.M., 1997. Isolation of the Pichia pastoris glyceraldehyde-3-phosphate dehydrogenase gene and regulation and use of its promoter. Gene 186, 37–44. doi:10.1016/S0378-1119(96)00675-0

Weninger, A., Fischer, J., Raschmanová, H., Kniely, C., Vogl, T., Glieder, A., 2017. Expanding the CRISPR/Cas9 toolkit for Pichia pastoris with efficient donor integration and alternative resistance markers. J. Cell. Biochem. doi:10.1002/jcb.26474

Weninger, A., Hatzl, A.-M., Schmid, C., Vogl, T., Glieder, A., 2016. Combinatorial optimization of CRISPR/Cas9 expression enables precision genome engineering in the methylotrophic yeast Pichia pastoris. J. Biotechnol. doi:10.1016/j.jbiotec.2016.03.027

Werten, M.W.T., de Wolf, F.A., 2005. Reduced Proteolysis of Secreted Gelatin and Yps1-Mediated -Factor Leader Processing in a Pichia pastoris kex2 Disruptant. Appl. Environ. Microbiol. 71, 2310–2317. doi:10.1128/AEM.71.5.2310-2317.2005

Werten, M.W.T., Van Den Bosch, T.J., Wind, R.D., Mooibroek, H., De Wolf, F.A., 1999. High-yield secretion of recombinant gelatins by Pichia pastoris. Yeast 15, 1087–1096. doi:10.1002/(SICI)1097-0061(199908)15:11<1087::AID-YEA436>3.0.CO;2-F

Whittle, B.A., Guy, G.W., Robson, P., 2001. Prospects for New *Cannabis*-Based Prescription Medicines. J. *Cannabis* Ther. 1, 183–205. doi:10.1300/J175v01n03_12

Yamamoto, H., Kimata, J., Senda, M., Inoue, K., 1997. Dimethylallyl diphosphate: Kaempferol 8-dimethylallyl transferase in Epimedium diphyllum cell suspension cultures. Phytochemistry 44, 23–28. doi:10.1016/S0031-9422(96)00484-0

Yang, J., Cai, H., Liu, J., Zeng, M., Chen, J., Cheng, Q., Zhang, L., 2018. Controlling AOX1 promoter strength in Pichia pastoris by manipulating poly (dA:dT) tracts. Sci. Rep. 8, 1401. doi:10.1038/s41598-018-19831-y

CHAPTER 3

Production of Δ^9-tetrahydrocannabinolic acid from cannabigerolic acid by whole cells of *Pichia* (*Komagataella*) *pastoris* expressing Δ^9-tetrahydrocannabinolic acid synthase from *Cannabis sativa* L.

Bastian Zirpel, Felix Stehle, Oliver Kayser

B.Z. performed all experiments regarding *K. phaffii*. The students Dirk Münker and David Dannheisig performed the experiments regarding *S. cerevisiae* and Madeleine Dorsch conducted the studies using *E. coli*. We are also grateful to Dr. Parijat Kusari for critically reading this manuscript. F.S. designed research. O.K. coordinated and supervised the study. All authors contributed to writing the manuscript.

Biotechnology Letters (2015) 37:1869–1875

3.1. ABSTRACT

Objective The Δ^9-tetrahydrocannabinolic acid synthase (THCAS) from *Cannabis sativa* was expressed intracellularly in different organisms to investigate the potential of a biotechnological production of Δ^9-tetrahydrocannabinolic acid (THCA) using whole cells.

Results Functional expression of THCAS was obtained in *Saccharomyces cerevisiae* and *Pichia* (*Komagataella*) *pastoris* using a signal peptide from the vacuolar protease Proteinase A. No functional expression was achieved in *Escherichia coli*. The highest volumetric activities obtained were 98 pkat ml^{-1} (intracellular) and 44 pkat ml^{-1} (extracellular) after 192 h of cultivation at 15 °C using *P. pastoris* cells. Low solubility of CBGA prevents the THCAS application in aqueous cell-free systems, thus whole cells were used for a bioconversion of cannabigerolic acid (CBGA) to THCA. Finally, 1 mM (0.36 g THCA l^{-1}) THCA could be produced by 10.5 g_{CDW} l^{-1} before enzyme activity was lost.

Conclusion Our findings indicate that *P. pastoris* whole cell catalysis offers the capability of pharmaceutical THCA production.

3.2. INTRODUCTION

Since the discovery of the psychoactive cannabinoid Δ9-tetrahydrocannabinol (THC) from *Cannabis sativa* in 1964, and the human endocannabinoid system, the effects and potential pharmaceutical applications of THC have been extensively studied. Nowadays, THC is widely used as therapeutic agent in treatment of chemotherapy-associated nausea and vomiting, AIDS related loss of appetite as well as pain and muscle spasms in multiple sclerosis. Further applications are still under investigation and the demand of pharmaceutical grade THC is still increasing (Carlini 2004; Pertwee 2006). Nevertheless, legal regulations for the cultivation of *C. sativa* in most countries, chemical syntheses of THC with low yields or expensive, chiral precursors are drawbacks for a cost-effective THC production (Mechoulam 1970; Trost and Dogra 2007). Therefore a biotechnological approach transferring the enzymes of the plant biosynthetic pathway of Δ9-tetrahydrocannabinolic acid (THCA), the precursor of THC, into a microbial production host might present an appropriate alternative. The enzyme Δ9-tetrahydrocannabinolic acid synthase (THCAS) catalyzing the last step of THCA biosynthesis (Fig. 2-1), the oxidative cyclization of cannabigerolic acid (CBGA), has been successfully expressed in low amounts in recombinant tobacco hairy roots, insect cell cultures and secreting *Pichia* (*Komagataella*) *pastoris* cultures (Sirikantaramas et al. 2004; Taura et al. 2007). Furthermore, a crystal structure of the enzyme is published indicating a covalently bound FAD moiety (bound to His114 and Cys176), a disulfide bond (between Cys37 and Cys99) and six N-linked glycosylation sites (Shoyama et al. 2012). Additionally, a catalytic mechanism of the oxidation of CBGA to THCA has been proposed, including H_2O_2 formation for the regeneration of FAD during catalysis.

Since a scale-up approach with the isolated THCAS is not suitable due to i) the low water solubility of the substrate CBGA, ii) the denaturing properties of H_2O_2, iii) the integral membrane enzyme CBGA synthase, that cannot be secreted and therefore not feasibly implemented into a cell-free production system, we focused in this study on the intracellular THCAS expression in *Escherichia coli*, *Saccharomyces cerevisiae* and *P. pastoris* cells and the possible application towards a whole cell production system of THCA.

3.3. MATERIAL AND METHODS

3.3.1. Chemicals

Δ^9-tetrahydrocannabinolic acid (THCA) was purchased from THC Pharm (Frankfurt am Main, Germany). Cannabigerolic acid (CBGA) was purchased from Taros Chemicals (Dortmund, Germany).

3.3.2. Microorganisms, genes and plasmids

Cloning strategies and a detailed list of all strains and plasmids used in this study are given in the supplementary material (Supplementary Table 1 and Supplementary Table 2). Synthetic coding sequences of THCAS (GenBank accession number AB057805) were codon optimized for expression in *Saccharomyces cerevisiae* and *Pichia pastoris* and purchased without signal peptide from GeneArt (Regensburg, Germany). Recombinant expression of THCAS was conducted with the following microorganisms: *Escherichia coli* SHuffle T7 Express and SHuffle T7 Express *lysY* (NEB, Frankfurt am Main, Germany), containing modifications to enable disulfide bond formation in the cytosol, were used with pET28a(+) and pET32a(+) vectors (Merck, Darmstadt, Germany); *Saccharomyces cerevisiae* CEN.PK2-1CΔ*gal1* (Euroscarf, Frankfurt am Main, Germany) deficient in the β-galactokinase and Δ*gal1*Δ*pep4* (this study) also deficient in the vacuolar Proteinase A; *Pichia pastoris* PichiaPink strains 1, 2 and 3 (Invitrogen, Darmstadt, Germany). All *Pichia* strains are adenine-auxotroph. Strain 2 and strain 3 contain additional knockouts of the vacuolar proteases Proteinase A (*pep4)* and Proteinase B (*prb1*), respectively. *Pichia* strains were transformed with linearized high copy (pPink_HC_THCAS) and low copy (pPink_LC_THCAS) vectors (Invitrogen, Darmstadt, Germany) for integration into chromosomal TRP2 gene and *Saccharomyces* strains were transformed with pDionysos_THCAS vector (Stehle et al. 2008), all containing a cDNA of THCAS with 3 additional histidines at the C-terminus and an additional N-terminal sequence coding for a 24 AA signal peptide from Proteinase A (UniProt accession number F2QUG8 in pPink vectors and P07267 in pDionysos vector) for targeting into the cell vacuoles.

3.3.3. Culture conditions

Detailed media compositions are described in the supplementary section. If not stated otherwise, cells were cultivated as follows. Recombinant *E. coli* cells were grown in 1 L flasks, containing 100 mL LB-medium (50 µg kanamycin ml^{-1}, 33 µg chloramphenicol ml^{-1}, 100 µg spectinomycin ml^{-1}) at 37 °C and 200 rpm to an OD_{600} of 0.6. THCAS expression was induced by addition of 1 mM IPTG and cells grown for 16 h at 20 °C. Recombinant *S. cerevisiae* cells were grown in minimal medium without leucine at 30 °C and 200 rpm for 24 h. Cells were used to inoculate 100 ml of 2 x YPAD medium at an OD_{600} of 0.5 and incubated after induction with 0.5 % (w/v) galactose at 20 °C and 200 rpm for 144 h. Recombinant *P. pastoris* cells were grown in BMGY at 30 °C and 200 rpm for 24 h. Afterwards, cells were harvested by centrifugation at 5,000 x g for 5 min and resuspended in modified BMMY (mBMMY) (Taura et al. 2007) to an OD_{600} of 20. Finally, Pichia cells were cultivated at 15 °C and 200 rpm until no increase in THCAS activity could be observed and supplemented with 0.5 % (v/v) methanol every 24 h for induction of protein expression.

3.3.4. Analytical methods

Cell density was measured at 600 nm and cell dry mass (CDW) was calculated according to Tolner et al. (2006) with a correlation of CDW [g l^{-1}] = 0.21 g l^{-1} x OD_{600}. Protein concentrations were measured using Bradford assay (Ernst and Zor 2010). Methanol concentrations were determined by HPLC-UV analysis at 210 nm using Hi-Plex H 300 x 7.7 mm column by isocratic elution (5 mM H_2SO_4 in H_2O) with a flow rate of 0.5 ml min^{-1} at 65 °C.

3.3.5. THCAS activity assay

A detailed protocol for cell lysis is described in the supplementary information. Briefly, cells were harvested by centrifugation. Cell pellets were resuspended in 100 mM Na-citrate buffer pH 5.5 and the supernatant was diluted to 50 % (v/v) with 100 mM Na-citrate buffer pH 5.5. Yeast cells were lysed by glass beads and *E. coli* cells by sonication. After centrifugation of cell debris, lysate supernatants and diluted culture supernatants were used for determination of THCAS activity at 37 °C by addition of CBGA (final concentration 100 µM, 1 % (v/v) DMSO). Activity assays were stopped by addition of 0.3 assay-volumes trifluoroacetic acid and 2.7 assay-volumes acetonitrile (ACN) followed by incubation on ice for 15 min. Supernatants were analyzed after centrifugation (13,100 x g, 4 °C, 30 min) by HPLC using a Nucleosil 100-5 C18 column. A flow rate of 0.7 ml min^{-1} was used with isocratic elution (25 % (v/v) H_2O with 0.1 % (v/v) FA/ 75 % (v/v) ACN). Identification of CBGA and THCA was performed by HPLC-MS and quantification by HPLC-UV at 225 nm and 35 °C.

3.4. RESULTS AND DISCUSSION

3.4.1. Comparison of THCAS activities of recombinant *Escherichia coli*, *Saccharomyces cerevisiae* and *Pichia pastoris* strains

The functional expression of Δ^9-tetrahydrocannabinolic acid synthase (THCAS) was investigated using different organisms (Table 3-1). X-ray structure analysis revealed a disulfide bond. Thus, achieving functional expression in a prokaryotic system, *E. coli* SHuffle T7 Express and SHuffle T7 Express *lysY* cells, that are able to establish disulfide bonds in the cytosol, were transformed with pET28a(+)_THCAS, containing the cDNA of THCAS without signal peptide. To rule out solubility issues during expression, cells were also transformed with pET32a(+)_THCAS containing an additional thioredoxin fusion tag for improved solubility. Unfortunately, no expression and activity of THCAS was obtained in *E. coli* cells. This indicates that functional expression of THCAS might require eukaryotic chaperones able to facilitate covalent binding of FAD to the THCAS or glycosylation of the protein. In both yeast expression systems, the THCAS was targeted into the vacuole of the cell using the signal peptides of the vacuolar Proteinase A from *S. cerevisiae* or *P. pastoris*, respectively. As vacuolar proteases might degrade THCAS, wild type strains and protease knockout strains were compared with each other. Therefore the PEP4 gene was knocked out by homologous recombination in *S. cerevisiae* CEN.PK2-1C Δ*gal1* (wt). PichiaPink strains 1 (wt), 2 (*pep4*) and 3 (*prb1*) were transformed with high and low copy vectors for genome integration. A screening of the different *Pichia* clones was conducted and is described in the supplementary section in detail. Data indicated that the strain containing the Proteinase A knockout transformed

with the high copy vector (PP2_HC) showed the highest THCAS activity among *P. pastoris* and *S. cerevisiae* strains. Therefore PP2_HC was chosen for subsequent optimization studies, since the obtained volumetric THCAS activity of PP2_HC cultures was only in the range of the latest published results (Taura et al. 2007).

Table 3-1: Comparison of different organisms regarding highest obtained Δ^9-tetrahydrocannabinolic acid synthase (THCAS) activity. Cultures were inoculated at 0.105 g_{CDW} ml^{-1} (OD_{600} of 0.5) and cultivated at 20 °C. Enzymatic activity of lysate supernatant was measured at 37 °C. Values are calculated from biological duplicates.

Strain	**Volumetric activity intracellular [pkat ml^{-1}]**	**Specific activity intracellular [pkat g_{CDW}^{-1}]**
***E. coli* (all tested strains)**	-	-
***S. cerevisiae* CEN.PK2-1C Δ*gal1*Δ*pep4* pDionysos_THCAS**	1.0 ± 0.1	5.6 ± 0.3
PichiaPink2 Δ*pep4* pPink_HC_THCAS (PP2_HC)	1.4 ± 0.1	12.4 ± 0.9

3.4.2. Optimization of THCAS expression in *P. pastoris*

Procedures and medium composition were taken from Taura et al. (2007) as a starting point for expression optimization. Preliminary experiments indicated that methanol feeding at low cell densities needed optimization due to a slow metabolic rate of the yeast cultures. To ensure that methanol did not accumulate over time but was consumed before next methanol supplementation, expression cultures of PP2_HC were inoculated from overnight precultures at a higher cell density of 4.2 g_{CDW} l^{-1} (OD_{600} of 20) in mBMMY. Methanol was added every 24 h at 0.5 % (v/v). Temperatures of 10 °C, 15 °C, 20 °C and 25 °C were tested for functional THCAS expression. The highest obtained activities during the cultivations are shown in Table 3-2. Detailed cultivation results of 10 °C, 20 °C and 25 °C are given in the supplementary information. The highest intracellular activity of THCAS (98 ± 5 pkat ml^{-1}) was obtained at 15 °C for 192 h of cultivation (Fig. 3-1). THCAS activity was also found in the culture supernatant (44 ± 4 pkat ml^{-1}) which might be due to misdirection into secretory vesicles upon overexpression (Rothman and Stevens 1986). Since microscopic analyses showed only intact cells and protein content was constant over the cultivation time in the supernatant (data not shown), cell lysis seems not responsible for supernatant activity. Considering the different assay temperatures used by Taura (30 °C) and in this study (37 °C) (Fig. 3-2), the obtained volumetric THCAS activities were increased by 6,350 % compared to the reported activity by Taura et al. (Taura et al. 2007a). Nevertheless, methanol was consumed at every feeding point at later stages of cultivation presenting a possibility for further optimization. Additionally, flocculation of cells could be observed in all PP2_HC cultivations. Together with the finding of increased functionally expressed THCAS at decreasing temperatures, it seems likely that at higher metabolic rates the correct folding of the THCAS might present a challenge for the cells, as it includes its oxidative folding in the ER together with an excessive production of reactive oxygen species (Delic et al. 2014).

Table 3-2: Comparison of intracellular and extracellular Δ^9-tetrahydrocannabinolic acid synthase (THCAS) activity at different cultivation temperatures. Activities of culture or lysate supernatant were measured at 37 °C. The maximum values obtained during each cultivation are shown. Values are calculated from biological triplicates with two technical replicates.

Temperature [°C]	**Time [h]**	**Volumetric activity intracellular [pkat ml^{-1}]**	**Volumetric activity extracellular [pkat ml^{-1}]**	**Specific activity intracellular [pkat g_{CDW}^{-1}]**	**Specific activity extracellular [pkat g_{CDW}^{-1}]**
10	240	54 ± 4	43 ± 3	189 ± 16	152 ± 10
15	192	98 ± 5	44 ± 4	405 ± 8	179 ± 17
20	144	41 ± 3	25 ± 3	185 ± 9	114 ± 10
25	96	14 ± 0.4	7.6 ± 0.7	74 ± 2	41 ± 4

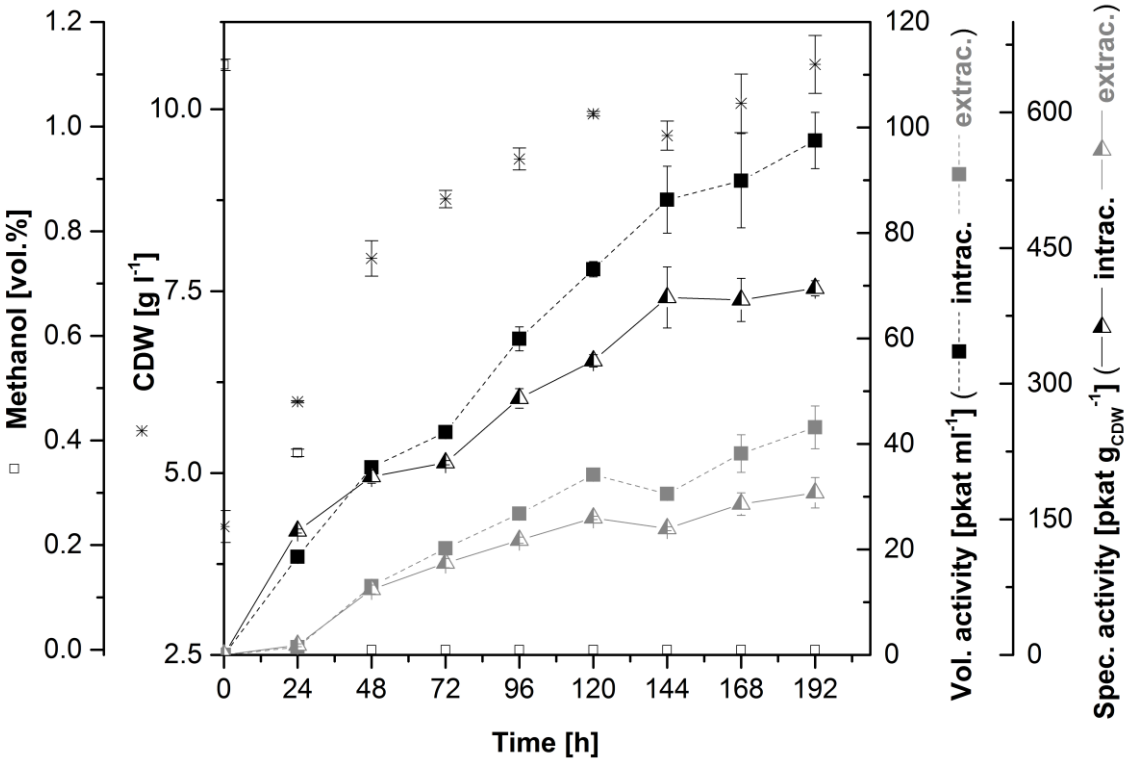

Fig. 3-1: Expression of THCAS using PP2_HC. Cultures were grown in 3-baffled shaking flasks at 200 rpm and 15 °C. Methanol was added every 24 h at a concentration of 0.5 % (v/v). Data points present the means of three biological replicates with two technical replicates and error bars present the standard deviation.

3.4.3. Whole cell bioconversion of cannabigerolic acid (CBGA) to Δ^9-tetrahydrocannabinolic acid (THCA) using *P. pastoris* cells

Preliminary experiments showed a low solubility of CBGA in aqueous solutions, e.g. around 200 µM in 100 mM Na-citrate buffer pH 5.5 (data not shown), impairing the production of higher amounts of THCA using cell-free aqueous systems or purified proteins. On the contrary, an immediate uptake of atleast 14 mM CBGA into the cells

could be observed (data not shown). Therefore, whole cell bioconversion of CBGA to THCA was investigated. A temperature dependency of THCAS activity in cell lysate supernatant is shown in Fig. 3-2.

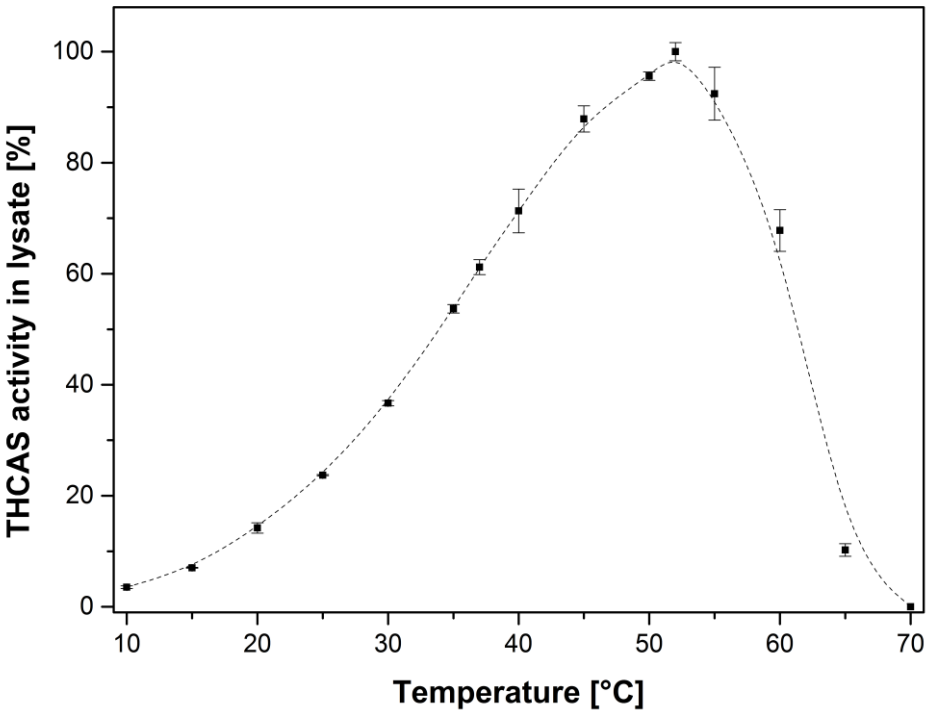

Fig. 3-2: Δ^9-tetrahydrocannabinolic acid synthase (THCAS) activity of cell lysate supernatant at different temperatures. Cells were lysed as described before and cell debris was centrifuged at 13,000 x g at 4 °C for 5 min. 100 % activity at 52 °C confers to 623 ± 10 pkat g_{CDW}^{-1}. At 37 °C 61 % of maximum THCAS activity is obtained (381 ± 8.3 pkat g_{CDW}^{-1}). Data points present the means of three biological replicates and error bars the standard deviation.

Whole cell assays were performed with 10.5 $g_{CDW}\,l^{-1}$ at the lysate's maximum activity (52 °C) and at a temperature where cells are still viable (37 °C) (Fig. 3-3, A). Maximum activities of whole cells at 37 °C and 52 °C were 328 ± 6 pkat g_{CDW}^{-1} and 601 ± 32 pkat g_{CDW}^{-1}, respectively (10.5 $g_{CDW}\,l^{-1}$ employed). During the whole assay time less than 1 % of added CBGA (and THCA at later time points) is present in the supernatant. This indicates that CBGA and THCA are embedded into the cell membranes due to their hydrophobic character. The substrate concentration available for the enzyme seems non-limiting for high catalytic rates, as the maximum activities of whole cells are comparable to cell-free enzyme assays. Furthermore, since no enzyme activity could be determined in the supernatant after centrifugation, cell lysis does not occur during the timeframe of bioconversion.

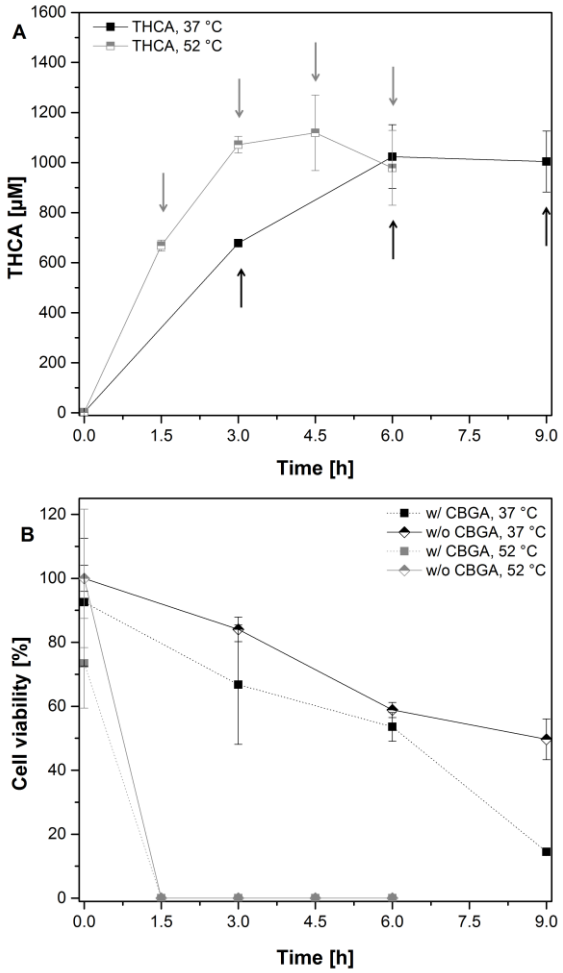

Fig. 3-3: Whole cell bioconversion of cannabigerolic acid (CBGA) to Δ^9-tetrahydrocannabinolic acid (THCA) using PP2_HC cells at 37 °C and 52 °C (A) and cell viability during bioconversion (B). Cells used were cultivated as described before, centrifuged, washed with 100 mM Na-citrate buffer pH 5.5 and finally resuspended in 400 µl 100 mM Na-citrate buffer pH 5.5 to 10.5 g_{CDW} l^{-1} (OD600 of 50). Conversion was started by addition of 1 mM CBGA (0 h). At every subsequent time-point, cells were separated from the supernatant and resuspended in fresh 100 mM Na-citrate buffer pH 5.5 before new substrate (1 mM) was added (marked with arrows for 37 °C (black) and 52 °C (grey)). CBGA and THCA concentrations in the supernatant as well as THCA synthase (THCAS) activity in the supernatant were measured at every time-point. CBGA and THCA concentrations in the supernatant were always below 10 µM and no THCAS activity could be measured in the supernatant (data not shown). 100 % cell viability at 37 °C and 52 °C confer to 340 ± 14 and 410 ± 89 colony forming units, respectively. Data points present the means of three biological replicates and error bars the standard deviation.

The employed amount of enzyme in the bioconversion is able to convert 1 mM CBGA to THCA (0.36 g THCA l^{-1}) before loss of activity arises. As this effect is not temperature-dependent (Fig. 3-3, B), the inactivation of enzyme might be due to H_2O_2 production upon FAD regeneration. Nevertheless, the concentration of THCA was increased by 400 % compared to reactions with lysate and by 900 % compared to reports from Taura et al (2007). Increasing the employed amount of cells could yield higher THCA levels. Furthermore, co-expression of a catalase or coupling THCA production to enzyme expression during cell growth could prolong enzymatic activity and thus increase THCA levels.

3.5. CONCLUSION

The expression of THCA synthase from *Cannabis sativa* L. was investigated using prokaryotic and eukaryotic expression systems. While no functional expression could be achieved in *E. coli*, the highest enzyme activity was

obtained in *P. pastoris* cultures. Under optimized conditions, volumetric THCAS activity levels were increased by 6,350 % compared to previous reports (Taura et al. 2007). The solubility issues in a biotechnological THCA production could be circumvented by employing *P. pastoris* whole cells. Finally, the whole cell bioconversion leads to the production of 1 mM THCA (0.36 g THCA l^{-1}). Thus, in future whole cells might provide an alternative method for the production of pharmaceutical THC.

3.6. REFERENCES

Carlini, E.., 2004. The good and the bad effects of (−) trans-delta-9-tetrahydrocannabinol (Δ9-THC) on humans. Toxicon 44, 461–467. doi:10.1016/j.toxicon.2004.05.009

Delic, M., Graf, A., Koellensperger, G., Haberhauer-Troyer, C., Hann, S., Mattanovich, D., Gasser, B., 2014. Overexpression of the transcription factor Yap1 modifies intracellular redox conditions and enhances recombinant protein secretion. Microb. Cell 1, 376–86. doi:10.15698/mic2014.11.173

Ernst, O., Zor, T., 2010. Linearization of the bradford protein assay. J. Vis. Exp. 1–6. doi:10.3791/1918

Mechoulam, R., 1970. Marihuana Chemistry. Science (80-.). 168, 1159–65. doi:10.1126/science.168.3936.1159

Pertwee, R.G., 2006. Cannabinoid pharmacology: the first 66 years. Br. J. Pharmacol. 147 Suppl, S163-71. doi:10.1038/sj.bjp.0706406

Rothman, J., Stevens, T.H., 1986. Protein Sorting in Yeast : Mutants Defective in Vacuole Biogenesis Mislocalize Vacuolar Proteins into the Late Secretory Pathway 47, 1041–51. doi:http://dx.doi.org/10.1016/0092-8674(86)90819-6

Shoyama, Y., Tamada, T., Kurihara, K., Takeuchi, A., Taura, F., Arai, S., Blaber, M., Shoyama, Y., Morimoto, S., Kuroki, R., 2012. Structure and Function of Δ1-Tetrahydrocannabinolic Acid (THCA) Synthase, the Enzyme Controlling the Psychoactivity of *Cannabis* sativa. J. Mol. Biol. 423, 96–105. doi:10.1016/j.jmb.2012.06.030

Sirikantaramas, S., Morimoto, S., Shoyama, Y., Ishikawa, Y., Wada, Y., Shoyama, Y., Taura, F., 2004. The Gene Controlling Marijuana Psychoactivity. J. Biol. Chem. 279, 39767–39774. doi:10.1074/jbc.M403693200

Stehle, F., Stubbs, M.T., Strack, D., Milkowski, C., 2008. Heterologous expression of a serine carboxypeptidase-like acyltransferase and characterization of the kinetic mechanism. FEBS J. 275, 775–87. doi:10.1111/j.1742-4658.2007.06244.x

Taura, F., Dono, E., Sirikantaramas, S., Yoshimura, K., Shoyama, Y., Morimoto, S., 2007. Production of Δ1-tetrahydrocannabinolic acid by the biosynthetic enzyme secreted from transgenic Pichia pastoris. Biochem. Biophys. Res. Commun. 361, 675–680. doi:10.1016/j.bbrc.2007.07.079

Tolner, B., Smith, L., Begent, R.H.J., Chester, K.A., 2006. Production of recombinant protein in Pichia pastoris by fermentation. Nat. Protoc. 1, 1006–1021. doi:10.1038/nprot.2006.126

Trost, B.M., Dogra, K., 2007. Synthesis of (-)-Delta9-trans-tetrahydrocannabinol: stereocontrol via Mo-catalyzed asymmetric allylic alkylation reaction. Org. Lett. 9, 861–3. doi:10.1021/ol063022k

CHAPTER 4

Optimization of Δ^9-tetrahydrocannabinolic acid-A synthase production in *Komagataella phaffii* via post-translational bottleneck identification

Bastian Zirpel, Friederike Degenhardt, Chantale Zammarelli, Daniel Wibberg, Jörn Kalinowski, Felix Stehle, Oliver Kayser

F.S. designed research. B.Z. planned the studies, performed the strain development, screening experiments and analyzed the data. F.D. helped with the Biolector experiments, discussions and trouble shoots. C.Z. supported the analytical measurements and helped with data analysis. F.S. helped with supervision of the study. D.W. and J.K. performed genome sequencing and analysis. O.K. coordinated and supervised the study. All authors contributed to writing the manuscript.

Submitted on 30.11.2017 in *Journal of Biotechnology*, accepted with minor revisions

4.1. ABSTRACT

Δ^9-tetrahydrocannabinolic acid (THCA) is a secondary natural product from the plant *Cannabis sativa* L. with therapeutic indications like analgesics for cancer pain or reducing spasticity associated with multiple sclerosis. Here, we investigated the influence of the co-expression of 12 helper protein genes from *Komagataella phaffii* (formerly *Pichia pastoris*) on the functional expression of the Δ^9-tetrahydrocannabinolic acid synthase (THCAS) heterologously expressed in *K. phaffii* by screening 21 clones of each transformation. Our findings substantiate the necessity of a suitable screening system when interfering with the secretory network of *K. phaffii*. We found that co-production of the chaperones CNE1p and Kar2p, the foldase PDI1p, the UPR-activator Hac1p as well as the FAD synthetase FAD1p enhanced THCAS activity levels within the *K. phaffii* cells. The strongest influence showed co-expression of *Hac1s* - increasing the volumetric THCAS activities 4.1-fold on average. We also combined co-production of Hac1p with the other beneficial helper proteins to further enhance THCAS activity levels. An optimized strain overexpressing *Hac1s*, *FAD1* and *CNE1* was isolated that showed 20-fold increased volumetric, intracellular THCAS activity compared to the starting strain. We used this strain for a whole cell bioconversion of cannabigerolic acid (CBGA) to THCA. After 8 h of incubation at 37 °C, the cells produced 3.05 g L^{-1} THCA corresponding to 12.5 % g_{THCA} g_{CDW}^{-1}.

4.2. INTRODUCTION

Cannabis sativa L. and its cannabinoids have gained increasing pharmaceutical importance in the last decades. Its most prominent cannabinoid, the major psychoactive Δ^9-tetrahydrocannabinol (THC), is nowadays used in several indications for treatment of chemotherapy-associated nausea and vomiting, AIDS-related loss of appetite as well as pain and muscle spasms in multiple sclerosis (Carlini, 2004; Pertwee, 2006). *In planta*, the acidic precursor of THC, namely Δ^9-tetrahydrocannabinolic acid (THCA), is produced by the Δ^9-tetrahydrocannabinolic acid synthase (THCAS) *via* oxidative cyclization from the precursor cannabigerolic acid (CBGA) and is decarboxylated upon heat induction. While THCA does not elicit psychoactive effects in humans, it is also currently examined for its immunomodulatory, anti-inflammatory, neuroprotective and anti-neoplastic effects (Moreno-Sanz, 2016).

Due to legal restrictions and drawbacks in chemical synthesis or agricultural production of cannabinoids for clinical use, researchers currently try to develop a controlled cannabinoid production platform in a heterologous host. Essential steps and recent advances towards development of such host were reviewed by Carvalho et al. (2017). The latest achievements and potentials of developing *Komagataella phaffii* (formerly *Pichia pastoris*) as a microorganism suitable for systems metabolic engineering have also been summarized (Schwarzhans et al., 2017). Additionally, the functional expression of *thcas* and *nphB* in *K. phaffii* has been reported as a major step towards this production in a heterologous host (Zirpel et al., 2017, 2015).

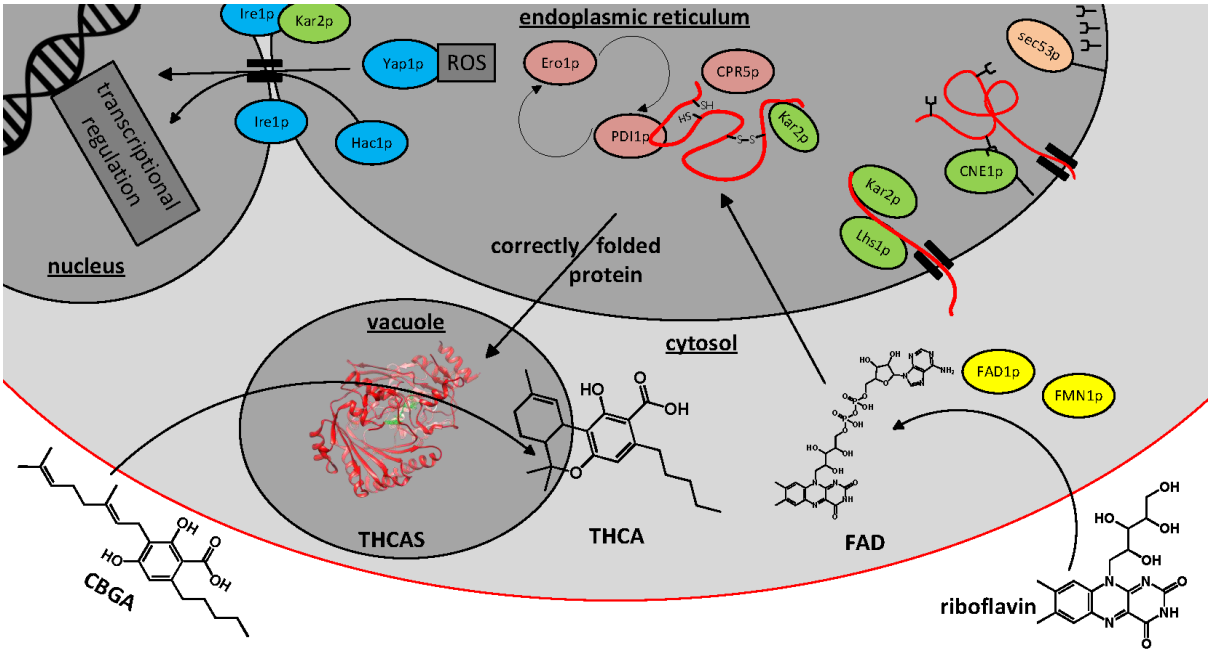

Fig. 4-1: Schematic overview of investigated bottlenecks during folding of functional THCAS. The THCAS (PDB: 3VTE) is targeted into the vacuole by using a *pep4* signal peptide (Zirpel et al., 2015). Proteins involved in folding and ER quality control (CNE1p, Lhs1p, Kar2p, PDIp, CPR5p, Ero1p), cofactor availability (FAD1p, FMN1p, Sec53p), reactive oxygen species (ROS) control (Yap1p) and unfolded protein response (Hac1p) were co-produced to enhance correctly folded THCAS. Riboflavin was added to the culture medium. After enzyme production, cells were used for a whole cell conversion of CBGA to THCA.

However, the THCAS possesses several structural features that might present obstacles in yielding high amounts of functionally active protein in the heterologous yeast. The enzyme contains a disulfide bond (C37, C99) and at least six *N*-glycosylation sites (N65, N89, N168, N329, N467, N499), as well as a bi-covalently attached flavin adenine dinucleotide (FAD) cofactor moiety (H114, C176) in its active site (Shoyama et al., 2012). Functional

expression of *thcas* in *K. phaffii* was reported first by Taura et al. (2007) and experimental data indicates that THCAS is produced in a strongly glycosylated form, although glycosylation was necessary rather for correct folding than for functionality as the THCAS was still active after EndoH deglycosylation. Furthermore, addition of riboflavin to the cultivation medium yielded higher THCAS activities in the supernatant of the expression cultures, pointing to an insufficient FAD-cofactor pool (Taura et al., 2007). Higher volumetric THCAS activities were achieved when expression cultivation was performed at lower temperatures (10 °C - 15 °C), again indicating folding issues in general. Compared to the wild-type strain not expressing the enzyme, a high degree of flocculation in the THCAS-overexpressing cells could be observed, which might be due to excessive generation of reactive oxygen species (ROS) upon excessive and/or incorrect protein folding (Delic et al., 2012; Zirpel et al., 2015).

We therefore wanted to identify bottlenecks during folding of the THCAS polypeptide chain by co-expressing different helper protein genes. There are many reviews about the impact of post-translational modifications of proteins, the involved helper proteins and the cell mechanisms on recombinant protein yields (Puxbaum et al., 2015; Schröder, 2008). An overview of the potential bottlenecks targeted in this study is shown in Fig. 4-1. After translocation of the nascent THCAS into the endoplasmic reticulum (ER), chaperones, co-chaperones and foldases prevent the polypeptide chain from aggregation and ensure proper folding. The ER-resident, essential Hsp70 chaperone Kar2p plays a major role by binding to hydrophobic patches of the unfolded polypeptide chains facilitating their transport through the ER lumen and preventing their agglomeration (Hale et al., 2010). The chaperone activity of Kar2p is regulated by its co-chaperones Sil1p and Lhs1p which also act as nucleotide exchange factors responsible for the regeneration of Kar2p ATPase cycles (Hale et al., 2010; Steel et al., 2004). The co-overexpression of Kar2p and Lhs1p has been successfully used to increase the levels of correctly folded recombinant proteins (Damasceno et al., 2007; de Ruijter et al., 2016). The chaperone CNE1p, the integral ER-membrane-bound calnexin-like protein, is responsible for correct folding and quality control of glycoproteins within the ER (Parlati et al., 1995). Co-expression of the respective *CNE1* was used to increase levels of a secreted target protein in *Hansenula polymorpha* as well as *K. phaffii* (Gu et al., 2015; Klabunde et al., 2007). Furthermore, foldases such as protein disulfide isomerase (PDI1p) and peptidyl-prolyl-*cis-trans* isomerase (PPIase/CPR5p) catalyze rate-limiting steps of protein folding. The major task of PDI1p is the correct arrangement of disulfide bonds of the polypeptide by an iterative cycle, but also a chaperone-like function can be assigned to the isomerase (Buck et al., 2007). PPIase catalyze the isomerization of peptidyl-prolyl bonds to facilitate folding of the peptide chain, however recently investigated PDI-PPIase interactions also substantiate the role in ER-chaperone/foldase partnerships. Co-overexpression of *PDI1* and *CPR5* has been utilized to enhance recombinant protein production in yeasts (de Ruijter et al., 2016; Inan et al., 2006). Likewise, a PDI1p-producing *K. phaffii* strain was used for the secretion of recombinant berberine-bridge-enzyme-like enzymes, which share high sequence and structural homology to the THCAS (Daniel et al., 2016). Another aspect to consider for THCAS production is the cofactor and precursor availability during processing of the nascent protein. Overproduction of Sec53p, a phosphomannomutase responsible for guanosine diphosphate mannose synthesis and involved in ER quality control, has been successfully realized previously (Gasser et al., 2007; Gu et al., 2015; Kepes and Schekman, 1988). The availability of bi-covalently bound cofactor FAD was investigated by co-overexpression of *FAD1*, coding for the FAD synthetase (FAD1p) which produces FAD from flavin mononucleotide (FMN) and co-overexpression of *FMN1*, the FMN synthase (FMN1p) which in return synthesizes FMN from riboflavin (Tu, 2000). While *FAD1* and *FMN1* are already upregulated in *K. phaffii* when growing on methanol, most of the FAD moieties presumably end up in the alcohol oxidase as well as endoplasmic thiol oxidase Ero1p (Rußmayer et al.,

2015). However, recombinant protein overexpression is often encompassed by oxidative stress due to production of ROS as well as induction of the unfolded-protein-response (UPR). The regeneration of PDI1p during its iterative cycle of disulfide bonding and rearrangements is enabled by the oxidation of Ero1p which is in return regenerated by oxidation of water to hydrogen peroxide. The increased amount of ROS activates Yap1p, a transcription factor involved in the response to oxidative stress. The role of Yap1p in maintaining the intracellular redox balance and thus in recombinant protein production was investigated recently and it could be shown that downregulation of *Yap1* led to accumulation of ROS and flocculation of the cells while constitutive overexpression of *Yap1* yielded higher amounts of secreted recombinant trypsinogen (Delic et al., 2014). The prolonged binding of unfolded or incorrectly folded proteins to Kar2p also triggers splicing of the *Hac1* mRNA which is subsequently transcribed into Hac1p. The transcriptional activator Hac1p up- and downregulate several genes involved in protein folding, secretion, ER quality control, glycosylation as well as ER-associated degradation. An overview of affected genes is given by Gasser *et al.* (Gasser et al., 2007). The splice-sites of Hac1p have recently been identified and co-overexpression of *Hac1s* (spliced, active version) was successfully used to increase titers of recombinantly produced protein (Guerfal et al., 2010). Here, we investigated the influence of the co-expression of twelve helper protein genes from *K. phaffii* on the functional, recombinant expression of the THCAS in this host.

4.3. MATERIALS AND METHODS

4.3.1. Materials

Chemicals were purchased from Invitrogen (Darmstadt, Germany), Sigma Aldrich (Darmstadt, Germany) and VWR (Darmstadt, Germany) if not stated otherwise. Δ^9-tetrahydrocannabinolic acid (THCA) was purchased from THC Pharm GmbH (Frankfurt am Main, Germany). Cannabigerolic acid (CBGA) was purchased from Taros Chemicals GmbH & Co. KG (Dortmund, Germany). All compounds have been checked for identity and purity by NMR analysis.

4.3.2. Plasmids and yeast strains

All strains used in this study are listed in Table 4-1. *Escherichia coli* DH5α was used for routine DNA transformations and plasmid isolations. PCR was performed using Q5® polymerase master mix (NEB, Frankfurt am Main, Germany) and the respective primers. Construction of plasmids was performed via Gibson assembly. For construction of plasmids pAXh_EV and pAXk_EV, the vector backbone was amplified from plasmid pAX_EV (Zirpel et al., 2017) with primers p_kanbb_fw and pkanbb_rv. The antibiotic resistance genes were amplified from vector pYTK079 (a gift from John Dueber (Addgene plasmid # 65186)) (Lee et al., 2015) and pUG6 (Euroscarf, Bad Homburg, Germany) with primers p_hygB_fw and p_hygB_rv or p_kan_fw and p_kan_rv, respectively. For generation of all other plasmids, the vector backbone was amplified from pAX_EV, pAXh_EV or pAXk_EV with primers p_pAX_fw and p_pAX_rv and the coding sequences were amplified (1 M betaine in PCR reaction) from isolated genomic DNA of PichiaPink™ strain 2 (Invitrogen, Darmstadt, Germany). A list of primers is given in Table S VIII-2.

Table 4-1: List of used strains. An overview of the used plasmids is given in Table S VIII-1.

Strain	**Relevant genotype of transformed strain**	**Transformed plasmid(s)**	**Expressed coding sequence(s)/ antibiotic resistance(s)**	**Gene accession number(s)**	**Reference(s)**
PP2_HC	*Komagataella phaffii* PichiaPink™ Δ*ade*Δ*pep4* (Invitrogen, Darmstadt, Germany)	pPink_HC_THCAS (*thcas* codon usage optimized for *K. phaffii*)	p_{AOX1}: *thcas*		(Zirpel et al., 2015)
PP2_EV	PP2_HC	pAX_EV	p_{AOX1}: - $Zeor^R$		This study
PP2_PDI1	PP2_HC	pAX_PDI1	p_{AOX1}: *PDI1* $Zeor^R$	CAC33587.1	This study
PP2_Ero1	PP2_HC	pAX_Ero1	p_{AOX1}: *Ero1* $Zeor^R$	CAY67364.1	This study
PP2_Yap1	PP2_HC	pAX_Yap1	p_{AOX1}: *Yap1* $Zeor^R$	CAY71861.1	This study
PP2_Hac1s	PP2_HC	pAX_Hac1s	p_{AOX1}: *Hac1s* $Zeor^R$	CAY67758.1	This study
PP2_Lhs1	PP2_HC	pAX_Lhs1	p_{AOX1}: *Lhs1* $Zeor^R$	CCA36228.1	This study
PP2_Kar2	PP2_HC	pAX_Kar2	p_{AOX1}: *Kar2* $Zeor^R$	AY965684.1	This study
PP2_FAD1	PP2_HC	pAX_FAD1	p_{AOX1}: *FAD1* $Zeor^R$	CAY67302.1	This study

Table 4-1: List of used strains - continued.

PP2_FAD1FMN1	PP2_HC	pAX_FAD1FMN1	p_{AOX1}: *FAD1* and *FMN1* separated via T2A sequence Zeor^R	CAY67302.1 CAY72070.1	This study; (Beekwilder et al., 2014a)
PP2_Sec53	PP2_HC	pAX_Sec53	p_{AOX1}: *Sec53* Zeor^R	CAY69880.1	This study
PP2_CNE1	PP2_HC	pAX_CNE1	p_{AOX1}: *CNE1* Zeor^R	CAY68938.1	This study
PP2_CPR5	PP2_HC	pAX_CPR5	p_{AOX1}: *CPR5* Zeor^R	CAY67638.1	This study
PP2Kar17_Hac1s	PP2_Kar2 C17	pAXh_Hac1s	p_{AOX1}: *Hac1s, Kar2* Zeor^R, HygB^R	CAY67758.1 AY965684.1	This study
PP2PDI21_Hac1s	PP2_PDI1 C21	pAXh_Hac1s	p_{AOX1}: *Hac1s, PDI1* Zeor^R, HygB^R	CAY67758.1 CAC33587.1	This study
PP2FAD22_Hac1s	PP2_FAD1 C22	pAXh_Hac1s	p_{AOX1}: *Hac1s, FAD1* Zeor^R, HygB^R	CAY67758.1 CAY67302.1	This study
PP2FF23_Hac1s	PP2_FAD1FMN1 C23	pAXh_Hac1s	p_{AOX1}: *Hac1s, FAD1, FMN1* Zeor^R, HygB^R	CAY67758.1 CAY67302.1 CAY72070.1	This study
PP2Hac14_Hac1s	PP2_Hac1s C14	pAXh_Hac1s	p_{AOX1}: *Hac1s, Hac1s* Zeor^R, HygB^R	CAY67758.1	This study
PP2CNE21_Hac1s	PP2_CNE1 C21	pAXh_Hac1s	p_{AOX1}: *Hac1s, CNE1* Zeor^R, HygB^R	CAY67758.1 CAY68938.1	This study
PP2CNE21Hac5_FAD1	PP2_CNE21_Hac1s C5	pAXk_FAD1	p_{AOX1}: *FAD1, CNE1, Hac1s* Zeor^R, HygB^R,G-418^R	CAY67758.1 CAY68938.1 CAY67302.1	This study

Preparation and transformation of electro-competent cells of *K. phaffii* was adapted from previous reports (Lin-Cereghino et al., 2005; Wu and Letchworth, 2004). An overnight culture of the respective strain was cultivated in YPD medium (2 % (w/v) peptone, 1 % (w/v) yeast extract, 2 % (w/v) glucose) at 30 °C and 200 rpm for inoculation of 100 ml fresh YPD medium at OD_{600} of 0.15 - 0.2. Cells were incubated in a 1 L baffled flask at 200 rpm, 30 °C

to an OD_{600} of 1. Cells (100 ml, OD_{600} of 1) were harvested by centrifugation at 500x g for 5 min and resuspended in 50 ml of Wu buffer (100 mM lithium acetate, 10 mM dithiothreitol, 0.6 M sorbitol, 10 mM Tris-HCl pH 7.5) and incubated for 30 min at room temperature. After centrifugation at 500 x g for 5 min, cells were resuspended in 6.25 ml BEDS buffer (3 % (v/v) ethylene glycol, 5 % (v/v) DMSO, 1 M sorbitol, 10 mM bicine-NaOH, pH 8.3) and aliquots of 1 ml were slowly frozen at - 80 °C. Electro-competent cells were thawed and washed 3 times with 1 ml of 1 M sorbitol solution before pellet was resuspended in 80 µl of 1 M sorbitol. Before transformation was performed in a 2 mm cuvette at 1800 V using the EquiBio Easyject Prima Electroporator, 2.5 µg of the respective *Pme*I-linearized vector DNA was added and cells incubated for 5 min on ice. After electroporation, 1 ml of ice-cold medium (0.5 ml YPD, 0.5 ml 1 M sorbitol) was added and cells incubated for 1.5 h at 30 °C, 200 rpm. Cells (50 µl) were plated on YPD agar with 100 µg ml^{-1} zeocin, 200 µg ml^{-1} G-418 or 300 µg ml^{-1} hygromycin B, respectively and grown for 2 days at 30 °C.

4.3.3. Determination of gene copy number of PP2_HC

The determination of copy number, integration direction and locus of *SpeI*-linearized plasmid pPink_HC_THCAS in strain PP2_HC (described in (Zirpel et al., 2015) was performed at the CeBiTec (Bielefeld University, Germany) and was described recently (Schwarzhans et al., 2016a). In brief, DNA of PP2_HC was isolated and quality controlled before sequencing. For sequencing of PP2_HC, a paired-end sequencing library (TruSeq sample preparation kit; Illumina, USA) was constructed according to the manufacturer's protocol. The genome sequence was established on the Illumina MiSeq. Based on a genome assembly using GS De Novo Assembler v2.8. (Roche Diagnostics, Mannheim, Germany) with default settings and an *in silico* approach (Wibberg et al., 2011), the copy number, integration direction and locus were analysed. The assembled draft sequence of the strain PP2_HC was deposited in the EMBL-EBI database under the accession numbers OCZY01000001-OCZY01000033 (PRJEB23195).

4.3.4. Screening of *K. phaffii* transformants for improved THCAS activities

Colonies of PP2_HC transformed with the respective *Pme*I-linearized vector DNA (sample colonies) were transferred to a sterile 48-round-well Biolector® plate (m2p-labs, Baesweiler, Germany) filled with 800 µl modified BMGY (10 g L^{-1} yeast extract , 20 g L^{-1} peptone, 5 g L^{-1} casamino acids, 100 mM Bis-Tris-HCl buffer pH 5.8, 13.8 g L^{-1} yeast nitrogen base, 0.4 mg L^{-1} biotin, 10 mg L^{-1} riboflavin, 1.5 % (w/v) glycerol) per well. Cells were cultivated using the Robolector™ system at 28 °C and 1200 rpm. Control cells (PP2_HC) were cultivated in triplicates together with 21 sample colonies. Due to non-disruptive, genomic integration into AOX1 promoter sequences of the transformed strain, gene expression of helper proteins as well as of *thcas* were under control of the AOX1 promoter and induced by methanol supplementation. After 24 h, expression cultures were inoculated by transferring 10 µl of each culture to a fresh well. After additional 18 h of cultivation and depletion of glycerol, 8 µl feeding solution (25 % (v/v) methanol, 200 g L^{-1} glycerol, 1.5 % (w/v) ammonium hydroxide) were fed every 2 h for 32 h. Cells were harvested by centrifugation of 650 µl culture volume. The pellet was washed by resuspension in 650 µl assay buffer (100 mM Na-citrate buffer pH 5.5) before pellet was resuspended in 500 µl assay buffer for cell lysis. Cell lysis was performed by vortexing at maximum speed (All-in-One Vortexer, Biozym Scientific GmbH, Hessisch Oldendorf, Germany) with glass beads (0.25 - 0.5 mm diameter) for 20 min at 4 °C.

The lysate was centrifuged and the supernatant used for THCAS activity assay (300 µM CBGA, 30 min, 37 °C, 1100 rpm). Activity assays of lysates were performed in duplicates.

Activity assays were stopped by addition of 0.3 assay-volumes formic acid (FA) and 2.7 assay-volumes acetonitrile (ACN) followed by incubation on ice for 15 min. Supernatants were filtered (0.45 µm, Nylon) after centrifugation (13,100 x g, 4 °C, 20 min) and analyzed by HPLC-DAD (Agilent 1260 Infinity HPLC, Waldbronn, Germany) at 225 nm. Separation of compounds was performed on a Poroshell 120 EC-C18, 2.1 x 100 mm, 2.7 µm column (Agilent, Waldbronn, Germany) (0.7 ml min^{-1}, 40 °C, 35 % (v/v) H_2O with 0.1 % (v/v) FA, 65 % (v/v) ACN). The volumetric THCAS activity of each sample colony was calculated and normalized on the average activity of the control cells used in each cultivation.

4.3.5. Shaking flask cultivation for THCAS production in *K. phaffii*

Cultivation experiments were performed in triplicates. Precultures of 100 ml YPD medium in 1 L baffled shaking flasks were inoculated with cell material of the respective strain (PP2HC, PP2CNE21Hac5FAD C7) and cultivated for 24 h at 200 rpm and 30 °C. Cultures were harvested and cell pellets resuspended in 100 ml fresh BMMY medium (10 g L^{-1} yeast extract, 20 g L^{-1} peptone, 5 g L^{-1} casamino acids, 100 mM Bis-Tris-HCl buffer pH 5.8, 13.8 g L^{-1} yeast nitrogen base, 0.4 mg L^{-1} biotin, 10 mg L^{-1} riboflavin, 1 % (v/v) methanol) to a starting OD_{600} of 20. Cultivation was performed in 1 L baffled shaking flasks at 15 °C and 200 rpm for 144 h. Methanol was fed every 24 h at a concentration of 0.5 % (v/v) after sampling was conducted. Samples were used for OD_{600} and THCAS activity determination of cells and cell culture supernatant. Cell lysis was performed as described above, but only 500 µl samples were taken. Cell lysis in 100 mM NaCitrate buffer pH 4.85 and activity measurements were performed in technical duplicates as described above. Supernatants were diluted 1:1 with 100 mM Nacitrate buffer pH 5.5 for activity measurements.

4.3.6. Whole cell bioconversion for THCA production

Cells of PP2CNE21Hac5FAD C7 from the shaking flask experiment were pelleted and resuspended in culture supernatant to an OD_{600} of 100 and pH adjusted to 4.85. Bioconversions were performed in triplicates by incubating 600 µl cell suspension for 8 h (1100 rpm, 37 °C, 2 mM CBGA starting concentration). After 1 h, 2 h, 4 h and 6 h of incubation, 2 mM CBGA were added to the cell suspension. Before addition of CBGA, 50 µl sample was taken and diluted with 150 µl of stop solution (10 % v/v FA, 90 % (v/v) ACN) for further HPLC-DAD (225 nm) and HPLC-MS analysis (m/z 359.21, positive mode). The cell dry weight (CDW) was calculated with the correlation CDW (g L^{-1}) = 0.21 g L^{-1} x OD_{600} (Tolner et al., 2006). The THCA content of the cells was estimated by % g_{THCA} g_{CDW}^{-1}= (100 % * g_{THCA} L^{-1}) * (g_{THCA} L^{-1} + g_{CDW} L^{-1})$^{-1}$.

4.4. RESULTS

4.4.1. Starting strain PP2_HC

Previously, we reported the optimization of *thcas* expression in *K. phaffii* leading to a 63.5-fold increase in activity levels compared to preceding reports (Zirpel et al., 2015). While at the time several transformation colonies were screened by an enzyme assay, the gene copy numbers (GCN) of the screened cells remained unknown. To determine the GCN of PP2_HC, the draft genome sequence was established on the Illumina MiSeq system. The run obtained 1,673,004 reads yielding 503 Mb sequence information for PP2_HC. The assembly generated 33 scaffolds including 99 contigs with a total size of 9.3 Mb. By an *in silico* approach, we determined the GCN of strain PP2_HC to be 24 ± 2 oriented in a head-to-tail direction within the targeted *TRP2*-locus (THCAS gene cluster). By co-production of helper proteins in this strain, we wanted to identify possible bottlenecks of correct folding of the THCAS.

We first investigated the homogeneity of the control strain PP2_HC, which was used for subsequent transformations, by comparing THCAS activity levels of the control with 21 single colonies obtained from an isolation streak plate of the control cells (Fig. 4-2A). By F-test analysis (p = 0.01) the variances of the populations were determined to be not significantly different, thus assuming a homogenous control cell population.

Transformations of *PmeI*-linearized pAX-plasmids were targeted into the *AOX1* promoter sequence which is present 25 ± 2 times in strain PP2_HC. To ensure that the integration of new genetic material into the THCAS gene cluster does not significantly affect THCAS activity levels, we transformed the *PmeI*-linearized empty vector pAX_EV into PP2_HC and compared 21 transformants regarding their THCAS activity levels with the control PP2_HC (Fig. 4-2B). The intracellular, volumetric THCAS activity levels of both populations were compared by non-parametric Mann-Whitney-U test and determined to be not significantly different (p = 0.05), concluding that the transformation of the empty vector does not affect the THCAS activities.

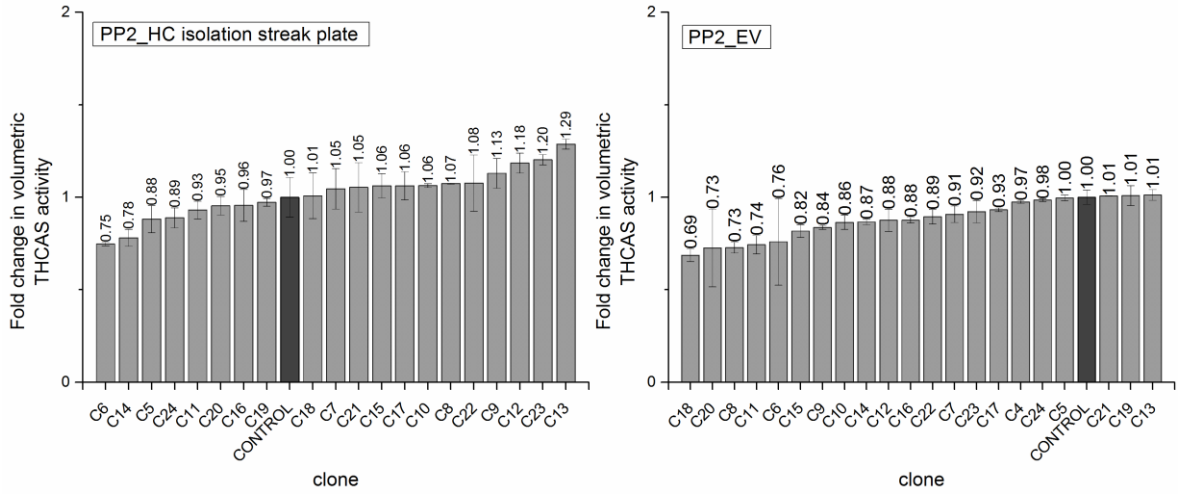

Fig. 4-2: Normalized intracellular, volumetric activity levels of colonies of PP2_HC obtained from an isolation streak plate (A) and transformants of PP2_HC with empty vector pAX_EV (B). Activities were normalized on the average control activity. Control activity was determined from triplicate cultivation of PP2_HC. All activity measurements of cell lysates were performed in duplicates.

4.4.2. Influence of co-produced helper proteins on THCAS activity

Next, we investigated the influence of the co-production of several helper proteins on the THCAS activity levels (Fig. 4-3). Significance was determined with Mann-Whitney-U test by comparing the normalized THCAS activities of the screened colonies against the empty-vector transformed population (PP2_EV) ($p = 0.05$).

Several co-produced proteins did not significantly increase the THCAS activity levels in the strain PP2_HC, namely the phosphomannomutase Sec53p, the PPIase CPR5p, the chaperone Lhs1p, as well as the thiol oxidase Ero1p or the transcriptional activator Yap1p (Fig. 4-3 and Fig. S VIII-1).

On the other side, the co-production of the glycoprotein-associated chaperone CNE1p, the FAD synthetase FAD1p, the foldase and protein disulfide isomerase PDI1p, the chaperone Kar2p and the UPR-related transcriptional activator Hac1p significantly increased the THCAS activity levels. The populations of PP2_Kar2 and PP2_CNE1 showed high clonal variabilities to the extent that several transformants presented significantly reduced THCAS activities while others benefited from co-production of the helper protein (Fig. 4-3). This observation was especially made for PP2_CNE1 (see Fig. S VIII-2) where 9 and 8 out of 21 clones showed significantly decreased or increased THCAS activities, respectively. The populations of PP2_FAD1, PP2_PDI1 and PP2_Hac1 also showed variabilities to some extent, but all screened transformants had increased THCAS activity levels compared to PP2_HC (Fig. 4-3). The volumetric activities of the PP2_FAD1FMN1 population, which are co-expressing both *FAD1* and *FMN1* (separated by a T2A sequence (Beekwilder et al., 2014)), were not significantly increased compared to PP2_FAD1 which is only co-expressing FAD1. The co-production of the transcriptional activator of UPR-related genes Hac1p enhanced THCAS activity levels the most - in average by 4.1-fold (Fig. 4-3).

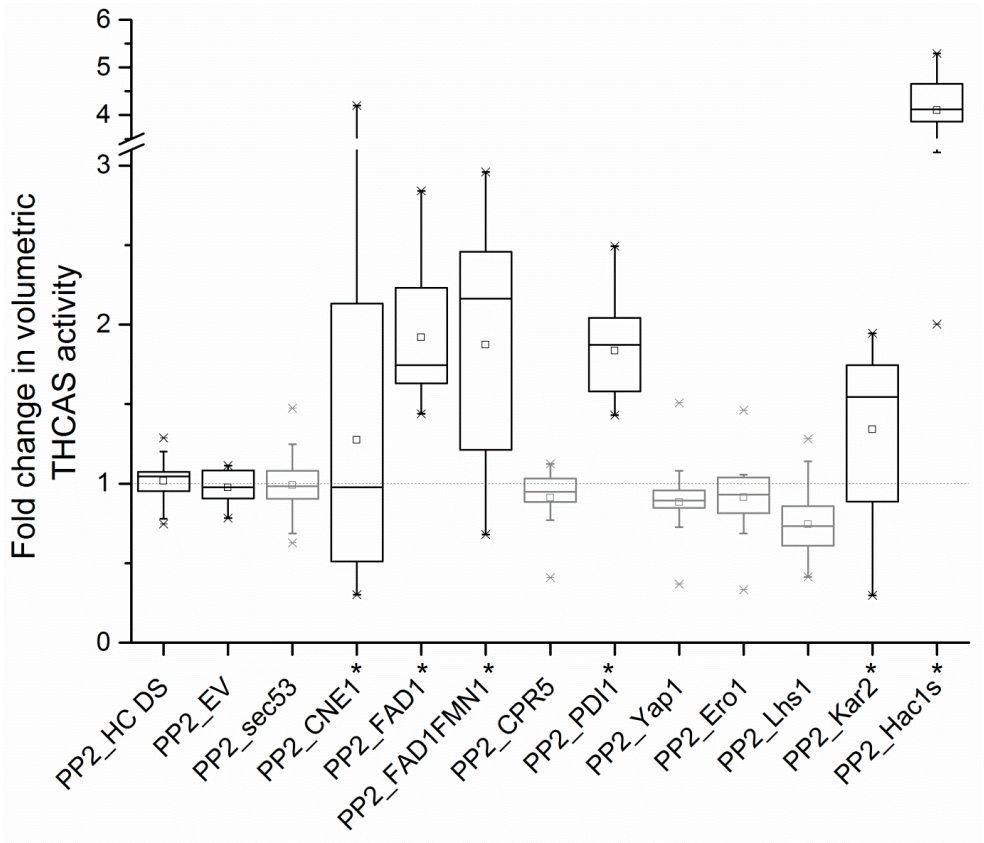

Fig. 4-3: Influence of co-produced helper proteins on THCAS activity levels in *K. phaffii* strain PP2_HC. Volumetric activities were determined in technical duplicates and normalized on the average activity of PP2_HC cultivated in biological triplicates. Significantly increased activities (marked with *) were determined with the Mann-Whitney-U test comparing against the empty-vector transformed population (PP2_EV) ($p = 0.05$).

After identification of helper proteins that exert a positive effect on the functional *thcas* expression, we used the clone with the highest intracellular, volumetric THCAS activity of the respective population (PP2_Hac C14, PP2_PDI1 C21, PP2_Kar2 C17, PP2_FAD1 C22, PP2_FAD1FMN1 C23, PP2_CNE1 C21) for subsequent transformations with pAXh_Hac1s. Antibiotic resistance genes were exchanged on pAX-plasmids (zeocin resistance) to generate vectors with hygromycin B resistance (pAXh-plasmids). To determine effects that cannot be contributed to Hac1p co-production alone, we compared the normalized, volumetric THCAS activities of the screened colonies against the Hac1s transformed population (PP2_Hac1s) and determined significance with the Mann-Whitney-U test ($p = 0.05$). It is important to note that further increase of Hac1p titers in the strain PP2_Hac1s C14, which is already overexpressing *Hac1s*, did not further improve functional *thcas* expression. Additionally, THCAS activities of the population of PP2FF23_Hac1s and PP2PDI21_Hac1s were not significantly improved compared to PP2_Hac1s. While we observed - compared to PP2_HC - slightly reduced growth and/or maximum OD_{600} values for all populations co-expressing helper protein genes, PP2FF23_Hac1s and PP2PDI21_Hac1s populations suffered from severe flocculation and most of the screened clones showed up to 50 % reduced final biomass in this experimental setup (see Fig. S VIII-4, Fig. S VIII-5, Fig. S VIII-6). However, additive effects of Hac1p co-production together with Kar2p, FAD1p, PDI1p and CNE1p were observed (Fig. 4-4). Based on these results, we subsequently transformed the clone with the highest THCAS activity of PP2CNE21_Hac1s (C5) with pAXk_FAD1. Under the tested conditions PP2CNE21Hac5_FAD1C7 showed the largest increase in functional *thcas* expression with a 20-fold enhanced activity compared to the initial strain PP2_HC.

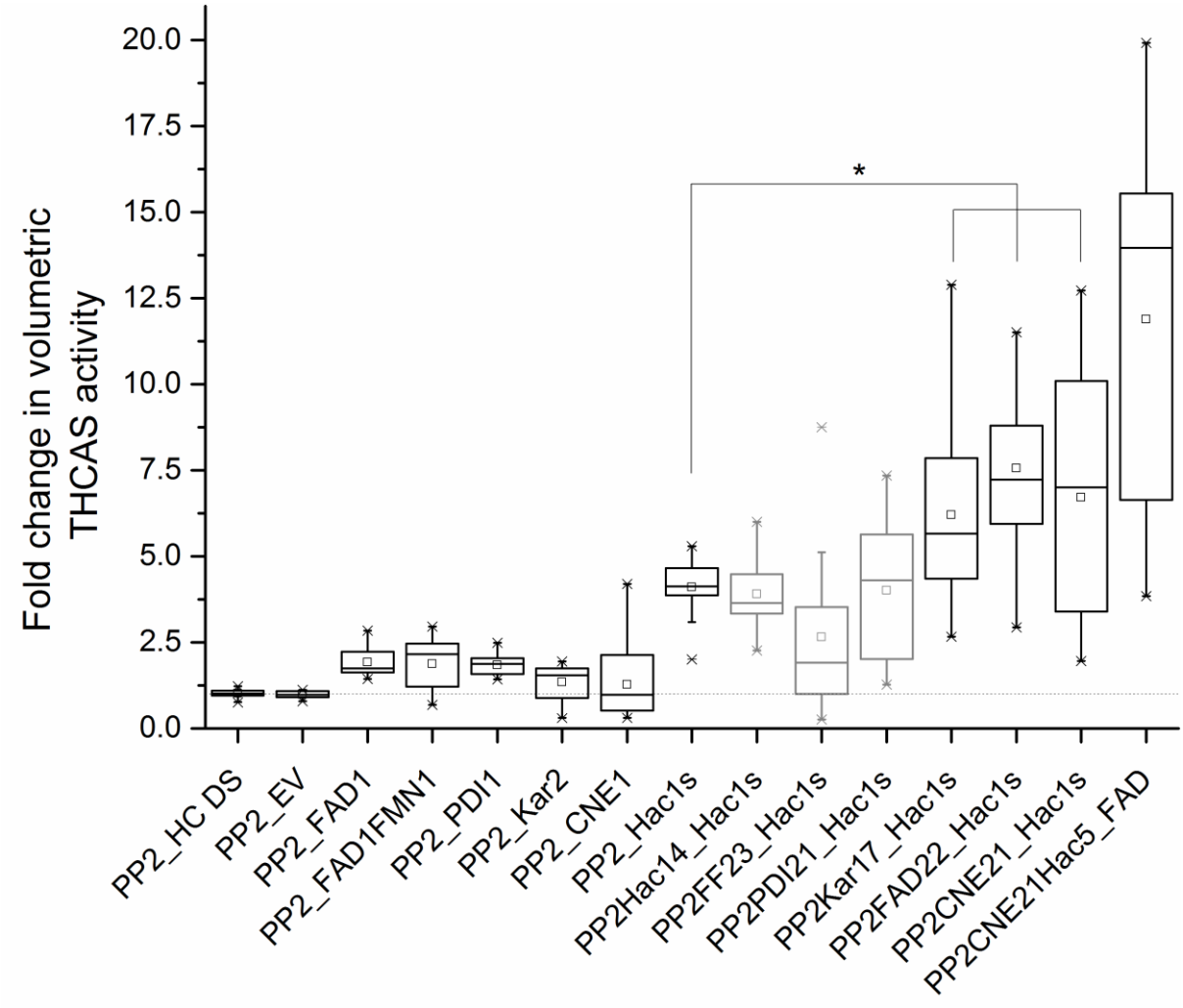

Fig. 4-4: Additive effects of co-produced helper proteins on THCAS activity levels. Volumetric activities were determined in technical duplicates and normalized on the average activity of the transformed strain cultivated in biological triplicates. Significantly increased activities (marked with *) were determined with Mann-Whitney-U test by comparing the normalized, volumetric THCAS activities of the screened colonies against the population of PP2_Hac1s (p = 0.05).

4.4.3. Optimized strain PP2CNE21Hac5_FAD1C7

We cultivated the optimized strain PP2CNE21Hac5_FAD1C7 and the initial strain PP2_HC at 15 °C as described previously (Zirpel et al., 2015). After 144 h of cultivation of the optimized strain, THCAS activities of 62.4 nkat g_{CDW}^{-1} (507 pkat ml^{-1}) intracellular and 9.78 nkat g_{CDW}^{-1} (79 pkat ml^{-1}) in the culture supernatant could be obtained (Fig. 4-5 A). Compared to the initial strain, the specific activity was 9.3-fold increased. The volumetric activity - due to lower maximum cell density obtained in this shaking flask cultivation setup – was 7.9-fold increased. The volumetric activities are shown in Fig. S VIII-7. Additionally, the relative amount of THCAS found intracellularly was increased in the optimized strain (after 144 h of cultivation at 15 °C: 86 % in PP2CNE21Hac5_FAD1C7 compared to 63 % in PP2_HC). After 144 h of cultivation, we adjusted the OD_{600} of the PP2CNE21Hac5_FAD1C7 culture to 100 and its pH to 4.85 and performed a whole cell biotransformation. After 8 h of incubation at 37 °C, the culture produced 3.05 g L^{-1} THCA corresponding to about 12.5 % g_{THCA} g_{CDW}^{-1}. At this point 85.2 % of the employed 10 mM CBGA were converted to THCA, although it is noteworthy that the bioconversion did not reach a plateau phase (Fig. 5 B).

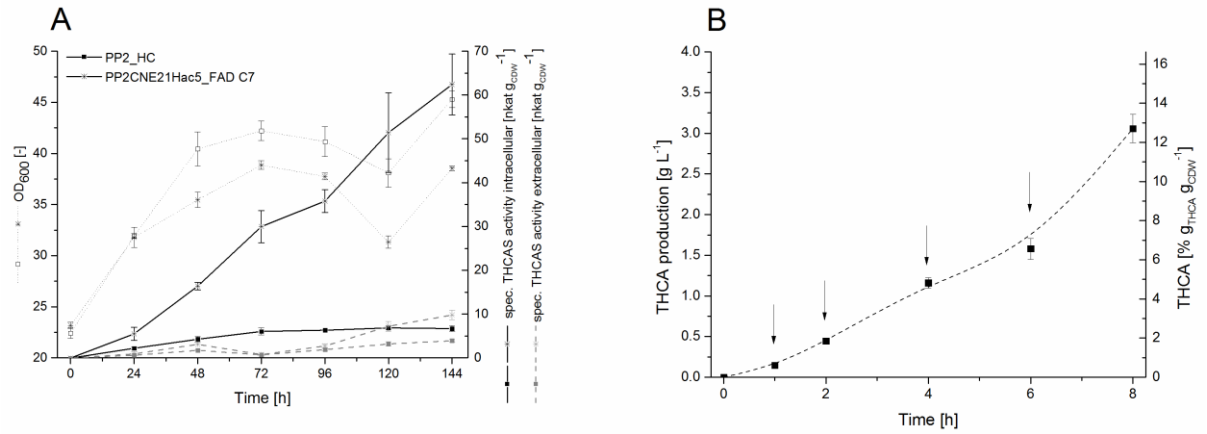

Fig. 4-5: A: Time-course of THCAS activity levels of initial strain PP2_HC and optimized strain PP2CNE21Hac5FAD C7 - Cultivation was performed at 15 °C, 0.5 % (v/v) methanol added every 24 h; B: Whole cell bioconversion of CBGA by strain PP2CNE21Hac5_FAD1C7 (OD_{600} 100) at 37 °C. Bioconversion was started with 2 mM CBGA and after every sampling additional 2 mM CBGA were added to the cells (marked with arrows).

4.5. DISCUSSION

4.5.1. Screening strategy and bottleneck identification of functional THCAS folding

In a previous study (Zirpel et al., 2015) we screened *K. phaffii* transformants for their THCAS activity and found a strain with a high gene copy number (GCN 24 ± 2) which should allow for a high protein synthesis rate. However, the THCAS activity was not proportionally increased compared to strains with a GCN of 1. Recently, studies of intracellular recombinant protein flux models supported that a higher GCN often correlates proportionally to protein synthesis rates as long as the secretory pathway capacity does not become saturated and limiting (Love et al., 2012; Pfeffer et al., 2011). Based on this, we expected this strain to possess a high potential for further enhancement of THCAS activity levels by identifying and overcoming these rate-limiting steps. We employed a standardized transformation, cultivation and screening protocol to evaluate the influence of co-overexpressed *K. phaffii* genes. To preserve a functional secretory network, the aspect of gene expression fine-tuning needs to be considered in the experiments, thus we tried to generate multi-copy integrations. By screening 21 clones per transformation, we expected to record different or unexpected integration events, such as head-to-head, head-to-tail or tail-to-tail integrations, which supposedly yield varying gene expression rates (Schwarzhans et al., 2016a, 2016b).

We identified PDI1p, CNE1p, FAD1p, Kar2p and Hac1p as positively influencing THCAS activity levels in *K. phaffii* strains. Thus, we assume that - amongst further issues not addressed in this study - a lacking pool of available cofactor FAD, the disulfide bond formation and iteration cycle as well as agglomeration processes lead to misfolding of the THCAS. Data suggest that *FAD1* expression is favorable for THCAS folding, but *FMN1* expression is not necessary to replenish the FAD pool. Admittedly, we cannot rule out any drawbacks of employing a T2A sequence (Beekwilder et al., 2014) for polycistronic expression which would conceal a positive influence of FMN1p co-production. With overexpression of the UPR-related transcription activator *Hac1s*, most of these bottlenecks are targeted in parallel, which is supported by the fact that it exerted the strongest impact on THCAS activities with an average 4.1-fold increase. However, we could not further increase the THCAS activities by increase of *Hac1s* expression (strain PP2Hac14_Hac1s, Fig. 4-4), while co-production of Hac1p and other

chaperones yielded even higher THCAS activity levels. Because the clonal variety of population PP2_Hac1s is low and most clones show a comparable increase in THCAS activity (Fig. S VIII-2), we assume that a single gene copy of *Hac1s* under control of the AOX1 promoter is already sufficient to maximally activate transcription of UPR related genes in this strain, *e.g.* because of saturation of binding sites of Hac1p for transcriptional activation. Thus, we investigated the combination of helper proteins by transformation of pAXh_Hac1s into the best expressing clones of PP2_CNE1, PP2_PDI1, PP2_Kar2, PP2_FAD1 and PP2_FAD1FMN1. Finally, the combination of *Hac1s*, *CNE1*, and *FAD1* resulted in a strain with 20-fold increased THCAS activity level (PP2CNE21Hac5FAD C7).

However, we are aware that gene expression under control of the AOX1 promoter might already be too strong, as *e.g.* co-production of Lhs1p showed a significantly negative effect (Fig. 4-3). Additionally, all genes are induced by methanol simultaneously with *thcas*, though for some genes a constitutive expression might be necessary to positively impact the THCAS production. This could be shown for a constitutive co-expression of *Yap1*, which significantly reduced the ER redox state of the cell and subsequently improved recombinant protein secretion (Delic et al., 2014). We also cannot exclude that all sequences of non-effective genes are correct as many of annotated *K. phaffii* genes have so far only been inferred from homology and not investigated experimentally, *e.g.* CPR5p.

4.5.2. Scope of the screening system and improved features of PP2CNE21Hac5FAD C7

It is difficult to make general suggestions which helper protein co-production will enhance recombinant protein titers as it mostly depends on the target protein's features. Therefore, a screening of several potential helper proteins is important. However, in studies of helper protein co-production to increase recombinant protein titers in *K. phaffii* often no data is given about the amount of transformed DNA or the GCN, number of screened clones or their variability. Even if a GCN is determined by qPCR, it does not necessarily correlate with the strain's productivity as has recently been comprehensively illustrated by Schwarzhans et al. (2016b), where green fluorescent protein production in *K. phaffii* transformants was correlated with qPCR- and whole-genome sequencing-determined GCNs. Thus, we decided not to determine a GCN by qPCR but to generate multi-copy integrations and screen 21 transformants of each population to support our conclusions with statistical significance.

The scope of the screening system specifies which properties of the screened colonies might be detected and enhanced ("You get what you screen for."). We previously showed that cultivation at lower temperatures (15 °C) is favorable for correct folding of THCAS (Zirpel et al., 2015). Reducing temperature is a suitable measure to increase specific target protein titers (Gasser et al., 2007). However, considering a platform organism producing cannabinoids from cheap carbon sources, a trade-off of target protein levels and metabolic rates for the production of precursors of CBGA such as geranyl diphosphate has to be made. By cultivating the cells at 28 °C, we screened for enhanced THCAS production at temperatures that would allow for a more feasible production process. The volumetric THCAS activity levels of strain PP2CNE21Hac5FAD C7 were increased 20-fold at 28 °C and 7.3-fold at 15 °C compared to PP2_HC, emphasizing that THCAS production was optimized for the temperature we screened at. To also allow for a more sensitive detection of secretory network disruption, we employed an increased methanol feeding rate putting the cells under increased ROS- and UPR-related stress. ROS will be produced when *K. phaffii* cells utilize methanol and upon excessive protein folding and misfolding in the ER (PDI1p-Ero1p cycle).

In case of PP2PDI21_Hac1s and PP2FF23_Hac1s this experimental setup resulted in severe flocculation and reduced final biomass in most but not all screened colonies presumably due to accumulation of excessive ROS (Delic et al., 2014). We also screened PP2FF23_Hac1s in an experimental setup with longer intervals for methanol feeding and no flocculation could be observed (data not shown). Therefore, we assume that these cells possess either an unbalanced secretory network or the secretory pathway capacities are limiting and thus did not further pursue enhancement of THCAS activities in these populations. Furthermore, we focused on the intracellular, volumetric THCAS activities of the different colonies to neglect clones with growth impairments and isolate clones with improved suitability for a whole cell bioconversion. Compared to the initial strain PP2_HC, the optimized strain PP2CNE21Hac5FAD C7 showed a higher THCAS retention inside the cell (86 % compared to 63 % in PP2_HC after 144 h at 15 °C). As THCAS is targeted to the cell vacuole, enzyme activity in the culture supernatant is unexpected. However, we could not detect cell lysis via microscopic analysis and rather assume a misdirection of the protein into secretory vesicles upon overexpression (Rothman and Stevens, 1986; Zirpel et al., 2015). Hence, we assume that the optimized strain exerts not only an improved intracellular THCAS activity but also an increased secretory pathway integrity.

4.6. CONCLUSION

We identified several bottlenecks during folding of the THCAS in *K. phaffii* and could counteract these by co-production of the foldase and protein disulfide isomerase PDI1p, the glycoprotein-associated chaperone CNE1p, the FAD synthetase FAD1p, the chaperone Kar2p and the UPR-related transcriptional activator Hac1p. Our data suggest that the potential of *Hac1s* overexpression is limiting in a wildtype strain as a single copy of *Hac1s* was sufficient to maximally activate UPR-related transcription. However, the secretory pathway capabilities could be further increased by combined expression of *Hac1s* with several other helper protein genes, although a comprehensive screening of the transformation populations was necessary to isolate clones with significantly increased THCAS activities. The strain with the highest THCAS activity was PP2CNE21Hac5FAD C7 - expressing *Hac1s*, *CNE1* and *FAD1* - which showed a 20-fold increase in activity levels compared to the starting strain PP2_HC and approximately more than 450-fold enhanced THCAS activity compared with the first reports from Taura in *K. phaffii* (Taura et al., 2007; Zirpel et al., 2015). This strain was able to produce 3.05 g L^{-1} THCA corresponding to 12.5 % g_{THCA} g_{CDW}^{-1} in a whole cell bioconversion of CBGA within 8 h of incubation. This highlights the possibilities of a cannabinoid production platform, whether it is the production of cannabinoids from a cheap carbon source or the controlled production of single cannabinoids from a precursor by production of a cannabinoid synthesizing enzyme. As the cannabidiolic acid synthase, cannabichromenic acid synthase and THCAS - the enzymes of *C. sativa* responsible for the production of the three main cannabinoids cannabidiolic acid, cannabichromenic acid and THCA - possess high sequence similarities (> 83 %), it is close at hand that similar protein titers and activities in *K. phaffii* could be achieved for those enzymes or improved enzyme variants of them. Findings might also prove applicable for the recombinant production of other similar enzymes of the class of berberine-bridge-enzyme-like enzymes.

4.7. REFERENCES

Beekwilder, J., van Rossum, H.M., Koopman, F., Sonntag, F., Buchhaupt, M., Schrader, J., Hall, R.D., Bosch, D., Pronk, J.T., van Maris, A.J.A., Daran, J.-M.M., 2014. Polycistronic expression of a β-carotene biosynthetic pathway in Saccharomyces cerevisiae coupled to β-ionone production. J. Biotechnol. 192, 383–392. doi:10.1016/j.jbiotec.2013.12.016

Buck, T.M., Wright, C.M., Brodsky, J.L., 2007. The activities and function of molecular chaperones in the endoplasmic reticulum. Semin. Cell Dev. Biol. 18, 751–761. doi:10.1016/j.semcdb.2007.09.001

Carlini, E.., 2004. The good and the bad effects of (−) trans-delta-9-tetrahydrocannabinol (Δ9-THC) on humans. Toxicon 44, 461–467. doi:10.1016/j.toxicon.2004.05.009

Carvalho, Â., Hansen, E.H., Kayser, O., Carlsen, S., Stehle, F., 2017. Designing microorganisms for heterologous biosynthesis of cannabinoids. FEMS Yeast Res. 17. doi:10.1093/femsyr/fox037

Damasceno, L.M., Anderson, K.A., Ritter, G., Cregg, J.M., Old, L.J., Batt, C.A., 2007. Cooverexpression of chaperones for enhanced secretion of a single-chain antibody fragment in Pichia pastoris. Appl. Microbiol. Biotechnol. 74, 381–389. doi:10.1007/s00253-006-0652-7

Daniel, B., Wallner, S., Steiner, B., Oberdorfer, G., Kumar, P., Van Der Graaff, E., Roitsch, T., Sensen, C.W., Gruber, K., Macheroux, P., 2016. Structure of a berberine bridge enzyme-like enzyme with an active site specific to the plant family Brassicaceae. PLoS One 11, 1–21. doi:10.1371/journal.pone.0156892

de Ruijter, J.C., Koskela, E. V., Frey, A.D., 2016. Enhancing antibody folding and secretion by tailoring the Saccharomyces cerevisiae endoplasmic reticulum. Microb. Cell Fact. 15, 87. doi:10.1186/s12934-016-0488-5

Delic, M., Graf, A., Koellensperger, G., Haberhauer-Troyer, C., Hann, S., Mattanovich, D., Gasser, B., 2014. Overexpression of the transcription factor Yap1 modifies intracellular redox conditions and enhances recombinant protein secretion. Microb. Cell 1, 376–86. doi:10.15698/mic2014.11.173

Delic, M., Rebnegger, C., Wanka, F., Puxbaum, V., Haberhauer-Troyer, C., Hann, S., K?llensperger, G., Mattanovich, D., Gasser, B., 2012. Oxidative protein folding and unfolded protein response elicit differing redox regulation in endoplasmic reticulum and cytosol of yeast. Free Radic. Biol. Med. 52, 2000–2012. doi:10.1016/j.freeradbiomed.2012.02.048

Gasser, B., Maurer, M., Rautio, J., Sauer, M., Bhattacharyya, A., Saloheimo, M., Penttilä, M., Mattanovich, D., 2007. Monitoring of transcriptional regulation in Pichia pastoris under protein production conditions. BMC Genomics 8, 179. doi:10.1186/1471-2164-8-179

Gu, L., Zhang, J., Du, G., Chen, J., 2015. Multivariate modular engineering of the protein secretory pathway for production of heterologous glucose oxidase in Pichia pastoris. Enzyme Microb. Technol. 68, 33–42. doi:10.1016/j.enzmictec.2014.10.006

Guerfal, M., Ryckaert, S., Jacobs, P.P., Ameloot, P., Van Craenenbroeck, K., Derycke, R., Callewaert, N., 2010.

The HAC1 gene from Pichia pastoris: characterization and effect of its overexpression on the production of secreted, surface displayed and membrane proteins. Microb. Cell Fact. 9, 49. doi:10.1186/1475-2859-9-49

Hale, S.J., Lovell, S.C., De Keyzer, J., Stirling, C.J., 2010. Interactions between Kar2p and its nucleotide exchange factors Sil1p and Lhs1p are mechanistically distinct. J. Biol. Chem. 285, 21600–21606. doi:10.1074/jbc.M110.111211

Inan, M., Aryasomayajula, D., Sinha, J., Meagher, M.M., 2006. Enhancement of protein secretion in Pichia pastoris by overexpression of protein disulfide isomerase. Biotechnol. Bioeng. 93, 771–778. doi:10.1002/bit.20762

Kepes, F., Schekman, R., 1988. The yeast SEC53 gene encodes phosphomannomutase. J. Biol. Chem. 263, 9155–9161.

Klabunde, J., Kleebank, S., Piontek, M., Hollenberg, C.P., Hellwig, S., Degelmann, A., 2007. Increase of calnexin gene dosage boosts the secretion of heterologous proteins by Hansenula polymorpha. FEMS Yeast Res. 7, 1168–1180. doi:10.1111/j.1567-1364.2007.00271.x

Lee, M.E., DeLoache, W.C., Cervantes, B., Dueber, J.E., 2015. A Highly Characterized Yeast Toolkit for Modular, Multipart Assembly. ACS Synth. Biol. 4, 975–986. doi:10.1021/sb500366v

Lin-Cereghino, J., Wong, W.W., Xiong, S., Giang, W., Luong, L.T., Vu, J., Johnson, S.D., Lin-Cereghino, G.P., 2005. Condensed protocol for competent cell preparation and transformation of the methylotrophic yeast Pichia pastoris. Biotechniques 38, 44, 46, 48.

Love, K.R., Politano, T.J., Panagiotou, V., Jiang, B., Stadheim, T.A., Love, J.C., 2012. Systematic single-cell analysis of pichia pastoris reveals secretory capacity limits productivity. PLoS One 7, 1–11. doi:10.1371/journal.pone.0037915

Moreno-Sanz, G., 2016. Can You Pass the Acid Test? Critical Review and Novel Therapeutic Perspectives of Δ 9 -Tetrahydrocannabinolic Acid A. *Cannabis* Cannabinoid Res. 1, 124–130. doi:10.1089/can.2016.0008

Parlati, F., Dominguez, M., Bergeron, J.J.M., Thomas, D.Y., 1995. Saccharomyces cerevisiae CNE1 Encodes an Endoplasmic Reticulum (ER) Membrane Protein with Sequence Similarity to Calnexin and Calreticulin and Functions as a Constituent of the ER Quality Control Apparatus. J. Biol. Chem. 270, 244–253. doi:10.1074/jbc.270.1.244

Pertwee, R.G., 2006. Cannabinoid pharmacology: the first 66 years. Br. J. Pharmacol. 147 Suppl, S163-71. doi:10.1038/sj.bjp.0706406

Pfeffer, M., Maurer, M., Köllensperger, G., Hann, S., Graf, A.B., Mattanovich, D., 2011. Modeling and measuring intracellular fluxes of secreted recombinant protein in Pichia pastoris with a novel 34S labeling procedure. Microb. Cell Fact. 10, 47. doi:10.1186/1475-2859-10-47

Puxbaum, V., Mattanovich, D., Gasser, B., 2015. Quo vadis? The challenges of recombinant protein folding and secretion in Pichia pastoris. Appl. Microbiol. Biotechnol. 99, 2925–2938. doi:10.1007/s00253-015-6470-z

Rothman, J., Stevens, T.H., 1986. Protein Sorting in Yeast : Mutants Defective in Vacuole Biogenesis Mislocalize

Vacuolar Proteins into the Late Secretory Pathway 47, 1041–51. doi:http://dx.doi.org/10.1016/0092-8674(86)90819-6

Rußmayer, H., Buchetics, M., Gruber, C., Valli, M., Grillitsch, K., Modarres, G., Guerrasio, R., Klavins, K., Neubauer, S., Drexler, H., Steiger, M., Troyer, C., Al Chalabi, A., Krebiehl, G., Sonntag, D., Zellnig, G., Daum, G., Graf, A.B., Altmann, F., Koellensperger, G., Hann, S., Sauer, M., Mattanovich, D., Gasser, B., 2015. Systems-level organization of yeast methylotrophic lifestyle. BMC Biol. 13, 80. doi:10.1186/s12915-015-0186-5

Schröder, M., 2008. Engineering eukaryotic protein factories. Biotechnol. Lett. 30, 187–196. doi:10.1007/s10529-007-9524-1

Schwarzhans, J.-P., Luttermann, T., Geier, M., Kalinowski, J., Friehs, K., 2017. Towards systems metabolic engineering in Pichia pastoris. Biotechnol. Adv. 35, 681–710. doi:10.1016/j.biotechadv.2017.07.009

Schwarzhans, J.-P., Wibberg, D., Winkler, A., Luttermann, T., Kalinowski, J., Friehs, K., 2016a. Integration event induced changes in recombinant protein productivity in Pichia pastoris discovered by whole genome sequencing and derived vector optimization. Microb. Cell Fact. 15, 84. doi:10.1186/s12934-016-0486-7

Schwarzhans, J.-P., Wibberg, D., Winkler, A., Luttermann, T., Kalinowski, J., Friehs, K., 2016b. Non-canonical integration events in Pichia pastoris encountered during standard transformation analysed with genome sequencing. Sci. Rep. 6, 38952. doi:10.1038/srep38952

Shoyama, Y.Y., Tamada, T., Kurihara, K., Takeuchi, A., Taura, F., Arai, S., Blaber, M., Morimoto, S., Kuroki, R., Shoyama, Y.Y., Morimoto, S., Kuroki, R., 2012. Structure and function of Δ1-tetrahydrocannabinolic acid (THCA) synthase, the enzyme controlling the psychoactivity of *Cannabis* sativa. J. Mol. Biol. 423, 96–105. doi:10.1016/j.jmb.2012.06.030

Steel, G.J., Fullerton, D.M., Tyson, J.R., Stirling, C.J., 2004. Coordinated activation of Hsp70 chaperones. Science 303, 98–101. doi:10.1126/science.1092287

Taura, F., Dono, E., Sirikantaramas, S., Yoshimura, K., Shoyama, Y., Morimoto, S., 2007. Production of Δ1-tetrahydrocannabinolic acid by the biosynthetic enzyme secreted from transgenic Pichia pastoris. Biochem. Biophys. Res. Commun. 361, 675–680. doi:10.1016/j.bbrc.2007.07.079

Tolner, B., Smith, L., Begent, R.H.J., Chester, K.A., 2006. Production of recombinant protein in Pichia pastoris by fermentation. Nat. Protoc. 1, 1006–1021. doi:10.1038/nprot.2006.126

Tu, B.P., 2000. Biochemical Basis of Oxidative Protein Folding in the Endoplasmic Reticulum. Science (80-.). 290, 1571–1574. doi:10.1126/science.290.5496.1571

Wu, S., Letchworth, G.J., 2004. High efficiency transformation by electroporation of Pichia pastoris pretreated with lithium acetate and dithiothreitol 36, 1–3.

Zirpel, B., Degenhardt, F., Martin, C., Kayser, O., Stehle, F., 2017. Engineering yeasts as platform organisms for cannabinoid biosynthesis. J. Biotechnol. 259, 204–212. doi:10.1016/j.jbiotec.2017.07.008

Zirpel, B., Stehle, F., Kayser, O., 2015. Production of Δ9-tetrahydrocannabinolic acid from cannabigerolic acid by whole cells of Pichia (Komagataella) pastoris expressing Δ9-tetrahydrocannabinolic acid synthase from *Cannabis* sativa l. Biotechnol. Lett. 37, 1869–1875. doi:10.1007/s10529-015-1853-x

CHAPTER 5

Elucidation of structure-function relationship of THCA and CBDA synthase from *Cannabis sativa* L.

Bastian Zirpel, Oliver Kayser, Felix Stehle

B.Z. and F.S. planned the experimental studies. B.Z. designed and generated all enzyme variants, performed all experimental studies and analyzed the data. O.K. coordinated and supervised the study. All authors contributed to write the manuscript.

Submitted on 07.02.2018 in *Journal of Biotechnology*

5.1. ABSTRACT

Cannabinoids are secondary natural products from the plant *Cannabis sativa* L. Therapeutic indications of cannabinoids currently comprise a significant area of medicinal research. We have expressed the Δ^9-tetrahydrocannabinolic acid synthase (THCAS) and cannabidiolic acid synthase (CBDAS) recombinantly in *Komagataella phaffii* and could detect eight different products with a cannabinoid scaffold after conversion of the precursor cannabigerolic acid (CBGA). Besides five products remaining to be identified, both enzymes were forming three major cannabinoids of *C. sativa* - Δ^9-tetrahydrocannabinolic acid (THCA), cannabidiolic acid (CBDA) and cannabichromenic acid (CBCA). In pursuit of improved enzyme properties for a biotechnological cannabinoid production, we performed site-directed mutagenesis to investigate the glycosylation pattern, the C-terminal berberine-bridge-enzyme (BBE) domain, the active site and the product specificity of both enzymes. The THCAS variant T_N89Q+N499Q (lacking two glycosylation sites) exerted about two-fold increased activity compared to wild-type enzyme. Variant T_H494C+R532C (additional disulfide bridge) exerted about 1.7-fold increased activity compared to wild-type enzyme and a shifted temperature optimum from 52 °C to 57 °C. We generated two CBDAS variants, C_S116A and C_A414V, with 2.8 and 3.3-fold increased catalytic activities for CBDA production. C_A414V additionally showed a broadened pH spectrum and a 19-fold increased catalytic activity for THCA production. These studies lay the groundwork for further research as well as biotechnological cannabinoid production.

5.2. INTRODUCTION

Cannabinoids are secondary natural products predominantly found in the oil compartments of trichomes of the plant *Cannabis sativa* L. Up to now more than 100 cannabinoids have been isolated (Rosenberg et al., 2017). Many of these phytocannabinoids are derived from the three major, most abundant acidic cannabinoids - namely Δ^9-tetrahydrocannabinolic acid-A (THCA), cannabichromenic acid (CBCA) and cannabidiolic acid (CBDA) - by non-enzymatic transformations and degradation reactions upon heat and light exposure as well as auto-oxidation (Crombie et al., 1968; Degenhardt et al., 2017). Since the discovery of the human endocannabinoid system, the potential pharmaceutical effects and applications of cannabinoids have been extensively studied. Nowadays, Δ^9-tetrahydrocannabinol (THC) is widely used as therapeutic agent in treatment of chemotherapy-associated nausea and vomiting, AIDS related loss of appetite as well as pain and muscle spasms in multiple sclerosis. Other potential applications are currently under investigation (Carlini, 2004; Chandra et al., 2017). While THCA does not elicit psycho-active effects in humans, it is currently examined for its immunomodulatory, anti-inflammatory, neuroprotective and anti-neoplastic effects (Moreno-Sanz, 2016). The other two primary, neutral cannabinoids cannabidiol (CBD) and cannabichromene (CBC) are currently not used as active pharmaceutical ingredients, but they are investigated for several therapeutical effects and features. CBD is investigated for its application in treatment of Alzheimer's disease, Parkinson's disease and epilepsy, as well as for its anti-tumor properties and neuroprotective efficacy (Pisanti et al., 2017). CBC is investigated for its anti-inflammatory, anti-fungal, antibiotic and analgesic effects (Elsohly et al., 1982; Maione et al., 2011; Romano et al., 2013).

In planta, the three major cannabinoids are produced by their respective enzymes from the precursor cannabigerolic acid (CBGA), the Δ^9-tetrahydrocannabinolic acid synthase (THCAS), the cannabidiolic acid synthase (CBDAS) and the cannabichromenic acid synthase (CBCAS). Coding sequences of the THCAS and CBDAS have been published (Sirikantaramas et al., 2004; Taura et al., 2007b) and THCAS has been purified to homogeneity from *Spodoptera frugiperda* Sf9 insect cells enabling the generation of a structural protein model (PDB: 3VTE) (Shoyama et al., 2012, 2005; Sirikantaramas et al., 2004). Furthermore, the THCAS has previously been expressed recombinantly in the yeasts *Saccharomyces cerevisiae* and *Komagataella phaffii* (formerly *Pichia pastoris*) (Taura et al., 2007a). The CBCAS protein has been identified, partially purified and characterized in the past (Morimoto et al., 1998), however until now - besides a filed patent containing a coding sequence - no further scientific research regarding the CBCAS has been published (Page and Stout, 2015).

The THCAS and CBDAS share a high sequence similarity of 83 % based on which a common ancestor was suggested initially (Taura et al., 2007b). Upon analysis of sequence variants of CBDAS and THCAS from different *C. sativa* L. strains, the CBDA synthase was considered as the ancestral synthase from which the THCAS evolved (Onofri et al., 2015). However, it is suggested that only a small number of amino acid residues would determine the product specificity of both these enzymes due to the functional similarities in their suspected catalytic mechanisms (Taura et al., 2007b). Elucidation of the crystal structure of the THCAS allowed the proposition of a catalytic mechanism of the THCAS. Shoyama et al. performed mutational studies of the THCAS and assumed a deprotonation of CBGA by the phenolate anion of Y484, which triggers the substrate oxidation by a hydride transfer from C3 of CBGA to the flavin adenine dinucleotide (FAD) moiety. Subsequent intramolecular cyclization of the carbon scaffold yields the tricyclic THCA product (Shoyama et al., 2012). While the substitution of Y484F abolished THCAS activity, Y417F, E442Q and H292A substitutions resulted in severely decreased enzyme

activity and these positions were hence presumed to play a major role in the catalytic mechanism, i.e. in substrate binding and stabilization. The FAD cofactor is bi-covalently bound to H114 and C176. Substitution H114A in both THCAS and CBDAS yielded inactive enzymes (Sirikantaramas et al., 2004; Taura et al., 2007b). Effects of other amino acid (AA) substitutions have been investigated as well either by recombinant production, purification and characterization of THCAS variants (Sirikantaramas et al., 2004) or by comparison of the coding sequences of CBDAS and THCAS with the respective cannabinoid contents and ratios in different *Cannabis* varieties (Onofri et al., 2015). The THCAS also contains a disulfide bond (C37, C99) and at least six *N*-glycosylation sites (N89, N168, N329, N467, N499), however two other possible sites (N297, N305) are insufficiently resolved in the published crystal structure (Shoyama et al., 2012).

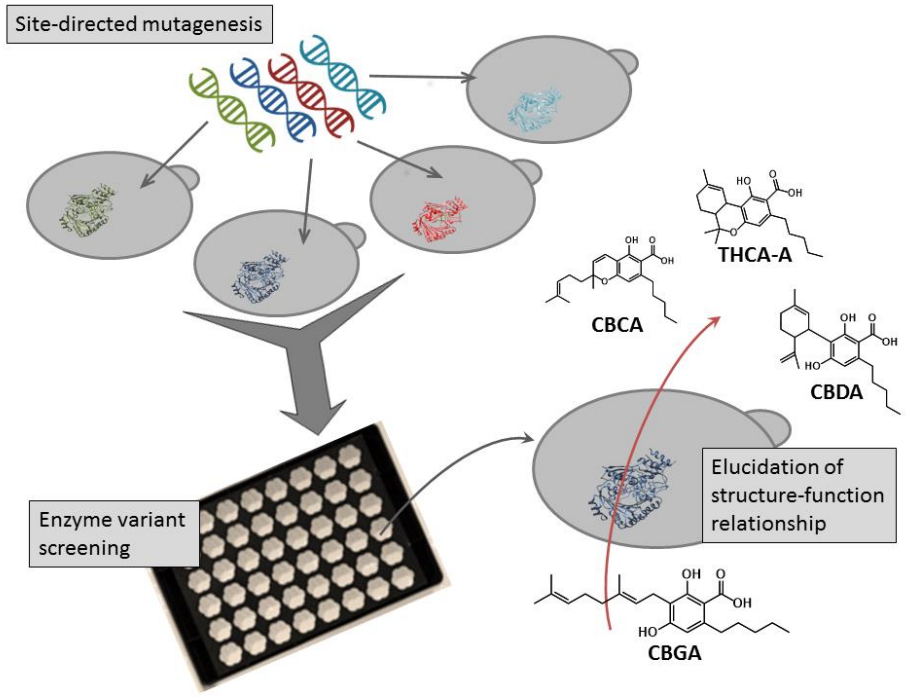

Fig. 5-1: Cannabinoids are secondary natural products from the plant *Cannabis sativa* L. with increasing pharmaceutical importance. We established a system for screening enzyme variants of the Δ^9-tetrahydrocannabinolic acid synthase and the cannabidiolic acid synthase regarding optimized properties, such as catalytic activity, stability, pH range and product specificity.

The THCAS has been recombinantly produced in *K. phaffii* and cultivation conditions have been optimized (Zirpel et al., 2015). The production has been improved manifold by co-production of several helper proteins which enabled sufficient functional enzyme expression for a low-throughput screening of rationally designed enzyme variants (Zirpel et al., 2017b). In pursuit of improved enzyme properties for a biotechnological cannabinoid production, we wanted to gain deeper insights into structure-function relationships of the THCAS and the CBDAS. By site-directed mutagenesis, we investigated the necessity of glycosylation sites and a disulfide bridge, influence of the berberine-bridge-enzyme (BBE)-domain and residues near the active site for catalytic activity of the enzymes.

5.3. MATERIAL AND METHODS

5.3.1. Materials

Chemicals were purchased from Invitrogen (Darmstadt, Germany), Sigma Aldrich (Darmstadt, Germany) and VWR (Darmstadt, Germany) if not stated otherwise. Δ^9-tetrahydrocannabinolic acid (THCA), Δ^9-tetrahydrocannabinol (THC) and cannabidiolic acid (CBDA) were purchased from THC Pharm GmbH (Frankfurt am Main, Germany). Cannabigerolic acid (CBGA) was purchased from Taros Chemicals GmbH & Co. KG (Dortmund, Germany).

5.3.2. Plasmid and yeast strains

E Escherichia coli DH5α was used for routine DNA transformations and plasmid isolations. A list of used primers is given in Table S1. A CBDAS cDNA sequence, codon-optimized for *K. phaffii* expression, was ordered from Centic Biotec (Heidelberg, Germany) (sequence in supplementary information). PCRs were performed using Q5 polymerase master mix (NEB, Frankfurt am Main, Germany) and the respective primers. Plasmids ppink_HC_Hac1S, pAX_Hac1s, pAX_pT and pAX_pC were generated via Gibson assembly. The vector backbones were amplified from ppink_HC (Invitrogen, Darmstadt, Germany) using primers ppink_fw and p_pAX_rv or from pAX_EV (Zirpel et al., 2017a) using primers p_pAX_fw and p_pAX_rv, respectively. The coding sequences were amplified from isolated genomic DNA of PichiaPink™ strain 2 (Invitrogen, Darmstadt, Germany) with primers p_Hac1_fw and p_Hac1s_rv2 (ppink_HC_Hac1s generation), p_Hac1_fw and p_Hac1s_rv (pAX_Hac1 generation), from ppink_HC_THCAS (Zirpel et al., 2015) with primers p_THCAS_fw and p_THCAS_rv (pAX_pT generation) or from ordered synthetic vector containing CBDAS cDNA with primers p_CBDAS_fw and p_CBDAS_rv (pAX_pC generation). For mutagenesis of pAX_pC and pAX_pT, primers were designed and PCRs performed as described in (Liu and Naismith, 2008), followed by 1 h *DpnI*-digest at 37 °C and subsequent transformation of 2 µL PCR mix into competent *E. coli* DH5α cells. Preparation and transformation of electro-competent cells of *K. phaffii* was performed according to previous reports (Lin-Cereghino et al., 2005; Wu and Letchworth, 2004). Strain PPHac was generated by transformation of electro-competent PichiaPink™ strain 2 with 5 µg of *SpeI*-linearized plasmid ppink_HC_Hac1S at 1800 V using the EquiBio Easyject Prima Electroporator, cultivation on pichia-adenine-dropout agar for 3 days at 30 °C and isolation of a white colony. Strain PP2_Hac1s was generated by transformation of *PmeI*-linearized vector pAX_Hac1s into strain PP2_HC (Zirpel et al., 2015) already expressing THCAS. Generation of strains producing CBDAS and THCAS enzyme variants was performed accordingly by transformation of electro-competent PPHac cells with 50-75 ng of the respective *PmeI*-linearized pAX-plasmids. Cells were grown for 2 days on YPD agar (10 g L^{-1} yeast extract, 20 g L^{-1} peptone, 2 g L^{-1} glucose, 20 g L^{-1} agar) with 100 µg mL^{-1} Zeocin.

5.3.3. Screening of THCAS and CBDAS variants in *K. phaffii*

PPHac was transformed with the respective *Pme*I-linearized vector DNA. Four colonies of each strain were transferred to a sterile 48-round-well Biolector® plate (m2p-labs, Baesweiler, Germany) filled with 900 µL modified BMGY (10 g L^{-1} yeast extract, 20 g L^{-1} peptone, 5 g L^{-1} casamino acids, 100 mM Bis-Tris-HCl buffer

pH 5.8, 13.8 g L^{-1} yeast nitrogen base, 0.4 mg L^{-1} biotin, 10 mg L^{-1} riboflavin, 1.5 % (w/v) glycerol) per well. Cells were cultivated using the Robolector™ system at 30 °C and 1200 rpm. After 22 h, expression cultures were inoculated by transferring 40 µL of each culture to a fresh well. After additional 12 h of cultivation and depletion of glycerol feeding of methanol was started. After 34 h and 36 h of cultivation, 8 µL feeding solution (25 % (v/v) methanol, 188 g L^{-1} sorbitol, 1.5 % (w/v) ammonium hydroxide) was added to each well, followed by addition of 16 µL feeding solution after 38 h, 40 h, 42 h and 44 h. After 47 h of cultivation, cells were harvested by centrifugation of 850 µL culture volume. The pellet was washed by resuspension in 850 µL wash buffer (10 mM Na-citrate buffer pH 4.6, 500 mM NaCl) before pellet was resuspended in 500 µL wash buffer for cell lysis. Cell lysis was performed by vortexing at maximum speed (All-in-One Vortexer, Biozym Scientific GmbH, Hessisch Oldendorf, Germany) with glass beads (0.25 - 0.5 mm diameter) for 20 min at 4 °C. The lysate was centrifuged and 90 µL of supernatant mixed with either 1 M Na-citrate buffer pH 4.6 or 1 M Bis-Tris-HCl buffer pH 6.5 for THCAS activity assays (300 µM CBGA, 37 °C, 1100 rpm, 30 min).

5.3.4. Purification of THCAS

A *K. phaffii* strain overexpressing *Hac1s* (Zirpel et al., 2017b) and *thcas* under control of the AOX1 promoter was cultivated at 15 °C as described in (Zirpel et al., 2015), but 100 mM Bis-Tris buffer pH 5.8 was used in BMMY medium. After 96 h of cultivation, the supernatant of 600 mL cell culture was collected by centrifugation (20 min, 29.000 x g, 4 °C). Supernatant was concentrated 16-fold by cross-flow filtration (Vivaflow 50R, Sartorius, Göttingen, Germany), supplemented with 15 mM imidazole and pH adjusted to 7.0. The concentrated supernatant was applied onto 2 x 1 mL HisTrap™ FF crude columns (in series) (GE Healthcare, Solingen, Germany) using the Bio-Rad Biologic DuoFlow system (Bio-Rad Laboratories GmbH, Munich, Germany). Washing was performed as described in the HisTrap^{FF} column manual at a flow rate of 1 mL min^{-1}. Elution was performed stepwise at 38 mM, 65 mM and 250 mM imidazole (Tris-HCl pH 7.0, 250 mM NaCl). Collected eluate at 250 mM imidazole was desalted to 100 mM Na-citrate buffer pH 4.6 using PD-10 desalting columns (GE Healthcare, Solingen, Germany).

5.3.5. Temperature and pH profiles

Investigation of residual activities of the THCAS at different pH values was performed with partially purified enzyme. For investigation of CBDAS and variant C_A414V, the respective strain was cultivated as described in (Zirpel et al., 2015). Cells were harvested by centrifugation and supernatant discarded. The cell pellet was resuspended in 100 mM Na-citrate buffer pH 4.6 to an OD_{600} of 100. Cells were lysed via french press and supernatant collected after centrifugation (20 min, 29.000 x g, 4 °C).

Supernatants or purified enzyme solutions were desalted in triplicates to the respective buffer solutions using Zeba™ Spin desalting columns (7K MWCO, 0.5 mL, Thermo Fisher Scientific, Schwerte, Germany) (100 mM Na-citrate in range pH 2.5 - pH 5.0; 100 mM Bis-Tris-HCl in range pH 5.5 - pH 6.5; 100 mM Tris-HCl in range pH 7.0 - pH 8.5). Residual activities were determined by activity assay at 37 °C (300 µM CBGA) and subsequent HPLC-MS and HPLC-DAD analysis.

Temperature profiles were obtained from determination of residual activities of the enzyme (100 mM Na-citrate, pH 4.6) at the respective temperature. Before addition of 300 µM CBGA, solutions were pre-incubated for 5 min at the respective temperature.

5.3.6. HPLC- DAD/ESI-MS

Activity assays were stopped by addition of 0.3 assay-volumes formic acid (FA) and 2.7 assay-volumes acetonitrile (ACN) followed by incubation on ice for 15 min. Supernatants were filtered (0.45 µm, Nylon) after centrifugation (13,100 x g, 4 °C, 20 min) and analyzed by HPLC-DAD (225 nm) and HPLC-ESI-MS (*m/z* 359.21) (Agilent 1260 Infinity HPLC, Waldbronn, Germany). Separation of compounds was performed on a Poroshell 120 EC-C18, 2.1 x 100 mm, 2.7 µm column (Agilent, Waldbronn, Germany) (0.7 mL min^{-1}, 40 °C, 35 % (v/v) H_2O with 0.1 % (v/v) FA, 65 % (v/v) ACN).

5.3.7. HPLC-ESI-MS^3

Partially purified THCAS and cell lysates of *K. phaffii* producing CBDAS or C_A414V were incubated with CBGA for 2 h or overnight at 37 °C and extracted with two assay-volumes of ethyl acetate. The ethyl acetate phase was evaporated and dried compounds solved in methanol. Compounds were separated using a EC 50/3 Nucleoshell RP18 2.7 µm column (Macherey Nagel, Düren, Germany) (0.35 mL min^{-1}, 30 °C, 38 % (v/v) H_2O with 0.1 % (v/v) FA, 62 % (v/v) ACN) and analyzed by HPLC-ESI-$HRMS^3$ on a high resolution LTQ-Orbitrap XL Mass spectrometer (Thermo Fisher Scientific, Waltham, USA) equipped with a HESI-II ion source (Thermo Fisher Scientific, Waltham, USA) coupled to an Agilent 1290 HPLC system (Agilent, Waldbronn, Germany).

5.3.8. NMR analysis of CBCA

Partially purified THCAS was employed in an overnight CBCA production from CBGA (35 mL 100 mM Tris-HCl buffer pH 7.7, 12.5 mg CBGA, 37 °C, 200 rpm). Extraction was performed by addition of 70 mL ethyl acetate and vortexing for 30 min. After centrifugation (5 min, 5.000 x g), ethyl acetate phase was collected and evaporated in a rotary evaporator (R200 system, Büchi, Essen, Germany). Compounds were resuspended in 200 µL methanol. Purification was performed on a Nucleodur C18 HTec, 250 x 10 mm, 5 µm column (Macherey Nagel GmbH & Co. KG, Düren, Germany) using an isocratic flow (4.0 mL min^{-1}, 40 °C, 35 % (v/v) H_2O/ 65 % (v/v) ACN). The separated peak was detected at 265 nm and fractionated with a FC-1 Dynamax fraction collector (Zinsser Analytik, Frankfurt am Main, Germany). After removal of solvent by rotary evaporation, lyophilization was performed (Alpha 1-4, Martin Christ, Osterode am Harz, Germany). Obtained compound was submitted for ^1H NMR measurement as described in (Zirpel et al., 2017a).

5.3.9. Shaking flask cultivation of PPHac_C_A414V+A46VT47A

Cultivation experiments were performed in triplicates. Precultures of 100 mL YPD medium (10 g L^{-1} yeast extract, 20 g L^{-1} peptone, 2 g L^{-1} glucose) in 1 L baffled shaking flasks were inoculated with cell material of strain PPHac_C_A414V+A46V+T47A cultivated for 24 h at 200 rpm and 30 °C. Cultures were harvested and cell pellets

resuspended in 100 mL fresh BMMY medium (10 g L^{-1} yeast extract , 20 g L^{-1} peptone, 5 g L^{-1} casamino acids , 100 mM Bis-Tris-HCl buffer pH 5.8, 13.8 g L^{-1} yeast nitrogen base, 0.4 mg L^{-1} biotin, 10 mg L^{-1} riboflavin, 1 % (v/v) methanol) to a starting OD_{600} of 20. Cultivation was performed in 1 L baffled shaking flasks at 15 °C and 200 rpm for 144 h. Methanol was fed every 24 h at a concentration of 0.5 % (v/v) after sampling was conducted. Samples were used for OD_{600} and THCAS activity determination of cells and cell culture supernatant. Cell lysis of each biological replicate was performed in technical duplicates in 100 mM Na-citrate buffer pH 4.6. The lysate was centrifuged and 100 µL of supernatant used for THCAS activity assays (300 µM CBGA, 37 °C, 1100 rpm, 30 min).

5.3.10. Whole cell bioconversion for CBDA production

Cells of PPHac_A414V+A46V+T47A from the shaking flask experiment were pelleted and resuspended in culture supernatant to an OD_{600} of 100 and pH adjusted to 4.85. Bioconversions were performed in triplicates by incubating 600 µL cell suspension for 8 h (1100 rpm, 37 °C, 2 mM CBGA starting concentration). After 1 h, 2 h, 4 h and 6 h, 2 mM additional CBGA were added after 50 µL sample was taken and diluted with 150 µL of stopping solution (10 % (v/v) FA, 90 % (v/v) ACN) for further HPLC-DAD (225 nm) and HPLC-MS analysis (*m/z* 359.21). The cell dry weight (CDW) was calculated with the correlation CDW (g L^{-1}) = 0.21 g L^{-1} x OD_{600} (Tolner et al., 2006). The THCA content of the cells was estimated by % $g_{product}$ g_{CDW}^{-1}= (100 % * $g_{product}$ L^{-1}) / ($g_{product}$ L^{-1} + g_{CDW} L^{-1}).

5.4. RESULTS AND DISCUSSION

5.4.1. Screening system for mutational studies of THCAS and CBDAS

We generated the strain PPHac by transforming *K. phaffii* cells (PichiaPink™ strain 2) with ppink_Hac1s - allowing for overproduction of Hac1s to enhance THCAS and CBDAS production (Guerfal et al., 2010). Only co-production of Hac1p allowed for cultivation of the cells in a multi-well plate format to obtain enzyme activities that were sufficient for detection of changes in activities and product specificities (Zirpel et al., 2017b). We ordered a codon-usage optimized cDNA of *cbdas* (see supplementary material) and generated several mutants of *thcas* and *cbdas* by site-directed mutagenesis. To increase the chance of generating single copy integrations, low amounts (50-70 ng) of *PmeI*-linearized plasmid DNA were transformed into PPHac cells. Cultivation and activity screenings were performed with four colonies of each transformation using the Robolector™ system. A table with all generated THCAS and CBDAS variants can be found in the supplementary material (Table S1). Selected variants are discussed in the next sections. After cultivation and expression at 30 °C, cells were harvested and lysed. The cell culture lysates were employed for activity assays at two different pH values (pH 4.6 and pH 6.5) to detect possible changes in the pH range of the enzyme variants. Enzyme activity was always normalized on the activity of co-cultivated PPHac cells producing THCAS or CBDAS wild-type enzymes, respectively. It should be noted that with the obtained data it is not possible to differentiate between altered catalytic properties of an enzyme variant and altered gene expression or enzyme folding.

5.4.2. Product specificity of THCAS and CBDAS

Recently it was suggested that the THCAS sequence arose from the CBDAS by duplication and divergence (Onofri et al., 2015). To verify if the THCAS still exhibits the capacity to form CBDA we used our previously established *K. phaffii* strain to produce THCA in high amounts (Zirpel et al., 2017b). To enable the detection of low product concentrations, the THCAS was partially purified from cultivation broth supernatant by concentration via cross-flow filtration and Ni-NTA purification (Fig. S IX-1). After desalting to assay buffer (100 mM Na-citrate buffer pH 4.6), the partially purified THCAS was used for CBGA conversion and the products were analyzed via HPLC-DAD/-MS/-MS^3. A chromatogram of the products with a *m/z* of 357.21 (HPLC-MS, negative mode) - which confers to *m/z* of cannabinoids CBDA, CBCA and THCA (Fig. 5-2) - is shown in Fig. 5-3.

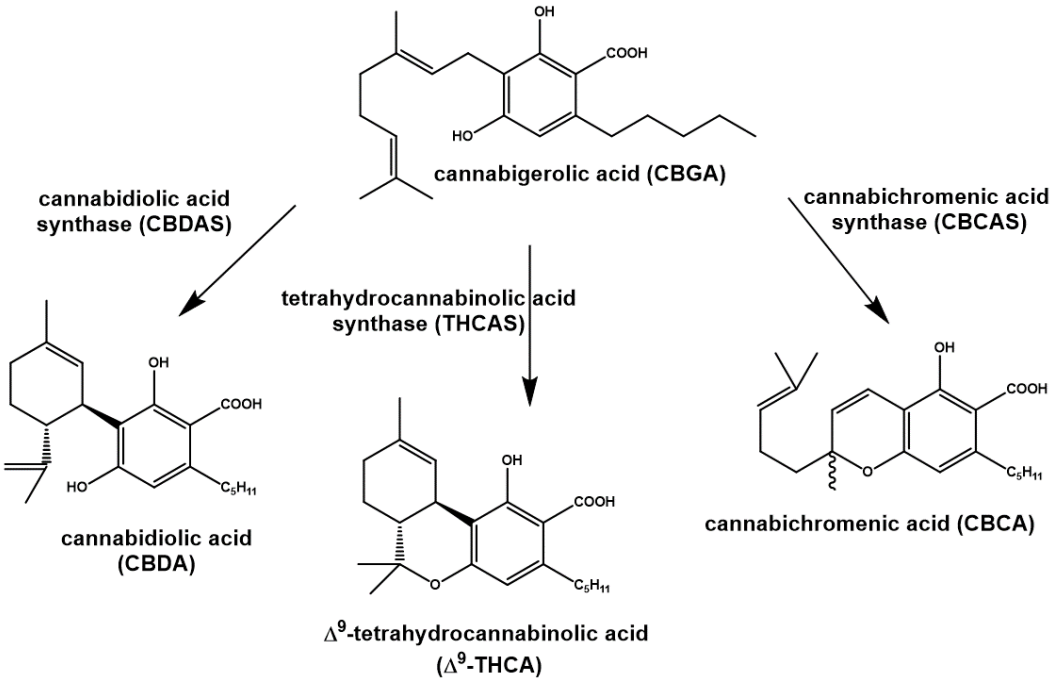

Fig. 5-2: Cannabinoid biosynthesis from precursor CBGA in *C. sativa* L.

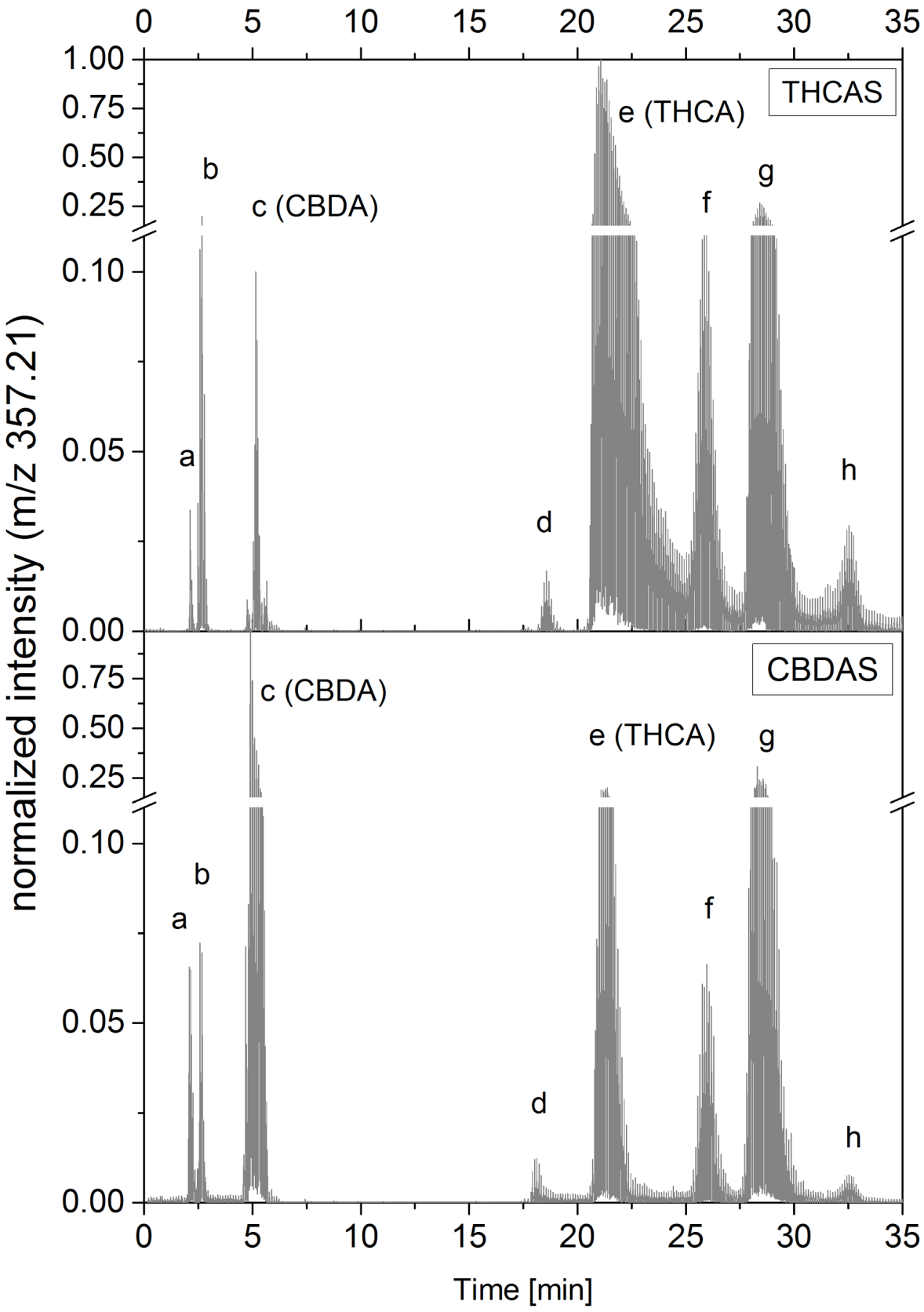

Fig. 5-3: Extracted ion chromatograms (*m/z* 357.21; negative mode) of CBGA conversions with THCAS (upper chromatogram) and CBDAS (bottom chromatogram) at 37 °C. Partially purified THCAS and PPHac_C (producing CBDAS) lysate supernatant were used, respectively. Eight different products (a - h) with a *m/z* of 357.21 could be detected in both assays.

Indeed, besides the formation of THCA the production of CBDA was verified by the comparison with commercial standards. Surprisingly, at least six additional product peaks (a, b, d, f - h) with the same *m/z* ratio were detected. The products were, however, not detected by incubation of enzyme solution without substrates or incubation of CBGA, CBDA and THCA without enzyme solution. Furthermore, we extracted the products from a full CBGA conversion and used them as substrates for a subsequent conversion by THCAS. Product ratios were consistent and no other products were obtained, indicating that THCAS is not using any obtained product as a substrate for subsequent catalytic reactions (results not shown). Additionally, product ratios were independent from incubation time and they were produced in a pH dependent manner (Fig. S IX-2). UV analysis of the formed products showed that the spectra of products f and g differ from the others by the existence of a single dominant absorption maximum at 255 nm (Fig. S IX-3) - contrary to the two absorption maxima at 225 nm and 270 nm of CBDA and THCA. So far only cannabichromenic acid (CBCA) is known to have such UV characteristics (Hazekamp et al., 2005). Subsequently, the partially purified THCAS was employed in an overnight assay at pH 7.7 at 37 °C to produce high amounts of product g for isolation and subsequent NMR analysis (Fig. S IX-7). Finally, by the comparison with previously published CBCA-NMR data (Lee and Wang, 2005), the production of CBCA by the THCAS was verified.

To determine whether the detected compounds share the same carbon scaffold, we analyzed the assays using HPLC-MS^3 in negative mode by collision induced fragmentation of ions with *m/z* 339.21 or *m/z* 313.21 of the fragmented precursor ion of *m/z* 357.21 (see Fig. S IX-4 for MS^2 data). The MS^3 spectra display a high similarity and show characteristic fragments for all product peaks (Fig. S IX-5, Fig. S IX-6). For each product a comparison with database spectra was performed (www.mzcloud.org) with available cannabinoid spectra of the three main cannabinoids CBDA, CBCA and THCA always being the most probable matches. Thus, we conclude that all products share the same carbon scaffold.

To check if the ancestral sequence of CBDA also exhibits such a broad product spectrum we also employed CBDAS from *K. phaffii* culture cell lysate to convert CBGA. In fact, the same product peaks were obtained, although in different ratios (Fig. 5-3). Morimoto et al. claimed that the CBCA synthase does not require molecular oxygen and cofactors and is therefore not related to THCAS or CBDAS (Morimoto et al., 1998). However, production of CBCA by both CBDAS and THCAS, which require molecular oxygen for FAD regeneration, substantiates that a potential CBCAS is indeed related to the other synthases.

Finally, the CBDAS and THCAS activities and product specificities were investigated at different pH values (Fig. 5-4 and Fig. S IX-2). The pH-optimum of both enzymes was determined at pH 4.5 for the production of CBDA and THCA, respectively, slightly lower as the previously reported pH 5.0 (Taura et al., 1996) or pH 5.5 - 6.0 (Taura et al., 1995). Most side-products are produced in less than 1 % of total product amounts. It has to be noted that due to a lack of commercial standards, we were only able to estimate product amounts via UV absorption at 225 nm (a, b, c, d, e, h) and 255 nm (f, g) (Fig. S IX-3), thus actual values slightly differ. While the THCAS produces several products (a, b, CBDA (c), d, THCA (e), h) in the same pH range, product formation of f and CBCA (g) was highest at pH values of 6.5 - 7.0. CBCA is the major side-product of the THCAS as it is produced up to 30 % of maximum THCAS activity at a pH of 7.0 (Fig. 5-4 A). Contrary, catalytic activity of CBDAS is lost at pH values above 6.5 (Fig. 5-4 B). Major side-products of the CBDAS are CBCA and THCA - each produced at about 5 % of the CBDA amount.

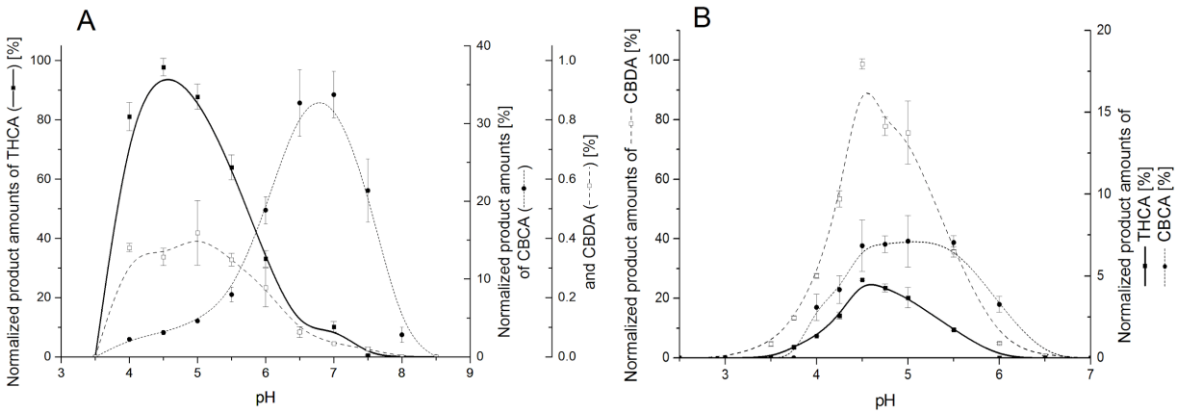

Fig. 5-4: pH-dependent product formations of THCAS (A) and CBDAS (B) regarding their conversion of CBGA to CBDA, THCA and CBCA. Product formation is normalized on the maximum amount of THCA (A) and CBDA (B), respectively. Amount of CBDA and THCA is estimated by UV absorption at 225 nm. Amount of CBCA is estimated by UV absorption at 255 nm.

Taking the different pH profiles (Fig. 5-4, Fig. S IX-2) and the UV spectra (Fig. S IX-3) into account, we conclude that product f possesses a carbon scaffold similar to CBCA and that it is catalyzed via the same mechanism, but the identity of the unknown products remains to be elucidated. Since we were only detecting m/z of 357.21, degradation products are unlikely but cannot be excluded. Cannabicyclolic acid is to our knowledge the only other cannabinoid with *m/z* of 357.21 and is occurring via irradiation of CBCA (Sirikantaramas et al., 2007). As the used separating setup is unsuitable for separation of enantiomers, structural isomers seem to be more likely.

For the first time we showed the product specificity of the THCAS and CBDAS. Besides five unknown products remaining to be identified, both enzymes are producing the three major cannabinoids of *C. sativa*: THCA, CBDA and CBCA. CBDA and THCA, which correspond to > 90 % of the formed products at pH 4.5, are the name-giving products of the CBDAS and THCAS, respectively. Additionally, depending on the pH, the THCAS has two main products - THCA at pH 4.5 and CBCA at pH 7 - and might also contribute to CBCA content within the plant depending on the pH in the oil compartments of the plant trichomes.

5.4.3. Structural elements of THCAS and CBDAS

The THCAS contains several structural elements that are supposedly imperative for correct folding. The structural model contains a disulfide bridge (C37, C99), a bi-covalently bound FAD cofactor (H114, C176) and at least six *N*-acetyl-glucosamine residues; however a potential glycosylation site (N305) is not fully resolved in the model. Substitution of C37S, C99S, C176A and H114A within the THCAS completely abolished its activity (Fig. 5-5 C), thus showing the imperative nature of these structural elements. In *K. phaffii*, THCAS is also produced in a hyperglycosylated form. Taura et al. recently investigated whether the glycosylation is necessary for THCAS activity by deglycosylating the purified THCAS with an endoglucanase (Taura et al., 2007a). The deglycosylated THCAS was reported to be 1.2-fold more active than the glycosylated form. Glycosylation and agglomeration processes of glyco-residues during protein biosynthesis might also present an obstacle for the cell for efficient THCAS production (Zirpel et al., 2017b). In this regard, we investigated the effects of each glycosylation on the THCAS and CBDAS production in *K. phaffii* and whether glycosylation in general is necessary for correct folding of THCAS (Fig. 5-5). We ordered a THCAS cDNA with seven AA substitutions lacking all glycosylation sites (T_deg: N65Q, N89Q, N168Q, N305Q, N329Q, N467Q, N499Q). However, no THCAS activity could be detected

in strain PPHac_T_deg (Fig. 5-5 B), thus we conclude that glycosylation is mandatory for functional expression in *K. phaffii*, but not necessary for maintaining THCAS tertiary structure and activity after folding. We further tried to assess the influence of every single potential glycosylation site of CBDAS and THCAS on the activity by step-wise substitution of the respective AAs (Fig. 5-5 A and B).

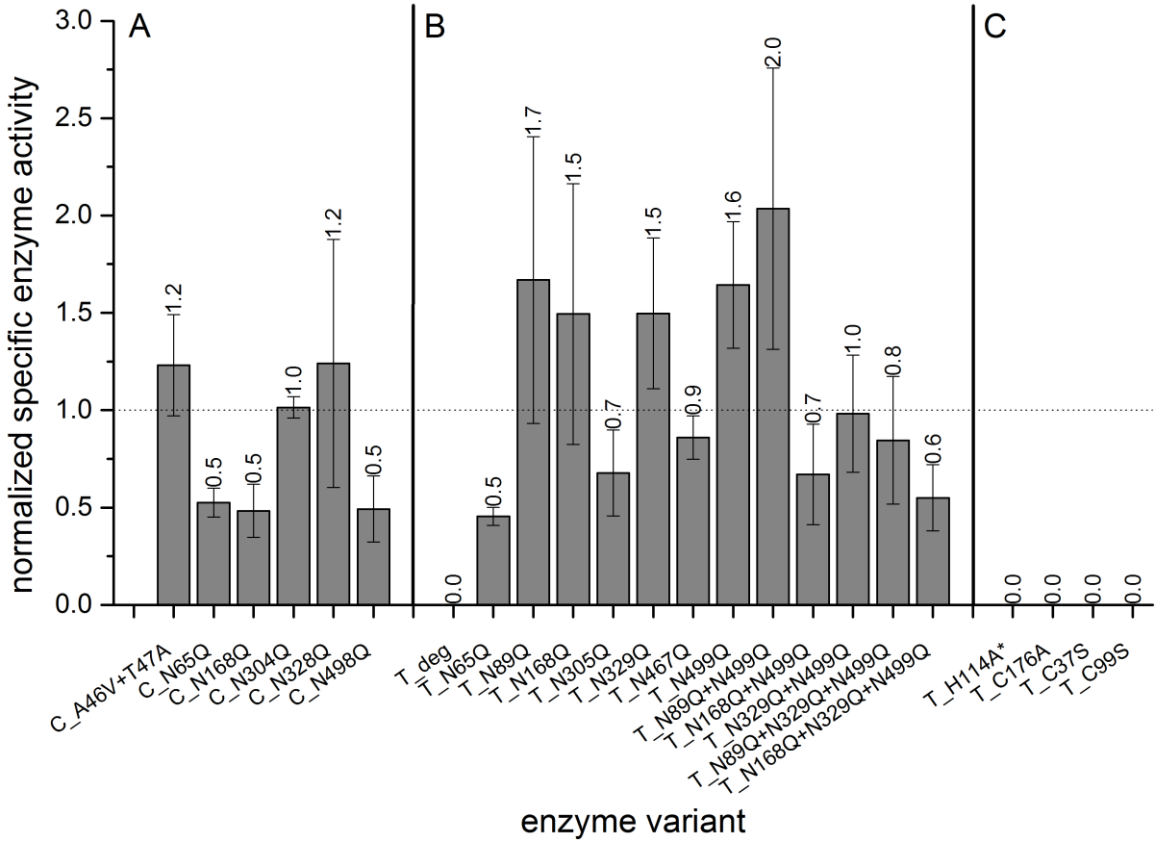

Fig. 5-5: Normalized, specific enzyme activities at pH 4.6 of CBDAS (C_) and THCAS (T_) variants with altered glycosylation pattern. Activities were normalized on the respective, specific wild-type enzyme activity. Result of THCAS variant T_H114A marked with * is taken from literature (Sirikantaramas et al., 2004).

THCAS variants T_N65Q, T_N305Q and T_N467Q showed decreased activity compared to the wild-type. In contrast, variants T_N89Q, T_N168Q, T_N329Q and T_N499Q showed about 1.5-fold increased activity. We subsequently combined multiple glycosylation site deletions that exerted on their own a positive effect (Fig. 5-5B). Unfortunately, decreasing enzyme activity is detected in the strains with increasing number of deleted glycosylation sites. However, strain PPHac_T_N89Q+N499Q with two deleted glycosylation sites still showed a 2.0-fold increased THCAS activity compared to PPHac_T. Due to lack of a structural model of the CBDAS we targeted the corresponding putative glycosylation sites (N45 (via enzyme variant C_A46V+T47A), N65, N168, N304, N328, N498). The CBDAS lacks potential sites at N89 and N467, but contains an additional putative site at N45. CBDAS variants C_A46V+T47A and C_N328Q showed slightly increased activity, while the other variants exerted similar or decreased activity compared to the wild-type (Fig. 5-5C).

It should be noted that a deletion of a glycosylation site within the THCAS does not exert the same effect as the corresponding substitution within the CBDAS, e.g. PPHac_T_N499Q showed 2.0-fold increase in activity compared to PP2_Hac_T while the activity of PPHac_C_N498Q was only 50 % of PPHac_C. It cannot be excluded that the substitution of N->Q itself influences enzyme activity or enzyme production due to a changed secondary

structure rather than the missing glyco-residues. However, if the deletion of a glycosylation site leads to an increased enzyme activity, it might indicate that the glycosylation - or hyperglycosylation in yeasts - exerts a negative effect on the folding of the enzyme.

5.4.4. C-terminal BBE-domain and catalytic base Y484 of THCAS

The THCAS as a member of the BBE-like-family possesses a loosely connected C-terminal region, the BBE-domain (AA477 to AA535). This region lacks stable secondary structures, however contains the AA residue Y484, the putative catalytic base of the active center of the THCAS and CBDAS essential for catalytic activity of the enzymes (Shoyama et al., 2012). We investigated amino acid residues of this domain by aligning the THCAS structural model to other enzyme models sharing high sequence and/or structural homology (Fig. 5-6 A). Several highly preserved and thus supposedly important residues were identified (e.g. K384, Y510, F531, Q535). The substitution of those AA residues with alanine resulted in enzyme variants with either no (Y510A, F531A, Q535A) or severely reduced (K384A) enzymatic activity (Fig. 5-6 B). These AA substitutions presumably remove crucial interactions between loop regions within the BBE domain and thus Y484 might no longer be stabilized in a position to act as the catalytic base. Several THCAS and CBDAS variants have been described in literature as well, although the effect of the AA-substitution on the positioning of the catalytic base in the active site was not considered. Onofri et al. suggested detrimental effects of substitutions L539Q, G489R and P476S on the catalytic activity of the CBDAS (Onofri et al., 2015). These AA substitutions would considerably affect stability within the BBE domain and/or positioning of the Y483 within the active site of the enzyme (Fig. 5-6 A). These findings might also suggest that Y483 of CBDAS acts as a catalytic base.

To further elucidate the characteristics of the BBE-domain, the C-terminus of the THCAS was shortened. The results substantiate the fragility of this domain as the deletion of AA538 to AA545 (T_537stop) fully diminished THCAS activity and step-wise addition of C-terminal amino acids AA538, AA539 and AA540 gradually re-established THCAS functionality and activity (Fig. 5-6 B). Additionally, we linked green fluorescent protein C-terminally to these THCAS variants (e.g. to T_537stop). Expression was detected by fluorescence, although no activity could be determined (data not shown). Thus, we conclude that folding of the THCAS was not affected but the dispositioning of the catalytic base Y484 most likely resulted in the complete loss of activity. Based on these findings we tried to stabilize the BBE-domain by introduction of an additional disulfide or salt bridge (Fig. 5-6 B and C). Most variants showed reduced activity (T_H494E+R532K, T_Q124C+H494C, T_Q124K+H494E, T_Y500K+L540E), however the variant T_H494C+R532C showed a 1.7-fold improved activity in our screening system.

We subsequently cultivated the strains PPHac_T_H494C+R532C and PPHac_T to compare enzyme stability in the cell lysate supernatants (Fig. 5-5C). Compared to the wild-type enzyme, the variant T_H494C+R532C showed 1.7-fold increased THCAS activity and the temperature optimum for catalytic activity was shifted from 52 °C to 57 °C. Furthermore, variant T_H494C+R532C exerted increased temperature stability with e.g. 30 % residual activity compared to complete loss of activity in the wild-type at 70 °C. This indicates that the disulfide bond was formed, however still has to be verified with additional experiments. While it remains to be elucidated whether the increased THCAS activity is due to an increased enzyme production or due to higher specific activities of the

enzyme, these features show that our approach to stabilize the C-terminal region in order to hold the Y484 in position is possible.

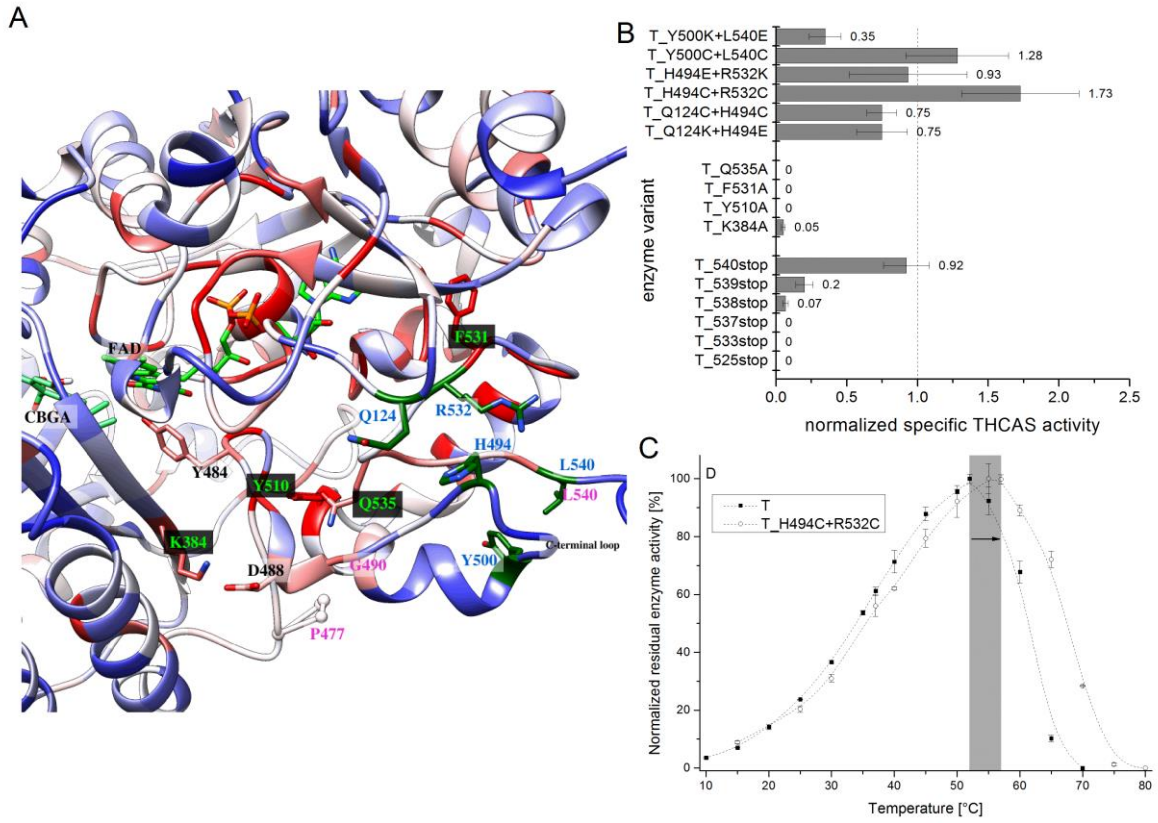

Fig. 5-6: A: Important amino acid residues of the BBE domain of the THCAS. The color code indicates the conservation of the amino acid residue (gradual shift from blue (low conservation) to red (high conservation)). The conservation was determined by aligning against structurally similar enzymes (PDBs: 5D79, 4UD8, 4DNS, 4PVE, 4PVJ, 3FW9, 5K8E, 3RJ8, 3W8W, 3POP, 2WDW, 1ZR6) to the structural model of THCAS (PDB: 3VTE). Green-labeled residues on dark background (K384, Y510, F531, Q535) were substituted by mutagenesis with alanine to generate inactive THCAS variants. Magenta-labeled residues (P477, G490, L540) mark corresponding THCAS positions that were reported crucial for the CBDAS (Onofri et al., 2015). Blue-labeled residues (Q124, H494, Y500, R532, L540) were substituted by mutagenesis with cysteine, lysine and/or glutamic acid to generate disulfide bond or salt-bridge stabilized enzyme variants. Graphic generated with Chimera (Pettersen et al., 2004). B: Normalized, specific enzyme activities at pH 4.6 of THCAS (T_) variants with altered BBE-domain. Activities were normalized on the respective, specific wild-type enzyme activity. C: Temperature profiles of THCAS wild-type (T) and variant T_H494+CR532C. Clarified cell lysates of PPHac_T and PPHac_T_H494C+R532C were incubated with 1 mM CBGA for 20 min at different temperatures. Before addition of CBGA, lysates were pre-incubated for 5 min at the respective temperature. Arrow indicates shift in temperature optimum from 52 °C to 57 °C in variant T_H494C+R532C by introducing cysteines for disulfide bridge formation.

5.4.5. Investigation of active site of THCAS and CBDAS

As described above, both the THCAS and CBDAS produced eight different products, although in different ratios. It was suggested that the THCAS sequence arose from the CBDAS by duplication and divergence and that only a few amino acid residues are responsible for differences in product specificity (Onofri et al., 2015; Taura et al., 2007b). We thus compared the sequences of CBDAS and THCAS and investigated whether AA differences near the active site are responsible for the different product specificities. The group of Taura et al. proposed a catalytic mechanism for THCA production by THCAS (Shoyama et al., 2012) and later on proposed another mechanism to account for the distinguished production of CBDA and THCA (Chandra et al., 2017). The catalytic base either

catalyzes deprotonation of *O*6´ of CBGA to produce THCA or deprotonation of a terminal methyl group of the geranyl residue of CBGA to produce CBDA.

A synthetic cDNA coding for a THCAS with 12 AA substitutions (T_12) (Fig. 5-7 A) was constructed, substituting AA residues near the active site with the respective AA of the CBDAS. Unfortunately, the strain PPHac_T_12 did not show detectable THCAS or CBDAS activity. We subsequently screened THCAS variants with single AA substitutions near the active site (Fig. 5-7 B). Variants T_Q69H and T_K377Q+K378N+T379G showed activities comparable to the wild-type enzyme, however most of the enzyme variants showed strongly decreased THCAS activity without enhanced CBDA production. Interestingly, the changes A415V and A116S resulted in almost inactive THCAS variants. Therefore, AA residues of the CBDAS were changed (S116A, V414A) to the homologous residues of THCAS (Fig. 5-7 C). In our screening system the strains PPHac_C_S116A and PPHac_C_A414V showed about 2.8- and 3.3-fold increased CBDA production compared to the wild-type CBDAS, respectively. The fact that AA414 is located directly in the active site and AA116 is proximal to the proposed catalytic base Y483 (of CBDAS) (Fig. 5-7 A) indicates that rather the specific activity of the CBDAS variants is increased and not their production within the cells. Product specificity and pH profile of C_A414V and CBDAS wild-type were compared (Fig. 5-7 D). Substitution of A414V yields a CBDAS variant displaying not only about 3-fold higher catalytic activity for the production of CBDA, but also characteristics of the THCAS, i.e. about 19-fold higher catalytic activity for the production of THCA and a broadened pH spectrum for the production of CBDA, THCA and CBCA. This is accompanied with a shift of the pH optimum from pH 4.5 to pH 5.0 regarding CBDA and THCA. Assuming that the enzyme production in strains PPHac_C_A414V, PPHac_C and PPHac_T is equivalent, the catalytic activity for the combined cannabinoid production of variant C_A414V is about 4.4-fold higher compared to CBDAS wild-type and about 2-fold higher than THCAS wild-type enzyme at pH 4.6. Contrary, the variant C_S116A showed the same increase in catalytic activity for the production of THCA and CBDA, respectively, while the pH range and pH optimum was not altered (data not shown). Furthermore, we investigated whether combination of both AA substitutions would be beneficial. Variant C_S116A+A414V though showed a decreased activity compared to the variants with single AA substitutions (Fig. 5-7 C).

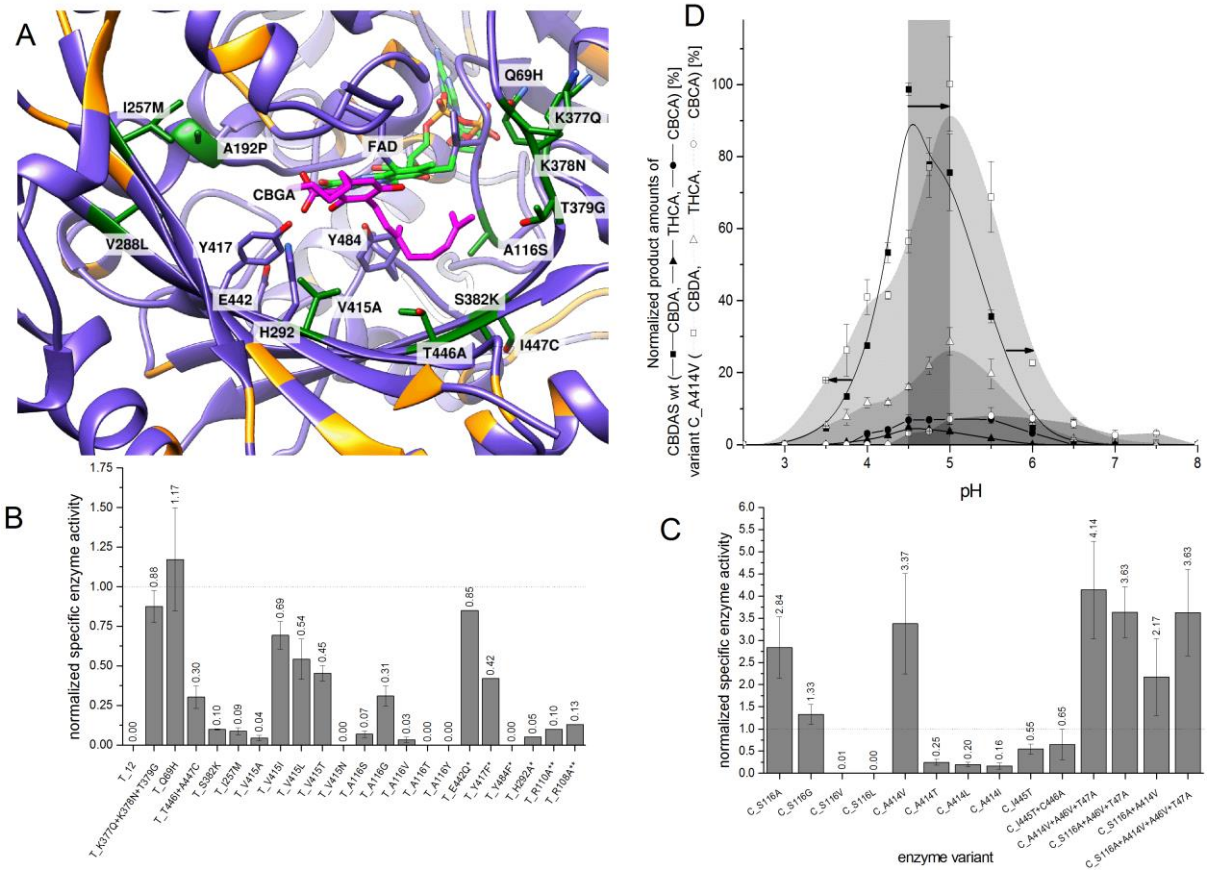

Fig. 5-7: A: Amino acid differences between THCAS and CBDAS sequences near active site. Orange and dark green: THCAS AA residues different to CBDAS residues. Magenta: Potential position of CBGA in active site. Light green: FAD cofactor. Dark green: 12 AA residues of THCAS near active site as potential targets for mutagenesis. Numberings refer to AA residues of THCAS. Graphic generated with Chimera (Pettersen et al., 2004). B + C: Normalized specific enzyme activities at pH 4.6 of THCAS (B) and CBDAS (C) variants. Activities were normalized on the respective, specific wild-type enzyme activity. Results of THCAS variants marked with * (Shoyama et al., 2012) and ** (Sirikantaramas et al., 2004) are taken from literature. D: pH-dependent CBDA, CBCA and THCA production of CBDAS wild-type and variant C_A414V. Product formation is normalized on the maximum amount of CBDA. Amount of CBDA and THCA is estimated by UV absorption at 225 nm. Amount of CBCA is estimated by UV absorption at 255 nm.

We further generated other enzyme variants of THCAS and CBDAS with changed amino acids at both of these positions (Fig. 5-7 B, C). Variants T_V415I, T_V415L and T_V415T exerted at least 50 % remaining THCAS activity while T_V415N showed no residual activity, suggesting that the size of the residue at this position is important. An alanine residue is presumably too small to stabilize surrounding AA residues and thus CBGA in a catalytically favorable position. Activities of enzyme variants with AA116 substitutions suggest that the proximal catalytic base Y484 (Y483 of CBDAS) is in both enzymes in a catalytically favorable position when an alanine is present at position 116. Smaller or bulkier AA residues at position 116 yield less active or inactive enzyme variants. Nonetheless, it is important to note that changes at AA116 do not alter the product specificity of the enzyme as is the case in position AA414 (corresponds to AA415 of THCAS). Strains producing CBDAS variants containing additional substitutions of A46V+T47A showed slightly increased activities compared to the strains producing variants without these substitutions as already described in the previous section.

In addition to T_12 being inactive, exchange of individual AA residues near the active site of the THCAS to its corresponding AA residue of the CBDAS did not alter the product specificity at all. However, the exchange of A414V within the CBDAS did influence product specificity, catalytic activity and pH profile of the enzyme. This indicates that the different product specificity between both enzymes is not only determined by AAs near the active

center and that more distant AA residues have to be considered for mutagenesis studies. It should also be noted that the available crystal structure of the THCAS was obtained without a bound substrate within the active site and therefore in the future crystal structures of the CBDAS and THCAS and/or their variants including substrate analogues will be helpful.

Nevertheless, our findings offer more insights into the catalytic mechanisms of the enzymes and the possibility to investigate additional enzyme variants. We also identified and characterized the improved CBDAS variant C_A414V. With its pH optimum shifted from pH 4.5 to pH 5.0 and a broadened pH range, this variant presents a more promising catalyst for the CBDA production in yeasts as it better fits the intracellular pH values.

5.4.6. Production of variant C_A414V+A46V+T47A in *K. phaffii* and whole cell bioconversion of CBGA

To conclude the experimental series, the strain PPHac_C_A414V+A46V+T47A was cultivated in shaking flasks at 15 °C as described in (Zirpel et al., 2015). After 144 h of incubation, the culture showed activities of 62.9 pkat mL^{-1} (8.2 nkat g_{CDW}^{-1}) intracellularly and 36.7 pkat mL^{-1} (4.7 nkat g_{CDW}^{-1}) extracellularly for the production of CBDA as well as 21.1 pkat mL^{-1} (2.7 nkat g_{CDW}^{-1}) intracellularly and 13.0 pkat mL^{-1} (1.7 nkat g_{CDW}^{-1}) extracellularly for the production of THCA (Fig. 5-8 A). Additionally, at the end of the cultivation the OD_{600} of the cell culture was adjusted to 100 and the pH to 4.85 for the whole cell bioconversion of CBGA to THCA and CBDA. After 6 h of incubation at 37 °C, cells were able to produce 0.42 g_{CBDA} L^{-1} and 0.13 g_{THCA} L^{-1} corresponding to 2.0 % g_{CBDA} g_{CDW}^{-1} and 0.63 % g_{THCA} g_{CDW}^{-1}, respectively (Fig. 5-8). This strain was able to produce similar amounts of cannabinoids as described for THCA production in PP2_HC previously (Zirpel et al., 2015) and thus shows the interchangeability of the last catalyst in the cannabinoid biosynthesis. However, strain PPHac_C_A414V+A46V+T47A shows low product specificity. Besides a high cannabinoid production, the ability to tailor the cannabinoid content and type by expressing different *thcas* or *cbdas* mutants is likewise important and thus further research on structure-function relationship regarding product specificity is necessary.

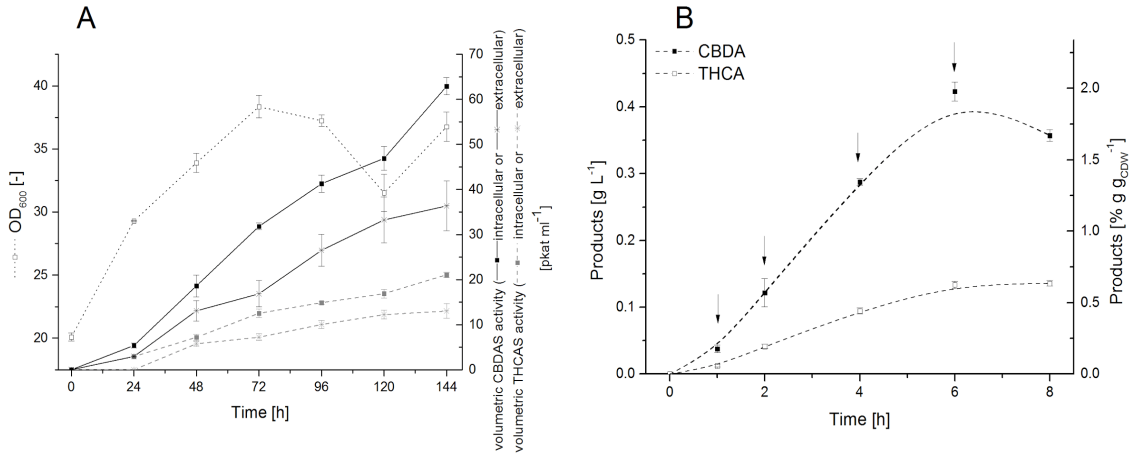

Fig. 5-8: A: Shaking flask cultivation of PPHac_C_A414V+A46V+T47A at 15 °C, 0.5 % (v/v) methanol added every 24 h; B: Whole cell bioconversion of CBGA by strain PPHac_T_A414V+A46V+T47A (OD_{600} 100) at 37 °C. Bioconversion was started with 2 mM CBGA and after every sampling additional 2 mM CBGA were added to the cells (marked with arrows).

5.5. CONCLUSION

We have expressed the *thcas* and *cbdas* recombinantly in *K. phaffii* and could detect up to eight different products for the conversion of CBGA that share a cannabinoid carbon scaffold. The major products of both enzymes were CBDA, THCA and CBCA, although produced in different ratios. The THCAS possesses two main products in THCA at pH 4.5 and CBCA at pH 7.0, the pH optimum of the CBDAS for production of its main product CBDA is pH 4.5. Five side-products remain to be identified.

A screening system for mutational studies of THCAS and CBDAS in *K. phaffii* using a *Hac1s* co-expressing strain was established and several promising enzyme variants of THCAs and CBDAS were identified laying the groundwork for biotechnological applications as well as proceeding research. Structural elements of both enzymes were investigated - in detail the glycosylation pattern and the BBE-domain. A THCAS variant without glycosylation sites (T_deg) yielded no active enzyme, thus demonstrating the necessity of glycosylation sites for the functional expression of THCAS in *K. phaffii*. In general, decreasing enzyme activity is detected in the strains with increasing number of deleted glycosylation sites. However, not all glycosylation sites are necessary for the functional expression. In fact, strain PPHac_T_N89Q+N499Q (THCAS variant lacking two glycosylation sites) exerted about 2.0-fold increased activity compared to strain PPHac_T. The importance of the integrity of the BBE domain which contains the proposed catalytic base Y484 (Y483 of CBDAS) was demonstrated. Strain PPHac_T_H494C+R532C (THCAS variant with potential disulfide bridge within BBE-domain) exerted about 1.7-fold increased activity compared to strain PPHac_T. In addition, the temperature optimum of this variant was shifted from 52 °C to 57 °C indicating successful stabilization of the BBE-domain.

While we could not elucidate how to change the product specificity of the THCAS, we generated two CBDAS variants with increased activities. Compared to the CBDAS wild-type, variant C_S116A showed about 2.8-fold increased catalytic activity for the production of CBDA without changing the product specificity. Variant C_A414V displayed about 3.3-fold increased catalytic activity for the production of CBDA and changed product specificity with about 19-fold increased activity for the production of THCA. This was accompanied by a broadened pH spectrum and a shift of pH optimum from pH 4.5 to pH 5.0 and provides the fundament for biotechnological applications. These findings offer more insights into the catalytic mechanisms of THCA and CBDA production. However, additional research for elucidation of structure-function relationships regarding the enzyme product specificity is necessary.

5.6. REFERENCES

Carlini, E.., 2004. The good and the bad effects of (−) trans-delta-9-tetrahydrocannabinol (Δ9-THC) on humans. Toxicon 44, 461–467. doi:10.1016/j.toxicon.2004.05.009

Chandra, S., Lata, H., ElSohly, M.A., 2017. *Cannabis* sativa L. - Botany and Biotechnology. Springer International Publishing, Cham. doi:10.1007/978-3-319-54564-6

Crombie, L., Ponsford, R., Shani, A., Yagnitinsky, B., Mechoulam, R., 1968. Hashish components. Photochemical production of cannabicyclol from cannabichromene. Tetrahedron Lett. 9, 5771–5772. doi:10.1016/S0040-4039(00)76346-5

Degenhardt, F., Stehle, F., Kayser, O., 2017. The Biosynthesis of Cannabinoids, in: Preedy, V. (Ed.), Handbook of *Cannabis* and Related Pathologies. Elsevier, pp. 13–23. doi:10.1016/B978-0-12-800756-3.00002-8

Elsohly, H.N., Turner, C.E., Clark, A.M., Elsohly, M.A., 1982. Synthesis and Antimicrobial Activities of Certain Cannabichromene and Cannabigerol Related Compounds. J. Pharm. Sci. 71, 1319–1323. doi:10.1002/jps.2600711204

Guerfal, M., Ryckaert, S., Jacobs, P.P., Ameloot, P., Van Craenenbroeck, K., Derycke, R., Callewaert, N., 2010. The HAC1 gene from Pichia pastoris: characterization and effect of its overexpression on the production of secreted, surface displayed and membrane proteins. Microb. Cell Fact. 9, 49. doi:10.1186/1475-2859-9-49

Hazekamp, A., Peltenburg, A., Verpoorte, R., Giroud, C., 2005. Chromatographic and Spectroscopic Data of Cannabinoids from *Cannabis* sativa L. J. Liq. Chromatogr. Relat. Technol. 28, 2361–2382. doi:10.1080/10826070500187558

Lee, Y.R., Wang, X., 2005. Concise Synthesis of Biologically Interesting (±)-Cannabichromene, (±)-Cannabichromenic Acid, and (±)-Daurichromenic Acid. Bull. Korean Chem. Soc. 26, 1933–1936. doi:10.5012/bkcs.2005.26.12.1933

Liu, H., Naismith, J.H., 2008. An efficient one-step site-directed deletion, insertion, single and multiple-site plasmid mutagenesis protocol. BMC Biotechnol. 8, 91. doi:10.1186/1472-6750-8-91

Maione, S., Piscitelli, F., Gatta, L., Vita, D., De Petrocellis, L., Palazzo, E., de Novellis, V., Di Marzo, V., 2011. Non-psychoactive cannabinoids modulate the descending pathway of antinociception in anaesthetized rats through several mechanisms of action. Br. J. Pharmacol. 162, 584–596. doi:10.1111/j.1476-5381.2010.01063.x

Moreno-Sanz, G., 2016. Can You Pass the Acid Test? Critical Review and Novel Therapeutic Perspectives of Δ 9 -Tetrahydrocannabinolic Acid A. *Cannabis* Cannabinoid Res. 1, 124–130. doi:10.1089/can.2016.0008

Morimoto, S., Komatsu, K., Taura, F., Shoyama, Y., 1998. Purification and characterization of cannabichromenic acid synthase from *Cannabis* sativa. Phytochemistry 49, 1525–9.

Onofri, C., de Meijer, E.P.M., Mandolino, G., 2015. Sequence heterogeneity of cannabidiolic- and tetrahydrocannabinolic acid-synthase in *Cannabis* sativa L. and its relationship with chemical phenotype.

Phytochemistry 116, 57–68. doi:10.1016/j.phytochem.2015.03.006

Page, J., Stout, J., 2015. CANNABICHROMENIC ACID SYNTHASE FROM *CANNABIS* SATIVA. WO2015196275.

Pettersen, E.F., Goddard, T.D., Huang, C.C., Couch, G.S., Greenblatt, D.M., Meng, E.C., Ferrin, T.E., 2004. UCSF Chimera - A visualization system for exploratory research and analysis. J. Comput. Chem. 25, 1605–1612. doi:10.1002/jcc.20084

Pisanti, S., Malfitano, A.M., Ciaglia, E., Lamberti, A., Ranieri, R., Cuomo, G., Abate, M., Faggiana, G., Proto, M.C., Fiore, D., Laezza, C., Bifulco, M., 2017. Cannabidiol: State of the art and new challenges for therapeutic applications. Pharmacol. Ther. 175, 133–150. doi:10.1016/j.pharmthera.2017.02.041

Romano, B., Borrelli, F., Fasolino, I., Capasso, R., Piscitelli, F., Cascio, M., Pertwee, R., Coppola, D., Vassallo, L., Orlando, P., Di Marzo, V., Izzo, A., 2013. The cannabinoid TRPA1 agonist cannabichromene inhibits nitric oxide production in macrophages and ameliorates murine colitis. Br. J. Pharmacol. 169, 213–229. doi:10.1111/bph.12120

Rosenberg, E.C., Patra, P.H., Whalley, B.J., 2017. Therapeutic effects of cannabinoids in animal models of seizures, epilepsy, epileptogenesis, and epilepsy-related neuroprotection. Epilepsy Behav. 70, 319–327. doi:10.1016/j.yebeh.2016.11.006

Shoyama, Y., Takeuchi, A., Taura, F., Tamada, T., Adachi, M., Kuroki, R., Shoyama, Y., Morimoto, S., 2005. Crystallization of Δ 1 -tetrahydrocannabinolic acid (THCA) synthase from *Cannabis* sativa. Acta Crystallogr. Sect. F Struct. Biol. Cryst. Commun. 61, 799–801. doi:10.1107/S1744309105023365

Shoyama, Y., Tamada, T., Kurihara, K., Takeuchi, A., Taura, F., Arai, S., Blaber, M., Shoyama, Y., Morimoto, S., Kuroki, R., 2012. Structure and Function of Δ1-Tetrahydrocannabinolic Acid (THCA) Synthase, the Enzyme Controlling the Psychoactivity of *Cannabis* sativa. J. Mol. Biol. 423, 96–105. doi:10.1016/j.jmb.2012.06.030

Sirikantaramas, S., Morimoto, S., Shoyama, Y., Ishikawa, Y., Wada, Y., Shoyama, Y., Taura, F., 2004. The Gene Controlling Marijuana Psychoactivity. J. Biol. Chem. 279, 39767–39774. doi:10.1074/jbc.M403693200

Taura, F., Dono, E., Sirikantaramas, S., Yoshimura, K., Shoyama, Y., Morimoto, S., 2007a. Production of Δ1-tetrahydrocannabinolic acid by the biosynthetic enzyme secreted from transgenic Pichia pastoris. Biochem. Biophys. Res. Commun. 361, 675–680. doi:10.1016/j.bbrc.2007.07.079

Taura, F., Morimoto, S., Shoyama, Y., 1996. Purification and Characterization of Cannabidiolic-acid Synthase from *Cannabis* sativa L. J. Biol. Chem. 271, 17411–17416. doi:10.1074/jbc.271.29.17411

Taura, F., Morimoto, S., Shoyama, Y., Mechoulam, R., 1995. First direct evidence for the mechanism of .DELTA.1-tetrahydrocannabinolic acid biosynthesis. J. Am. Chem. Soc. 117, 9766–9767. doi:10.1021/ja00143a024

Taura, F., Sirikantaramas, S., Shoyama, Y., Yoshikai, K., Shoyama, Y., Morimoto, S., 2007b. Cannabidiolic-acid

synthase, the chemotype-determining enzyme in the fiber-type *Cannabis* sativa. FEBS Lett. 581, 2929–2934. doi:10.1016/j.febslet.2007.05.043

Tolner, B., Smith, L., Begent, R.H.J., Chester, K.A., 2006. Production of recombinant protein in Pichia pastoris by fermentation. Nat. Protoc. 1, 1006–1021. doi:10.1038/nprot.2006.126

Zirpel, B., Degenhardt, F., Martin, C., Kayser, O., Stehle, F., 2017a. Engineering yeasts as platform organisms for cannabinoid biosynthesis. J. Biotechnol. 259, 204–212. doi:10.1016/j.jbiotec.2017.07.008

Zirpel, B., Degenhardt, F., Zammarelli, C., Wibberg, D., Kalinowski, J., Stehle, F., Kayser, O., 2017b. Optimization of Δ9-tetrahydrocannabinolic acid-A synthase production in Komagataella phaffii via post-translational bottleneck identification. Manuscr. Submitt. Publ.

Zirpel, B., Stehle, F., Kayser, O., 2015. Production of Δ9-tetrahydrocannabinolic acid from cannabigerolic acid by whole cells of Pichia (Komagataella) pastoris expressing Δ9-tetrahydrocannabinolic acid synthase from *Cannabis* sativa l. Biotechnol. Lett. 37, 1869–1875. doi:10.1007/s10529-015-1853-x

CHAPTER 6

Engineering yeasts as platform organisms for cannabinoid biosynthesis

Bastian Zirpel, Friederike Degenhardt, Chantale Martin, Oliver Kayser, Felix Stehle

F.S. and O.K. coordinated and supervised the study; C.M. synthesized GPP and supported analytical measurements; F.D. performed the studies in *S. cerevisiae*; B.Z. performed the studies in *K. phaffii*. All authors analyzed the data and contributed to write the manuscript.

Journal of Biotechnology (2017) 259:204–212

6.1. ABSTRACT

Δ^9-tetrahydrocannabinolic acid (THCA) is a plant derived secondary natural product from the plant *Cannabis sativa* L. The discovery of the human endocannabinoid system in the late 1980s resulted in a growing number of known physiological functions of both synthetic and plant derived cannabinoids. Thus, manifold therapeutic indications of cannabinoids currently comprise a significant area of research. Here we reconstituted the final biosynthetic cannabinoid pathway in yeasts. The use of the soluble prenyltransferase NphB from *Streptomyces* sp. strain CL190 enables the replacement of the native transmembrane prenyltransferase cannabigerolic acid synthase from *C. sativa*. In addition to the desired product cannabigerolic acid, NphB catalyzes an *O*-prenylation leading to 2-*O*-geranyl olivetolic acid. We show for the first time that the bacterial prenyltransferase and the final enzyme of the cannabinoid pathway tetrahydrocannabinolic acid synthase can both be actively expressed in the yeasts *Saccharomyces cerevisiae* and *Komagataella phaffii* simultaneously. While enzyme activities in *S. cerevisiae* were insufficient to produce THCA from olivetolic acid and geranyl diphosphate, genomic multi-copy integrations of the enzyme's coding sequences in *K. phaffii* resulted in successful synthesis of THCA from olivetolic acid and geranyl diphosphate. This study is an important step toward total biosynthesis of valuable cannabinoids and derivatives and demonstrates the potential for developing a sustainable and secure yeast bio-manufacturing platform.

6.2. INTRODUCTION

Cannabis sativa L. (hemp, marijuana; Cannabaceae) is well known for the biosynthesis of Δ^9-tetrahydrocannabinolic acid (THCA) and related cannabinoids. The plant has been used for more than 3,500 years in ethnomedicine and was used as legal herbal medicine before being banned as illicit drug beginning of last century. THCA is the pharmacologically active constituent whose structure was first elucidated in 1964 (Gaoni and Mechoulam, 1964a) and tested in various pharmacological assays as potential drug target to treat symptoms of different diseases like tremor in multiple sclerosis, vomiting during antineoplastic chemotherapy, posttraumatic stress and more (Gaoni and Mechoulam, 1964a; Ligresti, 2006). Besides THCA more than 100 other cannabinoids were described so far (Mehmedic et al., 2010) that are biosynthesized mainly in trichomes located on leaves and with high density on flower buds of *C. sativa* (Happyana et al., 2013; Sirikantaramas et al., 2005). Cannabinoids are terpenophenolics with mixed biosynthetic origins. Biosynthetically, cannabinoids are prenylated polyketides derived from the polyketide and MEP pathway delivering an alkylresorcinolic acid (predominantly olivetolic acid; OA) and a monoterpene moiety (predominantly geranyl diphosphate; GPP), respectively (Fig. 6-2). OA is biosynthesized by two type III polyketide synthases called olivetol synthase and olivetolic acid cyclase (Gagne et al., 2012). Biosynthetic precursor of the first committed metabolite towards a high diversity of cannabinoids is cannabigerolic acid (CBGA) being formed by a C-C Friedel-Craft alkylation of OA at position C3. *In planta*, this reaction is performed by the integral membrane protein cannabigerolic acid synthase (CBGAS), which is presumably located in the membranes of the plastids (Eisenreich et al., 2001; Fellermeier and Zenk, 1998). Finally, THCA and cannabidiolic acid (CBDA) are produced from CBGA via oxidative cyclization catalyzed by the tetrahydrocannabinolic acid synthase (THCAS) or the cannabidiolic acid synthase (CBDAS), respectively (Fig. 6-2). On the contrary, these enzymes are exported into the secretory cavities of the glandular trichomes, suggesting a transport mechanism of CBGA through the membranes by either active transport or diffusion (Sirikantaramas et al., 2005; Taura et al., 2007b).

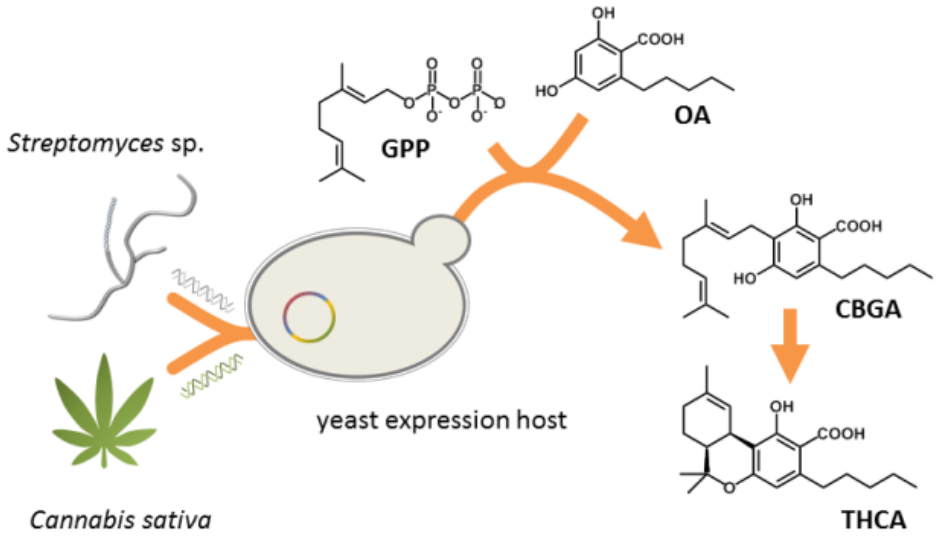

Fig. 6-1: Δ9-tetrahydrocannabinolic acid (THCA) is a plant derived secondary natural product from the plant *Cannabis sativa* L. with therapeutic indications like analgesics for cancer pain, decreasing intraocular pressure in glaucoma or reducing spasticity associated with multiple sclerosis. Here we reconstituted the late biosynthetic pathway for THCA production from *C. sativa* in yeasts by combining the bacterial prenyltransferase NphB with the THCA forming enzyme. These engineered yeasts mark a significant step toward the total biosynthesis of valuable cannabinoids in microbial hosts.

Engineering microbial strains for the production of secondary natural products provides an interesting alternative to chemical synthesis or plant based production. The reconstitution of the cannabinoid pathway in a microbial system offers the possibility of the modulation of formed products by incorporation of different starter units, by tailoring involved enzymes or by elongation of the biosynthetic pathway resulting in non-natural cannabinoids with altered pharmacological properties. However, genetic reconstruction of biosynthetic routes raises many engineering challenges either on the level of genetic pathway assembly or regulation networks. Yeast, especially *Saccharomyces cerevisiae*, is one of the major platform organisms, and geneticists and biotechnologists have demonstrated in an impressive way how various plant pathways leading to dihydroartemisinine, (Paddon and Keasling, 2014) thebaine (Thodey et al., 2014) or resveratrol (Li et al., 2016) can be successfully reconstructed. Nevertheless, *Komagataella phaffii (*formerly *Pichia pastoris)* often shows better protein production rates and could therefore present an interesting alternative production host for plant derived pharmacologically active metabolites. Secondary natural product pathways of plants in particular, present a number of challenges to microorganisms due to complex and branched pathways, unsuitable catalytic properties of the involved enzymes, compartmentalization, and specific regulation mechanisms in different organs. For example, THCAS is directed into the secretory pathway and is a soluble enzyme in *C. sativa*. In contrast, CBGAS is an integral membrane protein most likely localized in plastids of the plant. Since the functional expression of the THCAS as cytosolic protein in a prokaryotic host failed (Zirpel et al., 2015), the reconstitution of the cannabinoid pathway also comprises a compartmentation of the different biosynthetic enzymes. Feeding experiments of *thcas* expressing yeasts with CBGA showed that THCA was formed. Thus, a transport of the intermediate product CBGA through membranes is not limiting (Zirpel et al., 2015).

Besides expressing sufficient amounts of catalytically slow enzymes of secondary metabolism, the application of integral membrane proteins (like CBGAS) in a heterologous biosynthetic pathway is challenging due to problems of correct protein folding and incorrect organelle localization accompanied with additional compartmentation issues. To circumvent these unpredictable barriers we alternatively chose the soluble aromatic prenyltransferase NphB from *Streptomyces* sp. strain CL190 (Bonitz et al., 2011; Kuzuyama et al., 2005) to replace CBGAS. NphB catalyzes the transfer of geranyl moieties to various aromatic acceptor molecules. In previous studies it was shown that NphB is capable to prenylate dihydroxy naphthalenes, several flavonoids and polyketides particularly olivetol, the decarboxylated form of OA, at the C2 and C4 position (Kumano et al., 2008). Beside the formation of C-geranylation NphB catalyzes the formation of O-prenyl linkage to the aromatic substrates. In contrast to the promiscuous specificity towards the aromatic substrates NphB only accepts GPP as prenyl donor. But regardless its relaxed substrate specificity, NphB often shows a high regioselectivity for the prenyl group transfer. In conclusion, this makes NphB a promising candidate for the substitution of plant derived membrane bound prenyltransferases.

We previously described the functional intracellular expression of THCAS in *S. cerevisiae* and *K. phaffii* using a signal peptide from the vacuolar protease, proteinase A (Zirpel et al., 2015). In continuation of our research to develop yeasts as platform organisms for cannabinoid biosynthesis we established NphB as alternative biocatalyst for production of CBGA. Subsequently, we coupled the expression of the prenyltransferase to THCAS in *K. phaffii* resulting in the successful production of THCA from OA and GPP. Thereby, 82 ± 4.6 pmol L^{-1} OD^{-1} h^{-1} THCA were produced.

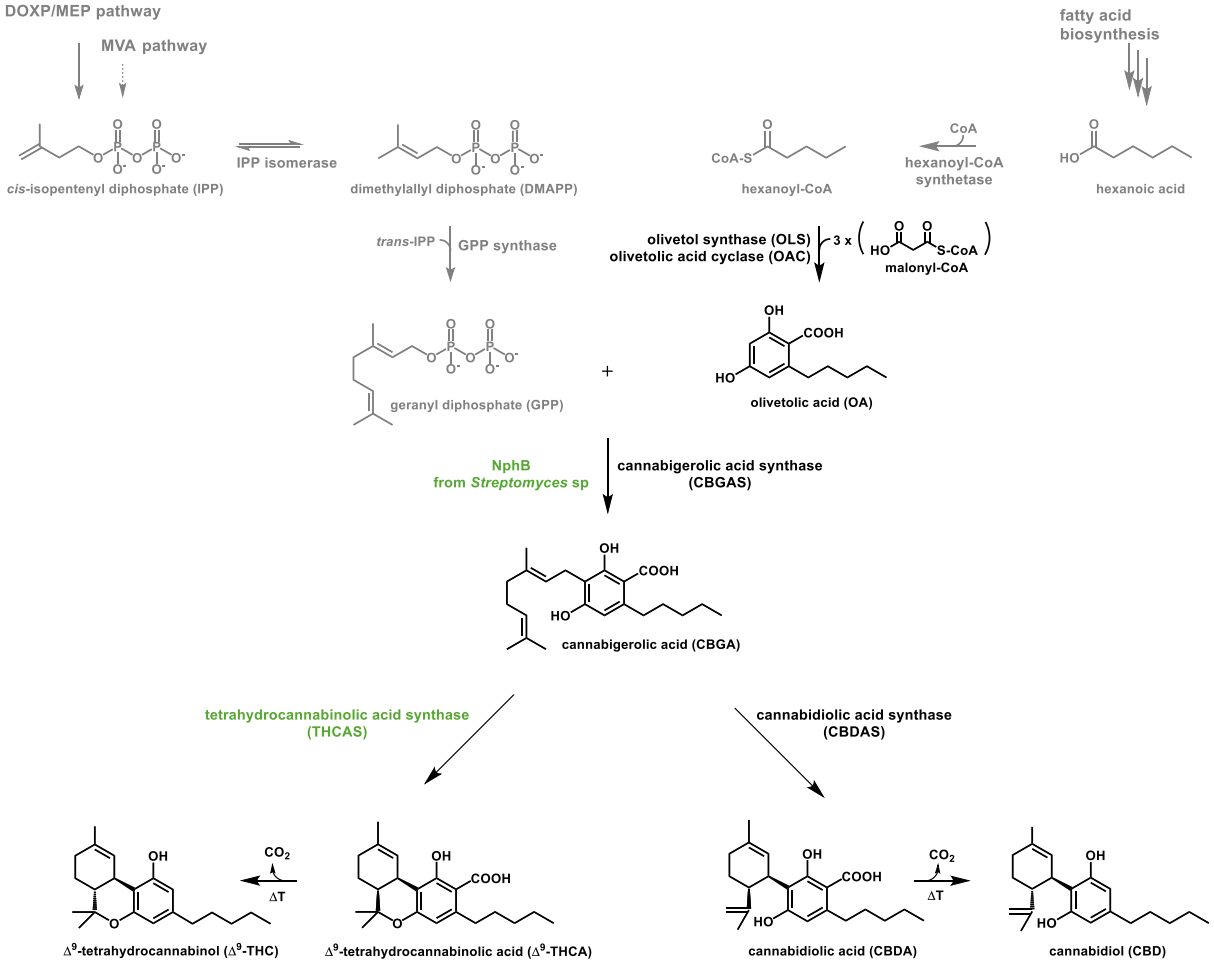

Fig. 6-2: Biosynthetic pathway of cannabinoids in *C. sativa*. The precursors geranyl diphosphate (GPP) and olivetolic acid (OA) are converted to the central intermediate of the cannabinoid pathway cannabigerolic acid (CBGA). Subsequently CBGA is further converted by two different oxidoreductases tetrahydrocannabinolic acid synthase (THCAS) and cannabidiolic acid synthase (CBDAS) to the acidic forms of THC and CBD accumulating in the glandular trichomes. Heterologously expressed enzymes of this study are highlighted in green. Intermediates of the primary metabolism are displayed in grey. MEP, 2C methyl-D-erythritol-4 phosphate; DOXP, 1 deoxy- D-xylulose-5 phosphate; MVA, mevalonate; IPP, cis-isopentenyl diphosphate; DMAPP, dimethylallyl diphosphate; AAE1, hexanoyl-CoA synthetase; OLS, olivetol synthase; OAC, olivetolic acid cyclase; CBGAS, cannabigerolic acid synthase; NphB, aromatic prenyltransferase from *Streptomyces* sp. strain CL190; Δ^9-THCA, Δ^9-tetrahydrocannabinolic acid; Δ^9-tetrahydrocannabinol; CBDA, cannabidiolic acid; CBD, cannabidiol; Modified from Degenhardt et al. (Degenhardt et al., 2017)

6.3. MATERIAL AND METHODS

6.3.1. Screening of *K. phaffii* transformants for high NphB activities

Colonies of PP2_HC transformed with *Pme*I-linearized pAX_NphB vector were transferred to a sterile 48-round-well Biolector® plate (m2p-labs, Baesweiler, Germany) containing 800 µL BMGY medium (15 g L^{-1} glycerol, 10 g L^{-1} yeast extract, 20 g L^{-1} peptone, 5 g L^{-1} casamino acids, 13.8 g L^{-1} yeast nitrogen base, 100 mM Bis-Tris buffer pH 5.8, 0.4 mg L^{-1} biotin) per well. Precultures were incubated using the Biolector® (m2p-labs, Baesweiler, Germany) at 1200 rpm and 28 °C for 22 h for complete use-up of glycerol. From precultures 10 µL were transferred by an attached pipetting robot Sias Xantus (Tecan Group Ltd., Männedorf, Switzerland) to fresh BMGY medium. After 18 h of incubation, feeding of cultures with 8 µL nutrient solution (200 g L^{-1} glycerol, 1.5 % (v/v) ammonium hydroxide, 25 % (v/v) methanol) every 2 h was started and continued for 32 h. Cells were harvested by

centrifugation of 650 µL of culture and resuspension of the pellet in 500 µL assay buffer (50 mM Tris-HCl buffer pH 7.5, 10 % (w/v) glycerol, 100 mM sodium chloride). Cell lysis was performed as described previously (Zirpel et al., 2015). Lysate supernatant was used for NphB activity assay (1 mM GPP, 1 mM OA, 5 mM magnesium chloride, 37 °C, 1100 rpm, 4 h).

6.3.2. Expression of *nphB* and *thcas* in *S. cerevisiae*

The expression of SC_TT2AN and SC_N as well as the respective strains expressing only NphB (SC_N) or THCAS (SC_T, SC_T2) was performed with two precultures followed by one main culture. After inoculation of synthetic mineral salt medium without leucine (6.7 g L^{-1} YNB without amino acids, 1.6 g L^{-1} drop out supplements without leucine, 20 g L^{-1} fructose) the cells were incubated overnight at 30 °C and 200 rpm. The first preculture was used for the inoculation of the second preculture which was incubated at 30 °C and 200 rpm for 12 h. 100 mL complex medium (20 g L^{-1} yeast extract, 40 g L^{-1} peptone, 80 mg L^{-1} adenine hemisulfate, 40 g L^{-1} fructose, 5 g L^{-1} galactose; 100 mM potassium citrate buffer pH 5.5) in 1 L baffled flasks were inoculated with OD_{600} of 0.5 for main culture. Cultures were incubated at 15 °C and 200 rpm over 168 h. Samples were taken every 24 h for measurement of optical density (600 nm) and activity assays.

Cell culture volumes correlating with an OD_{600} of 125 were harvested by centrifugation (2,000 x g, 4 °C, 10 min). Supernatants were discarded and cells resuspended in 500 µL assay buffer (50 mM Tris-HCl buffer pH 7.5, 10 % (w/v) glycerol, 100 mM sodium chloride). Cell suspension was transferred to 0.5 mL tubes and filled with 0.4 - 0.6 mm glass beads. Cells were lysed by vortexing at maximum speed at 4 °C for 30 min. Cell lysate was centrifuged and supernatant used for NphB activity assays (5 mM magnesium chloride, 1 mM GPP, 1 mM OA, 37 °C, 1100 rpm, 4 h) and THCAS assays (0.3 mM CBGA, 37 °C, 1100 rpm, 4 h).

6.3.3. Expression of *nphB* and *thcas* in *K. phaffii*

Clones of PP2_HC pAX_N C1 and C23 as well as the respective control strains expressing only NphB (PP2_EV pAX_N) or THCAS (PP2_HC) were used for inoculation of 100 mL BMGY medium in baffled 1 L shaking flasks. Cultures were incubated at 200 rpm and 30 °C overnight. Cells were harvested and used for inoculation of 50 mL BMMY (1 % (v/v) methanol, 10 g L^{-1} yeast extract, 20 g L^{-1} peptone, 5 g L^{-1} casamino acids, 13.8 g L^{-1} yeast nitrogen base, 100 mM Bis-Tris buffer pH 5.8, 0.4 mg L^{-1} biotin) at an OD_{600} of 10. Cultivation was conducted at 160 rpm and 15 °C for 96 h and 500 µL methanol was added every 24 h after sampling. Samples were taken for measurement of optical density (600 nm), NphB activity assays (described above) and THCAS activity assays. Cell lysis was performed as described previously (Zirpel et al., 2015), but 2 mL of cell culture were harvested and cell pellets resuspended in 500 µL assay buffer (50 mM Tris-HCl buffer pH 7.5, 10 % (w/v) glycerol, 100 mM sodium chloride). For measurement of THCAS activity, lysate supernatant was incubated with 0.3 mM CBGA for 4 h at 37 °C and 1100 rpm.

6.3.4. HPLC-ESI-MS/MS

Activity assays were stopped by addition of 0.1 assay-volumes trichloroacetic acid (*K. phaffii*) or formic acid (*S. cerevisiae*) and 2.9 assay-volumes acetonitrile (ACN) followed by incubation on ice for 15 min. Supernatants were

filtered (0.45 µm, Nylon) after centrifugation (13,100 x g, 4 °C, 20 min) and analyzed by HPLC-DAD (Agilent 1260 Infinity HPLC, Waldbronn, Germany). Separation of compounds from *S. cerevisiae* extracts was performed on a EC 100/2 Nucleoshell RP18 2.7 µm column (Macherey Nagel, Düren, Germany) (0.8 mL min^{-1}, 40 °C, 35 % (v/v) H_2O with 0.1 % (v/v) formic acid (FA), 65 % (v/v) ACN). Separation of compounds from *K. phaffii* extracts was performed on a EC 100/2 Nucleoshell RP18 2.7 µm column (Macherey Nagel, Düren, Germany) (0.8 mL min^{-1}, 40 °C, 39 % (v/v) H_2O with 0.1 % (v/v) FA, 61 % (v/v) ACN). Quantification of products was based on integrated peak areas of the UV-chromatograms at 225 nm. Standard curves were generated for CBGA and THCA and the CBGA standard curve was used to estimate the concentration of the side-product 2-*O*-GOA. The identity of all compounds was confirmed by comparing mass and tandem mass spectra of each sample with coeluting standards analyzed by Bruker compact™ ESI-Q-TOF (Bruker, Bremen, Germany) using positive ionization mode.

6.3.5. Preparative RP-HPLC

The isolation of 2-*O*-GOA was done by extraction with ethyl acetate. The purification was performed on a Nucleodur C18 HTec 5 µm (250 x 10 mm) column (Macherey Nagel, Düren, Germany) using an isocratic gradient (4.0 mL min^{-1}, 40 °C, 35 % (v/v) H_2O/ 65 % (v/v) ACN). The separated peak was detected at 225 nm and fractionated with a FC-1 Dynamax fraction collector (Zinsser Analytik, Frankfurt am Main, Germany). After removal of solvent a lyophilisation was performed. Obtained compound was submitted for ^1H NMR measurement.

6.4. RESULTS

6.4.1. NphB is able to produce CBGA

In a first approach, the heterologous expression of the native CBGA forming enzyme CBGAS from *C. sativa* (Page and Boubakir, 2014) was investigated in *S. cerevisiae*, but no functionally active protein was obtained. To circumvent the problems expressing the integral membrane protein CBGAS, we tried to use the soluble aromatic prenyltransferase NphB from *Streptomyces* sp. CL190 strain. Previous studies indicated that NphB is able to prenylate OA (Kuzuyama et al., 2005). Thus, *S. cerevisiae* CEN.PK cells carrying the coding sequence of NphB under the control of the GAL1 promoter (SC_N) were used to express the soluble prenyltransferase. HPLC analysis of the activity assay with GPP and OA revealed the formation of two products with m/z of 361.23. The peak with a retention time of 1.6 min was identical to the standard compound of CBGA (Fig. 6-3) indicating that NphB is indeed able to prenylate OA to CBGA. The second peak at 1.7 min showed the same m/z of 361.23 but a different MS^2 spectrum (Supporting Fig. S X-1), suggesting that NphB prenylates OA at a different position. According to Kuzuyama et al. (2005) and Kumano et al. (2010) NphB catalyzes carbon-carbon and carbon-oxygen-based geranylation of many hydroxyl-containing aromatic acceptors. Possible prenylation sites of OA by NphB are shown in Fig. 6-4. For further elucidation of the unknown compound the corresponding peak was isolated via preparative RP-HPLC followed by NMR analysis (Supplementary information). That suggested that NphB is able to geranylate OA preferentially at the 2-*O* position resulting in 2-*O*-geranyl olivetolic acid (2-*O*-GOA). Other prenylation products with m/z of 361.23 could not be detected via HPLC-MS.

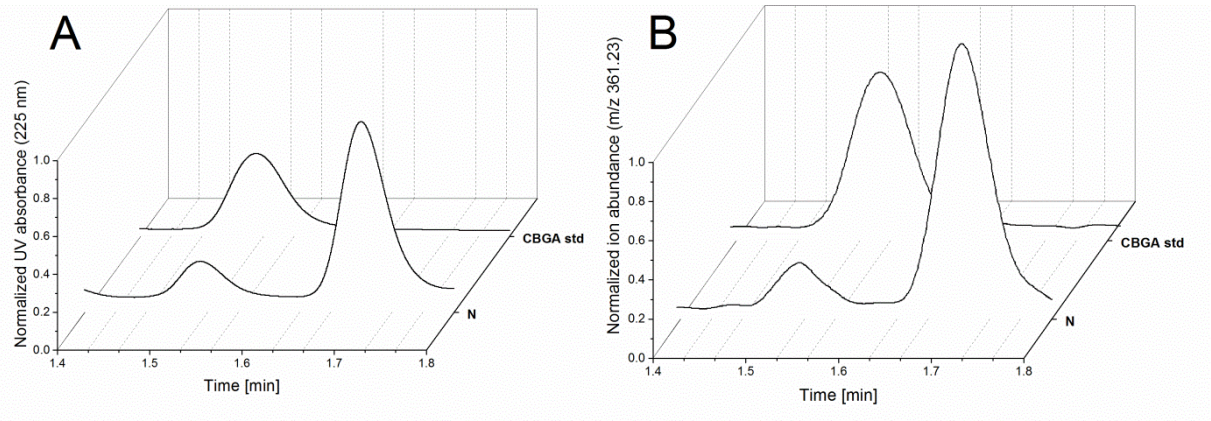

Fig. 6-3: LC-MS analysis of cannabinoids produced with cell lysates of *S. cerevisiae* expressing *nphB*. The yeast lysates were incubated with 1 mM GPP and OA, respectively. (A) HPLC-UV chromatograms at 225 nm of the standard CBGA and the assay products. (B) Extracted ion chromatograms (EIC) of m/z 361.23 (CBGA) of the standard CBGA and the assay products. N – assay of SC_N lysates.

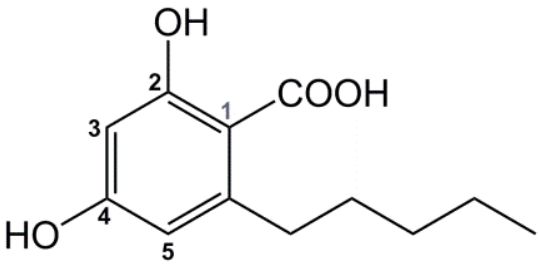

Fig. 6-4: Possible geranylation sites of OA by NphB. The aromatic prenyltransferase NphB is able to catalyze carbon-carbon and carbon-oxygen based geranylation of hydroxyl-containing aromatic acceptors. Possible *O*-geranylation can take place at positions 2 and 4. C-C prenylation is possible at positions 3 (CBGA) and 5.

6.4.2. Whole cell assay of *S. cerevisiae*

Based on these results we tested whether *S. cerevisiae* is able to take up OA and GPP from the medium to set up a whole cell assay. Initial tests suggested that OA concentrations up to 5 mM are not toxic to *S. cerevisiae* cells (data not shown). SC_N cells were cultivated in complex medium for 72 h at 15 °C and 200 rpm. The cells were harvested and resuspended in assay buffer. Cells were either (a) lysed for a subsequent NphB activity assay to determine if NphB is functionally expressed or (b) directly supplemented with 3 mM OA and 3 mM GPP. Finally, the cells of the whole cell assay were extracted using ethyl acetate to determine CBGA formation upon uptake of OA and GPP.

The results indicate that although NphB is functionally expressed, the substrate uptake by whole cells is not occurring or insufficient under tested conditions as cultivation of cells in the presence of OA and GPP did not yield in CBGA or 2-*O*-GOA formation (Supporting Fig. S X-2).

6.4.3. Fusion of NphB and THCAS

We showed that yeast extracts expressing *nphB* catalyze the prenylation of OA by GPP to form CBGA, the substrate of the THCAS to form THCA. Based on these results we tried to express both enzymes simultaneously in *S. cerevisiae*. In a first approach, separation of the two coding sequences of THCAS and NphB was achieved

by a viral T2A sequence that enables the eukaryotic expression of both enzymes driven by a single promoter (Beekwilder et al., 2014b). The construct was designed with upstream *thcas* and downstream *nphB* as it is unknown whether the function of the N-terminal leader peptide of THCAS would be negatively affected by an additional proline upon co-translational cleavage of the T2A peptide sequence.

The yeast strain SC was transformed with pDionysos_TT2AN and cultivated for 168 h. Samples for OD_{600} measurement and activity assays were taken every 24 h. Product formation was analyzed after supplementing OA and GPP to the cell lysates. Results depicted in Fig. 6-5 and Supporting Fig. S X-3 show production of CBGA and 2-*O*-GOA but no THCA was formed. The low CBGA production rate of 2.5 pmol L^{-1} OD^{-1} h^{-1} indicates that the CBGA concentration might not be sufficiently high for a subsequent oxidative cyclization by THCAS. Enzyme activities of SC_N lysates supplemented with OA and GPP indicate that expression rates of separately expressed *nphB* is higher than co-expressed with *thcas* (Fig. 6-5). The highest CBGA production rate of SC_N was detectable 144 h after induction (12 pmol L^{-1} OD^{-1} h^{-1}, Fig. 6-5). The highest possible THCA production rate of SC_TT2AN lysates supplemented with CBGA was detectable 120 h after induction (126 pmol L^{-1} OD^{-1} h^{-1}, Fig. 6-5) whereas the highest THCA production rate of SC_T was already reached 96 h after induction (427 pmol L^{-1} OD^{-1} h^{-1}, Supporting Fig. S X-4).

The expression of *nphB* and *thcas* driven by a single *Gal1* promoter did not result in THCA formation. On this account we tested the bidirectional Gal10/Gal1 promoter system of yeast since the repeated application of identical promoter sequences in the same system might lead to instability of constructs caused by the highly active homologous recombination machinery of yeast (Siddiqui et al., 2012). The construct pDio2_THCAS was cloned in order to test whether *thcas* is functionally expressed under pGal10. The yeast strain SC was transformed with the desired plasmid and cultivated for 168 h. Samples for OD_{600} measurement and activity assay were taken every 24 h. Enzyme activities of SC_T2 lysates supplemented with CBGA show that the highest THCA production rate was obtained 72 h after induction (272 pmol L^{-1} OD^{-1} h^{-1} (Supporting Fig. S X-4). A comparison of SC_T and SC_T2 indicates that *thcas* expressed using pGal1 is more active than *thcas* expressed under pGal10. THCAS expression under pGal1 resulted, 72 h after induction, in a THCA production rate of 348 pmol L^{-1} OD^{-1} h^{-1}.

Based on the results we decided to use pGal1 for *nphB* expression. The yeast strain SC was transformed with pDio2_NT and cultivated for 168 h. Samples for OD_{600} measurements and activity assays were taken every 24 h. Product formation was analyzed after supplementing OA and GPP to the cell lysates. Results shown in Fig. 6-5 indicate that CBGA and 2-*O*-GOA were formed, but no THCA. The highest CBGA production rate was obtained 96 h after induction (8 pmol L^{-1} OD^{-1} h^{-1}, Fig. 6-5). The formation of 2-*O*-GOA is constant between 96 and 168 h after induction (Supporting Fig. S X-5). The highest possible THCA production rate of SC_NT lysates supplemented with CBGA was detectable 168 h after induction (233 pmol L^{-1} OD^{-1} h^{-1}, Fig. 6-5).

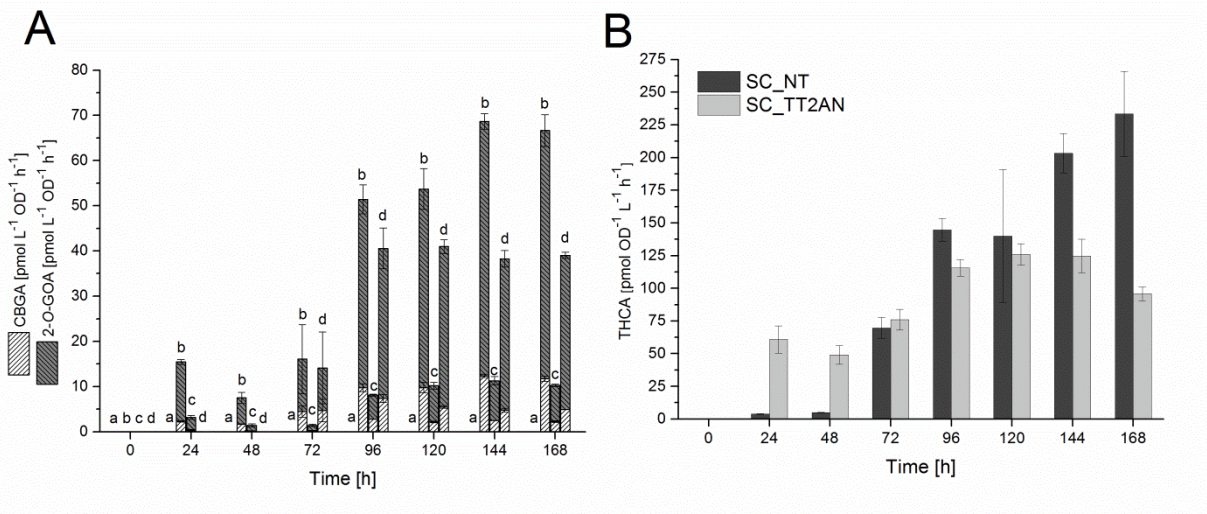

Fig. 6-5: Shaking flask cultivation of *S. cerevisiae* cells and analysis of product formation. (A) Comparison of cells expressing only *thcas* (SC_T, (a)), only *nphB* (SC_N, (b)) or *nphB* and *thcas* ((SC_TT2AN, (c)), (SC_NT, (d)); (B) THCAS activities in (c) and (d); Expression cultures were inoculated at OD_{600} of 0.5 and incubated for 168 h at 15 °C, 200 rpm in 1 L baffled shaking flasks (10 % filling volume); cell lysate supernatants were incubated with either 1 mM OA, 1 mM GPP, 5 mM $MgCl_2$ at 37 °C for 4 h to determine CBGA, 2-*O*-GOA and THCA formation (A) or with 0.3 mM CBGA at 37 °C for 4 h to determine the highest possible THCA production under the tested conditions (B); assays were analyzed via HPLC-MS and product formation normalized on cell culture OD_{600}, cell culture volume and assay incubation time. Data points are calculated from biological triplicates each analyzed in technical duplicates.

Neither expression of *thcas* and *nphB* driven by the same promoter nor the expression of both enzymes using a bidirectional Gal10/Gal1 promoter system led to formation of sufficient amounts of CBGA which could serve as substrate for THCAS. To test if higher expression levels of *nphB* and *thcas* will lead to the formation of THCA we switched to *K. phaffii* as expression host.

6.4.4. Screening of different *K. phaffii* strains for highest cannabinoid formation

In order to improve *nphB* expression we tried to make use of *K. phaffii*'s ability to express proteins at high levels upon multi-copy integration of the coding sequences into its genome. Therefore we used the previously reported strain PP2_HC (Zirpel et al., 2015) which is already able to functionally express *thca*s intracellularly at high levels and transformed it with high amounts of linearized vector DNA pAX_NphB containing the coding sequence of *nphB*. Subsequently, 24 transformants were checked via colony PCR for successful integration of the vector DNA and screened in a 48-well format for their product formation capabilities (CBGA, 2-*G*-GOA, THCA) upon supplementation of OA and GPP to the cell lysates (Fig. 6-6). The results indicate a high phenotypic variety supposedly due to varying copy numbers of pAX_NphB leading to product formations from 20 to 280 pmol L^{-1} OD^{-1} h^{-1}. For a more detailed elucidation of THCA production capabilities of *K. phaffii*, clone C23 (high THCA production) and clone C1 (low THCA production) were cultivated at a larger scale in a shaking flask experiment.

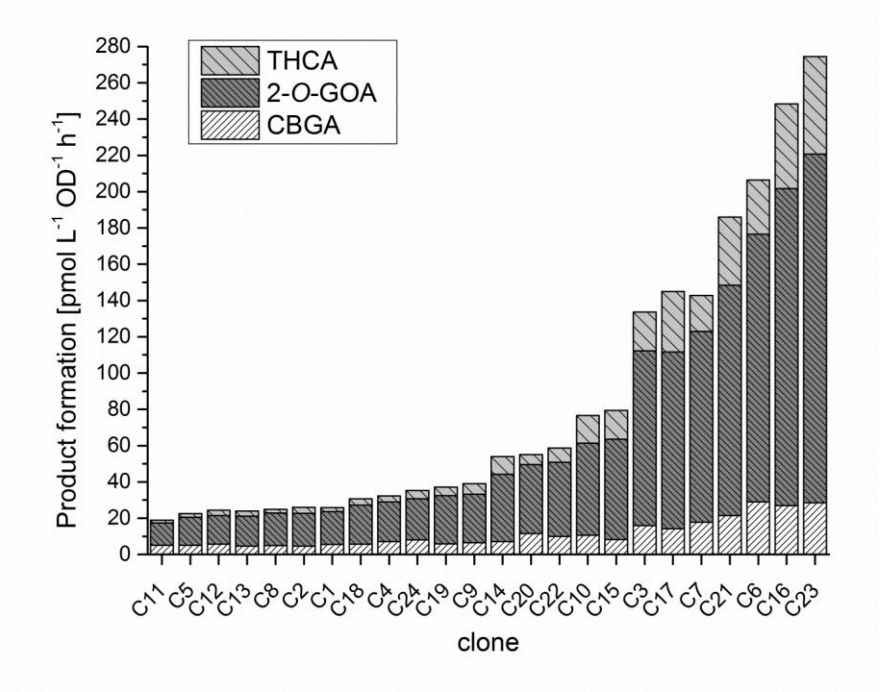

Fig. 6-6: Screening of 24 different *K. phaffii* transformants expressing *nphB* and *thcas* (PP2_NT). Expression cultures were grown for 32 h at 28 °C in deep-well plates; cell lysate supernatants were incubated with 1 mM OA, 1 mM GPP, 5 mM $MgCl_2$ at 37 °C for 4 h; assays were analyzed via HPLC-MS and product formation normalized on cell culture OD_{600}, cell culture volume and assay incubation time.

6.4.5. Time dependent expression in *K. phaffii*

K. phaffii clones C1 and C23 expressing both *nphB* and *thcas* as well as control strains expressing only one of the enzymes were incubated in shaking flasks to investigate enzyme activities over time (Fig. 6-7). Cultivation conditions were adapted to optimal *thcas* expression conditions as reported before (Zirpel et al., 2015). As expected, NphB was functionally expressed and accumulation of CBGA and 2-*O*-GOA occurred in lysates of cells lacking THCAS (PP2_N, Fig. 6-8). THCA is only produced from GPP and OA in strains expressing both *nphB* and *thcas* (PP2_NT). Furthermore, the side-product 2-*O*-GOA is not accepted as a substrate by the THCAS. Finally, the performed screening for strains with higher NphB activities yielded a strain with a 5-fold increased production rate. PP2_NT C23 was able to produce 615 pmol L^{-1} OD^{-1} h^{-1} whereas clone C1 only produced 125 pmol L^{-1} OD^{-1} h^{-1}. Similar results are obtained for the production of THCA which was 6-fold increased with clone C23 compared to C1.

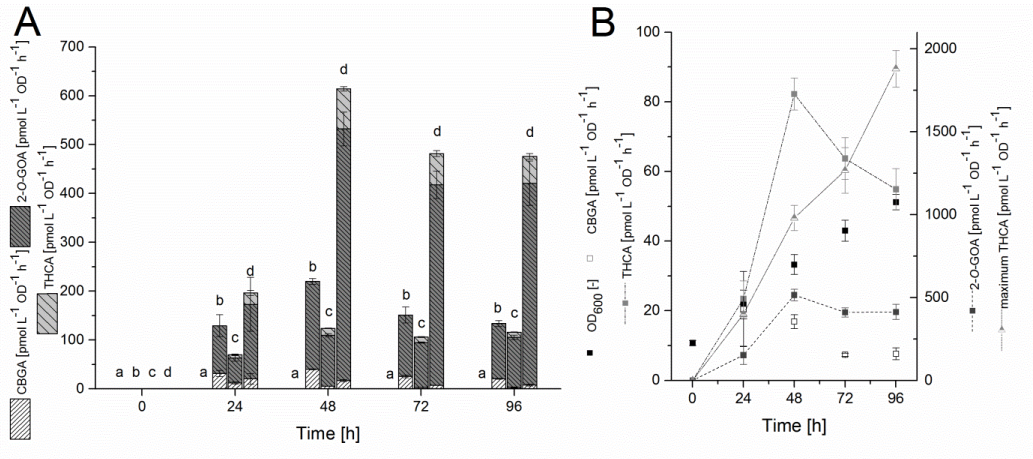

Fig. 6-7: Shaking flask cultivation of *K. phaffii* cells and analysis of product formation. (A) Comparison of cells expressing only *thcas* (PP2_HC, (a)), only *nphB* (PP2_N, (b)) or *nphB* and *thcas* (PP2_NT clone C1 (c), PP2_NT clone C23 (d)); (B) Cultivation of PP2_NT clone C23; expression cultures were inoculated at OD_{600} of 10 and incubated for 96 h at 15 °C, 160 rpm in 500 mL baffled shaking flasks (10 % filling volume); cell lysate supernatants were incubated with either 1 mM OA, 1 mM GPP, 5 mM $MgCl_2$ at 37 °C for 4 h to determine CBGA, 2-*O*-GOA and THCA formation or with 0.3 mM CBGA at 37 °C for 4 h to determine the highest possible THCA production under the tested conditions; assays were analyzed via HPLC-MS and product formation normalized on cell culture OD_{600}, cell culture volume and assay incubation time. Data points are calculated from biological triplicates each analyzed in technical duplicates.

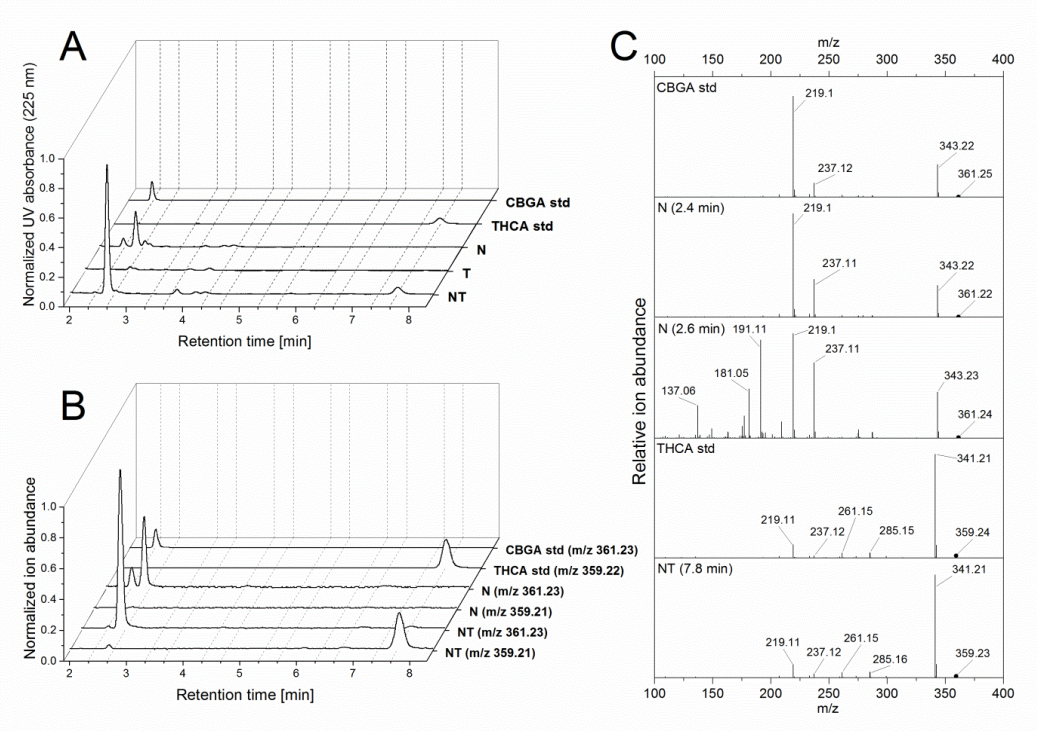

Fig. 6-8: LC-MS analysis of cannabinoids produced with extracts of *K. phaffii* expressing both *nphB* and/or *thcas*. The yeast extracts were incubated with 1 mM GPP and OA, respectively. (A) HPLC-UV chromatograms at 225 nm of the standards CBGA, THCA and the assay products. (B) Extracted ion chromatograms (EIC) of m/z 361.23 (CBGA) and m/z 359.21 (THCA) of the standards CBGA, THCA and the assay products. (C) Tandem mass spectra of CBGA and THCA standards and the product peaks of chromatograms in (A). 2-*O*-GOA (RT 2.6 min) was identified by NMR. All standards were also analyzed by NMR (Supplementary information). N – assay of lysed yeast expressing only NphB; T – assay of lysed yeast expressing only THCAS; NT – assay of lysed yeast expressing both NphB and THCAS.

6.5. DISCUSSION

6.5.1. Replacement of the native plant prenyltransferase

In view of the difficulties of implementing an integral membrane protein, like CBGAS, into a heterologous production strain for cannabinoids we decided to replace CBGAS by NphB, a soluble prenyltransferase from *Streptomyces* sp. strain CL190. It was described previously that OA might serve as prenyl acceptor molecule for NphB (Kuzuyama et al., 2005). Here we show for the first time that NphB is able to catalyze the formation of CBGA. Nevertheless, a major side-product formation (~85 %) was detected resulting in the formation of an *O*-prenylated product, 2-*O*-GOA (Fig. 6-3 and Fig. 6-9), which presents a bottleneck in the coupling of both *nphB* and *thcas* in the same host. In future, a rational protein engineering approach based on the crystal structure of NphB together with homology modelling and substrate docking studies might enable the improvement of the specificity towards CBGA and higher specific activities.

6.5.2. Expression capacity limitations of *S. cerevisiae*

S. cerevisiae is a well-established and well characterized host for the implementation of heterologous biosynthetic pathways. For example baker's yeast served as platform organism for the complete biosynthesis of opioids published by the group of Smolke (Galanie et al., 2015). Our studies show that *S. cerevisiae* is able to produce all expressed coding sequences in a functional and active manner but the expression levels are not sufficient to couple different enzyme activities in order to set up a whole new biosynthetic pathway. The first attempt to combine coding sequences of *thcas* and *nphB* separated by a T2A sequence under the control of a single promoter did not result in the formation of the final product THCA, although both enzymes were active. Based on these results we decided to use a bidirectional promoter system consisting of pGal1 and pGal10, which are both classified as strong inducible promoters in yeast (Partow et al., 2010). A comparison of the enzyme activities of SC_T and SC_T2 lysates indicated that pGal1 is a stronger promoter than pGal10. These results are also supported by West et al. (West et al., 1987) and Cartwright et al. (Cartwright et al., 1994). One reason that the two promoter strategy yields higher enzyme activities compared to the T2A-single-promoter system might be difficulties during cleavage of the T2A fusion proteins.

6.5.3. Reconstitution of the late cannabinoid pathway

Based on the results of the whole cell assay, yeast cell lysates have to be tested for activity rather than intact cells. However, taking the total biosynthetic pathway into consideration, whole cell catalysis might still be feasible upon expression of olivetolic acid cyclase (Gagne et al., 2012) and olivetol synthase (Taura et al., 2009) as well as GPP synthase (Marks et al., 2009) while feeding hexanoate/malonate.

Contrary to *S. cerevisiae*, *K. phaffii* was able to form THCA from OA and GPP (Supporting Fig. S X-5). The quantity of produced 2-*O*-GOA correlates with the produced intermediate CBGA and thus with the amount of functionally active NphB within the cell. The produced amounts of CBGA and 2-*O*-GOA of strain *K. phaffii* C19

(Fig. 6-6), based on activity measurements, are comparable to the ones in SC_NT (Fig. 6-5A, 168 h) and in strain C19 the produced amount of CBGA is sufficient for the formed amount of THCAS to catalyze the formation of THCA. Therefore, rather the enzyme expression level of *thcas* than *nphB* is the crucial factor that needs to be optimized in the first place. However, if baker's yeast should be used in future as platform organism for the reconstitution of the whole biosynthetic pathway both enzyme activities need to be improved by increasing the expression levels or the specific enzyme activities upon protein engineering.

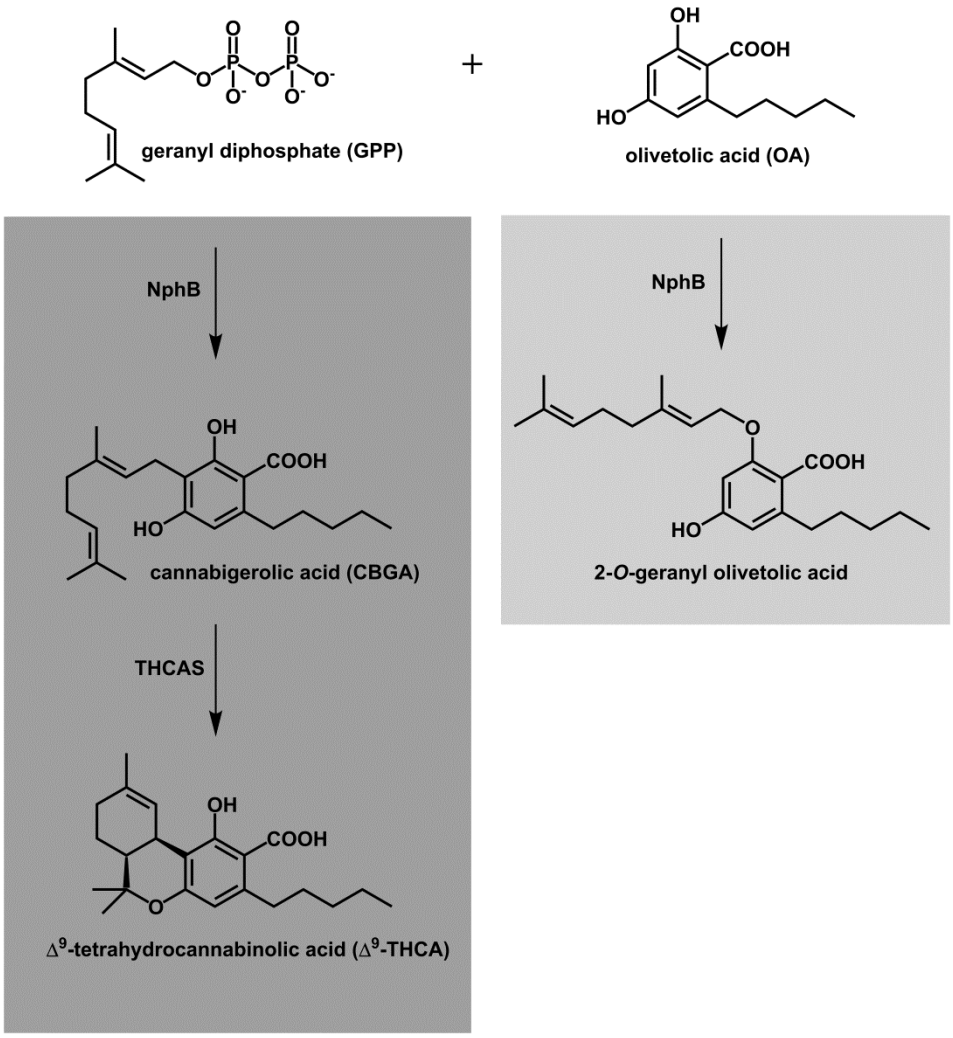

Fig. 6-9: Reconstitution of the final biosynthetic cannabinoid pathway of *C. sativa* in yeast. The main route resulting in THCA is dark grey shaded. The formation of the side product 2-*O*-GOA is highlighted in light grey. NphB - soluble prenyltransferase from a naphterpin biosynthetic gene cluster from Streptomyces sp. strain CL190, THCAS - tetrahydrocannabinolic acid synthase from *C. sativa*.

In contrast, the *K. phaffii* results show (Fig. 6-7B) that at the tested conditions NphB activity levels are limiting the THCA production as the cell lysates after 48 h of cultivation contain enough THCAS to produce 34-fold more THCA (maximum THCA production in the THCAS assay compared to THCA production in NphB/THCAS-coupled assay after 96 h of cell growth) if NphB would supply enough CBGA as substrate. The highest specific production rates were obtained after 48 h of cultivation presumably due to no further increase in cytosolic *nphB* expression levels. However, we cannot rule out that substrates, intermediates and products are metabolized by other yeast enzymes. On the contrary, THCAS levels are still increasing over time (see Fig. 6-7B) which corresponds to the results reported previously (Zirpel et al., 2015). Consistent observations regarding maximum

activities can be made for all strains expressing *nphB*. While THCAS is targeted into the vacuole in a strain lacking the vacuolar proteinase A, presumably facilitating accumulation of the protein in the vacuole, cytosolic NphB turnover might present an additional bottleneck for increased enzyme levels. Besides, we chose assay conditions for the coupled enzyme reaction which are more favorable for NphB rather than THCAS (pH 7.5, 37 °C). However, considering a whole metabolic process, a more acidic pH in the cytosol (Valli et al., 2005) might reduce the enzyme activity of NphB within the cell. On the contrary, THCAS has a lower pH optimum at 4.5 that fits with the vacuolar localization of the enzyme in yeast. Additionally, substrate limitations that might occur as the result of the different compartmentation of the biosynthetic enzymes or the assumed low polarity of the substrates pose further challenges in the whole cell process.

Taken all this into consideration NphB levels have to be improved extensively. One excellent possibility offers the post-transformational vector amplification in *K. phaffii* that subsequently enables to increase gene copy numbers inside the cell (Aw and Polizzi, 2016). This might be even more important with regard to the complete biosynthesis of cannabinoids as it allows for belated elimination of catalytic bottlenecks.

6.6. CONCLUSION

Our study shows that the coupling of both enzymes, NphB and THCAS, was successful using *K. phaffii* as expression host. While *K. phaffii* has so far mainly been used for excessive secreted protein production, purification and characterization, it proves its potential in metabolic engineering when linear secondary biosynthetic pathways should be integrated into a heterologous host. We effectively generated and screened gene multi-copy clones in a multi-well plate experiment and characterized the best expressing strain regarding its capability to produce THCA from OA and GPP. The cell lysate was able to produce 82 ± 4.6 pmol L^{-1} OD^{-1} h^{-1} THCA (Fig. 6-7A), but NphB activities were limiting in this strain and a considerable amount of side-product 2-*O*-GOA was produced. Overcoming NphB activity and product specificity issues by means of directed mutagenesis will be a major task, as – assuming the same expression and specific activity of a NphB mutant producing only CBGA - it would be possible to produce 34-fold more THCA within this yeast system conferring to THCA production rates in the hundred milligrams per liter and hour scale. While product titers and rates are still low in the generated heterologous systems, we hereby present a possibility to circumvent the troublesome expression of the integral membrane-bound CBGAS from *C. sativa* and demonstrate the potential for developing a sustainable and secure cannabinoid producing yeast platform.

6.7. REFERENCES

Aw, R., Polizzi, K.M., 2016. Liquid PTVA: a faster and cheaper alternative for generating multi-copy clones in Pichia pastoris. Microb. Cell Fact. 15, 29. doi:10.1186/s12934-016-0432-8

Beekwilder, J., van Rossum, H.M., Koopman, F., Sonntag, F., Buchhaupt, M., Schrader, J., Hall, R.D., Bosch, D., Pronk, J.T., van Maris, A.J. a, Daran, J.M., 2014. Polycistronic expression of a beta-carotene biosynthetic pathway in *Saccharomyces cerevisiae* coupled to beta-ionone production. J. Biotechnol. 192, 383–392. doi:10.1016/j.jbiotec.2013.12.016

Bonitz, T., Alva, V., Saleh, O., Lupas, A.N., Heide, L., 2011. Evolutionary Relationships of Microbial Aromatic Prenyltransferases. PLoS One 6, e27336. doi:10.1371/journal.pone.0027336

Cartwright, C.P., Li, Y., Zhu, Y.-S., Kang, Y.-S., Tipper, D.J., 1994. Use of β-lactamase as a secreted reporter of promoter function in yeast. Yeast 10, 497–508. doi:10.1002/yea.320100409

Degenhardt, F., Stehle, F., Kayser, O., 2017. The Biosynthesis of Cannabinoids, in: Preedy, V. (Ed.), Handbook of *Cannabis* and Related Pathologies. Elsevier, pp. 13–23. doi:10.1016/B978-0-12-800756-3.00002-8

Eisenreich, W., Rohdich, F., Bacher, A., 2001. Deoxyxylulose phosphate pathway to terpenoids. Trends Plant Sci. 6, 78–84. doi:10.1016/S1360-1385(00)01812-4

Fellermeier, M., Zenk, M.H., 1998. Prenylation of olivetolate by a hemp transferase yields cannabigerolic acid, the precursor of tetrahydrocannabinol. FEBS Lett. 427, 283–5.

Gagne, S.J., Stout, J.M., Liu, E., Boubakir, Z., Clark, S.M., Page, J.E., 2012. Identification of olivetolic acid cyclase from *Cannabis* sativa reveals a unique catalytic route to plant polyketides. Proc. Natl. Acad. Sci. 109, 12811–12816. doi:10.1073/pnas.1200330109

Galanie, S., Thodey, K., Trenchard, I.J., Filsinger Interrante, M., Smolke, C.D., 2015. Complete biosynthesis of opioids in yeast. Science (80-.). 349, 1095–1100. doi:10.1126/science.aac9373

Gaoni, Y., Mechoulam, R., 1964. Isolation, Structure, and Partial Synthesis of an Active Constituent of Hashish. J. Am. Chem. Soc. 86, 1646–1647. doi:10.1021/ja01062a046

Happyana, N., Agnolet, S., Muntendam, R., Van Dam, A., Schneider, B., Kayser, O., 2013. Analysis of cannabinoids in laser-microdissected trichomes of medicinal *Cannabis* sativa using LCMS and cryogenic NMR. Phytochemistry 87, 51–59. doi:10.1016/j.phytochem.2012.11.001

Kumano, T., Richard, S.B., Noel, J.P., Nishiyama, M., Kuzuyama, T., 2008. Chemoenzymatic syntheses of prenylated aromatic small molecules using Streptomyces prenyltransferases with relaxed substrate specificities. Bioorg. Med. Chem. 16, 8117–8126. doi:10.1016/j.bmc.2008.07.052

Kumano, T., Tomita, T., Nishiyama, M., Kuzuyama, T., 2010. Functional characterization of the promiscuous prenyltransferase responsible for furaquinocin biosynthesis: identification of a physiological polyketide substrate and its prenylated reaction products. J. Biol. Chem. 285, 39663–71. doi:10.1074/jbc.M110.153957

Kuzuyama, T., Noel, J.P., Richard, S.B., 2005. Structural basis for the promiscuous biosynthetic prenylation of aromatic natural products. Nature 435, 983–7. doi:10.1038/nature03668

Li, M., Schneider, K., Kristensen, M., Borodina, I., Nielsen, J., 2016. Engineering yeast for high-level production of stilbenoid antioxidants. Sci. Rep. 6, 36827. doi:10.1038/srep36827

Ligresti, A., 2006. Antitumor Activity of Plant Cannabinoids with Emphasis on the Effect of Cannabidiol on Human Breast Carcinoma. J. Pharmacol. Exp. Ther. 318, 1375–1387. doi:10.1124/jpet.106.105247

Marks, M.D., Tian, L., Wenger, J.P., Omburo, S.N., Soto-Fuentes, W., He, J., Gang, D.R., Weiblen, G.D., Dixon, R. a, 2009. Identification of candidate genes affecting Delta9-tetrahydrocannabinol biosynthesis in *Cannabis sativa*. J. Exp. Bot. 60, 3715–26. doi:10.1093/jxb/erp210

Mehmedic, Z., Chandra, S., Slade, D., Denham, H., Foster, S., Patel, A.S., Ross, S.A., Khan, I.A., ElSohly, M.A., 2010. Potency Trends of Δ9-THC and Other Cannabinoids in Confiscated *Cannabis* Preparations from 1993 to 2008*. J. Forensic Sci. 55, 1209–1217. doi:10.1111/j.1556-4029.2010.01441.x

Paddon, C.J., Keasling, J.D., 2014. Semi-synthetic artemisinin: a model for the use of synthetic biology in pharmaceutical development. Nat. Rev. Microbiol. 12, 355–367. doi:10.1038/nrmicro3240

Page, J.E., Boubakir, Z., 2014. Aromatic prenyltransferase from *Cannabis*. US 20120144523 A1.

Partow, S., Siewers, V., Bjørn, S., Nielsen, J., Maury, J., 2010. Characterization of chromosomal integration sites for heterologous gene expression in *Saccharomyces cerevisiae*. Yeast 27, 955–964. doi:10.1002/yea

Siddiqui, M.S., Thodey, K., Trenchard, I., Smolke, C.D., 2012. Advancing secondary metabolite biosynthesis in yeast with synthetic biology tools. FEMS Yeast Res. 12, 144–170. doi:10.1111/j.1567-1364.2011.00774.x

Sirikantaramas, S., Taura, F., Tanaka, Y., Ishikawa, Y., Morimoto, S., Shoyama, Y., 2005. Tetrahydrocannabinolic Acid Synthase, the Enzyme Controlling Marijuana Psychoactivity, is Secreted into the Storage Cavity of the Glandular Trichomes. Plant Cell Physiol. 46, 1578–1582. doi:10.1093/pcp/pci166

Taura, F., Sirikantaramas, S., Shoyama, Y., Yoshikai, K., Shoyama, Y., Morimoto, S., 2007. Cannabidiolic-acid synthase, the chemotype-determining enzyme in the fiber-type *Cannabis* sativa. FEBS Lett. 581, 2929–2934. doi:10.1016/j.febslet.2007.05.043

Taura, F., Tanaka, S., Taguchi, C., Fukamizu, T., Tanaka, H., Shoyama, Y., Morimoto, S., 2009. Characterization of olivetol synthase, a polyketide synthase putatively involved in cannabinoid biosynthetic pathway. FEBS Lett. 583, 2061–2066. doi:10.1016/j.febslet.2009.05.024

Thodey, K., Galanie, S., Smolke, C.D., 2014. A microbial biomanufacturing platform for natural and semisynthetic opioids. Nat. Chem. Biol. 10, 837–844. doi:10.1038/nchembio.1613

Valli, M., Sauer, M., Branduardi, P., Borth, N., D, 2005. Intracellular pH distribution in *Saccharomyces cerevisiae* cell populations, analyzed by flow cytometry. Appl. Environ. Microbiol. 71, 1515–1521. doi:10.1128/AEM.71.3.1515

West, R.W., Chen, S.M., Putz, H., Butler, G., Banerjee, M., 1987. GAL1-GAL10 divergent promoter region of Saccharomyces cerevisiae contains negative control elements in addition to functionally separate and possibly overlapping upstream activating sequences. Genes Dev. 1, 1118–1131. doi:10.1101/gad.1.10.1118

Zirpel, B., Stehle, F., Kayser, O., 2015. Production of Δ9-tetrahydrocannabinolic acid from cannabigerolic acid by whole cells of Pichia (Komagataella) pastoris expressing Δ9-tetrahydrocannabinolic acid synthase from *Cannabis* sativa l. Biotechnol. Lett. 37, 1869–1875. doi:10.1007/s10529-015-1853-x

CHAPTER 7

Discussion and Outlook

7.1. CHOICE OF HETEROLOGOUS EXPRESSION SYSTEM

As discussed in chapter 4, the THCAS possesses several features that might affect functional gene expression, i.e. formation of a disulfide bond, covalent attachment of the FAD cofactor and several glycosylation sites. We initially investigated recombinant THCAS production in *E. coli*, *S. cerevisiae* and *K. phaffii*. However, functional expression of *thcas* was achieved in neither *E. coli* BL21 cells nor *E. coli* SHuffle T7 Express *lysY* cells, the latter being able to form disulfide bonds within the cytosol (see chapter 3). Contrary, in the investigated eukaryotic hosts functional gene expression was achieved when THCAS polypeptide chain was targeted through the endoplasmic reticulum (ER) to the vacuole using the PEP4 signal sequence. The THCAS variants lacking the disulfide bond (T_C37S, T_C99S) were not active in *K. phaffii*, indicating the necessity of the disulfide bond for an active enzyme. It could also be shown that the THCAS variant lacking all glycosylation sites (T_deg, Fig. 5-5) could not be actively produced in *K. phaffii* cells, however deglycosylation via EndoH treatment of functional, glycosylated THCAS did not reduce enzyme activity (Taura et al., 2007a). As *E. coli* SHuffle T7 Express *lysY* cells are able to form disulfide bonds and *E. coli* is naturally able to produce enzymes with covalently attached FAD cofactor, e.g. the fumarate reductase (Starbird et al., 2017), it is therefore likely that glycosylation facilitates the correct folding of the enzyme and thus functional expression of *thcas* failed in *E. coli* cells. Whether this is true or not, could be investigated using an engineered *E. coli* strain allowing for *N*-linked protein glycosylations (Nothaft and Szymanski, 2013; Valderrama-Rincon et al., 2012). The THCAS - besides its origin *C. sativa* - is functionally expressed in *S. frugiperda*, *S. cerevisiae* and *K. phaffii*, all of them exerting differences in their *N*-glycosylation apparatus and pattern, therefore indicating that rather the presence of glycosylation and not the type of glycoresidues impact the successful folding.

We hence focused on the THCAS production in recombinant yeasts. Obtained THCAS activity levels in *K. phaffii* were already higher compared to *S. cerevisiae* before optimization of expression (chapter 3). After optimization of the cultivation conditions, about 150 pkat ml^{-1} of total THCAS activity were achieved in shaking flask experiments using *K. phaffii*, corresponding to an 64-fold increase compared to previous reports (Taura et al., 2007a) and about 15-fold increase compared to optimized *S. cerevisiae* cultivations (results not shown; ~10 pkat ml^{-1} achieved after optimization of cultivation conditions). Based on these initial experiments, in subsequent studies we focused on *K. phaffii* as heterologous host for the production of cannabinoid producing enzymes. It is known that the secretory pathway and the protein production capacities of *K. phaffii* are superior to those of *S. cerevisiae*. Still, the fact that by co-production of helper proteins (chapter 4.4) the THCAS activity levels within the cell could be increased up to 20-fold shows that the THCAS protein presents a challenge even for the *K. phaffii* cells.

We showed that THCAS activity within the cell is higher at lower expression temperatures (15 °C showed highest activity levels in *K. phaffii* and *S. cerevisiae*, chapter 3). While low temperatures are rather unfeasible for an industrial production process, by co-production of helper proteins the cell's ability to produce THCAS at higher temperatures (28 °C) was improved on the one hand. On the other hand the identification of helper proteins with a positive effect on *thcas* expression also allowed for the development of a small-scale low-throughput screening system for rational protein design using *K. phaffii* as recombinant host (see chapter 7.2.1).

However, not only for proteins directed through the secretory pathway, but also for the cytosolic protein NphB *K phaffii* showed the superior production capacity of both tested eukaryotic hosts. The results depicted in chapter 6 present *K. phaffii* as a more promising host for the production of cannabinoids compared to *S. cerevisiae* (see also chapter 7.2.2 for further discussion).

7.2. THE FUNDAMENT FOR SUBSEQUENT STUDIES

7.2.1. Mutational studies on cannabinoid producing enzymes

We wanted to optimize enzyme properties of the THCAS and CBDAS via site-directed mutagenesis for the application in a heterologous, cannabinoid producing yeast. Taking this into account, we targeted the enzymes into the cell vacuole, although enzyme secretion might enable a faster and less laborious measurement of enzyme activity. Furthermore, the ability to measure enzyme activity at different pH values was important and more feasible when cells could be lysed at different pH values.

Generally, when performing mutational studies of a protein, changes in the protein properties have to be identified using a screening system. Important features of a screening system comprise expenses, robustness, reproducibility, sensitivity and throughput. Depending on the purpose of the screening system, different emphases are put on these factors and often compromises have to be made.

The goal of our screening system was to identify not only altered enzyme activities at the wild-type optimal pH value (pH 4.5), but also to detect changes in the enzyme pH profile at higher pH values (pH 6.5 - pH 7.0). As the THCAS and CBDAS have strongly reduced activities at these higher pH values (Fig. 5-4), sensitivity was an important factor for the establishment of the screening system. In this regard, the amount of functionally expressed enzyme was considered critical. Although the use of an episomal expression system using *S. cerevisiae* as recombinant host promised a high reproducibility, the obtained enzyme activities were insufficient for our screening purpose. On the other hand, the possibility of generating multi-copy strains in *K. phaffii* to increase gene expression (as described in chapter 3) is not feasible as it lacks reproducibility. Hence, the elucidation of the influence of co-produced helper proteins on the THCAS activity was utilized for the successful establishment of a screening system (chapter 4.4). The subsequent generation of a chassis strain producing the UPR-related transcription activator Hac1p allowed for sufficient enzyme activities when aiming for single copy transformants. This led to the establishment of a low-throughput screening system for rational mutagenesis of cannabinoid producing enzymes using *K. phaffii* (chapter 5.4.1).

The data provided by this system was satisfactory for the identification of enzyme variants with optimized features enabling their subsequent investigation and characterization. However, a lacking reproducibility compromised the informative value and significance of the obtained results. The experimental setup itself proved to be robust with low standard deviations when the same cell material was investigated in replicates (chapter 4.4). On the other hand, high variations were obtained when comparing different transformed colonies even if low amounts of DNA were transformed in a standardized manner. Therefore, it is likely that differences in replicates were due to a strong clonal variability of the transformants (chapter 2.4.2).

An alternative approach to overcome this problem presents the use of episomal expression vectors in *K. phaffii*. However, only recently substantial advances in development of stable episomal expression systems using *K. phaffii* have been accomplished (Chen et al., 2017; Schwarzhans et al., 2017b). Protein production levels are reported to be similar to chromosomal single copy integrations and a high vector stability is presented when selection pressure is maintained (Schwarzhans et al., 2017b). Reduced clonal variability (episomal vector) paired with a potent chassis strain for the production of cannabinoid producing enzymes (co-production of Hac1p) will effectively increase the informative value of the obtained results. Additionally, clonal homogeneity might also be increased when using *K. phaffii* CBS7435 *ku70*, a strain with reduced occurrence of NHEJ events, and single copy integrations facilitated with the recently established CRISPR/Cas9 system (Weninger et al., 2017). Furthermore, the implementation of promoter alternatives, e.g. GAP promoter or $P_{AOX1\text{-}syn(d6)}$, eliminates the necessity of methanol feeding and thus might offer possibilities to increase reproducibility and robustness of the screening system. As the mutational studies performed within this thesis do merely provide a fundament for subsequent experiments, it is highly recommended to evaluate these expression systems for future mutational studies.

Several questions should be investigated in these future experiments. First of all, interesting variants should be purified for more accurate characterization studies. A chassis strain, co-producing at least Hac1p, should be used for the secretion of the His-tagged protein variants to the supernatant and unproblematic purification via Ni-NTA chromatography as described in chapter 5.3.4. Furthermore, the identification of the unknown products formed by CBDAS and THCAS during CBGA conversion should be pursued in the next future.

Data suggests that THCAS is a challenging protein for yeast to produce (chapter 3 and 4). Next to the necessity of several glycosylation sites, the stability of the C-terminal BBE-domain, which also contains the suggested catalytic base Y484, was considered crucial for an active protein as well (chapter 5). While we could generate an enzyme variant (T_H494C+R532C) that not only showed a higher temperature stability (temperature optimum shifted from 52 °C to 57 °C, residual activity detected at 70 °C vs. 65 °C (wild-type), Fig. 5-6), but also an increased activity level within the cells, it should be investigated whether this variant exerts a higher specific activity or increased activity was detected due to increased enzyme production within the cell. Further introductions of disulfide or salt bridges to stabilize the C-terminal region should be investigated as well. As depicted in Fig. 5-6 A and B, residues K384 and D488 are highly conserved in the aligned proteins, therefore suggesting that the salt bridge between these residues plays an important role for the enzyme, presumably in holding the adjacent loop region with residue Y484 in correct place in the active site (T_K384A showed ~ 5 % residual wild-type activity). Hence, possible variants holding this loop region in place should be analyzed and investigated.

We also tried to elucidate mechanistical differences between THCAS and CBDAS by comparing their sequences and investigating influences of amino acid residue differences near the catalytic center (Fig. 5-7). While several amino acid changes yielded THCAS variants with no or strongly decreased activity compared to the wild-type enzyme, none of the investigated THCAS variants exerted increased specificity for the production of CBDA. Contrary, subsequent AA substitutions at the respective positions within the CBDAS (variants C_S116A, C_A414V) displayed an increased activity and/or an altered pH profile and product specificity. Based on these results and variants T_S382K and T_I257M displaying strongly decreased activities as well, the respective CBDAS variants C_K381S and C_M256I should be investigated. However, to gain additional insight into the mechanistical differences between CBDAS and THCAS, it should be considered to purify large quantities of the

CBDAS and/or THCAS for crystallization, x-ray analysis and subsequent comparison of both structures and their catalytic centers. While the group of Shoyama et al. failed to obtain crystals when co-crystallizing THCAS with its substrate CBGA, a substrate analogue or product THCA (2012), data provided in chapters 3, 4 and 5 will allow for easy production and purification of large amounts of THCAS or CBDAS to pursue co-crystallization.

Another disadvantage of our screening system is the rather low throughput. The measurement of product formation via HPLC-MS analysis subsequent to cultivation of single colonies harboring different genetic enzyme mutants, the cell lysis and activity assays is time consuming and requires a lot of effort. To improve throughput, in particular the detection method should be changed. Ideally, enzyme variants can be analyzed on a single cell basis *in vivo*, e.g. via fluorescence-activated cell sorting, allowing for a higher throughput and enabling random mutagenesis studies of the enzymes. As the cannabinoid producing enzymes catalyze an oxidative cyclization with only hydrogen peroxide as side-product and similar spectrophotometrical features of substrate and products, the direct detection of the substrate conversion proves difficult. Often, surrogate substrates are developed and used to detect enzyme activities. The development of a surrogate substrate which after conversion yields a detectable product, e.g. via spectrophotometric or fluorescence detection, is, however, unlikely for the THCAS or CBDAS as a cyclization reaction is performed. The most promising approach is the detection of the side-product hydrogen peroxide which is produced in equimolar concentrations to the products (Sirikantaramas et al., 2004).

There are several hydrogen peroxide probes available, such as systems based on small molecule complex formation like Europiumchloride-Tetracycline-Complex (Wolfbeis et al., 2002) or pentafluoro-benzene-sulfonyl-fluorescein (Maeda et al., 2004), systems based on subsequent enzymatic conversion like horseradish peroxidase-systems or systems based on protein binding like HyPer3 (Bilan et al., 2013). Most of these require the external addition of substrates or molecules to the cells and their diffusion into the cell which might prove problematic. HyPer3 on the other hand, is a combination of the hydrogen peroxide sensing OxyR protein coupled to a yellow fluorescent protein. Besides the possibility to determine the amount of produced HyPer3 in a cell via fluorescence, upon binding of hydrogen peroxide absorption and emission spectra of the protein differ and can be detected. A *K. phaffii* chassis strain producing HyPer3 might thus enable feasible random mutagenesis studies of the cannabinoid producing enzymes and should be investigated in the future.

7.2.2. Engineering *K. phaffii* as a host for cannabinoid biosynthesis

To produce cannabinoids in *K. phaffii*, a sufficient supply of GPP and OA are necessary from which subsequently CBGA is synthesized and cyclized to the final cannabinoid. GPP is synthesized from IPP which is supplied via the host's own MVA pathway and for the production of OA from hexanoyl-CoA and malonyl-CoA the host has to be able to produce both of the involved enzymes from *C. sativa*, OAC and OLS (see Fig. S VI-1, Fig. S VI-2, chapter 2.2.1). However, the major bottleneck was considered to be the prenylation of OA to yield CBGA. While an enzyme, the CBGAS; is described in literature to perform this step, scientific knowledge is inconclusive. Reports are divided about the CBGAS being a soluble (Fellermeier and Zenk, 1998) or transmembrane protein (Ohara et al., 2009; Yamamoto et al., 1997) while the sequence registered in a patent is of a transmembrane protein (Page and Boubakir, 2014). However, it could never be shown that this sequence is indeed coding for an active CBGAS. Combined with the fact that transmembrane proteins are rather difficult targets to produce recombinantly as

membrane compositions of different hosts is often varying significantly, we decided to find a soluble substitute protein.

We chose the soluble aromatic prenyltransferase NphB from *Streptomyces* sp. strain CL190 (Bonitz et al., 2011; Kuzuyama et al., 2005) to replace the CBGAS (see chapter 6). NphB catalysis the transfer of geranyl moieties to various aromatic acceptor molecules and we could show that it also prenylates OA to form CBGA. Furthermore, we were able to produce both enzymes, NphB and THCAS, within the same cell. As the substrates OA and GPP are not diffusing through the cell membrane, we had to use cell lysate for the production of THCA from OA and GPP. Nevertheless, at pH 7.5 the lysate of the *K. phaffii* cells was able to produce THCA. Again, it should be emphasized that the same experiments were conducted using a *S. cerevisiae* strain as well, although its lysate did only produce CBGA and no THCA could be detected. On the one hand, not only THCAS activity but also NphB activity levels were about 10-fold lower in *S. cerevisiae* compared to *K. phaffii* cells. On the other hand, peak enzyme activities of *K. phaffii* cultures were reached already after 48 h compared to the 144 h of *S. cerevisiae* cultures, also introducing a considerable time factor into the cultivation process. As these results were presumably due to the lower protein production capacity of *S. cerevisiae*, the importance of a host able to achieve high protein yields is unequivocal. Unfortunately, the wild-type enzyme was producing CBGA only as a side product while 2-*O*-GOA was the main product. Using the lysate of these highlighted strains (chapter 6), the prenylation performed by NphB presented the bottleneck, although the reaction was already performed at a pH favorable for NphB activity rather than THCAS.

The coupling of NphB with a cannabinoid producing enzyme *in vivo* might therefore present a challenge as well. The intracellular pH of *S. cerevisiae* is dependent on whether cells are in stationary or exponential phase, the extracellular pH and the intracellular pH and can vary significantly (pH 5 - pH 7) (Valli et al., 2005). The vacuolar pH is more acidic and can vary between pH 5.0 and pH 6.5 depending on cultivation conditions (Diakov et al., 2013; Li and Kane, 2009). In general, the interplay of enzyme activity and product specificity at different pH values has to be taken into account. While the pH optimum for NphB activity is alkaline (pH 7.5 - pH 8.5, not published, oral communication with Friederike Degenhardt), THCAS produces THCA at the highest rate at pH 4.5 and CBCA at pH 7.0. The CBDAS wild-type however has a pH optimum at pH 4.5 for the production of CBDA and is not active at pH 7.0 (Fig. 5-4). The vacuolar environment might be a good fit for the THCAS as discussed in chapter 6.5. However, the pH range of the THCAS (pH 3.75 - pH 7.5 for production of THCA) is naturally broader than that of the CBDAS (pH 3.5 - pH 6.0 for production of CBDA). Although we could show that CBDAS can be readily produced within *K. phaffii* (see chapter 5), this might present a problem regarding the interchangeability of the last catalyst in the cannabinoid producing platform organism. The generation of a CBDAS variant (C_A414V) with a broader pH range and a shift of the pH optimum from pH 4.5 to pH 5.0 was a first step in the right direction in spite of a decreased product specificity.

An acidic cytosolic pH will, however, further decrease enzyme activity of NphB. While mutational studies are also underway to increase the product specificity of NphB for the production of CBGA, its catalytic activity and pH profile, the bottleneck might also be minimized by optimizing the expression in *K. phaffii*. The co-production of several helper proteins (chapter 4), *inter alia* ER-resident chaperones, was successfully applied to enhance activity levels of the vacuole-targeted THCAS. A similar strategy could be applied to investigate influence of several cytosol-resident chaperones to optimize the expression of *nphB* (Gasser et al., 2007; Gong et al., 2009).

Another approach might present the additional compartmentalization of the biosynthetic pathway. In *S. cerevisiae*, the peroxisomal pH was investigated and compared to the cytosolic pH using pH-sensitive yellow fluorescent proteins (van Roermund, 2004). In their studies, the cytosolic pH was determined to be 7.0 compared to 8.2 in the peroxisome. It has to be taken into account that cultivation conditions might influence these conditions, however it is likely that the peroxisomal pH in yeast is more alkaline than its cytosol and thus more favorable for NphB activity. Despite the potential advantage regarding NphB activity, the compartmentalization of the CBGA production into the yeast peroxisome could also have other benefits, especially with regard to the implementation and enhancement of production of precursors OA and GPP.

On the one hand, the β-oxidation pathway is taking place within the yeast peroxisome and ultimately feeds acetyl-CoA into the cell's metabolism and the MVA pathway for IPP supply. Based on this, a pathway was transferred to the peroxisome of *K. phaffii* for the biosynthesis of lycopene from IPP and farnesyl diphosphate (FPP) (Bhataya et al., 2009). The final lycopene yield was about 4-times higher than reported for a cytosolic lycopene biosynthesis (Araya-Garay et al., 2012). While Bhataya et al. used the native peroxisome targeting sequence 1 (PTS1), the sequence was recently optimized to improve transport rates independent of protein properties (DeLoache et al., 2016). Other studies in *S. cerevisiae* also proposed to use the peroxisome for production of β-oxidation-derived metabolites (DeLoache et al., 2016; Sheng et al., 2016; Zhou et al., 2016).

On the other hand, the peroxisome of methylotrophic yeasts can constitute to up to 80 % of the total cell volume indicating a large potential for protein intake and thus metabolite production within the peroxisome (Gleeson and Sudbery, 1988). Peroxisome biogenesis in *K. phaffii* can be induced via methanol and oleate due to the MUT and β-oxidation pathway taking place in the peroxisome. However, both pathways are independent from each other and accordingly a down-regulation of genes involved in the β-oxidation of fatty acids has been observed when cells were grown on methanol (Prielhofer et al., 2015; Rußmayer et al., 2015). When cells are grown on glucose limitation however, an increased β-oxidation pathway activity was observed which has to be considered for promoter selection within the engineering and fermentation strategy. Using the methanol-independent, oleate-inducible promoter P_{POX1}, it was possible to combine a glucose growth phase with oleate-induced peroxisome biogenesis and simultaneous gene expression to enable the polyhydroxyalkanoate production within the peroxisomes of *K. phaffii* (Poirier, 2002). Furthermore, *K. phaffii* shows robust growth compared to the poor growth of *S. cerevisiae* in culture media containing only fatty acids as the carbon source (Poirier, 2002).

K. phaffii has recently been used for the production of (+)-nootkatone (Wriessnegger et al., 2014) and dammarenediol-II (Liu et al., 2015) from FPP with the dammarenediol-II system - without optimization of the MVA pathway flux - already surpassing yields obtained from *S. cerevisiae* production systems with an optimized MVA pathway flux (Schwarzhans et al., 2017a). That the flux optimization of the MVA pathway enhances the terpenoids production in *S. cerevisiae* is well-known (Asadollahi et al., 2010), however Wriessnegger et al. were the first to deploy such strategy in *K. phaffii* to improve (+)-nootkatone production. While the yields were also significantly higher compared to *S. cerevisiae* systems producing (+)-nootkatone, a more promising insight was presented by this group. Unlike for *S. cerevisiae* cultures, at concentrations > 100 mg (+)-nootkatone no cytotoxic effects on *K. phaffii* could be observed (Gavira et al., 2013). This might indicate a higher robustness of *K. phaffii* compared to *S. cerevisiae* for the production of many metabolites.

Potential necessary steps to enable the cannabinoid production in yeast from a cheap carbon source have been discussed in detail by Carvalho et al. (2017). Generally, in addition to expressing *nphB* and *thcas* or *cbdas*, the flux through the MVA pathway has to be increased and the formation of GPP instead of FPP prioritized by making use of a FPP synthase variant with optimized product specificity regarding GPP. The native FPP synthase in yeasts produces GPP exclusively as an intermediate and side-product in low amounts. However, a FPP synthase variant is known that has been engineered into a GPP synthase (Ignea et al., 2014). Furthermore, the supply of OA might be realized by expressing *oac* and *ols* from *C. sativa*. As the market price of hexanoate is relatively low, it might be fed to the cells instead of expressing necessary genes for its production. Still, hexanoate has to be activated to hexanoyl-CoA by an acyl activating enzyme within the cell. Activation can be realized using expression of *aae1* from *C. sativa* or upregulation of the native genes if possible.

Data indicates that CBGA and THCA are accumulating within the cell membranes due to their hydrophobic character (chapter 3). As CBGA was also available for vacuolar THCAS, we assume that CBGA and THCA will ultimately diffuse through the membranes of compartments, however most of the metabolites might accumulate in the membranes. Thus, CBGA produced in the peroxisome might be available for the THCAS or CBDAS in the vacuole. Nevertheless, it has to be clarified that this also poses a threat for membrane integrity and subsequently metabolic activity and cell viability. Therefore it might be difficult to obtain high cannabinoid contents within yeast cells.

Carvalho et al. depict the various advantages and disadvantages of several potential heterologous hosts for the cannabinoid production (Carvalho et al., 2017). Admittedly, there have been not many metabolic engineering projects in *K. phaffii* compared to *S: cerevisiae*. It should, however, be noted that this was mainly due to a lack of available genetic tools and strains and a significantly smaller scientific community. The advantage of *S. cerevisiae* over *K. phaffii* in terms of available genetic tools as well as available strains, vectors and promoters becomes more and more insignificant with the recently established episomal vectors, the CRISPR/Cas9 system, the Golden*Pi*CS system, the increasing number and variety in strains and promoters (*K. phaffii* toolkit) as well as the possibilities to tackle the clonal variety in *K. phaffii* (see chapter 2.4.1 and 2.4.2). Therefore, with the new tools at hand, the conclusion from solely the experimental results, i.e. a 10-fold higher NphB activity level and a more than 70-fold higher THCAS activity level (comparing optimized strain PP2CNE21Hac5FAD C7 (chapter 4.4.3) and SC_NT (chapter 6.4)), should be to pursue a strain engineering of the methylotrophic yeast *K. phaffii* for an industrial cannabinoid production platform. Combined with a presumably higher robustness of *K. phaffii* compared to *S. cerevisiae* to excess metabolite production and the possibility to transfer the CBGA production into the peroxisome, which can make up to 80 % of the cell volume in methylotrophic yeasts, this approach should involve the compartmentalization of the biosynthetic pathway.

7.3. OUTLOOK

Future developments are uncertain as the global legislation for the use of medical *Cannabis* is changing rapidly towards opening *Cannabis* to the public, although *Cannabis* is still not FDA and EMA approved for safety and efficacy. It should not be desirable to fully legalize *Cannabis* due to public health and abuse risks. While European countries currently do not plan to do so, a growing number of citizen petitions demand legalization. However the legislation will change, the demand for pharmaceutical grade cannabinoids is already rising and will presumably still do in the near future as cannabinoids are being under investigation for additional medical applications. The rapidly increasing demand can currently not be met and people are hence still drawn to the black market with its inherent lack of quality control and thus health risks.

The biotechnological approach presents an alternative to tackle these problems. The prospect of processes with a high controllability and reproducibility, GMP-compliance, a high scalability to cover demands as well as more environmentally friendly and agricultural area-saving conditions are desirable.

In this regard, the work presented in this thesis provides a promising basis for future research regarding the biosynthesis of cannabinoids in yeasts, especially *K. phaffii*. Based on the presented results and recent advances of the scientific community, *K. phaffii* should be considered the more promising host compared to *S. cerevisiae* not only for the production of large amounts of these cannabinoid producing enzymes, e.g. for protein crystallization studies or further mutational studies, but also for the metabolic engineering project. Employment of the newly available episomal vectors as well as synthetic promoters should lead to a significant decrease of the clonal variability in the screening system and thus increased sensitivity for the detection of promising enzyme variants. Furthermore, the recent development and optimization of a CRISPR/Cas9 system combined with the established Golden*Pi*Cs system negates most of the previous disadvantages of *K. phaffii* compared with *S. cerevisiae* regarding its genetic toolbox for metabolic engineering.

Implementing some of the proposed approaches to realize the cannabinoid biosynthesis in *K. phaffii*, it should be possible to develop a yeast producing different cannabinoids or cannabinoid compositions from a cheap carbon source. Whether the process will be competitive to other production methods, depends, however, on several factors. Foremost, to achieve high product titers, the precursor supply is critical. While there is extensive experimental knowledge available to boost the IPP and GPP production within the yeast, it is lacking for the supply of olivetolic acid up to now. In addition, the inherent toxicity of the cannabinoids potentially presents a major bottleneck as well. Finding solutions to these problems should be next in line. Nevertheless, the studies presented here contribute to increased fundamental and industrially relevant knowledge and will help promoting a biotechnological cannabinoid production in yeasts.

7.4. REFERENCES

Araya-Garay, J.M., Feijoo-Siota, L., Rosa-dos-Santos, F., Veiga-Crespo, P., Villa, T.G., 2012. Construction of new Pichia pastoris X-33 strains for production of lycopene and β-carotene. Appl. Microbiol. Biotechnol. 93, 2483–2492. doi:10.1007/s00253-011-3764-7

Asadollahi, M. a, Maury, J., Schalk, M., Clark, A., Nielsen, J., 2010. Enhancement of farnesyl diphosphate pool as direct precursor of sesquiterpenes through metabolic engineering of the mevalonate pathway in Saccharomyces cerevisiae. Biotechnol. Bioeng. 106, n/a-n/a. doi:10.1002/bit.22668

Bhataya, A., Schmidt-Dannert, C., Lee, P.C., 2009. Metabolic engineering of Pichia pastoris X-33 for lycopene production. Process Biochem. 44, 1095–1102. doi:10.1016/j.procbio.2009.05.012

Bilan, D.S., Pase, L., Joosen, L., Gorokhovatsky, A.Y., Ermakova, Y.G., Gadella, T.W.J., Grabher, C., Schultz, C., Lukyanov, S., Belousov, V. V., 2013. HyPer-3: A Genetically Encoded H 2 O 2 Probe with Improved Performance for Ratiometric and Fluorescence Lifetime Imaging. ACS Chem. Biol. 8, 535–542. doi:10.1021/cb300625g

Bonitz, T., Alva, V., Saleh, O., Lupas, A.N., Heide, L., 2011. Evolutionary Relationships of Microbial Aromatic Prenyltransferases. PLoS One 6, e27336. doi:10.1371/journal.pone.0027336

Carvalho, Â., Hansen, E.H., Kayser, O., Carlsen, S., Stehle, F., 2017. Designing microorganisms for heterologous biosynthesis of cannabinoids. FEMS Yeast Res. 17. doi:10.1093/femsyr/fox037

Chen, H., Cao, C., Kulinich, A., Liu, L., Jung, Y.-S., Voglmeir, J., 2017. Engineering of an episomal plasmid suitable for high-throughput expression in Pichia pastoris. Comb. Chem. High Throughput Screen. 20, 1–23. doi:10.2174/1386207320666170925145531

DeLoache, W.C., Russ, Z.N., Dueber, J.E., 2016. Towards repurposing the yeast peroxisome for compartmentalizing heterologous metabolic pathways. Nat. Commun. 7, 11152. doi:10.1038/ncomms11152

Diakov, T.T., Tarsio, M., Kane, P.M., 2013. Measurement of Vacuolar and Cytosolic pH In Vivo in Yeast Cell Suspensions. J. Vis. Exp. 1–7. doi:10.3791/50261

Fellermeier, M., Zenk, M.H., 1998. Prenylation of olivetolate by a hemp transferase yields cannabigerolic acid, the precursor of tetrahydrocannabinol. FEBS Lett. 427, 283–5.

Gasser, B., Maurer, M., Rautio, J., Sauer, M., Bhattacharyya, A., Saloheimo, M., Penttilä, M., Mattanovich, D., 2007. Monitoring of transcriptional regulation in Pichia pastoris under protein production conditions. BMC Genomics 8, 179. doi:10.1186/1471-2164-8-179

Gavira, C., Höfer, R., Lesot, A., Lambert, F., Zucca, J., Werck-Reichhart, D., 2013. Challenges and pitfalls of P450-dependent (+)-valencene bioconversion by Saccharomyces cerevisiae. Metab. Eng. 18, 25–35. doi:10.1016/j.ymben.2013.02.003

Gleeson, M.A., Sudbery, P.E., 1988. The methylotrophic yeasts. Yeast 4, 1–15. doi:10.1002/yea.320040102

Gong, Y., Kakihara, Y., Krogan, N., Greenblatt, J., Emili, A., Zhang, Z., Houry, W. a, 2009. An atlas of chaperone-protein interactions in Saccharomyces cerevisiae: implications to protein folding pathways in the cell. Mol. Syst. Biol. 5, 275. doi:10.1038/msb.2009.26

Ignea, C., Pontini, M., Maffei, M.E., Makris, A.M., Kampranis, S.C., 2014. Engineering Monoterpene Production in Yeast Using a Synthetic Dominant Negative Geranyl Diphosphate Synthase. ACS Synth. Biol. 3, 298–306. doi:10.1021/sb400115e

Kuzuyama, T., Noel, J.P., Richard, S.B., 2005. Structural basis for the promiscuous biosynthetic prenylation of aromatic natural products. Nature 435, 983–7. doi:10.1038/nature03668

Li, S.C., Kane, P.M., 2009. The yeast lysosome-like vacuole: Endpoint and crossroads. Biochim. Biophys. Acta - Mol. Cell Res. 1793, 650–663. doi:10.1016/j.bbamcr.2008.08.003

Liu, X.-B., Liu, M., Tao, X.-Y., Zhang, Z.-X., Wang, F.-Q., Wei, D.-Z., 2015. Metabolic engineering of Pichia pastoris for the production of dammarenediol-II. J. Biotechnol. 216, 47–55. doi:10.1016/j.jbiotec.2015.10.005

Maeda, H., Fukuyasu, Y., Yoshida, S., Fukuda, M., Saeki, K., Matsuno, H., Yamauchi, Y., Yoshida, K., Hirata, K., Miyamoto, K., 2004. Fluorescent Probes for Hydrogen Peroxide Based on a Non-Oxidative Mechanism. Angew. Chemie Int. Ed. 43, 2389–2391. doi:10.1002/anie.200452381

Nothaft, H., Szymanski, C.M., 2013. Bacterial Protein N -Glycosylation: New Perspectives and Applications. J. Biol. Chem. 288, 6912–6920. doi:10.1074/jbc.R112.417857

Ohara, K., Muroya, A., Fukushima, N., Yazaki, K., 2009. Functional characterization of LePGT1, a membrane-bound prenyltransferase involved in the geranylation of p -hydroxybenzoic acid. Biochem. J. 421, 231–241. doi:10.1042/BJ20081968

Page, J.E., Boubakir, Z., 2014. Aromatic prenyltransferase from *Cannabis*. US 20120144523 A1.

Poirier, Y., 2002. Synthesis of polyhydroxyalkanoate in the peroxisome of Pichia pastoris. FEMS Microbiol. Lett. 207, 97–102. doi:10.1016/S0378-1097(01)00567-5

Prielhofer, R., Cartwright, S.P., Graf, A.B., Valli, M., Bill, R.M., Mattanovich, D., Gasser, B., 2015. Pichia pastoris regulates its gene-specific response to different carbon sources at the transcriptional, rather than the translational, level. BMC Genomics 16, 167. doi:10.1186/s12864-015-1393-8

Rußmayer, H., Buchetics, M., Gruber, C., Valli, M., Grillitsch, K., Modarres, G., Guerrasio, R., Klavins, K., Neubauer, S., Drexler, H., Steiger, M., Troyer, C., Al Chalabi, A., Krebiehl, G., Sonntag, D., Zellnig, G., Daum, G., Graf, A.B., Altmann, F., Koellensperger, G., Hann, S., Sauer, M., Mattanovich, D., Gasser, B., 2015. Systems-level organization of yeast methylotrophic lifestyle. BMC Biol. 13, 80. doi:10.1186/s12915-015-0186-5

Schwarzhans, J.-P., Luttermann, T., Geier, M., Kalinowski, J., Friehs, K., 2017a. Towards systems metabolic engineering in Pichia pastoris. Biotechnol. Adv. 35, 681–710. doi:10.1016/j.biotechadv.2017.07.009

Schwarzhans, J.-P., Luttermann, T., Wibberg, D., Winkler, A., Hübner, W., Huser, T., Kalinowski, J., Friehs, K., 2017b. A Mitochondrial Autonomously Replicating Sequence from Pichia pastoris for Uniform High Level Recombinant Protein Production. Front. Microbiol. 8, 1–15. doi:10.3389/fmicb.2017.00780

Sheng, J., Stevens, J., Feng, X., 2016. Pathway Compartmentalization in Peroxisome of Saccharomyces cerevisiae to Produce Versatile Medium Chain Fatty Alcohols. Sci. Rep. 6, 26884. doi:10.1038/srep26884

Shoyama, Y., Tamada, T., Kurihara, K., Takeuchi, A., Taura, F., Arai, S., Blaber, M., Shoyama, Y., Morimoto, S., Kuroki, R., 2012. Structure and Function of Δ1-Tetrahydrocannabinolic Acid (THCA) Synthase, the Enzyme Controlling the Psychoactivity of *Cannabis* sativa. J. Mol. Biol. 423, 96–105. doi:10.1016/j.jmb.2012.06.030

Sirikantaramas, S., Morimoto, S., Shoyama, Y., Ishikawa, Y., Wada, Y., Shoyama, Y., Taura, F., 2004. The Gene Controlling Marijuana Psychoactivity. J. Biol. Chem. 279, 39767–39774. doi:10.1074/jbc.M403693200

Starbird, C.A., Maklashina, E., Sharma, P., Qualls-Histed, S., Cecchini, G., Iverson, T.M., 2017. Structural and biochemical analyses reveal insights into covalent flavinylation of the Escherichia coli Complex II homolog quinol:fumarate reductase. J. Biol. Chem. 292, 12921–12933. doi:10.1074/jbc.M117.795120

Taura, F., Dono, E., Sirikantaramas, S., Yoshimura, K., Shoyama, Y., Morimoto, S., 2007. Production of Δ1-tetrahydrocannabinolic acid by the biosynthetic enzyme secreted from transgenic Pichia pastoris. Biochem. Biophys. Res. Commun. 361, 675–680. doi:10.1016/j.bbrc.2007.07.079

Valderrama-Rincon, J.D., Fisher, A.C., Merritt, J.H., Fan, Y., Reading, C.A., Chhiba, K., Heiss, C., Azadi, P., Aebi, M., DeLisa, M.P., 2012. An engineered eukaryotic protein glycosylation pathway in Escherichia coli. Nat. Chem. Biol. 8, 434–436. doi:10.1038/nchembio.921

Valli, M., Sauer, M., Branduardi, P., Borth, N., D, 2005. Intracellular pH distribution in *Saccharomyces cerevisiae* cell populations, analyzed by flow cytometry. Appl. Environ. Microbiol. 71, 1515–1521. doi:10.1128/AEM.71.3.1515

van Roermund, C.W.T., 2004. The peroxisomal lumen in Saccharomyces cerevisiae is alkaline. J. Cell Sci. 117, 4231–4237. doi:10.1242/jcs.01305

Weninger, A., Fischer, J., Raschmanová, H., Kniely, C., Vogl, T., Glieder, A., 2017. Expanding the CRISPR/Cas9 toolkit for *Pichia pastoris* with efficient donor integration and alternative resistance markers. J. Cell. Biochem. doi:10.1002/jcb.26474

Wolfbeis, O.S., Dürkop, A., Wu, M., Lin, Z., 2002. A Europium-Ion-Based Luminescent Sensing Probe for Hydrogen Peroxide. Angew. Chemie Int. Ed. 41, 4495–4498. doi:10.1002/1521-3773(20021202)41:23<4495::AID-ANIE4495>3.0.CO;2-I

Wriessnegger, T., Augustin, P., Engleder, M., Leitner, E., Müller, M., Kaluzna, I., Schürmann, M., Mink, D., Zellnig, G., Schwab, H., Pichler, H., 2014. Production of the sesquiterpenoid (+)-nootkatone by metabolic engineering of Pichia pastoris. Metab. Eng. 24, 18–29. doi:10.1016/j.ymben.2014.04.001

Yamamoto, H., Kimata, J., Senda, M., Inoue, K., 1997. Dimethylallyl diphosphate: Kaempferol 8-dimethylallyl transferase in Epimedium diphyllum cell suspension cultures. Phytochemistry 44, 23–28. doi:10.1016/S0031-9422(96)00484-0

Zhou, Y.J., Buijs, N.A., Zhu, Z., Gómez, D.O., Boonsombuti, A., Siewers, V., Nielsen, J., 2016. Harnessing Yeast Peroxisomes for Biosynthesis of Fatty-Acid-Derived Biofuels and Chemicals with Relieved Side-Pathway Competition. J. Am. Chem. Soc. 138, 15368–15377. doi:10.1021/jacs.6b07394

SUPPLEMENTARY MATERIAL

II. LIST OF ABBREVIATIONS

2-*O*-GOA	2-*O*-geranyl olivetolic acid
AA	amino acid
ADP	adenosine diphosphate
ATP	adenosine triphosphate
ARS	autonomously replicating sequence
BBE	berberine-bridge enzyme
Cas9	CRISPR-associated protein-9
CBC	cannabichromene
CBCA	cannabichromenic acid
CBCAS	CBCA synthase
CBD	cannabidiol
CBDA	cannabidiolic acid
CBDAS	CBDA synthase
CBDV	cannabidivarin
CBG	cannabigerol
CBGA	cannabigerolic acid
CBGAS	cannabigerolic acid synthase
CBNA	cannabinolic acid
CID	collision induced dissociation
CNE1p	calnexin-like protein
CPR5p	ER-resident peptidyl-prolyl-*cis*-*trans*-isomerase
CRISPR	clustered regularly interspaced short palindromic repeat
DMAPP	dimetyhlallyl diphosphate
DOXP	1-deoxy-D-xylulose 5-phosphate
ECS	endo-cannabinoid system
ER	endoplasmic reticulum
Ero1p	endoplasmic reticulum Oxidoreductin 1
FAAH	fatty acid amide hydrolase
FAD	flavin adenine dinucleotide
FAD1p	FAD synthetase
FMN1p	riboflavin kinase
GCN	gene copy number
GPP	geranyl diphosphate
Hac1p	basic leucine zipper transcription factor
Hac1s	spliced gene version of basic leucine zipper transcription factor
HR	homologous recombination
IPP	isopentyl diphosphate
Kar2p	chaperone of the endoplasmic reticulum lumen
Lhs1p	chaperone of the endoplasmic reticulum lumen

m/z	mass per charge ratio
MAGL	monoacylglycerol lipase
MEP	2-C-methyl-D-erythritol 4-phosphate
MVA	mevalonate/mevalonic acid
NHEJ	non-homologous end joining
Ni-NTA	Nickel-nitrilotriacetic acid
OA	olivetolic acid
OAC	olivetolic acid cyclase
OLS	olivetol synthase
PDI1p	protein disulfide isomerase
RT	retention time
ROS	reactive oxygen species
Sec53p	phosphomannomutase
Δ^9-THC	Δ^9-tetrahydrocannabinol
THC	Δ^9-tetrahydrocannabinol
THCA	Δ^9-tetrahydrocannabinolic acid
THCAS	Δ^9-tetrahydrocannabinolic acid synthase
THCV	Δ^9-tetrahydrocannabivarin
UPR	unfolded protein response
Yap1p	basic leucine zipper transcription factor

III. LIST OF FIGURES

IV. LIST OF TABLES

V. SUPPLEMENTARY MATERIAL CHAPTER 2

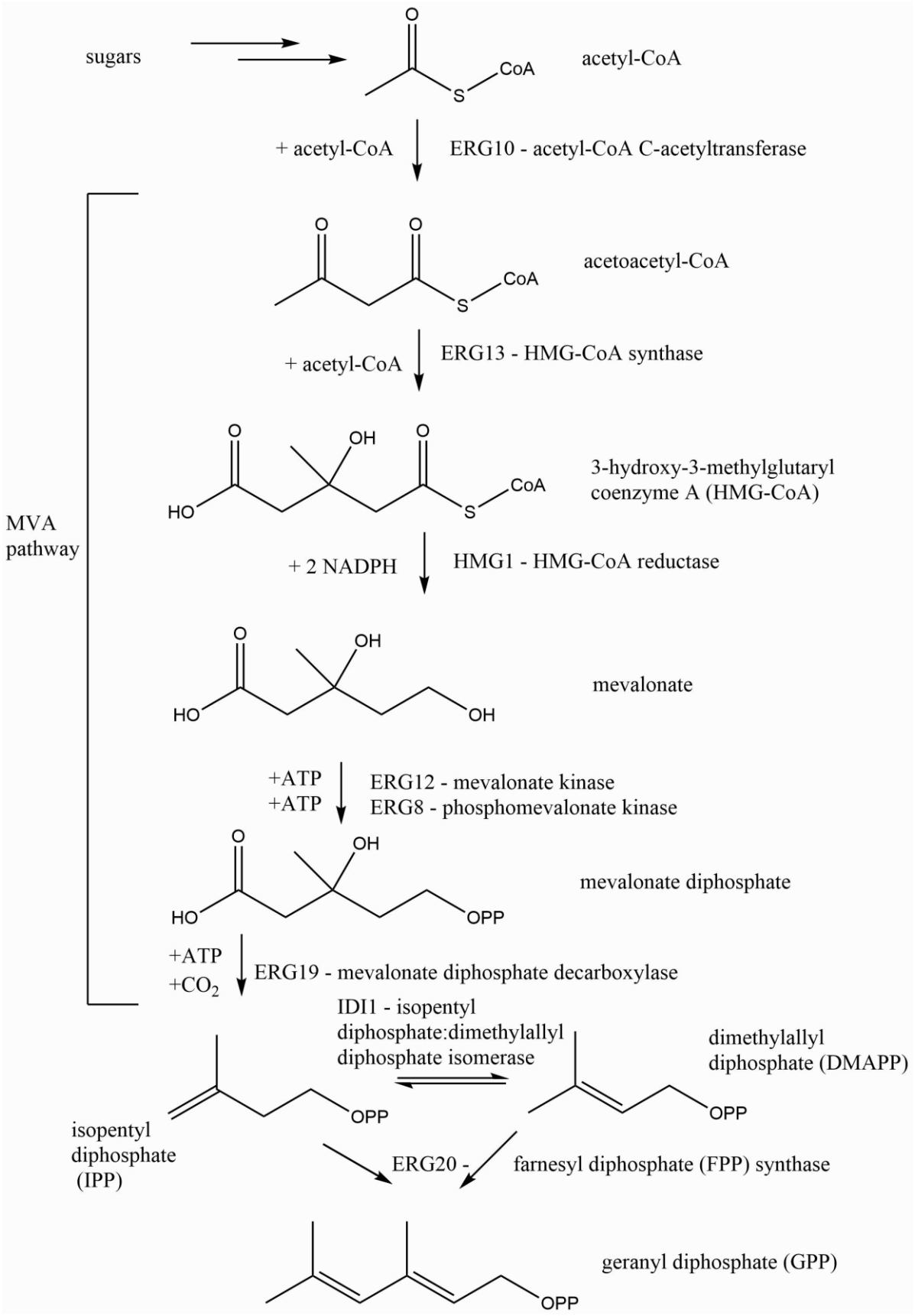

Fig. S VI-1: MVA pathway in *S. cerevisiae*. Adapted from Carvalho et al. (2017).

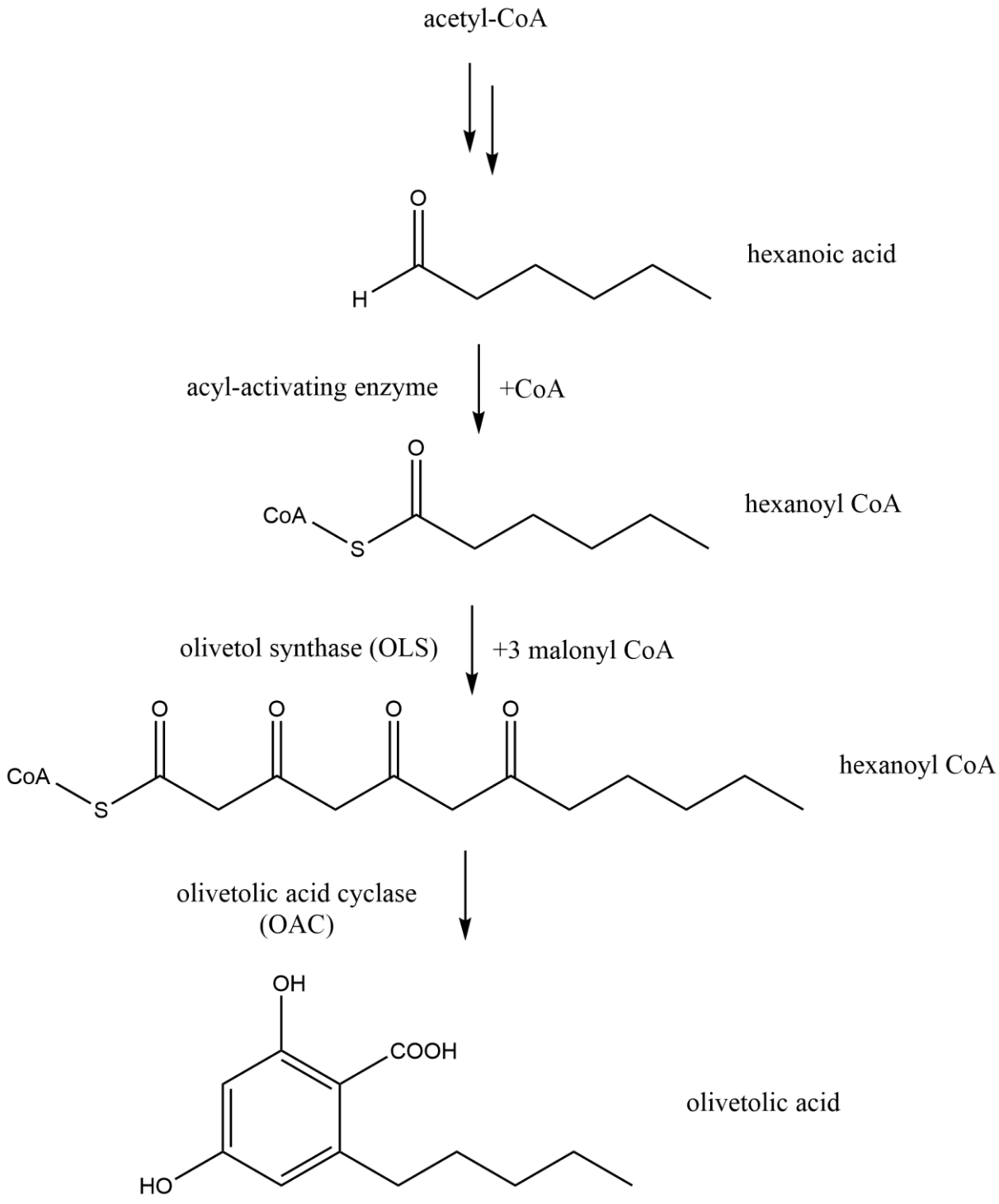

Fig. S VI-2: Olivetolic acid biosynthesis in *Cannabis sativa* L. Adapted from Carvalho et al. (2017).

VI. SUPPLEMENTARY MATERIAL CHAPTER 3

Table S VI-1: List of microorganisms used for expression of THCAS.

Organism	**Strain**	**Company**	**Genotype**
E. coli	SHuffle T7 Express	NEB, Frankfurt, Germany	fhuA2 lacZ::T7 gene1 [lon] ompT ahpC gal λatt::pNEB3-r1-cDsbC (SpecR, lacIq) ΔtrxB sulA11 R(mcr-73::miniTn10--TetS)2 [dcm] R(zgb-210::Tn10--TetS) endA1 Δgor Δ(mcrC-mrr)114::IS10
E. coli	SHuffle T7 Express *lysY*	NEB, Frankfurt, Germany	lacZ::T7 gene1 [lon] ompT ahpC gal λatt::pNEB3-r1-cDsbC (SpecR, lacIq) ΔtrxB sulA11 R(mcr-73::miniTn10--TetS)2 [dcm] R(zgb-210::Tn10--TetS) endA1 Δgor Δ(mcrC-mrr)114::IS10
S. cerevisiae	CEN.PK2-1C Δ*gal1*	Euroscarf, Frankfurt, Germany	*MAT*a; *gal1::loxP; ura3-52; trp1-289; leu2-3,112; his3Δ 1; MAL2-8C; SUC2*
S. cerevisiae	CEN.PK2-1C Δ*gal1*Δ*pep4*	this work	*MAT*a; *gal1::loxP; pep4::loxP; ura3-52; trp1-289; leu2-3,112; his3Δ 1; MAL2-8C; SUC2*
P. pastoris	PichiaPink1	Invitrogen, Darmstadt, Germany	*ade2*
P. pastoris	PichiaPink2	Invitrogen, Darmstadt, Germany	*ade2; pep4*
P. pastoris	PichiaPink3	Invitrogen, Darmstadt, Germany	*ade2; prb1*

Table S VI-2: List of plasmids.

Plasmid	**Features**
pET28a(+)_THCAS	pET28(a+) (Merck, Darmstadt, Germany) with cDNA of THCAS; cloned into *Nde*I and *Hin*dIII restriction sites
pET32a(+)_THCAS	pET32a(+) (Merck, Darmstadt, Germany) with cDNA of THCAS; cloned into *Nco*I and *Hin*dIII restriction sites
pDionysos_THCAS	pDionysos with cDNA of THCAS codon usage optimized for *S. cerevisiae*; N-terminal 5'UTR (AAAAAA) followed by sequence coding for 24 aa signal peptide of proteinase A (Uniprot P07267); C-terminal sequence coding for 3 additional histidines; cloned into *Hin*dIII and *Xba*I restriction sites
pPink_HC_THCAS	pPink-HC (Invitrogen, Darmstadt, Germany) with cDNA of THCAS codon usage optimized for *P. pastoris*; N-terminal 5'UTR (AAAAAA) followed by sequence coding for 24 aa signal peptide of proteinase A (Uniprot F2QUG8); C-terminal sequence coding for 3 additional histidines; cloned into *Eco*RI and *Kpn*I restriction sites
pPink_LC_THCAS	pPink-LC (Invitrogen, Darmstadt, Germany) with cDNA of THCAS codon usage optimized for *P. pastoris*; N-terminal 5'UTR (AAAAAA) followed by sequence coding for 24 aa signal peptide of proteinase A (Uniprot F2QUG8); C-terminal sequence coding for 3 additional histidines; cloned into *Eco*RI and *Kpn*I restriction sites

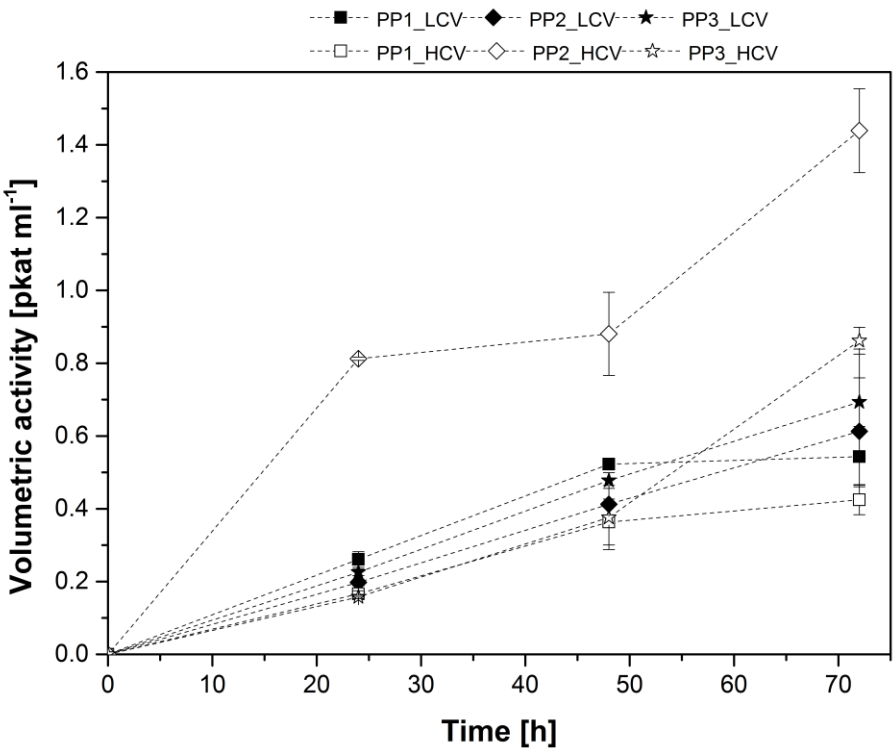

Fig. S VI-1: Screening of *P. pastoris* clones - volumetric THCAS activity. Cultures were inoculated at 0.105 g_{CDW} l^{-1}. Cultures were grown at 200 rpm and 20 °C. Methanol was added every 24 h at a concentration of 0.5 % (v/v). Values are calculated from biological duplicates.

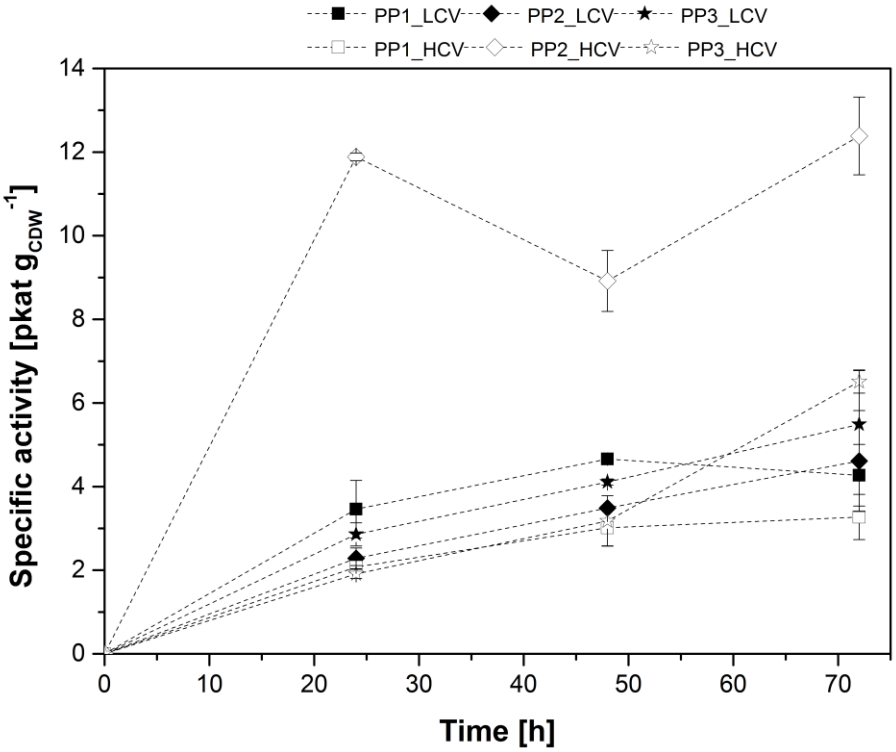

Fig. S VI-2: Screening of *P. pastoris* clones - specific THCAS activity. Cultures were inoculated at 0.105 g_{CDW} l^{-1}. Cultures were grown at 200 rpm and 20 °C. Methanol was added every 24 h at a concentration of 0.5 % (v/v). Values are calculated from biological duplicates.

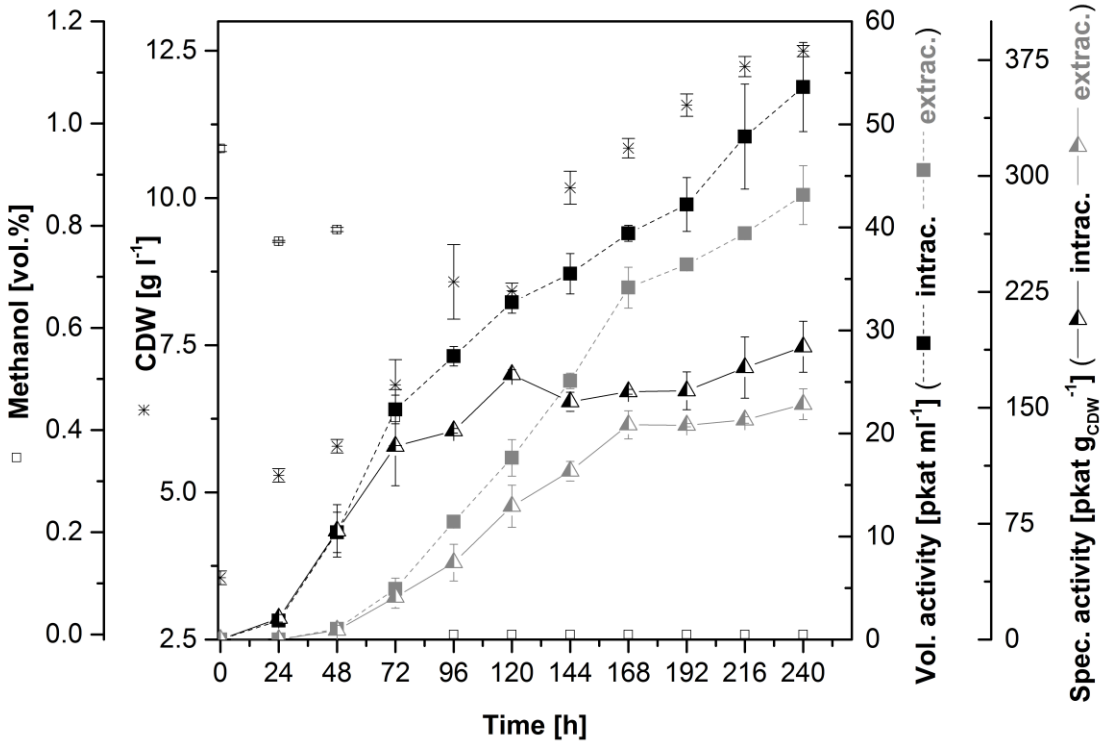

Fig. S VI-3: Expression of THCAS using PP2_HC. Cultures were grown in 3-baffled shaking flasks at 200 rpm and 10 °C. Methanol was added every 24 h at a concentration of 0.5 % (v/v). Data points present the means of three biological replicates with two technical replicates and error bars present the standard deviation.

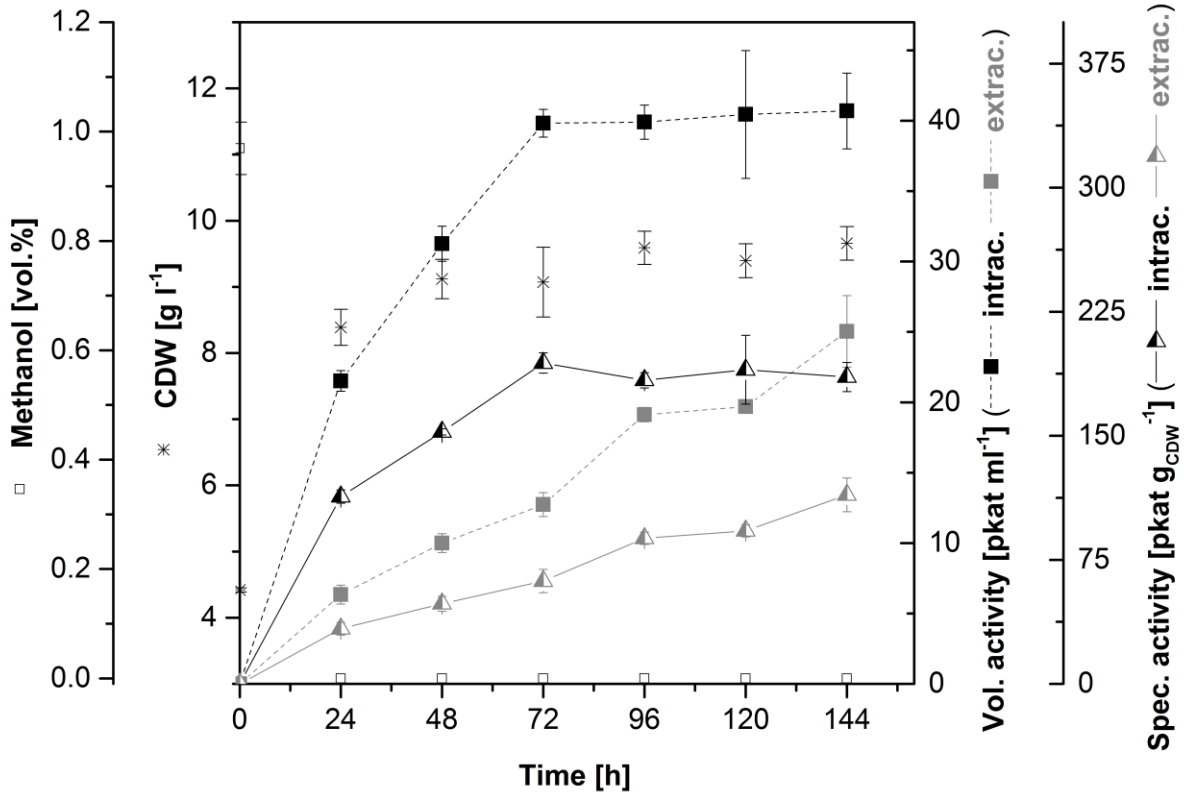

Fig. S VI-4: Expression of THCAS using PP2_HC. Cultures were grown in 3-baffled shaking flasks at 200 rpm and 20 °C. Methanol was added every 24 h at a concentration of 0.5 % (v/v). Data points present the means of three biological replicates with two technical replicates and error bars present the standard deviation.

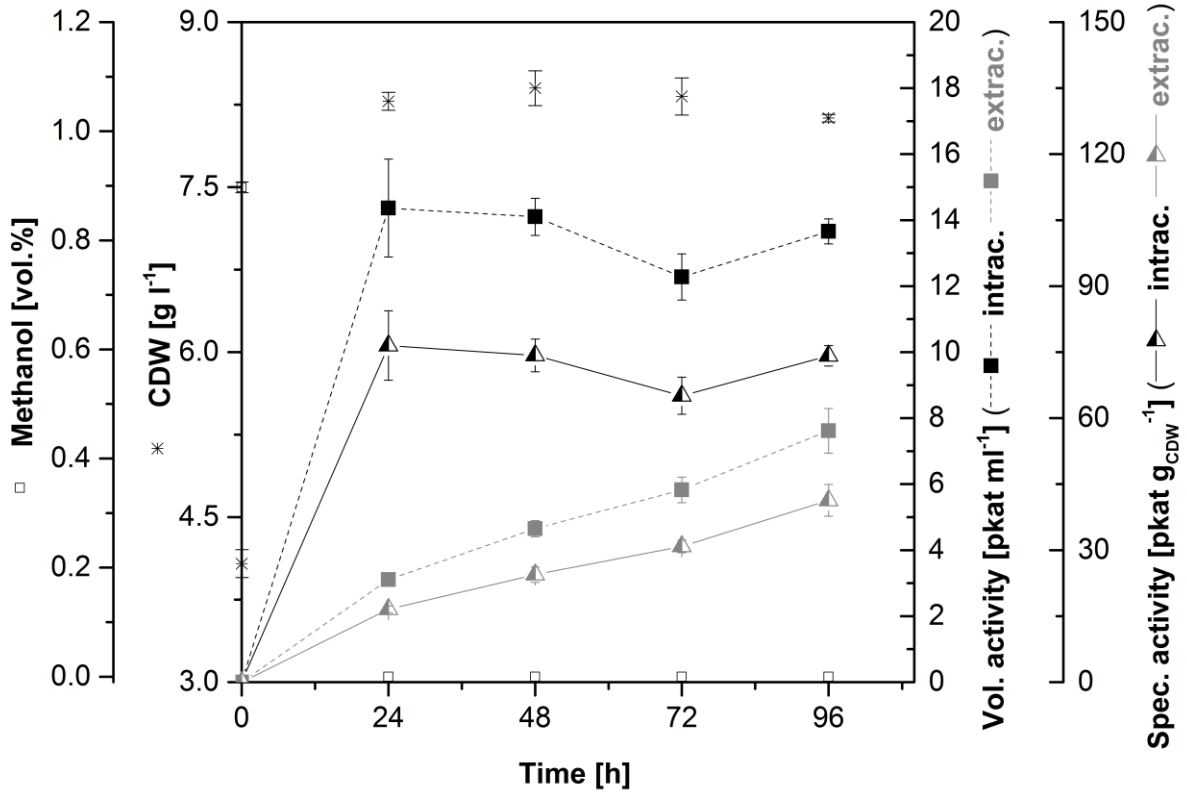

Fig. S VI-5: Expression of THCAS using PP2_HC. Cultures were grown in 3-baffled shaking flasks at 200 rpm and 25 °C. Methanol was added every 24 h at a concentration of 0.5 % (v/v). Data points present the means of three biological replicates with two technical replicates and error bars present the standard deviation.

Media composition

2 x YPAD medium (pH 5.5): 20 g yeast extract l^{-1}, 40 g peptone l^{-1}, 4.41 g citric acid monohydrate l^{-1}, 25.63 g tripotassium citrate monohydrate l^{-1}, 10 mg riboflavin l^{-1}, 80 mg adenine hemisulfate l^{-1}, 40 g fructose l^{-1}, 5 g galactose l^{-1}.

BMGY medium (pH 6): 10 g yeast extract l^{-1}, 20 g peptone l^{-1}, 100 mM phosphate buffer pH 6.0, 13.8 g yeast nitrogen base l^{-1}, 0.4 mg biotin l^{-1}, 10 g glycerol l^{-1}.

Modified BMMY (mBMMY) medium (pH 5.5) (adapted from Taura et al. 2007): 10 g yeast extract l^{-1}, 20 g peptone l^{-1}, 5 g casamino acids l^{-1}, 100 mM Na-citrate buffer pH 5.5, 13.8 g yeast nitrogen base l^{-1}, 0.4 mg biotin l^{-1}, 10 mg riboflavin l^{-1}, 1 % (v/v) methanol.

Generation of *E. coli* strains for intracellular THCAS expression

pGEM-T-easy(modified) carrying the plant cDNA of THCAS – THCAS sequence was amplified using the primers (5'-GATCCATATGAATCCTCGAGAAAACTTCCTTAAATGCTTCT-3' and 5'-GCATAAGCTT CTATTAATGATGATGCGGTGGAAGAGG-3') and cut with *Nde*I and *Hin*dIII for insertion into pET28a(+) or with primers (5'-GACTCCATGGCTAATCCTCGAGAAAACTTCCTTAAATGCTTCT-3' and 5'-GCATA AGCTTCTATTAATGATGATGCGGTGGAAGAGG-3') and cut with *Nco*I and *Hin*dIII for insertion into pET32a(+). The vectors generated contained the cDNA of THCAS without signal peptide and were transformed into *E. coli* SHuffle T7 Express and *E. coli* SHuffle T7 Express *lysY*.

Generation of *S. cerevisiae* strains for intracellular THCAS expression

A cDNA coding for the THCAS without the first 84 bp (native signal peptide) and optimized for the codon-usage in *S. cerevisiae* was obtained from GeneArt (Regensburg, Germany). The cDNA was amplified by PCR with gene-specific primers (5'-GGGAATTCAAGCTTAAAAAAATGTCCAGCTT GAAAGCATTATTGCCATTGGCCTTGTTGTTGGTCAGCGCCAACCAAGTTGCTGCAAACCCTAGAGA AAACTTTTTGAAATG-3' and 5'-GACTTCTAGATCATTAATGATGATGATGGTGATGTGGAGGCAATG GAGGGATGG-3') to introduce a 5'UTR consensus sequence from *S. cerevisiae* in the 5' untranslated region followed by a sequence coding for a 24 amino acid signal peptide from *S. cerevisiae* vacuolar proteinase A (UniProt accession number P07267) and 3 histidine residues to complement a His6-tag at the C-terminus of the protein. The PCR product was purified from gel and cloned into pDionysos using *Hin*dIII and *Xba*I restriction sites. The empty vector was transformed as negative control. Transformants were selected on minimal medium agar without leucine.

Generation of *P. pastoris* strains for intracellular THCAS expression

A cDNA coding for the THCAS without the first 84 bp (native signal peptide) and optimized for the codon-usage in *P. pastoris* was ordered from GeneArt. The cDNA was amplified by PCR with gene-specific primers (5'-GCATACGAATTCAAAAAAATGTCTATATTTGACGGTACTACGATGTCAATTGCC ATTGGTTTGCTCTCTACTCTAGGTATTGGTGCTGAAGCCAACCCAAGAGAAAACTTCTTGAAGTG-3' and 5'-CGCTAGGGTACCTTATTAATGATGATGATGATGATGTGGTGGCAATGG-3') to introduce a 5'UTR consensus sequence from *S. cerevisiae* in front of the start codon followed by a sequence coding for a 24 amino acid signal peptide from *P. pastoris* vacuolar proteinase A (UniProt accession number F2QUG8) and 3 histidine residues to complement a His6-tag at the C-terminus of the protein. The PCR product was purified from gel and cloned into the low copy number (pPink -LC) and high copy number (pPink -HC) vectors downstream of the AOX1 promoter using *Eco*RI and *Kpn*I restriction sites. The three PichiaPink strains 1, 2 and 3 were transformed with linearized (cut with *Spe*I; chromosomal introduction into TRP2 gene) pPink-LC_THCAS or pPink –HC_THCA plasmids. The empty vectors were transformed as negative controls. Transformants were selected on Pichia adenine dropout (PAD) agar.

Cell lysis of *E. coli* cells

Cell cultures were centrifuged for 20 min at 4 °C and 5.000 x g. Cell pellet was resuspended in 6 ml 100 mM Na-citrate buffer pH 5.5. The cell suspension was supplemented with 10 mg lysozyme ml^{-1} and incubated for 20 min at room temperature. Afterwards 10 mg DNaseI ml^{-1} was added and the cell suspension incubated at room temperature for 10 min. Cells were lysed by sonication on ice at an amplitude of 10 % (10 x 6 s pulse on, 30 s pulse off). The lysate was centrifuged for 30 min at 5.000 x g and 4 °C and the supernatant used for activity assays.

Cell lysis of *S. cerevisiae* and *P. pastoris* cells

Cells were harvested by centrifugation of 450 µl cell suspension at 13,000 x g at 4 °C for 5 min. Supernatants were discarded and cells resuspended in 450 µl 100 mM Na-citrate buffer pH 5.5. After addition of 75 U lyticase ml^{-1} (Sigma Aldrich, Hamburg, Germany), cells were incubated at 37 °C and 1,100 rpm for 10 min in a shaking incubator. Cell suspension was transferred to 0.5 ml tubes and filled with 0.25 mm – 0.5 mm glass beads. Cells

were lysed by vortexing at maximum speed at 4 °C for 10 min. Cell lysate was centrifuged and supernatant used for activity assays.

Screening of *P. pastoris* transformants for high THCAS activity

From PAD agar plates 5 white colonies of each strain were picked for inoculation of 2 ml BMGY in glass tubes. Cells were incubated at 30 °C in a rotary shaker. After 24 h cultures were centrifuged and pellet washed with 0.9 % NaCl, centrifuged and pellet resuspended in 2 ml of BMMY. 50 µl of the suspensions was used to inoculate 2 ml of BMMY in glass tubes, respectively. Cells were cultivated at 30 °C in the rotary shaker for 72 h. The clone with the highest activity was selected of each strain and used for inoculation of 50 ml BMGY in 500 ml non-baffled flasks. Cultures were incubated at 200 rpm at 30 °C for 24 h. After washing with 0.9 % NaCl, the pellets were resuspended in BMMY and used for inoculation of 50 ml BMMY in 500 ml baffled flasks at a starting OD_{600} of 0.5. Cultures were grown at 20 °C, 200 rpm and supplemented every 24 h with 0.5 % (v/v) methanol.

VII. SUPPLEMENTARY MATERIAL CHAPTER 4

Table S VIII-1: List of used plasmids. References include additional informations that cannot be obtained from gene accession number.

Plasmid	**Initial plasmid**	**Expressed coding sequence(s)/ antibiotic resistance(s)**	**Gene Accession number (s)**	**References**
pAX_EV	pGAPZ A	p_{AOX1}: - Zeo^R	-	(Zirpel et al., 2017a)
pAX_PDI1	pAX_EV	p_{AOX1}: *PDI* Zeo^R	**CAC33587.1**	This study
pAX_Ero1	pAX_EV	p_{AOX1}: *Ero1* Zeo^R	**CAY67364.1**	This study
pAX_Yap1	pAX_EV	p_{AOX1}: *Yap1* Zeo^R	**CAY71861.1**	This study
pAX_Hac1s	pAX_EV	p_{AOX1}: *Hac1s* Zeo^R	**CAY67758.1**	This study; (Guerfal et al., 2010)
pAX_Lhs1	pAX_EV	p_{AOX1}: *Lhs1* Zeo^R	**CCA36228.1**	This study
pAX_Kar2	pAX_EV	p_{AOX1}: *Kar2* Zeo^R	**AY965684.1**	This study
pAX_FAD1	pAX_EV	p_{AOX1}: *FAD1* Zeo^R	**CAY67302.1**	This study
pAX_FAD1FMN1	pAX_FAD1	p_{AOX1}: *FAD1* and *FMN1* separated via T2A sequence Zeo^R	**CAY67302.1** **CAY72070.1**	This study; (Beekwilder et al., 2014a)
pAX_Sec53	pAX_EV	p_{AOX1}: *Sec53* Zeo^R	**CAY69880.1**	This study
pAX_CNE1	pAX_EV	p_{AOX1}: *CNE1* Zeo^R	**CAY68938.1**	This study
pAX_CPR5	pAX_EV	p_{AOX1}: *CPR5* Zeo^R	**CAY67638.1**	This study
pAXh_EV	pAX_EV	p_{AOX1i}: - $HygB^R$	-	This study; (Lee et al., 2015)
pAXh_Hac1s	pAXh_EV	p_{AOX1i}: *Hac1s* $HygB^R$	**CAY67758.1**	This study; (Guerfal et al., 2010)

Table S VIII-1: List of plasmids - continued.

pAXk_EV	pAX_EV	p_{AOX1}: - Kan^R, G-418^R	-	This study
pAXk_FAD1	pAXk_EV	p_{AOX1}: *FAD1* Kan^R, G-418^R	**CAY67302.1**	This study

Table S VIII-2: List of used primers.

Primer	**Sequence 5'->3'**	**Purpose**
p_Ero1_fw	CAAAAAACAACTAATTATTCGAAACGATGAGGATAGTAAGGAGCGTAGCTATCG	Amplification of helper protein gene
p_Ero1_rv	TGAGTTTTTGTTCGGGCCCTTATTACAAGTCTACTCTATATGTGGTATCT	Amplification of helper protein gene
p_PDI_fw	CAAAAAACAACTAATTATTCGAAACGATGCAATTCAACTGGGATATTAAAACTG	Amplification of helper protein gene
p_PDI_rv	TTGTTCGGGCCCTTATTAAAGCTCGTCGTGAGCGTCTG	Amplification of helper protein gene
p_Yap1_fw	CAAAAAACAACTAATTATTCGAAACGATGAGTGACGTGGTAAACAAGAGA	Amplification of helper protein gene
p_Yap1_rv	TGAGTTTTTGTTCGGGCCCTTATTATTTAAACATGGAAAAATCGACAACATCT	Amplification of helper protein gene
p_Kar2_fw	CAAAAAACAACTAATTATTCGAAACGATGCTGTCGTTAAAACCATCTTGGCTGACTT	Amplification of helper protein gene
p_Kar2_rv	TGAGTTTTTGTTCGGGCCCTTATTACAACTCATCATGATCATAGTCATAGTCGTAGTCAAA	Amplification of helper protein gene
p_Hac1s_fw	CAAAAAACAACTAATTATTCGAAACGATGCCCGTAGATTCTTCTCATAAGACAG	Amplification of helper protein gene
p_Hac1s_rv	TCTGAGATGAGTTTTTGTTCGGGCCTTATTCCTGGAAGAATACAAAGTCATTTAAATCAAATGCATTAGCGGTAAATGGTGCTGCTGGATGATGCAACCGATTCGACTCGCTAA	Amplification of helper protein gene

Table S-VIII-2: List of used primers - continued.

p_FAD1_fw	CAAAAAACAACTAATTATTCGAAACGATGGTAACTGTTCTCTCCAATAGTAGTAAG	Amplification of helper protein gene
p_FAD1_rv	TGAGTTTTTGTTCGGGCCCTTATTATAATCTACTGGATCTTTCCTTTTCGGAATC	Amplification of helper protein gene
p_FMN1_fw	TGCGGTGACGTTGAGGAAAACCCAGGTCCAATGACTCGACCGGTGATACC	Amplification of helper protein gene
p_FMN1_rv	CTCTTCTGAGATGAGTTTTTGTTCGGGCCCTTATTATTTAACATTATGGACCTGTTCT	Amplification of helper protein gene
p_CNE1_fw	AGATCAAAAAACAACTAATTATTCGAAACGATGAAGATCTCTACCATTGCAAGTTCTA	Amplification of helper protein gene
p_CNE1_rv	CCTCTTCTGAGATGAGTTTTTGTTCGGGCCCTAGGTTCTCTTTGTAGCTTTA	Amplification of helper protein gene
p_CPR5_fw	AGATCAAAAAACAACTAATTATTCGAAACGATGAAATTGTTGAACTTTCTGCTTAG	Amplification of helper protein gene
p_CPR5_rv	CCTCTTCTGAGATGAGTTTTTGTTCGGGCCCTACAACTCATCTTTCACGACCTCCT	Amplification of helper protein gene
p_Sec53_fw	AGATCAAAAAACAACTAATTATTCGAAACGATGTCGTTTTCTAATAAAGAAGATC	Amplification of helper protein gene
p_Sec53_rv	TTCTGAGATGAGTTTTTGTTCGGGCCCTTATTACAGGGAAAAGAGCTCCTTTA	Amplification of helper protein gene
p_Lhs1_fw	AGATCAAAAAACAACTAATTATTCGAAACGATGAGAACACAAAAGATAGTAACA	Amplification of helper protein gene
p_Lhs1_rv	CCTCTTCTGAGATGAGTTTTTGTTCGGGCCCTACAACTCATCATGGGATGTTT	Amplification of helper protein gene
p_pAX_fw	GGCCCGAACAAAAACTCATCTCA	Integration of helper protein genes into pAX_EV
p_pAX_rv	CGTTTCGAATAATTAGTTGTTTTTTG	Integration of helper protein genes into pAX_EV

Table S VIII-2: List of used primers - continued.

p_kanbb_fw	CACGTCCGACGGCGGCCCACGGGTC	Generation of pAXk/pAXh_EV
p_kanbb_fw	GGTTTAGTTCCTCACCTTGTCGTATTATACTATGCCGATATACTATGCCGATGA	Generation of pAXk/pAXh_EV
p_hygB_fw	GTATAATACGACAAGGTGAGGAACTAAACCATGGGTAAAAAGCCTGAACT	Amplification of hygromycin B resistance gene
p_hygB_rv	CCTGGGACCCGTGGGCCGCCGTCGGACGTGTTATTCCTTTGCCCTCGGACGAG	Amplification of hygromycin B resistance gene
p_kan_fw	ATACGACAAGGTGAGGAACTAAACCATGGGTAAGGAAAAGACTCACG	Amplification of Kanamycin/G418 resistance gene
p_kan_rv	GACCCGTGGGCCGCCGTCGGACGTGTTAGAAAAACTCATCGAGCATCAAA	Amplification of Kanamycin/G418 resistance gene

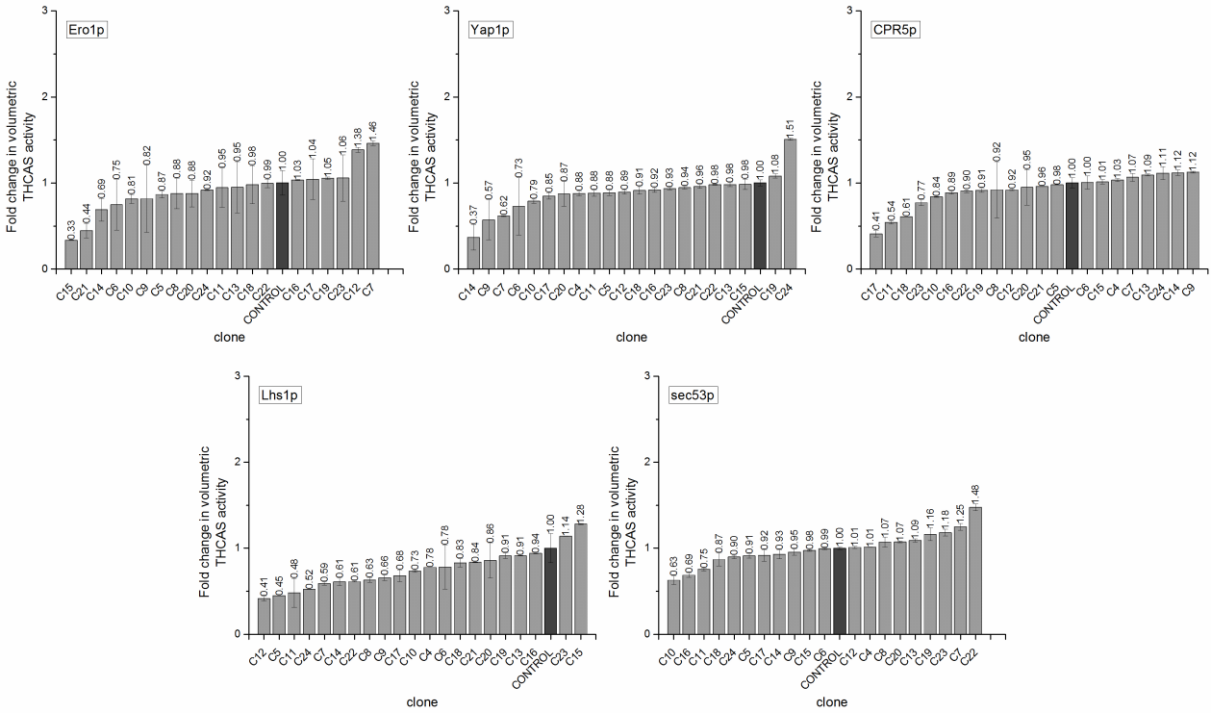

Fig. S VIII-1: Helper proteins without positive effect on measured THCAS activity. Shown is the change of normalized, volumetric, intracellular THCAS activities when cells were co-producing either Ero1p, Yap1p, CPR5p, Lhs1p or Sec53p.

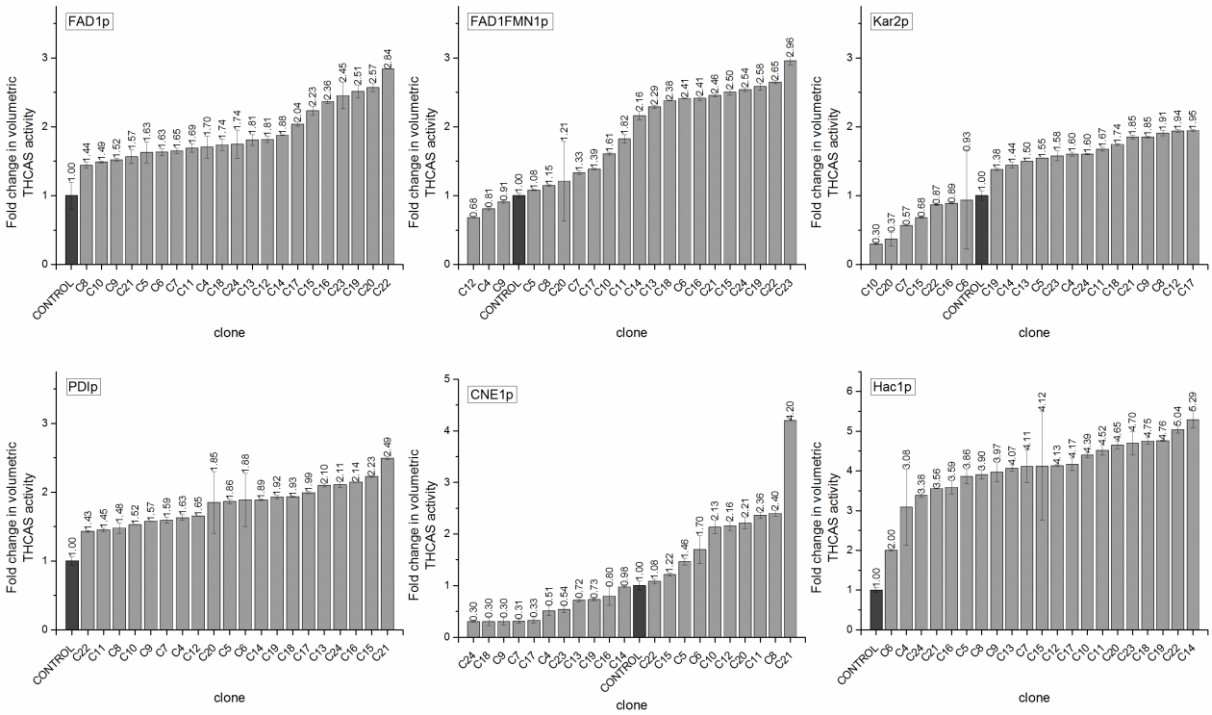

Fig. S VIII-2: Helper proteins with positive effect on measured THCAS activity. Shown is the change of normalized, volumetric, intracellular THCAS activities when cells were co-producing either FAD1p, FAD1p and FMN1p together, Kar2p, PDI1p, CNE1p or Hac1p.

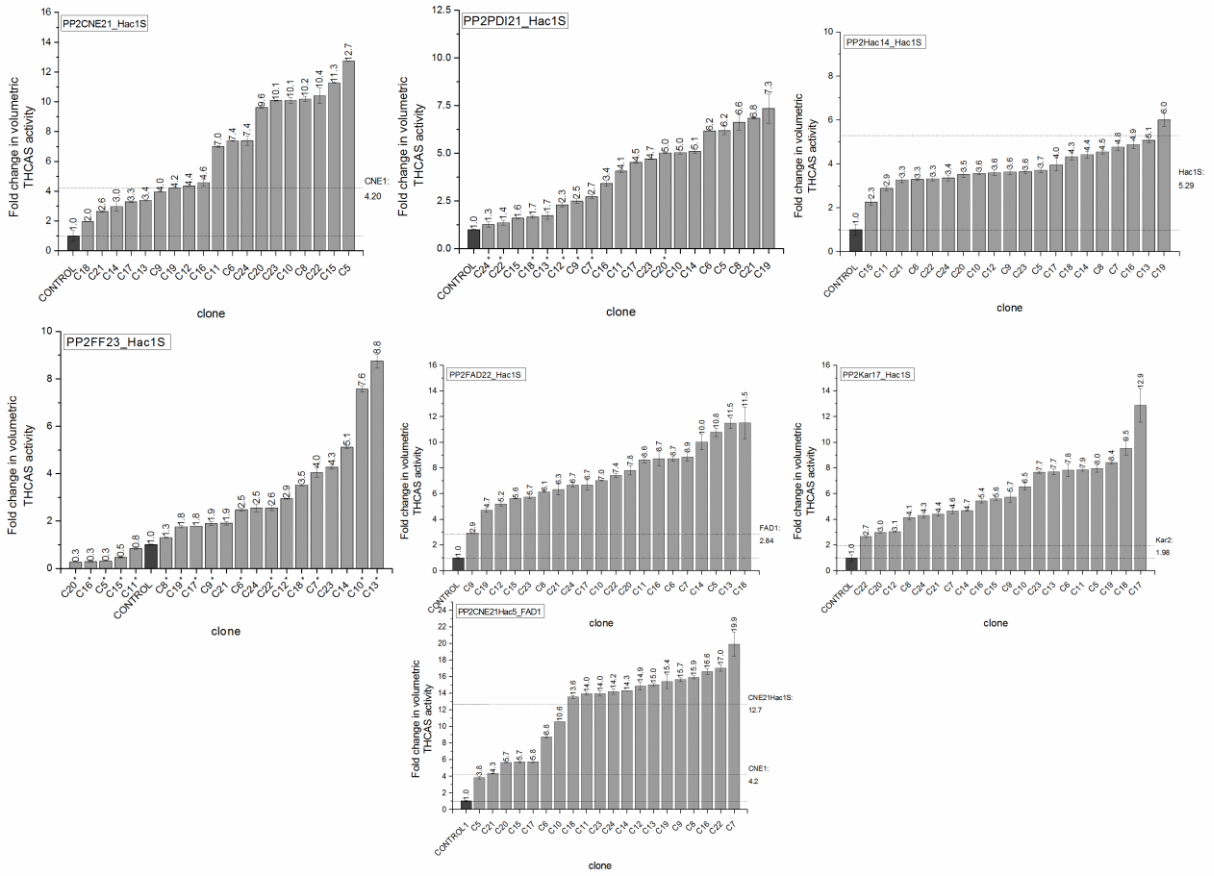

Fig. S VII-3: Influence of co-production of more than one helper protein on THCAS activities. Shown is the change of normalized, volumetric, intracellular THCAS activities when cells were co-producing Hac1p and either FAD1p, FAD1p and FMN1p, Kar2p, PDI1p, CNE1p or Hac1p.

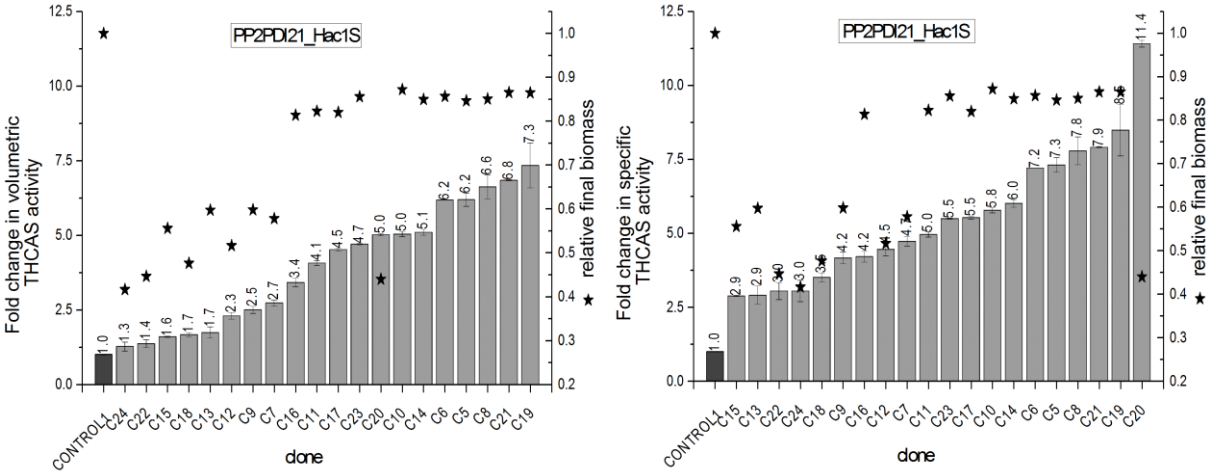

Fig. S VIII-4: Fold change in volumetric or specific THCAS activity in the population of PP2PDI21_Hac1s. Clones marked with a (*) showed severe growth impairment and flocculation under experimental conditions.

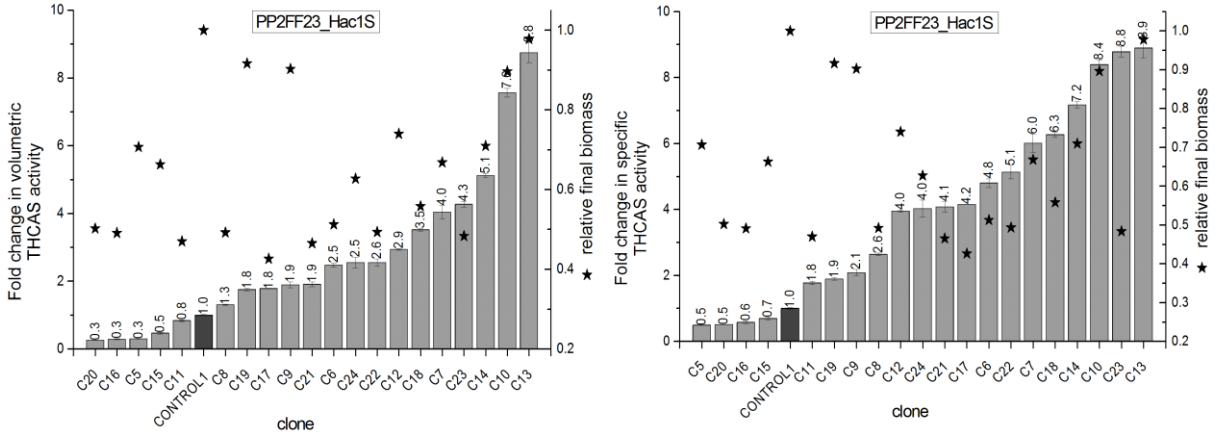

Fig. S VIII-5: Fold change in volumetric or specific THCAS activity in the population of PP2FF23_Hac1s. Clones marked with a (*) showed severe growth impairment and flocculation under experimental conditions.

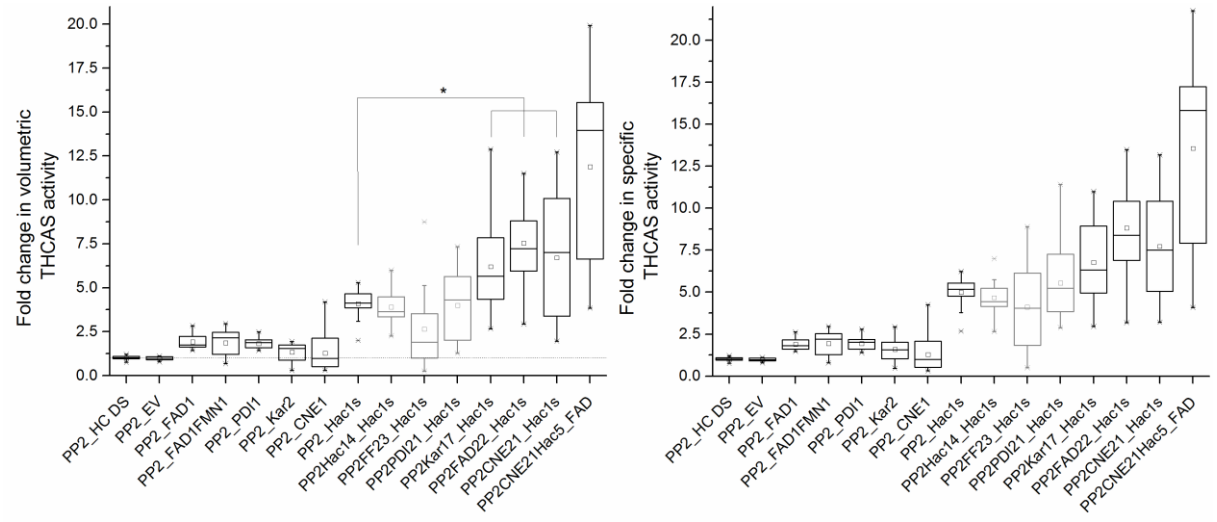

Fig. S VIII-6: Boxplots of the fold change in volumetric or specific THCAS activity. Clones of PP2PDI21_Hac1s and PP2FF23_Hac1s showed severe growth impairment and flocculation under experimental conditions. Significantly increased activities (marked with *) were determined with the Mann-Whitney-U test comparing against the empty-vector transformed population (PP2_EV) (p = 0.05).

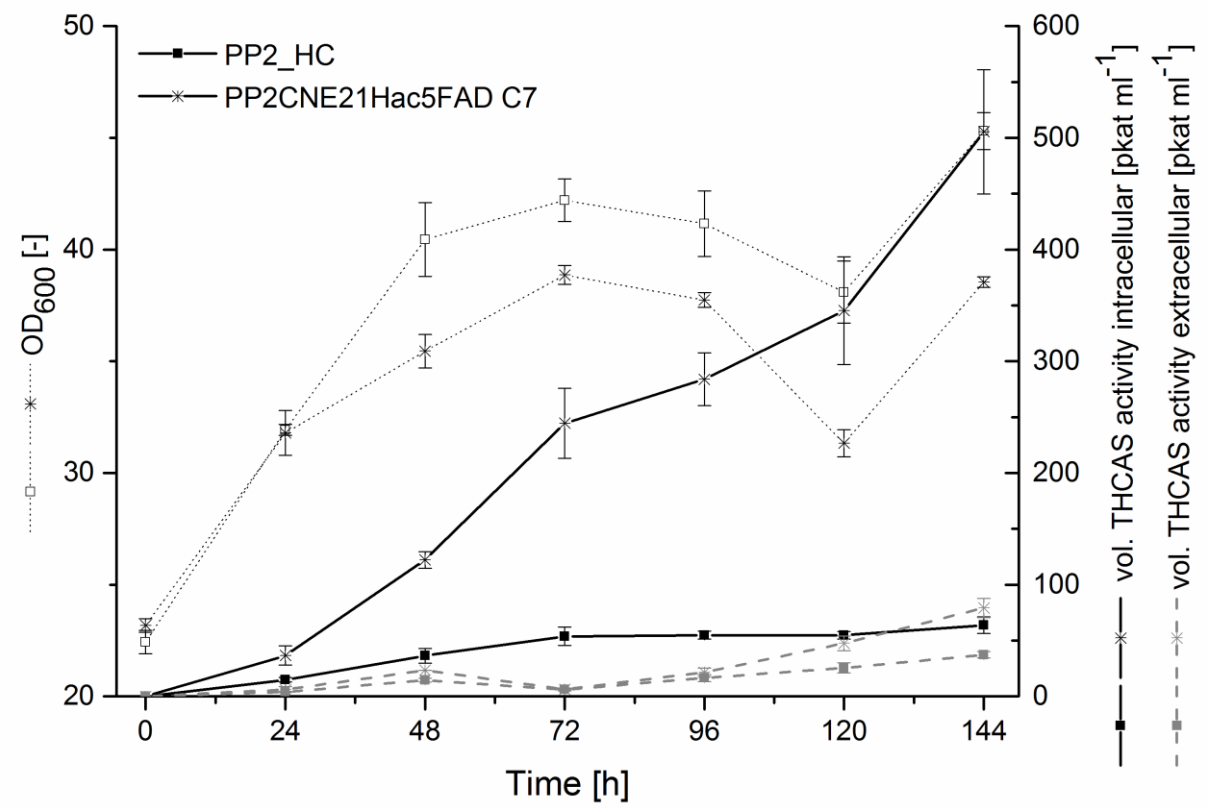

Fig. S VIII-7: Time-course of volumetric THCAS activity levels of starting strain PP2_HC and optimized strain PP2CNE21Hac5FAD C7. Cultivation was performed at 15 °C, 0.5 % (v/v) methanol added every 24 h.

VIII. SUPPLEMENTARY MATERIAL CHAPTER 5

CBDAS sequence:

ATGTCCATTTTCGACGGTACTACTATGTCCATTGCTATCGGTTTGTTGTCCACTTTGGGTATCGGTGC
TGAAGCTAACCCAAGAGAAAACTTCTTGAAGTGTTTTTCCCAGTACATCCCAAACAACGCTACAAA
CTTGAAGTTGGTTTACACTCAGAACAACCCATTGTACATGTCCGTTTTGAACTCCACTATCCACAAC
TTGAGATTCACTTCCGACACTACTCCAAAGCCATTGGTTATCGTTACTCCATCCCACGTTTCCCACA
TCCAGGGTACTATTTTGTGTTCCAAGAAGGTTGGATTGCAGATCAGAACAAGATCCGGTGGTCACG
ACTCTGAAGGTATGTCCTACATTTCCCAGGTTCCTTTCGTTATCGTTGACTTGAGAAACATGAGATC
CATCAAGATCGACGTTCACTCCCAGACTGCTTGGGTTGAAGCTGGTGCTACTTTGGGTGAAGTTTAC
TACTGGGTTAACGAGAAGAACGAGAACTTGTCCTTGGCTGCTGGTTACTGTCCAACTGTTTGTGCTG
GTGGTCATTTCGGTGGTGGTGGTTATGGTCCATTGATGAGAAACTACGGTTTGGCTGCTGACAACA
TCATCGACGCTCACTTGGTTAACGTTCACGGTAAGGTTTTGGACAGAAAGTCTATGGGTGAGGACT
TGTTCTGGGCTTTGAGAGGTGGTGGTGCTGAATCCTTCGGTATTATCGTTGCTTGGAAGATCAGATT
GGTTGCTGTTCCAAAGTCCACTATGTTCTCCGTTAAGAAAATCATGGAAATCCACGAATTGGTTAA
GTTGGTTAACAAGTGGCAGAACATTGCTTACAAGTACGACAAGGATTTGTTGTTGATGACTCACTT
CATCACTAGAAACATCACTGACAACCAGGGTAAGAACAAGACTGCTATCCACACTTACTTCTCTTC
CGTTTTCTTGGGTGGTGTTGACTCCTTGGTTGATTTGATGAACAAGTCTTTCCCAGAGTTGGGTATC
AAGAAAACTGACTGTAGACAGTTGTCCTGGATCGACACTATCATCTTCTACTCCGGTGTTGTTAACT
ACGACACAGACAACTTCAACAAAGAGATTTTGTTGGACAGATCCGCTGGACAGAACGGTGCTTTCA
AGATCAAGTTGGACTACGTTAAGAAGCCAATCCCAGAGTCCGTTTTCGTTCAGATTTTGGAGAAGT
TGTACGAAGAGGACATTGGTGCTGGTATGTACGCTTTGTACCCATACGGTGGTATCATGGACGAAA
TTTCCGAGTCCGCTATTCCATTCCCACACAGAGCTGGTATCTTGTACGAGTTGTGGTACATCTGTTC
TTGGGAGAAGCAAGAGGACAACGAGAAGCACTTGAACTGGATCAGAAACATCTACAACTTCATGA
CTCCATACGTTTCCAAGAACCCAAGATTGGCTTACTTGAACTACAGAGACTTGGACATCGGTATCA
ACGACCCAAAGAACCCTAACAACTACACTCAGGCTAGAATCTGGGGTGAAAAGTACTTCGGTAAG
AACTTCGACAGATTGGTTAAGGTTAAGACTTTGGTTGACCCAAACAATTTCTTCAGAAACGAGCAG
TCCATCCCTCCATTGCCAAGACATAGACATTAA

Table S VIII-1: List of used primers.

Primer	**Sequence 5'->3'**	**Purpose**
p_pAX_fw	GGCCCGAACAAAAACTCATCTCA	Generation of pAX_pT and pAX_pC
p_pAX_rv	CGTTTCGAATAATTAGTTGTTTTTTG	Generation of ppink_HC_Hac1s, pAX_pT and pAX_pC
ppink_fw	ATACAGGCCCCTTTTCCTTTGTC	Generation of ppink_HC_Hac1s
p_Hac1_fw	CAAAAAACAACTAATTATTCGAAACGATGCCCGTAGATTCTTCTCATAAGACAG	Generation of ppink_HC_Hac1s and pAX_Hac1s
p_Hac1s_rv	TCTGAGATGAGTTTTTGTTCGGGCCTTATTCCTGGAAGAATACAAAGTCATTTAAATCAAATGCATTAGCGGTAAATGGTGCTGCTGGATGATGCAACCGATTCGACTCGCTAA	Generation of pAX_Hac1s
p_Hac1s_rv2	TGATATCGACAAAGGAAAAGGGGCCTGTATTTATTCCTGGAAGAATACAAAGTCATTTAAATCAAATGCATTAGCGGTAAATGGTGCTGCTGGATGATGCAACCGATTCGACTCGCTAA	Generation of ppink_HC_Hac1s
p_CBDAS_fw	AGATCAAAAAACAACTAATTATTCGAAACGATGTCCATTTTCGACGGTACTAC	Generation of pAX_pC
p_CBDAS_rv	AGATGAGTTTTTGTTCGGGCCCTTATTAATGTCTATGTCTTGGCAATGGA	Generation of pAX_pC
p_THCAS_fw	AACTAATTATTCGAAACGGAATTCGAAACGATGTCTATATTTGACGGTACTAC	Generation of pAX_pT
p_THCAS_rv	TGAGTTTTTGTTCGGGCCCTTATTAATGATGATGTGGTGGCAATGG	Generation of pAX_pT

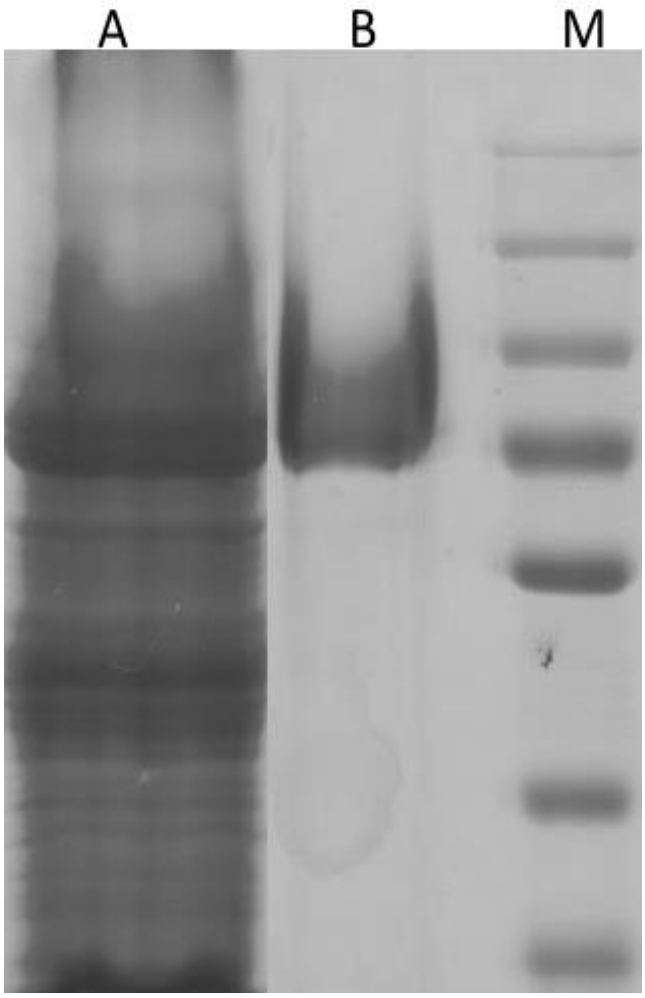

Fig. S IX-1: SDS-gel of purified THCAS from culture supernatant. Lane A: Concentrate (16-fold) of PP2_Hac1S culture supernatant. Lane B: Eluate from Ni-NTA column at 250 mM imidazole. Lane M: PageRuler™ Plus Prestained Protein Ladder, 10 to 250 kDa (Thermo Fisher Scientific, Schwerte, Germany) - band sizes (top to bottom): 250 kDa, 130 kDa, 100 kDa, 70 kDa, 55 kDa, 35 kDa, 25 kDa.

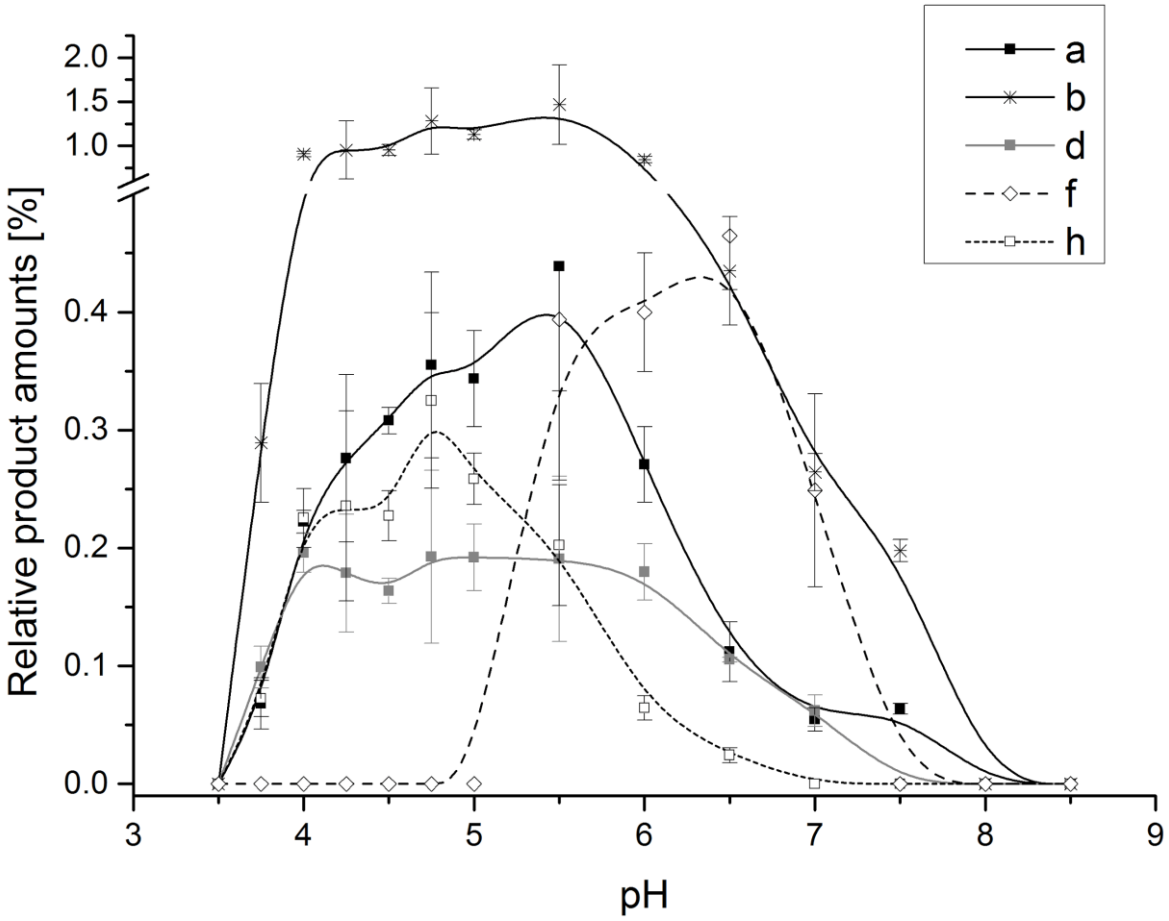

Fig. S IX-2: pH-dependent side-product formation of THCAS. Relative product amounts were normalized on maximum THCA production. Amounts of a, b, d, h are estimated via UV absorption at 225 nm and amount of product f is estimated via UV absorption at 255 nm.

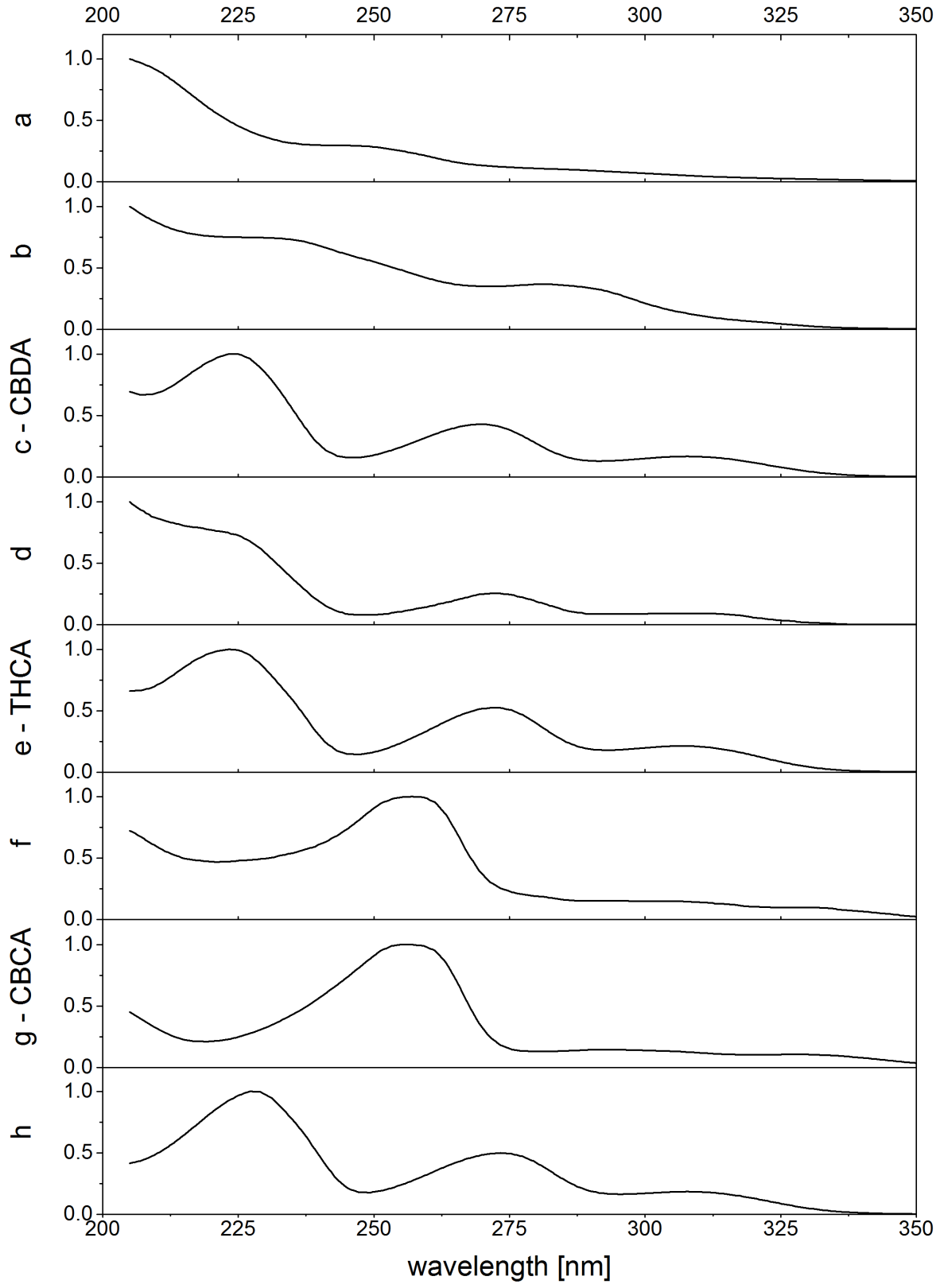

Fig. S IX-3: UV spectra of THCAS and CBDAS products.

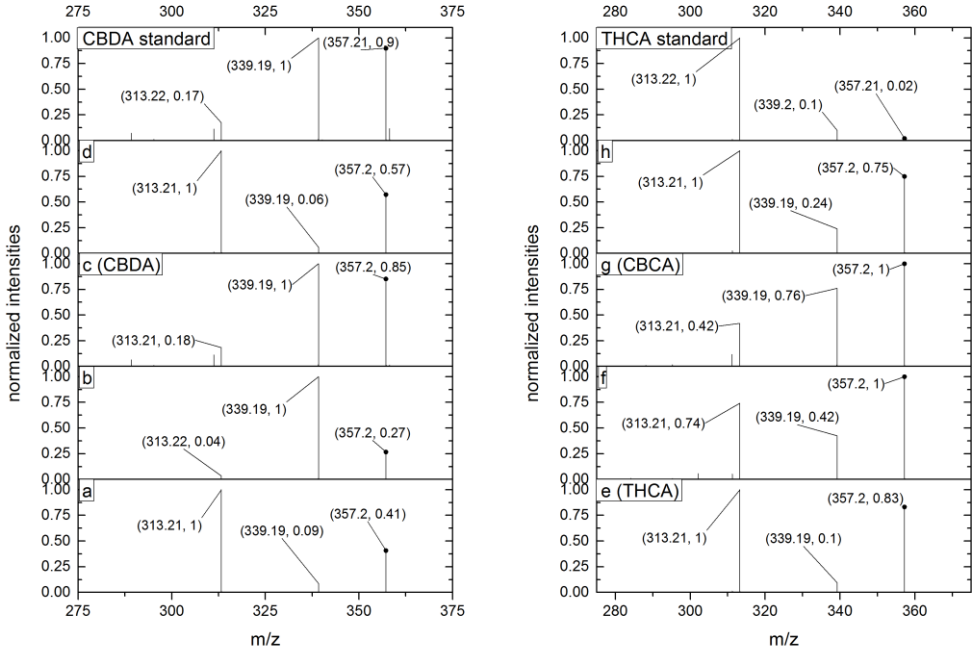

Fig. S IX-4: MS2 spectra of products obtained from CBGA conversion by THCAS and CBDAS (negative mode, MS2 spectra from 357.21@cid28.00 eV). Relative intensities of fragment ions are shown. Labels show ion m/z ratio and its relative intensity. Precursor ion is marked with dot.

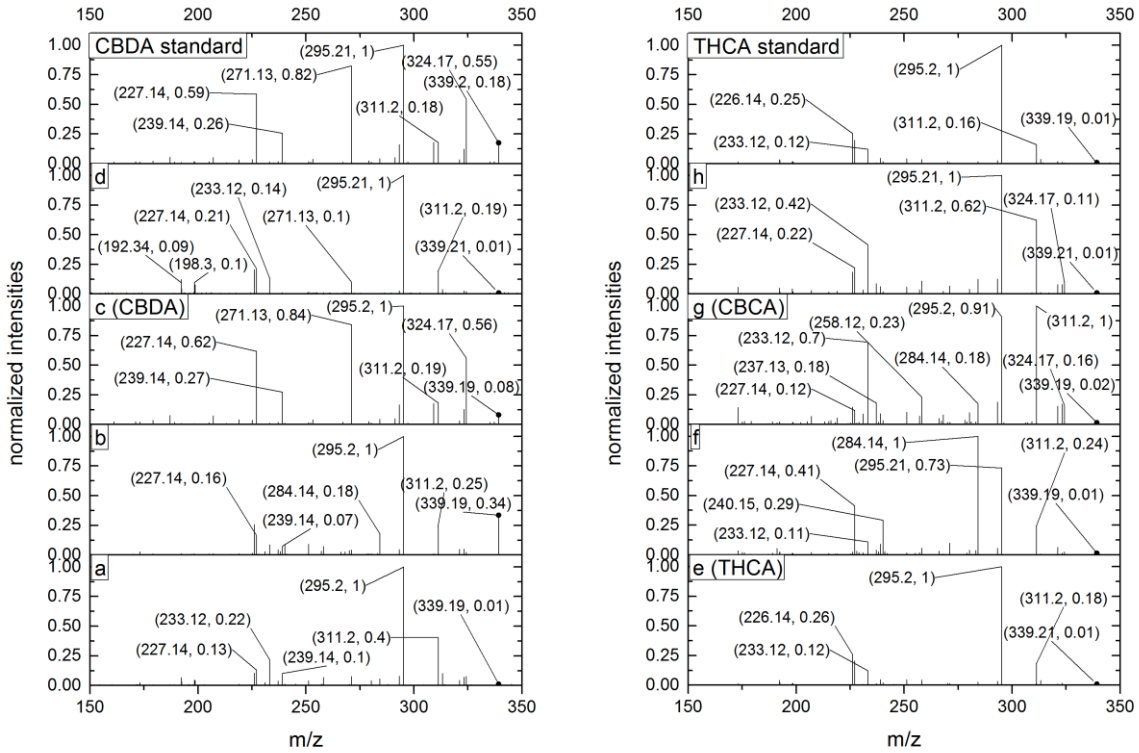

Fig. S IX-5: MS3 spectra of products obtained from CBGA conversion by THCAS and CBDAS (negative mode, MS3 spectra from 357.21@cid35.00 eV -> 339.20@cid35.00 eV). Relative intensities of fragment ions are shown. Labels show ion m/z ratio and its relative intensity. Precursor ion is marked with dot.

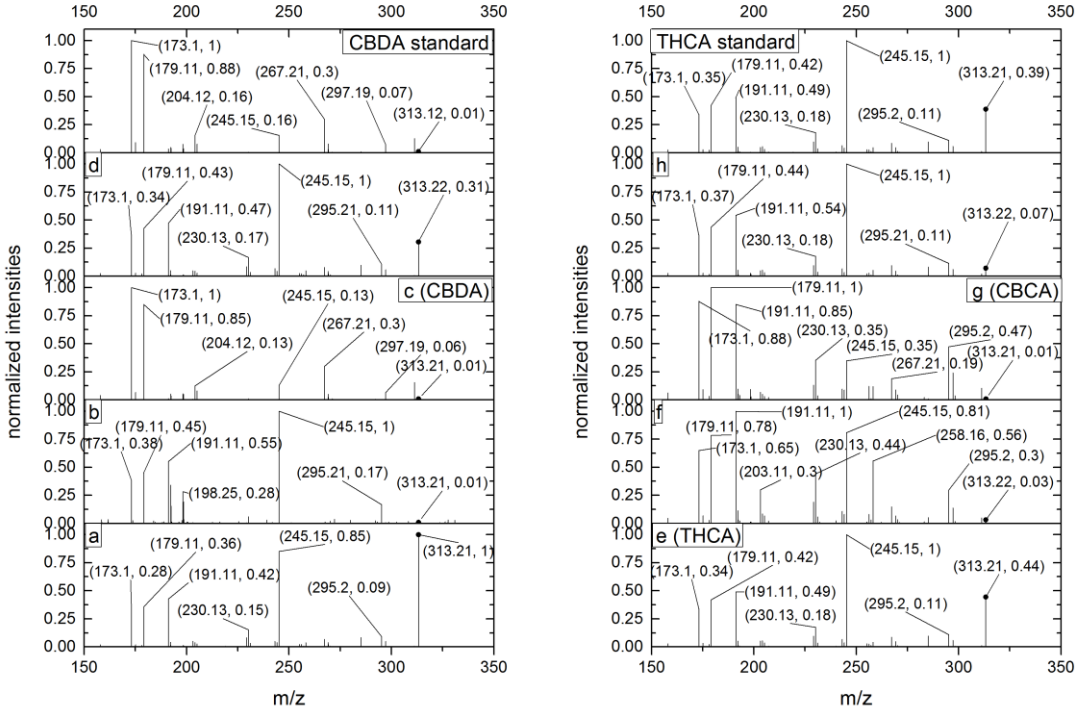

Fig. S IX-6: MS3 spectra of products obtained from CBGA conversion by THCAS and CBDAS (negative mode, MS3 spectra from 357.21@cid35.00 eV -> 313.21@cid35.00 eV). Relative intensities of fragment ions are shown. Labels show ion m/z ratio and its relative intensity. Precursor ion is marked with dot.

^{1}H NMR of CBCA (600 MHz, $CDCl_3$):

δ [ppm]: 0.89 (3H, t, J = 6.4 Hz), 1.28-1.36 (4H, m), 1.40 (s) 1.57 (3H, s), 1.65 (3H, s), 1.58-1.80 (4H, m), 2.03-2.11 (2H, m), 2.85 (2H, d, 7.8 Hz), 5.09 (1H, t, J = 7.03 Hz), 5.47 (1H, d, J = 10.1 Hz), 6.23 (1H, s), 6.73 (1H, d, 10.1 Hz), 11.88 (1H, s)

Fig. S IX-7: ^{1}H-NMR data of purified product g - CBCA.

Table S VIII-2: Normalized, specific activities of THCAS and CBDAS compared to the respective wild-type enzyme.

Enzyme variant	**Amino acid substitution(s) /deletion(s)**	**Normalized, specific enzyme activity (normalized on activity of respective wild-type enzyme)**	**Notes**
T	-	1 ± 0.15	wild-type
T_12	Q69H, A116S, A192P, V288L, I316V, K377Q, K378N, T379G, S382K, V415A, T446A, I447C	0.0	
T_12+489-496	Q69H, A116S, A192P, V288L, I316V, K377Q, K378N, T379G, S382K, V415A, T446A, I447C, L489I, K491I T492N N493D H494P A495K S496N	0.02	0.02 CBDA produced at pH 4.6
T_489-496	L489I, K491I T492N N493D H494P A495K S496N	1.39 ± 0.16	
T_H292F	H292F	0.0	
T_H292K	H292K	0.0	
T_H292N	H292N	0.02	0.02 CBCA produced at pH 4.6
T_H292R	H292R	0.0	0.04 CBCA produced at pH 4.6
T_H292Y	H292Y	0.02	0.04 CBCA produced at pH 4.6
T_A116S	A116S	0.07 ± 0.02	
T_A116Y	A116Y	0.0	
T_A116L	A116L	0.03 ± 0.02	

Table S IX-2: Normalized, specific activities of THCAS and CBDAS - continued.

T_A116N	A116N	0.0	
T_A116V	A116V	0.03 ± 0.02	
T_A116G	A116G	0.31 ± 0.07	
T_A116T	A116T	0.0	
T_Q69H	Q69H	1.17 ± 0.33	
T_Q69HA116S	Q69H, A116S	0.04 ± 0.01	
T_Q69HT446IA447C	Q69H, T446I, A447C	0.24 ± 0.04	
T_V415A	V415A	0.04 ± 0.02	
T_V415I	V415I	0.69 ± 0.09	
T_V415L	V415L	0.54 ± 0.13	
T_V415T	V415T	0.45 ± 0.05	
T_V415N	V415N	0.0	
T_KKT377QNG	K377Q, K378N, K379G	0.88 ± 0.1	
T_T446IA447C	T446I, A447C	0.3 ± 0.07	
T_N237S	N237S	0.93 ± 0.23	
T_I257M	I257M	0.09 ± 0.02	
T_S382K	S382K	0.1 ± 0.01	
T_K384A	K384A	0.05 ± 0.01	
T_Y510A	Y510A	0.0	

Table S IX-2: Normalized, specific activities of THCAS and CBDAS - continued.

T_F531A	F531A	0.0	
T_Q535A	Q535A	0.0	
T_C37S	C37S	0.0	
T_C99S	C99S	0.0	
T_C176A	C176A	0.0	
T_540stop	Δ541-545	0.92 ± 0.16	
T_539stop	Δ540-545	0.2 ± 0.06	
T_538stop	Δ539-545	0.07 ± 0.02	
T_537stop	Δ538-545	0.0	
T_533stop	Δ534-545	0.0	
T_525stop	Δ526-545	0.0	
T_Y500CL540C	Y500C, L540C	1.28 ± 0.36	
T_Y500KL540E	Y500K, L540E	0.35 ± 0.11	
T_H494CR532C	H494C, R532C	1.73 ± 0.41	
T_H494ER532K	H494E, R532K	0.93 ± 0.42	
T_Q124KH494E	Q124K, H494E	0.75 ± 0.18	
T_Q124CH494C	Q124C, H494C	0.75 ± 0.1	
T_deg	N65Q, N89Q, N168Q, N305Q, N329Q, N467Q, N499Q	0	
T_N499Q	N499Q	1.64 ± 0.32	

Table S IX-2: Normalized, specific activities of THCAS and CBDAS - continued.

T_N467Q	N467Q	0.86 ± 0.11	
T_N329Q	N329Q	1.5 ± 0.39	
T_N305Q	N305Q	0.68 ± 0.22	
T_N168Q	N168Q	1.49 ± 0.67	
T_N89Q	N89Q	1.67 ± 0.74	
T_N65Q	N65Q	0.45 ± 0.05	
T_N89QN499Q	N89Q, N499Q	2.03 ± 0.72	
T_N168QN499Q	N168Q, N499Q	0.67 ± 0.26	
T_N329QN499Q	N329Q, N499Q	0.99 ± 0.3	
T_N89QN168QN499Q	N89Q, N168Q, N499Q	0.84 ± 0.33	
T_N168QN329QN499Q	N168Q, N329Q, N499Q	0.55 ± 0.17	
C	-	1.0 ± 0.15	wild-type
C_A414V	A414V	3.37 ± 1.13	~19-fold increased THCA production compared to CBDAS wild-type
C_A414I	A414I	0.16 ± 0.07	
C_A414T	A414T	0.25 ± 0.06	
C_A414L	A414L	0.2 ± 0.05	
C_S116A	S116A	2.93 ± 0.33	~2.6-fold increased THCA production compared to CBDAS wild-type

Table S IX-2: Normalized, specific activities of THCAS and CBDAS - continued.

C_S116V	S116V	0.01	
C_S116G	S116G	1.33 ± 0.22	
C_S116L	S116L	0	
C_S116AA414V	A414V, S116A	2.17 ± 0.87	
C_S116A+A46VT47A	S116A, A46V, T47A	2.83 ± 0.45	
C_A414V+A46VT47A	A46V, T47A, A414V	4.14 ± 1.1	
C_S116AA414V+A46V T47A	S116A, A46V, T47A, A414V	3.63 ± 0.98	
C_I445T	I445T	0.55 ± 0.12	
C_I445TC446A	I445T, C446A	0.49 ± 0.17	
C_A46VT47A	A46V, T47A	1.23 ± 0.26	
C_N65Q	N65Q	0.52 ± 0.07	
C_N168Q	N168Q	0.48 ± 0.14	
C_N304Q	N304Q	1.01 ± 0.05	
C_N328Q	N328Q	1.24 ± 0.64	
C_N498Q	N498Q	0.49 ± 0.17	

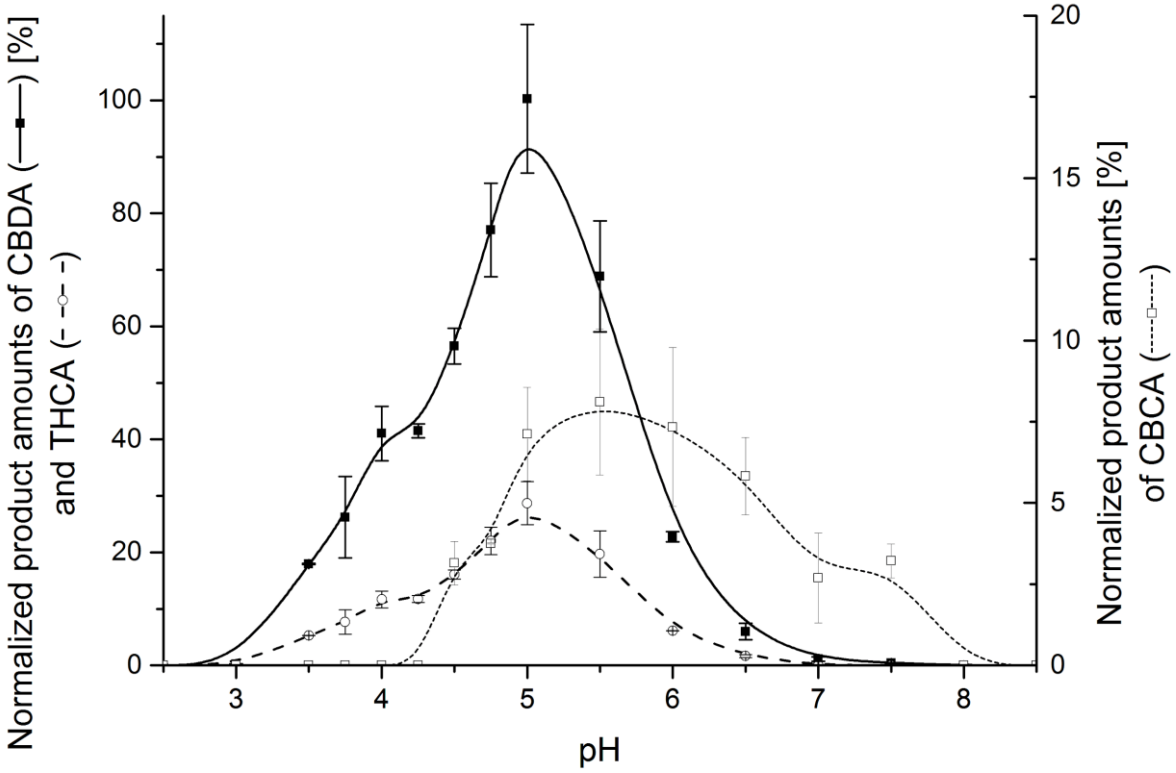

Fig. S VIII-8: pH profile of CBDAS variant C_A414V regarding its three major products CBDA, THCA and CBCA. Product formation is normalized on the maximum amount of CBDA. Amount of THCA and CBDA are estimated by UV absorption at 225 nm. Amount of CBCA is estimated by UV absorption at 255 nm

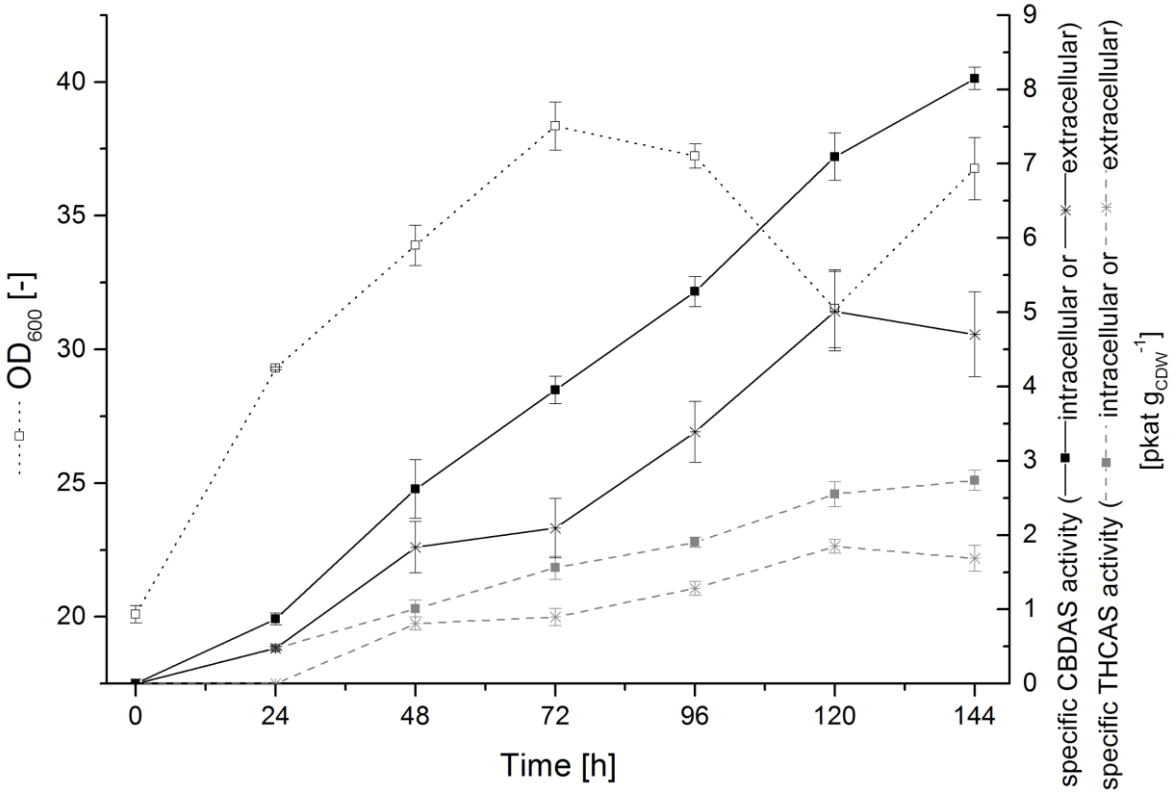

Fig. S VIII-9: Shaking flask cultivation of PPHac_C_A414V+A46V+T47A at 15 °C, 0.5 % (v/v) methanol added every 24 h.

IX. SUPPLEMENTARY MATERIAL CHAPTER 6

Table S IX-1: List of used strains.

Strain	**Relevant genotype/transformed strain**	**Transformed plasmid(s)**	**Reference**
SC	*Saccharomyces cerevisiae* CEN.PK2-1C *Δpep4Δgal1Δgal80*	-	This study
SC_EV	SC	pDionysos	This study
SC_N	SC	pDionysos_NphB	This study
SC_T	SC	pDionysos_THCAS	This study
SC_TT2AN	SC	pDionysos TT2AN	This study
SC_T2	SC	pDio2_THCAS	This study
SC_NT	SC	pDio2_THCAS-NphB	This study
PP2_HC	*Komagataella phaffii* PichiaPink Δ*ade*Δ*pep4* (Invitrogen, Darmstadt, Germany)	pPink_HC_THCAS	(Zirpel et al., 2015)
PP2_EV	*Komagataella phaffii* PichiaPink Δ*ade*Δ*pep4* (Invitrogen, Darmstadt, Germany)	pPink_HC	(Zirpel et al., 2015)
PP_N	PP2_EV	pAX_NphB	This study
PP_NT	PP2_HC	pAX_NphB	This study

Table S IX-2: List of used primers.

Primer	**Sequence 5'->3'**	**Purpose**
p_pAX_fw	GGCCCGAACAAAAACTCATCTCA	Generation of pAX_NphB
p_pAX_rv	CGTTTCGAATAATTAGTTGTTTTTTG	Generation of pAX_NphB
p_Ncoy_fw	CAAAAAACAACTAATTATTCGAAACGATGTCT GAAGCGGCGGACGTT	Generation of pAX_NphB
p_Ncoy_rv	TCTGAGATGAGTTTTTGTTCGGGCCTCAATCTT CCAAAGAATCAAAAG	Generation of pAX_NphB; Colony PCR *K. phaffii*
S1	GCTGCCCTGTCTTAAACC	Colony PCR *K. phaffii*
Gal1 Gluc rep free_fw	GCTCCGAACAATAAAGATTCGAAGCGATGATT TTTGATCTATTAA	Generation of mutated *Gal1* promoter in pDionysos
Gal1 Gluc rep free_rv	AGATCAAAATCATCGCTTCGAATCTTTATTGTT CGGAGCAGTGCGGCGCGAG	
Vf-pDio-THCAS	TGATCTAGAGGGCCGCATCATGTAATTAGTTAT GTCACGCTTACATTCACG	Generation of pDionysos_TT2AN
Vr-pDio-THCAS	ATGGTGATGTGGAGGCAATGGAGGGATGGATT GTTCGTTTCTAAAGAAGTTGTTTGGGTCGACTT TAGTCTTGACTTTGACTAATCTAT	
1f-ORF-2-o(Vec)-NphB (Cod)	CCCTCCATTGCCTCCACATCACCATAGAGCTGA GGGTAGAGGAAGTCTACTAACATGCGGTGACG TAGAAGAAAACCCTGGTCCTTCTGAAGCGGCG GACGTT	
1r-ORF-2-o(Vec)-NphB (Cod)	TTACATGATGCGGCCCTCTAGATCATCAATCTT CCAAAGAATCAAAAGCCTTCAA	

Table S X-2: List of used primers - continued.

Vf-pDio (Str_codon_yeast)	TCTAGAGGGCCGCATCATGTAATTAGT	Generation of pDionysos_NphB
Vr-pDio (Str_codon_yeast)	AAGCTTAATATTCCCTATAGTGAGTCGT	
1f-AAAAAA+NphB-o(Str_codon yeast)	CGACTCACTATAGGGAATATTAAGCTTAAAAAAATGTCTGAAGCGGCGGAC	
1r-AAAAAA+NphB-o(Str_codon yeast)	TAATTACATGATGCGGCCCTCTAGATTATCAATCTTCCAAAGAATCAAAAGCCTTCAA	
pDio-Gal10_fw	AGTACGGATTAGAAGCCGCCGAGCGGGTGA	Generation of pDio2
pDio-Gal10_rv	AGTGGATCATCCCCACGCGCCCTGT	
Gal10-NphB-ADH1_fw	ACAGGGCGCGTGGGGATGATCCACTGAGCGACCTCATGCTATACC	
Gal10-NphB-ADH1_rv	CGCTCGGCGGCTTCTAATCCGTACTTCAATATAGCAATGAGCAGTTAAGCGTA	
Vf_pDio-ADH1	TGGAGACTTGACCAAACCTCTGGCGAAGAAT	Generation of pDio2_THCAS
Vr_pDio-ADH1	TGTTGACACTTCTAAATAAGCGAATTTCTTATGATTTATGA	
1f_THCAS (1-)o(pDio2)	ATTCGCTTATTTAGAAGTGTCAACATTAATGATGATGATGGTGATGTGG	
1r_THCAS (1-)o(pDio2)	CGCCAGAGGTTTGGTCAAGTCTCCAAAAAAATGTCCAGCTTGAAAGCATTAT	
pDio-Gal10_fw	AGTACGGATTAGAAGCCGCCGAGCGGGTGA	Generation of pDio2_THCAS-NphB
pDio-Gal10_rv	AGTGGATCATCCCCACGCGCCCTGT	
Gal10-NphB-ADH1_fw	ACAGGGCGCGTGGGGATGATCCACTGAGCGACCTCATGCTATACC	
Gal10-NphB-ADH1_rv	CGCTCGGCGGCTTCTAATCCGTACTTCAATATAGCAATGAGCAGTTAAGCGTA	

Table S X-2: List of used primers - continued.

HR_Gal80_fw	ATGGACTACAACAAGAGATCTTCGGTCTCAAC CGTGCCTAATGCAGCTCCGTACGCTGCAGGTC GACAAC	Generation of the *Gal80* knockout in the genome of *S. cerevisiae* CEN.PK2-1C *Δpep4Δgal1*
HR_Gal80_rv	TTATAAACTATAATGCGAGATATTGCTAACGTT TAATGTGGAGCCCATCAGCATAGGCCACTAGT GGATCTGATAT	

Table S IX-3: List of used plasmids.

Plasmid	**Resistance/auxotrophy marker**	**Expressed coding sequence**	**Reference**
pET28a	Kanamycin	-	Merck Millipore, Darmstadt, Germany
pDionysos	Ampicillin, Uracil, Leucine	-	(Stehle et al., 2008)
pESC-URA	Ampicillin, Uracil	-	Agilent Technologies, Waldbronn, Germany
pDionysos_THCAS	Ampicillin, Uracil, Leucine	P_{GAL1}: THCAS	(Zirpel et al., 2015)
pDionysos_TT2AN	Ampicillin, Uracil, Leucine	P_{GAL1}: THCAS T2A NphB	This study
pDionysos_NphB	Ampicillin, Uracil, Leucine	P_{GAL1}: NphB	This study
pDio2_THCAS	Ampicillin, Uracil, Leucine	P_{GAL10}: THCAS	This study
pDio2_THCAS-NphB	Ampicillin, Uracil, Leucine	P_{GAL10}: THCAS P_{GAL1}: NphB	This study
pAX_EV	Zeocin	-	This study
pAX_NphB	Zeocin	P_{AOX1}: NphB	This study

Table S IX-4: Genotype of used *S. cerevisiae* strains

Organism	**Strain**	**Reference**	**Genotype**
S. cerevisiae	CEN.PK2-1C *Δpep4Δgal1*	(Zirpel et al., 2015)	*MAT*a; *gal1::loxP; pep4::loxP; ura3-52; trp1-289; leu2-3,112; his3Δ 1; MAL2-8C; SUC2*
S. cerevisiae	CEN.PK2-1C *Δpep4Δgal1Δgal80*	This study	*MAT*a; *gal1::loxP; pep4::loxP; gal80::loxP; ura3-52; trp1-289; leu2-3,112; his3Δ 1; MAL2-8C; SUC2*

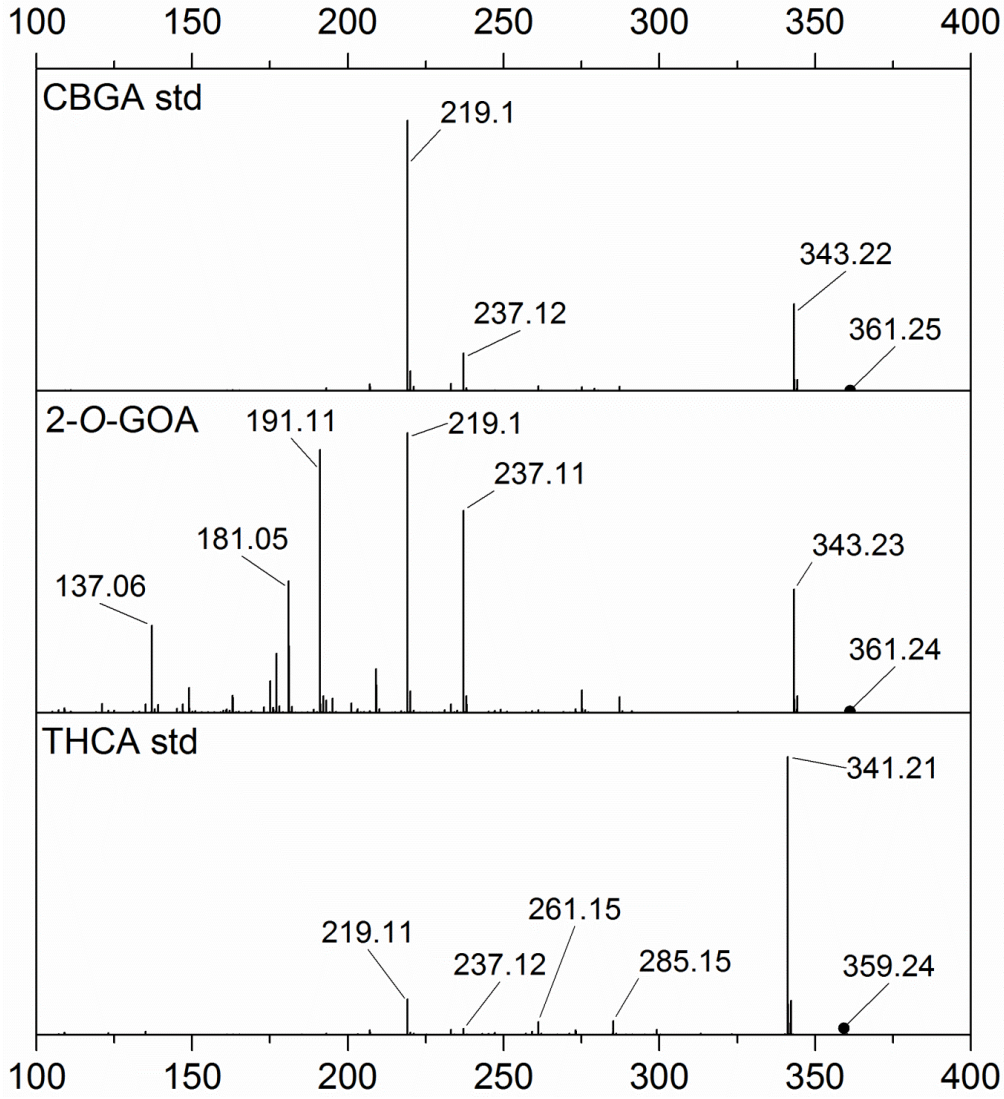

Fig. S X-1: Tandem mass spectra of standard compounds CBGA and THCA as well as side-product 2-*O*-GOA. Data were collected with the same column, pump and gradient as described in the material and method section. The system was run in positive electrospray (ESI) mode with a collision energy of 28 eV.

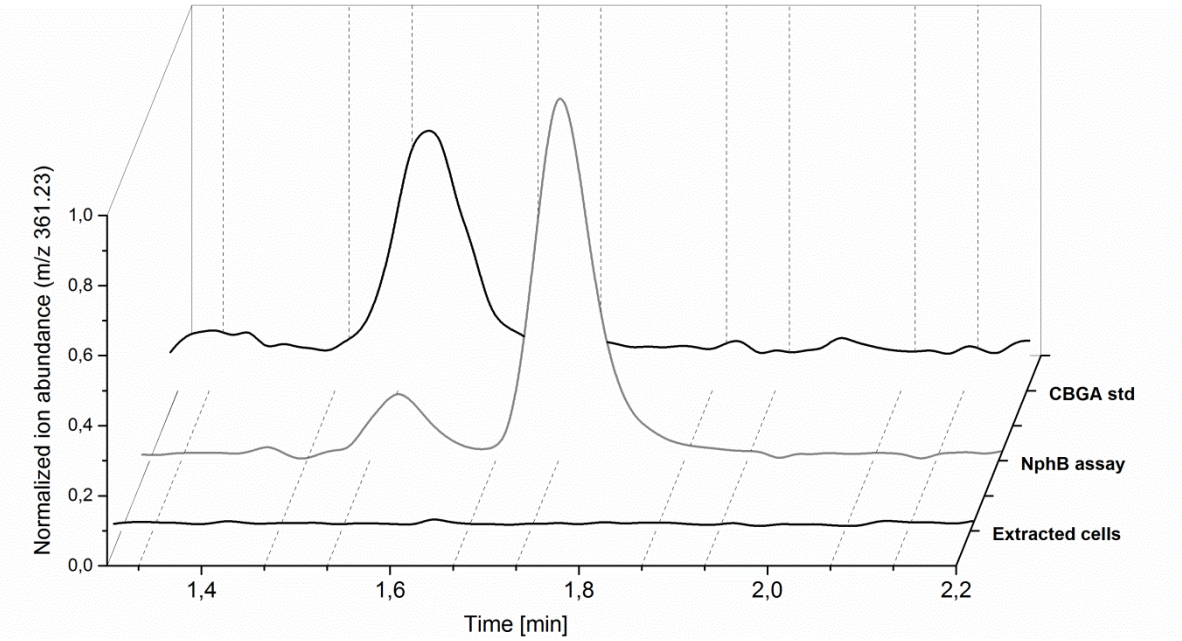

Fig. S X-2: Membrane permeability of OA and geranyl diphosphate for NphB activity. Cultivation of SC_N; expression cultures were inoculated at OD600 of 0.5 and incubated for 72 h at 15°C and 200 rpm in 500 mL baffled shaking flasks (10 % filling volume); after harvest cells were resuspended and either used for cell lysis or supplemented with 3 mM OA and 3 mM GPP (4 h, 37 °C); cell lysate supernatants were incubated with 1 mM OA, 1 mM GPP, 5 mM MgCl2 at 37°C for 4 h to determine CBGA and 2-*O*-GOA formation; cells supplemented with OA and GPP were harvested and extracted with ethyl acetate; extracts were vacuum dried and resuspended in ACN; assays and extracts were analyzed via HPLC-MS.

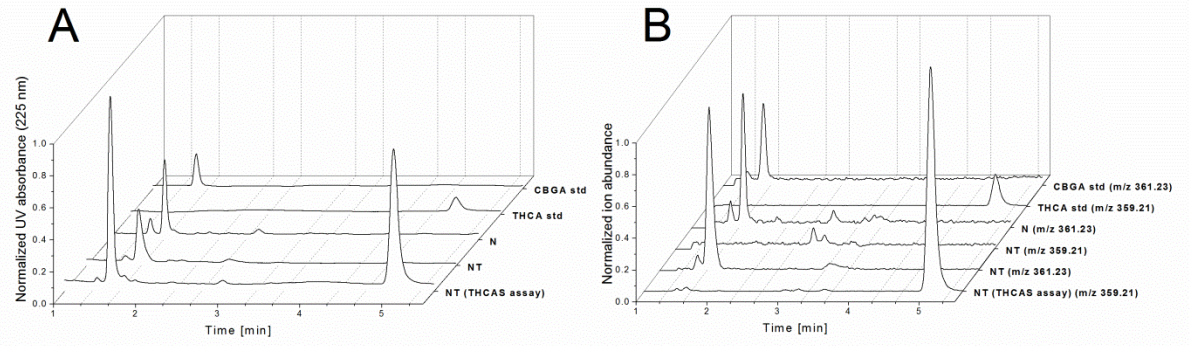

Fig. S X-3: LC-MS analysis of cannabinoids produced with cell lysates of *S. cerevisiae* expressing both *nphB* and/or *thcas*. The yeast lysates were incubated with 1 mM GPP and OA, respectively. (A) HPLC-UV chromatograms at 225 nm of the standards CBGA, THCA and the assay products. (B) Extracted ion chromatograms (EIC) of m/z 361.23 (CBGA) and m/z 359.21 (THCA) of the standards CBGA, THCA and the assay products. N – assay of yeast lysates expressing only NphB; NT – assay of yeast lysate expression both NphB and THCAS (SC_NT), supplemented with 0.3 mM CBGA

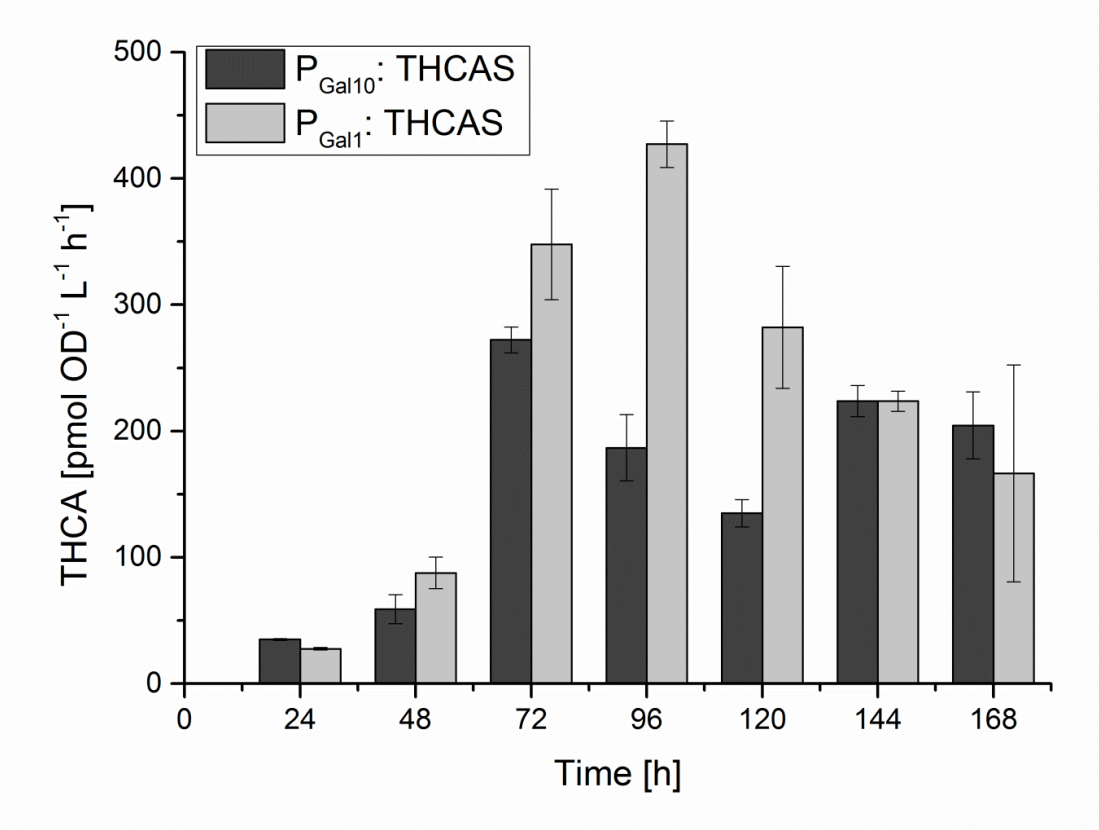

Fig. S X-4: Shaking flask cultivation of S. cerevisiae cells and analysis of THCA production. Expression cultures (SC_T and SC_T2) were inoculated at OD600 of 0.5 and incubated at 15 °C and 200 rpm for 168 h in 1 L baffled shaking flasks (10 % filling volume); cell lysate supernatants were incubated with 0.3 mM CBGA at 37 °C for 4 h; assays were analyzed via HPLC-MS and product formation normalized on cell culture OD600, cell culture volume and assay incubation time. Data points are calculated from biological triplicates each analyzed in technical duplicates.

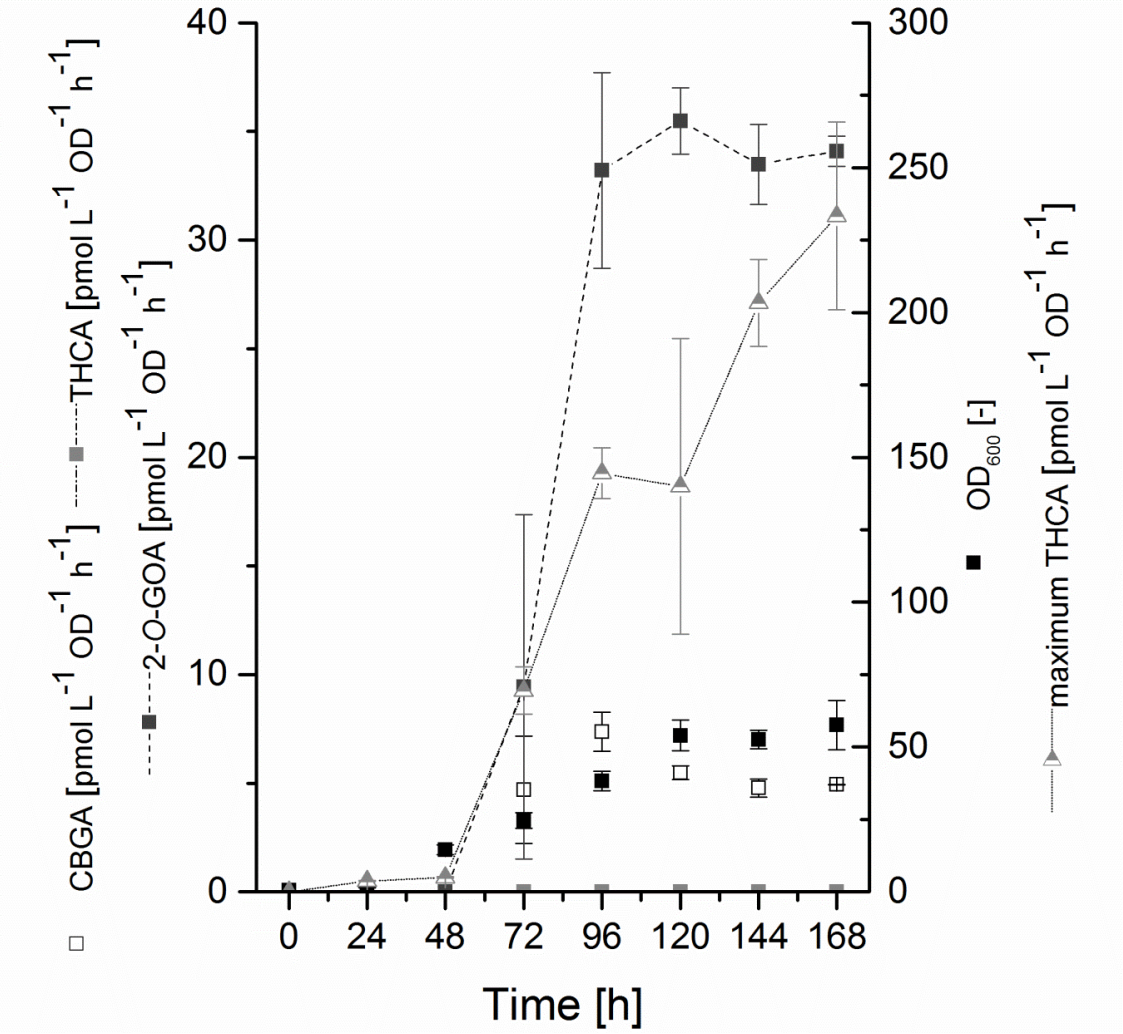

Fig. S X-5: Shaking flask cultivation of SC_NT cells and analysis of product formation. Expression cultures were inoculated at OD600 of 0.5 and incubated at 15 °C and 200 rpm for 168 h in 1 L baffled shaking flasks (10 % filling volume); cell lysate supernatants were incubated with either 1 mM OA, 1 mM GPP, 5 mM MgCl2 at 37 °C for 4 h to determine CBGA, 2-*O*-GOA and THCA formation or with 0.3 mM CBGA at 37 °C for 4 h to determine the highest possible THCA production under the tested conditions; assays were analyzed via HPLC-MS and product formation normalized on cell culture OD600, cell culture volume and assay incubation time. Data points are calculated from biological triplicates each analyzed in technical duplicates.

^{1}H-NMR analysis

Data were recorded on a Bruker AV 500 Avance III HD (Prodigy), Bruker (Karlsruhe, Germany). Olivetolic acid was dissolved in d6-DMSO (99.8%). 10 mg of in-house synthesized GPP was measured in D2O (99.8%) with a few drops of NaOD (99.8%) to keep it stable during measurement. CBGA and THCA were dissolved in CDCl3 (99.8%). Approximately 500 µg of isolated 2-O-GOA were dissolved in 500 µL CDCl3 (99.8%) and measured on a Bruker AV 700 Avance III HD (Cryo Probe), (Bruker, Karlsruhe, Germany).

NMR data: OA

^{1}H-NMR (500 MHz, d6-DMSO) δ: 1.61 ppm (s, 3H, methyl) 1.68 ppm (s, 3H, methyl) 1.70 ppm (s, 3H, methyl) 2.09 ppm (m, 4H, CH2 at C4 and C5) 4.46 ppm (t, 2H, J 1H,1H =6.5 Hz, CH2 at C1) 5.20 ppm (broad, 1 H, J 1H,1H =6.5 Hz, H at C6) and 5.45 ppm (t, 1 H, J 1H,1H =6.5 Hz, H at C2)

NMR data: GPP

^{1}H-NMR (500 MHz, D2O + NaOD) δ: 0.86 ppm (t, 3H, J= 6.8 Hz) 1.28 ppm (m, 4H) 1.49-1.46 ppm (m, 2H) 2.74 (t, 2H, J 1H,1H= 7.2 Hz) 6.12 (d, 1H, J 1H,1H = 2.4 Hz) 6.15 (d, 1H, J 1H,1H = 2.4 Hz) 10.05 (broad, 1 H)

NMR data: CBGA

^{1}H-NMR (500 MHz, CDCl3) δ: 0.84 ppm (t, 3H, J 1H,1H= 7.2 Hz) 1.28 ppm (m) 1.53 ppm (s) 1.61 ppm (m) 1.65 (s) 1.75 ppm (s) 2.02 ppm (m) 2.21 ppm (m) 2.82 ppm (t, J 1H,1H= 7.2 Hz) 3.38 ppm (d, J 1H,1H= 7.0 Hz) 4.99 ppm (t, J 1H,1H = 7.0 Hz) 5.52 ppm (t, J 1H,1H = 7.0 Hz) 6.22 ppm (s)

NMR data: 2-*O*-GOA

^{1}H-NMR (700 MHz, CDCl3) δ: 0.88 ppm (t) 1.55 ppm (m) 5.35 ppm (m) 6.17 ppm (s) 6.24 ppm (s). The shifts (6.17 and 6.24 ppm) indicate an alpha prenylation at the C2 hydroxyl group.

NMR data: THCA

^{1}H-NMR (500 MHz, CDCl3) δ: 0.84 ppm (t, J 1H,1H= 6.4 Hz) 1.09 ppm (s) 1.39 ppm (m) 1.42 ppm (s) 1.65 (s) 1.54 ppm (m) 1.69 ppm (s) 2.21 ppm (m) 1.70 ppm (m) 2.10 ppm (m) 2.78, 2.90 ppm (m) 3.18 ppm (d, J 1H,1H =10.4 Hz) 6.18 ppm (s) 6.39 ppm (s)

Chemicals were purchased from Invitrogen (Darmstadt, Germany), Sigma Aldrich (Darmstadt, Germany), Carl Roth (Karlsruhe, Germany) and VWR (Darmstadt, Germany) if not stated otherwise.

Δ9-tetrahydrocannabinolic acid (THCA) was purchased from THC Pharm (Frankfurt am Main, Germany). Cannabigerolic acid (CBGA) was purchased from Taros Chemicals (Dortmund, Germany). Olivetolic acid (OA) was purchased from Santa Cruz Biotechnology, Inc. (Heidelberg, Germany). All compounds were checked for purity and identity by ^{1}H NMR and mass spectroscopy.

Geranyl diphosphate (GPP) was synthesized in-house according to Woodside et al. (Woodside et al., 2003). The educts were freshly distilled directly before use to sequester impurities (purchased geraniol with 98% chemical purity). Finally, synthesized GPP was analyzed by 1H NMR.

A synthetic gene coding for lyticase (GenBank accession number AAA25520.1) with an additional C-terminal histidine tag was ordered from GeneArt (Life Technologies; Regensburg, Germany) and cloned via NcoI/HindIII into the pET28a vector. The active protein was purified from Escherichia coli expression cultures via affinity chromatography according to Shen et al. (Shen et al., 1991)

Plasmids and yeast strains

All strains used in this study are listed in Supporting Table S 1. *E.coli* DH5α was used for routine DNA transformations and plasmid isolations. Synthetic gene sequence of *NphB* (GenBank accession number AB187169) was codon optimized for expression in Saccharomyces cerevisiae and ordered from GeneArt (Life Technologies; Regensburg, Germany). Generation of plasmids was performed via Gibson assembly and a list of primers is given in the supplementary information (Supporting Table S 2). Plasmid pAX_EV was generated by

exchange of the GAP promoter of pGAPZ A (Invitrogen, Darmstadt, Germany) with the AOX1 promoter from ppink_HC (Invitrogen, Darmstadt, Germany).

Generation of *S. cerevisiae* plasmids

A list of all generates Plasmids is given in Supporting Table S 3. The cDNA of yeast-codon-optimized NphB was amplified by PCR with gene-specific primers (Supporting Table S 2) and cloned into pDionysos using Gibson Assembly. The gal80 knockout of S. cerevisiae CEN.PK2-1C Δpep4Δgal1 (Supporting Table S 4) (Zirpel et al., 2015) was performed using the Cre/loxP system published by (Güldener et al., 1996). Plasmid-free cells were recovered by growth in the presence of 5-fluoroorotic acid (5-FOA) (Boeke et al., 1984) and 5-fluoroanthranilic acid (5-FAA). All plasmids used for S. cerevisiae studies contain a mutated Gal1 promoter with deleted mig1 binding sites.(Johnston et al., 1994) Generation of mig1 deletion site vectors was realized via site-directed mutagenesis. Coding sequences of thcas and nphB of pDionysos_TT2AN were separated by a T2A sequence published by Beekwilder et al.(Beekwilder et al., 2014) Assembly of the plasmid was performed by Gibson cloning. The T2A sequence was integrated by PCR primer. The bidirectional Gal10/Gal1 promoter system was obtained from the pESC-URA plasmid. The pGal10-TADH1 cassette was inserted into pDionysos. The coding sequence of thcas under control of pGal10 and nphB under control of pGal1 were integrated by Gibson assembly.

Preparation of competent cells

Preparation and transformation of electro-competent cells of *K. phaffii* was performed according to previous reports.(Lin-Cereghino et al., 2005; Wu and Letchworth, 2004) Electro-competent cells were transformed with 2 to 3 µg of PmeI-linearized DNA of pAX_NphB at 1800 V using EquiBio Easyject Prima Electroporator. Cells were grown for 2 days on YPD agar with 100 µg mL-1 Zeocin and successful integration into genome was investigated via colony PCR using primers S1 and p_Ncoy_rv. Cells were resuspended in 10 µL dH2O, incubated in the microwave for 5 min at 700 W and 1 µL used for colony PCR.

Preparation and transformation of frozen competent S. cerevisiae cells was performed according to Gietz et al.(Gietz and Schiestl, 2007) After heat shock the cells were plated on agar plates containing synthetic mineral salt medium without uracil (6.7 g L-1 YNB without amino acids, 1.9 g L-1 drop out supplements without uracil, 20 g L-1 glucose, 20g L-1 agar) and incubated at 30 °C for 2-3 days. A few colonies from that plate were resuspended in dH2O and plated on synthetic mineral salt medium without leucine (6.7 g L-1 YNB without amino acids, 1.6 g L-1 drop out supplements without leucine, 20 g L-1 glucose, 20 g L-1 agar) .

Membrane permeability of OA and GPP

The cultivation of SC_N with leucine as an auxotrophic marker was carried out with two precultures followed by one main culture. After inoculation of synthetic mineral salt medium without leucine (6.7 g L-1 YNB without amino, 1.6 g L-1 drop out supplements without leucine, 20 g L-1 fructose) the cells were incubated overnight at 30 °C and 200 rpm. The first preculture was used for the inoculation of the second preculture which was grown at 30 °C and 200 rpm for 12 h. For expression culture 50 mL complex medium (20 g L-1 yeast extract, 40 g L-1 peptone, 80 mg L-1 adenine hemisulfate, 40 g L-1 fructose, 5 g L-1 galactose, 100 mM potassium citrate buffer pH 5.5) in 500 mL baffled flasks were inoculated with OD600 of 0.5. The cells were incubated for 72 h at 200 rpm and 15 °C.

Cell culture volumes correlating with an OD600 of 500 were harvested by centrifugation (2,000 x g, 4 °C, 10 min). Supernatants were discarded and cells resuspended in 2 mL assay buffer (50 mM Tris-HCl buffer pH 7.5, 10 % (w/v) glycerol, 100 mM sodium chloride). The cell suspension was divided into two 1 mL aliquots: (1) One aliquot was supplemented with 3 mM OA and 3 mM GPP and incubated for 4 h at 1400 rpm and 37°C. Cells were harvested by centrifugation (2,000 x g, 4 °C, 10 min) and used for ethyl acetate extraction. The extracts were dried under vacuum, resuspended in ACN, filtrated (0.45 µm, Nylon) and analyzed by HPLC-MS. Ethyl acetate extraction was performed in duplicates. (2) The second aliquot was used for cell lysis. 500 µL cell suspension was transferred to 0.5 mL tubes and filled with 0.4 - 0.6 mm glass beads. Cells were lysed by vortexing at maximum speed at 4 °C for 30 min. Cell lysate was centrifuged and supernatant used for NphB activity assay (5 mM magnesium chloride, 1 mM GPP, 1 mM OA, 37 °C, 1100 rpm, 4 h). Cell lysis and NphB activity assay were performed in duplicates.

X. SUPPLEMENTARY MATERIAL REFERENCES

Beekwilder, J., van Rossum, H.M., Koopman, F., Sonntag, F., Buchhaupt, M., Schrader, J., Hall, R.D., Bosch, D., Pronk, J.T., van Maris, A.J.A., Daran, J.-M.M., 2014. Polycistronic expression of a β-carotene biosynthetic pathway in Saccharomyces cerevisiae coupled to β-ionone production. J. Biotechnol. 192, 383–392. doi:10.1016/j.jbiotec.2013.12.016

Carvalho, Â., Hansen, E.H., Kayser, O., Carlsen, S., Stehle, F., 2017. Designing microorganisms for heterologous biosynthesis of cannabinoids. FEMS Yeast Res. 17. doi:10.1093/femsyr/fox037

Guerfal, M., Ryckaert, S., Jacobs, P.P., Ameloot, P., Van Craenenbroeck, K., Derycke, R., Callewaert, N., 2010. The HAC1 gene from Pichia pastoris: characterization and effect of its overexpression on the production of secreted, surface displayed and membrane proteins. Microb. Cell Fact. 9, 49. doi:10.1186/1475-2859-9-49

Lee, M.E., DeLoache, W.C., Cervantes, B., Dueber, J.E., 2015. A Highly Characterized Yeast Toolkit for Modular, Multipart Assembly. ACS Synth. Biol. 4, 975–986. doi:10.1021/sb500366v

Shen, S., Chretien, P., Bastien, L., Slilaty, S.N., 1991. Primary Sequence of the Glucanase Gene from Oerskovia xanthineolytica. J. Biol. Chem. 266, 1058–1063.

Stehle, F., Stubbs, M.T., Strack, D., Milkowski, C., 2008. Heterologous expression of a serine carboxypeptidase-like acyltransferase and characterization of the kinetic mechanism. FEBS J. 275, 775–87. doi:10.1111/j.1742-4658.2007.06244.x

Taura, F., Dono, E., Sirikantaramas, S., Yoshimura, K., Shoyama, Y., Morimoto, S., 2007. Production of Δ1-tetrahydrocannabinolic acid by the biosynthetic enzyme secreted from transgenic Pichia pastoris. Biochem. Biophys. Res. Commun. 361, 675–680. doi:10.1016/j.bbrc.2007.07.079

Woodside, A.B., Huang, Z., Poulter, C.D., 2003. Trisammonium Geranyl Diphosphate, in: Organic Syntheses. John Wiley & Sons, Inc., Hoboken, NJ, USA, NJ, USA, pp. 211–211. doi:10.1002/0471264180.os066.27

Zirpel, B., Degenhardt, F., Martin, C., Kayser, O., Stehle, F., 2017. Engineering yeasts as platform organisms for cannabinoid biosynthesis. J. Biotechnol. 259, 204–212. doi:10.1016/j.jbiotec.2017.07.008

Zirpel, B., Stehle, F., Kayser, O., 2015. Production of Δ9-tetrahydrocannabinolic acid from cannabigerolic acid by whole cells of Pichia (Komagataella) pastoris expressing Δ9-tetrahydrocannabinolic acid synthase from *Cannabis* sativa l. Biotechnol. Lett. 37, 1869–1875. doi:10.1007/s10529-015-1853-x

CURRICULUM VITAE

Name	Zirpel
First name	Bastian
Date of birth	21.02.1986
Place of birth	Hanover
Nationality	German

Academic education

06/2013 – 05/2018	**PhD student** Technical biochemistry, Biochemical and chemical engineering, TU Dortmund
06/2013 – 05/2017	**Research associate** Technical biochemistry, Biochemical and chemical engineering, TU Dortmund
06/2013 – 05/2016	**Graduate cluster fellow** Graduate cluster of industrial biotechnology (CLIB-GC within CLIB2021)
04/2011 – 03/2013	**M.Sc. Molecular/ Applied Biotechnology (grade 1.10)** Department Biology, RWTH Aachen
10/2006 – 03/2011	**B.Sc. Biotechnology (grade 1.59 with distinction)** Department Technology, Hochschule Emden-Leer
09/2009 – 06/2010	**B.Sc. Toxicology, Level 7 (81.9 % with distinction)** Department Life Science, Athlone Institute of Technology, Ireland

School education

06/2015	A-levels
1998 – 2005	Gymnasium Langenhagen

Internships

04/2013 – 05/2013	Graduate assistance – supervision of practical course „General biotechnology“, RWTH Aachen
06/2013 – 11/2013	Internship at the Fraunhofer-Institut for Toxikology and experimental Medicine, Brunswick

List of publications

- **Zirpel B**, Stehle F, Kayser O., 2015. "Production of Δ^9-tetrahydrocannabinolic acid from cannabigerolic acid by whole cells of *Pichia (Komagataella) pastoris* expressing Δ^9-tetrahydrocannabinolic acid synthase from *Cannabis sativa* L." Biotechnol Lett. 2015 Sep;37(9):1869-75
- **Zirpel B**, Degenhardt F, Martin C, Kayser O, Stehle F., 2017. „Engineering yeasts as platform organisms for cannabinoid biosynthesis." J Biotechnol. 2017 Oct 10;259:204-212.
- **Zirpel B**, Degenhardt F, Zammarelli C, Wibberg D, Kalinowski J, Stehle F, Kayser O. "Optimization of Δ9-tetrahydrocannabinolic acid-A synthase production in Komagataella phaffii via post-translational bottleneck identification" J. Biotechnol. 272–273, 40–47.
- **Zirpel B**, Kayser O, Stehle F, „Elucidation of structure-function relationship of THCA and CBDA synthase from *Cannabis sativa* L." – submitted to Journal of Biotechnology in 02/2018

List of presentations

- Recombinant expression and functional characterization of THCA synthase in yeasts. Oral presentation at CLIB-GC conference, Wermelskirchen, March 2016
- Recombinant expression of Δ^9-tetrahydrocannabinolic acid synthase from *Cannabis sativa* L. in *Pichia pastoris*. Poster presentation at CLIB-GC conference, March 2014
- Recombinant expression of THCA synthase in *Pichia pastoris* and its functional characterization. Poster presentation at CLIB-GC conference, Lünen, March 2015
- Production of Δ^9-tetrahydrocannabinolic acid from cannabigerolic acid by whole cells of *Pichia (Komagataella) pastoris* expressing Δ^9-tetrahydrocannabinolic acid synthase from *Cannabis sativa* L. Poster presentation at CLIB-GC conference, Wermelskirchen, March 2016